



Measurement of pathologically relevant adipocyte-derived extracellular vesicles

By

Donna Mathew

A thesis submitted for the degree

DOCTOR OF PHILOSOPHY

Neurosciences & Mental Health Research Institute

School of Medicine

Cardiff University

2019

DECLARATION

This work has not been submitted in substance for any other degree or award at this or any other university or place of learning, nor is being submitted concurrently in candidature for any degree or other award.

Signed (Candidate) Date

STATEMENT 1

This thesis is being submitted in partial fulfilment of the requirements for the degree of PhD

Signed (Candidate) Date

STATEMENT 2

This thesis is the result of my own independent work/investigation, except where otherwise stated. Other sources are acknowledged by explicit references. The views expressed are my own.

Signed (Candidate) Date

STATEMENT 3

I hereby give consent for my thesis, if accepted, to be available online in the University's Open Access repository and for inter-library loan, and for the title and summary to be made available to outside organisations.

Signed (Candidate) Date

Word Count: approximately 52, 000

*To my beloved parents and brother,
for their love*

Acknowledgements

First and foremost, I express my sincere and heartfelt gratitude to my supervisors, Professor Philip James and Dr Aled Rees, for granting me the research opportunity; and for their unflagging support, motivation and commitment that helped me strive through the years of my research study. I could not have asked for better mentors.

My gratitude further extends to my fellow research colleagues, Dr Katie Connolly, Dr Rebecca Wadey, Dr Nicholas Burnley-Hall, Dr Justyna Witzcak and Dr Rhiannon Roberts, who contributed with their knowledge and made this PhD truly a great learning and enjoyable experience. The knowledge and research skills I gained through their guidance and companionship is a blessing. My sincere thanks also go to Dr Aled Clayton and his team for sharing the lab facilities and timely advice. A special thanks to Mrs. Maggie Munnery and Ms Laura Watkeys, lab technicians and friends at Cardiff Metropolitan University.

A special mention to thank Dr Dev Dutta and his peers at University Hospital Llandough, for accommodating me into their clinics and arranging patients for sample. A further thank you to all the volunteers that contributed to this research work.

Lastly, special thanks to my dear friends back home who provided me with happy distraction that kept me sane, to my parents and brother, who believed in me and supported me from start to finish and my best friend turned husband Mr. Sajan Devaiah, for standing by me through the tough times and made this endeavour a journey to cherish.

Table of Contents

1. Literature Review	1
1.1 Extracellular vesicles.....	2
1.1.1 Nomenclature and Classification of EVs.....	2
1.1.2 Molecular composition	7
1.1.3 Biogenesis of Extracellular vesicles	11
1.1.4 Techniques for the isolation and characterisation of EVs	16
1.1.5 Characterisation of EVs	21
1.1.6 Functional Role of EVs.....	29
1.2 Adipose Tissue	36
1.2.1 Types of adipose tissue	37
1.2.2 Function of Adipocytes.....	41
1.2.3 Process of Adipocyte differentiation	44
1.2.4 Models to study adipocyte & adipogenesis	49
1.2.5 Adipocyte-derived Extracellular vesicles (ADEVs).....	59
1.3 Obesity and Cardiovascular disease	64
1.3.1 Vascular Endothelium.....	64
1.3.2 Endothelial Dysfunction	66
1.3.3 Endothelial Dysfunction and Atherogenesis.....	68
1.3.4 Obesity and Atherosclerosis	72
1.3.4 Role of EVs in atherosclerosis.....	76
1.4 Thesis aims and objectives	78
1.4.1 Hypothesis	78
1.4.2 Overall aim	78
1.4.3 Specific objectives	78
2. Methods	79
2.1 3T3-L1 cell culture.....	79

2.1.1 Cell Culture and cell counting	80
2.1.2 Oil Red O-staining	83
2.2 Extracellular Vesicle Isolation	84
2.2.1 Isolation of Extracellular vesicles from 3T3-L1 (Cell-derived EVs)	84
2.2.2 Isolation of EVs from human blood plasma (Plasma-derived EVs).....	84
2.3 Nanoparticle Tracking Analysis	86
2.3.1 Working principle	86
2.3.2 Experimental method.....	86
2.4 Time resolved Fluorescence (TRF)	89
2.4.1 Assay design	89
2.4.2 Experimental method.....	90
2.5 Bicinchoninic acid protein assay	92
2.5.1 Principle	92
2.5.2 Experimental procedure	92
2.6 NanoDrop Spectrophotometer.....	93
2.7 Western blotting	94
2.7.1 Sample preparation	94
2.7.2 Protein Separation by SDS-PAGE.....	94
2.7.3 Electroblotting	94
2.7.4 Antibody Incubation	95
2.7.5 Detection	95
2.8 Size-Exclusion chromatography.....	97
2.8.1 Column preparation	97
2.8.2 EV isolation	97
2.9 Adipokine array	98
2.9.1 Assay principle	98
2.9.2 Experimental procedure.....	98

2.10 Immunoassay	100
2.10.1 Magnetic bead capture using Dynabeads.....	100
2.10.2 Solid-phase capture of EVs.....	101
2.11 Human Umbilical Vein Endothelial Cell isolation.....	102
2.12 Leukocyte adhesion assay	104
2.12.1 Isolation of leukocytes	104
2.12.2 Leukocyte adhesion assay	104
2.13 Statistical analysis	105
2.14 Sample size.....	105
3. Results I: Isolation and phenotyping of adipocyte and plasma EVs	106
3. Perspective.....	107
3.1 Introduction	109
3.1.1 Objectives:	111
3.2 Methods	112
3.2.1 Cell Culture and EV isolation.....	112
3.2.2 Oil Red O staining	112
3.2.3 Nanoparticle Tracking Analysis	112
3.2.4 Western blotting.....	112
3.2.5 Time Resolved Fluorescence based Immunoassay (TRFIA)	112
3.2.6 Column chromatography	112
3.2.7 Statistical Analysis.....	112
3.3 Results	113
3.3.1 Measurement of size and concentration by NTA	113
3.3.2 Confirmation of Adipogenesis.....	115
3.3.3 Size and Concentration in cell and plasma derived EV sample	117
3.3.4 Analysis of EV protein markers by Western blotting.....	118

3.3.5 Analysis of EV protein markers using a Time Resolved Fluorescence Immuno-Assay	119
3.3.6 Separation of soluble, free protein from EVs within a sample	121
3.3.6.1 Column purification of 3T3-L1 - derived EVs	121
3.3.6.2 Column purification of plasma EVs	123
3.4 Discussion	126
3.4.1 Main discussion	126
3.4.2 Limitations and Conclusion	132
4. Results II: EVs with adipocyte character in circulation	134
4. Perspective	135
4.1 Introduction	136
4.1.1 Overall Aim:	138
4.2 Methods	139
4.2.1 3T3-L1 cell culture and isolation of extracellular vesicles	139
4.2.2 Isolation of plasma-derived EVs	139
4.2.3 Selective capture of EV populations	139
4.2.4 Detection of proteins in EVs	139
4.2.5 Adipokine array	140
4.2.6 Sequential depletion of EV population	140
4.2.7 Statistical Analysis	140
4.3 Results	141
4.3.1 Magnetic bead capture of selective EV population	141
4.3.2 Effect of magnetic bead capture on column purified EV samples	145
4.3.3 Analysis of plasma-derived EVs using size-exclusion chromatography	149
4.3.4 Sequential depletion of EV sub-populations with “column purified” plasma-derived EVs	152
4.3.5 Measurement of adipokines in pre- and post-depletion samples	155
4.4 Discussion	158

4.4.1 Limitations and Conclusion	167
5. Results III: Effect of circulating adipocyte-derived EVs on leukocyte attachment to endothelial cells	168
Perspective.....	169
5.1 Background	170
5.1.1 Aims:.....	172
5.2 Methods	173
5.2.1 HUVEC isolation and culture	173
5.2.2 Recruitment of obese subjects for study	173
5.2.3 Isolation and purification of ADEVs from plasma.....	173
5.2.4 Leukocyte Adhesion Assay	174
5.2.5 Western blot.....	174
5.2.6 Statistical analysis.....	174
5.3 Results	175
5.3.1 Subject characteristics.....	175
5.3.2 Collection (Isolation) of Human umbilical vein endothelial cells (HUVECs)	176
5.3.2 Effect of TNF- α on leukocyte-endothelial cell adhesion.....	177
5.3.3 Effect of ADEVs (post-depletion) from Healthy and Obese subjects on leukocyte- endothelial cell adhesion.....	179
5.4 Discussion	181
5.4.1 Limitations and future studies	189
6. General discussion	190
6.1 Thesis summary.....	191
6.2 Future directions.....	198
References	200
Appendix	261

SUMMARY

Extracellular vesicles (EVs) are microscopic membrane-bound vesicles, habitually released by different cell types into the local tissue and circulation to serve as intercellular signal communicators. They play an active role in the normal physiology as well as pathogenesis of diseases. *In vitro* studies from animal models and human adipose tissue explants have established the release of EVs from adipocytes, also known as adipocyte-derived EVs (ADEVs). These have been identified *in vitro* studies as possible endocrine mediators in the metabolic function of adipose tissue. Biological fluids, particularly, plasma is one of the channels for movement of EVs. Therefore, this thesis aimed to provide evidence for the presence of ADEVs in circulating plasma.

With the field being relatively young and expanding, there is a lack of standardisation in EV isolation and analytical techniques. Ultracentrifugation (UC) and size-exclusion chromatography (SEC) proved efficient in isolating an optimal population of EVs from plasma, whereas nanoparticle tracking analysis, time resolved fluorescence and western blotting were used to phenotype EV populations.

EV-rich sample was isolated from platelet-free plasma obtained from healthy individuals. Two techniques of magnetic bead capture and solid-phase immunoassay was used to selectively and sequentially deplete major circulating EV populations derived from platelets, leukocytes, endothelial and erythrocytes. Post-depleted samples retained an EV population positive for adipocyte markers and contained a range of adipokines.

Accumulating evidence has implicated ADEVs in obesity-associated cardiovascular diseases, through onset of endothelial dysfunction mediated by inflammation. Leukocyte-adhesion assays performed on HUVECs pre-treated with ADEVs, showed enhanced endothelial activation by ADEVs obtained from obese as compared to healthy subjects. This implies adipocytes release EVs into the circulation and could have a significant role in the development of endothelial dysfunction and atherosclerosis. This thesis suggests the role of plasma-borne ADEVs warrants further investigation as novel biomarkers and for potential therapeutic opportunities in treating cardiovascular diseases.

Abbreviations

A

Ab	Antibody
AMP-kinase	5' adenosine monophosphate-activated protein kinase
APC	Antigen presenting cells
ARRDC1	Arrestin Domain Containing 1
ASCs	Adipose-Derived Stem Cells (ASCs)
AT	Adipose tissue

B

BAT	Brown adipose tissue
BCA	Bicinchoninic-acid assay

C

C/EBP	CCAAT/enhancer-binding proteins
cAMP	Cyclic adenosine monophosphate
CD	Cluster of differentiation
COX	Cyclooxygenase
CVD	Cardiovascular diseases

D

DELFLIA	Dissociation-enhanced lanthanide fluorescence immunoassay
DLS	Dynamic light scattering
DMEM	Dulbecco's Modified Eagle Medium
DNA	Deoxyribonucleic acid

E

ECs	Endothelial cells
ELISA	Enzyme-linked immunosorbent assay
EpCAM	Epithelial cell adhesion molecule
ESCRT	Endosomal sorting complex required for transport
ET-1	Endothelin 1
Eu	Europium
EV	Extracellular Vesicles

F

FABP4	Fatty Acid-Binding Protein 4
FC	Flow cytometry
FCS	Fetal calf serum
Fst	Follistatin

H

HIF-1	Hypoxia-inducible factor 1
hnRNP	Heterogeneous nuclear ribonucleoproteins
HUVEC	Human umbilical vein endothelial cells

I

IA	Immunoassay
ICAM-1	Intercellular adhesion molecule 1
IL-1	Interleukin-1
ILV	Intraluminal vesicles
IR	Insulin resistance
ISEV	International Society on Extracellular Vesicles

L

LAMP	lysosome-associated membrane protein
LDL	Low-density lipoprotein
IEVs	large extracellular vesicles
LPS	Lipopolysaccharide

M

MCP-1	Monocyte chemoattractant protein-1
MFGE8	Milk fat globule–epidermal growth factor-factor VIII
MHC	Major histocompatibility complex
MIF	Macrophage migration inhibitory factor
mins	minutes
miRISC	miRNA-induced silencing complex
miRNA	MicroRNAs
ml	millilitres
mRNA	messenger Ribonucleic acid
mRNA	Messenger RNA

MV	Microvesicles
MVB	Multi vesicular bodies
MVEs	Multivesicular endosome
N	
NF- κ B	Nuclear factor kappa-light-chain-enhancer of activated B cells
NLRP3	Nucleotide-binding domain and leucine-rich repeat containing protein 3
nm	nanometer
NO	Nitric oxide
NTA	Nanoparticle tracking analysis
P	
PBS	Phosphate buffered saline
PECAM	Platelet endothelial cell adhesion molecule-1
PM	Plasma membrane
PMN	Polymorphonuclear neutrophils
PPAR- γ	Peroxisome proliferator-activated receptor gamma
PPP	Platelet poor plasma
PREF-1	Preadipocyte factor 1
PSGL-1	P-selectin glycoprotein ligand-1
R	
RIPA	Radioimmunoprecipitation assay
RNA	Ribonucleic acid
S	
SAT	Subcutaneous adipose tissue
SD	Standard deviation
SEC	Size-exclusion chromatography
SEM	Scanning electron microscopy
SFM	Serum free medium
SIMPLE	Small integral membrane protein of lysosomes and late endosomes
SMCs	Smooth muscle cells
STAM	Signal transducing adaptor molecule

T

T1D	Type1 Diabetes
TDEs	Tumour derived EVs
TEM	Transmission electron microscopy
TF+	Tissue Factor
TfR	transferrin receptor
TGF- β	Transforming growth factor- β
TNF- α	Tumour necrosis factor- α
TRF	Time Resolved Fluorescence
TRFIA	Time Resolved Fluorescence Immunoassay
tRNA	transfer RNA
TRPS	Tuneable resistive pulse sensing
TSG101	Tumour susceptibility gene 101
TSG-101	Tumour susceptibility gene-101
TXA2	Thromboxane synthase

U

UC	Ultracentrifugation
UCP-1	Uncoupling protein 1

V

VAT	Visceral adipose tissue
VCAM-1	Vascular cell adhesion molecule 1
VPS4	Vacuolar protein sorting-associated protein 4

W

WAT	White adipose tissue
β 1 AR	beta-1 adrenergic receptor
β 3-AR	beta-3 adrenergic receptor (β 3-AR)
μ l	microlitres

List of Figures

Figure 1.1 Nomenclatures of EVs.....	4
Figure 1.2 Types of EVs released from a cell.....	5
Figure 1.3 Molecular composition of extracellular vesicles EVs.....	10
Figure 1.4 EV isolation by ultracentrifugation.....	17
Figure 1.5 Schematic illustration of sequential filtration.....	18
Figure 1.6 Schematic view of the EV Array.....	26
Figure 1.7 Principle of Lanthanide luminescence measurements.....	28
Figure 1.8 Overview of the mouse models used in the study of adipogenesis.....	50
Figure 1.9 Overview of Human models to study the adipogenesis process.....	55
Figure 2.1 Microscopic images of 3T3-L1 on Day 0 and Day 14.....	81
Figure 2.2 Representative Timeline for growth of 3T3-L1.....	82
Figure 2.3 Isolation of EV.....	85
Figure 2.4 Principle of Nanoparticle Tracking Analysis.....	87
Figure 2.5 Concept of TRF assay to detect EVs.....	89
Figure 2.6 BCA assay standard curve.....	92
Figure 2.7 NanoDrop spectrophotometer.....	93
Figure 2.8 Electroblothing stack.....	95
Figure 2.9 Representative blot of the adipokine array post development on film.....	99
Figure 2.10 Principle of magnetic bead capture.....	101
Figure 2.11 Isolation of HUVECs from human umbilical cord.....	103
Figure 3.1 NTA analysis of size and concentration of polystyrene beads.....	115
Figure 3.2 Evidence of Adipogenesis in 3T3-L1 cells.....	116
Figure 3.3 Measurement of the size and concentration of EVs.....	117

Figure 3.4 Western blot analysis of adipocyte markers in EV lysates.....	118
Figure 3.5 Measurement of EV protein content by TRF-IA.....	120
Figure 3.6 The elution of 3T3-L1 EVs through a size exclusion column.....	122
Figure 3.7 Evaluation of plasma eluent through a size exclusion column.....	124
Figure 4.1 Analysis of magnetic bead capture by NTA and TRFIA in crude prep....	142
Figure 4.2 Effect of FABP4+ve EV pullout on plasma EV populations.....	144
Figure 4.3 Control experiment on 3T3-EVs through a CD9+ magnetic bead capture.....	144
Figure 4.4 Evaluation of CD9+ve and FABP4+ve magnetic bead pullout on 3T3- derived and plasma-derived EVs post column (SEC) purification.....	146
Figure 4.5 Validating efficiency of magnetic bead and solid phase assay in depleting EV-sub population.....	148
Figure 4.6 Evaluation of human plasma on SEC.....	150
Figure 4.7 Investigation of pooled plasma EVs.....	151
Figure 4.8 Evaluation of adipocyte and EV markers in the post-magnetic bead and solid phase depletion sample.....	154
Figure 4.9 Profile of adipokines in the pre- and post-depleted samples using a protein array kit.....	156
Figure 4.10 Adipokine array results.....	158
Figure 5.1 Immunofluorescence staining of HUVECs.....	176
Figure 5.2 Effect of varying doses of TNF- α on leukocyte attachment to HUVECs.....	178
Figure 5.3 Effect of ADEVs from healthy and obese subjects on leukocyte attachment to HUVECs.....	180
Figure 5.4 Conceptual illustration of the role of ADEVs in endothelial dysfunction.....	188

List of Tables

Table 1.1 Classification of EVs based on key characteristics.....	6
Table 1.2 Overview of the types of adipocytes in human.....	40
Table 2.1 Media used in the culture of 3T3-L1.....	80
Table 2.2 Pre- and post-analytical settings used for NTA experiments.....	88
Table 2.3 List of primary antibodies used in TRF assays.....	91
Table 2.4 List of primary antibodies used in Western blot experiments.....	96
Table 2.5 HUVEC media constituents.....	103
Table 3.1 Calibration beads evaluated by Nanoparticle tracking analysis.....	113
Table 3.2 Comparison of EV size and concentration of EVs following UC and SEC.....	125
Table 5.1 Summary of subject characteristics.....	175

Publications

Connolly, K., Wadey, R., **Mathew, D.**, Johnson, E., Rees, D. and James, P. (2018). Evidence for Adipocyte-Derived Extracellular Vesicles in the Human Circulation. *Endocrinology*, 159(9), pp.3259-3267.

Wadey, R., Connolly, K., **Mathew, D.**, Walters, G., Rees, D. and James, P. (2019). Inflammatory adipocyte-derived extracellular vesicles promote leukocyte attachment to vascular endothelial cells. *Atherosclerosis*, 283, pp.19-27.

1. Introduction

1.1 Extracellular vesicles

Cells from different organisms, including all eukaryotes (from amoebae, *Caenorhabditis elegans*, and parasites to mammals) but also prokaryotic cells have been demonstrated to release vesicles into the extracellular environment. In multicellular organisms, such vesicles have been isolated from diverse bodily fluids, including blood, urine, saliva, breast milk, amniotic fluid, ascites, cerebrospinal fluid, bile and semen. Extracellular vesicles (EVs) are membrane bound and contain cytosolic matter (proteins, lipids and nucleic acids) from the secreting cells enclosed in a lipid bilayer. Their sizes range from 40-1000nm and their biogenesis is regulated and conserved throughout evolution (Raposo and Stoorvogel 2013a; Colombo et al. 2014). Intercellular communication is an essential hallmark of multicellular organisms for routine metabolic function, which is mediated through direct cell-cell contact or transfer of secreted molecules. In the recent years, another mechanism has been understood for intercellular communication that involves intercellular transfer of EVs. Although the release of apoptotic bodies during apoptosis has been long known (Hristov et al. 2004), the fact that perfectly healthy cells also shed vesicles from their plasma membrane has only relatively recently become appreciated. EVs were first reported in 1946 as ‘pro-coagulant platelet-derived particles’, particulate materials released from platelets and found in serum (Chargaff and West 1946). This was later identified as microvesicles from platelets and called ‘platelets dust’ (Wolf 1967). The interest in the biology of EVs grew gradually over the years and within the last decade there was a rapid expansion in EV research groups and publication (Yiran et al. 2015).

1.1.1 Nomenclature and Classification of EVs

As the shedding of vesicles from different tissues began gaining biological significance, they were addressed under various terms among the researchers based on their tissue origin (prostasomes, oncosomes, cardiosomes, ectosomes), their proposed functions (calcifying matrix vesicles, argosomes, tolerosomes), or simply their presence outside the cells (prefix exo or ecto: ectosomes, exosomes, exovesicles, exosome-like vesicles) (Holme et al. 1994; Cocucci et al. 2009; Colombo et al. 2014). **Figure 1.1** lists the terms used in the nomenclature of EVs by researchers to date.

Exosomes are initially intraluminal vesicles of endocytic origin that are formed by inward budding of the limiting membrane to form multivesicular endosomes (MVEs) that are subsequently released by cells upon fusion with the plasma membrane. Their size distribution is relatively homogeneous ranging from 30-120nm (Raposo and Stoorvogel 2013b; Willms et al. 2018). Exosomes are commonly enriched in endosome-associated proteins such as Rab GTPases, soluble NSF attachment protein receptor (SNAREs), Annexins, and flotillin, due to their endocytic origin. Some of these proteins (e.g. Alix and TSG101) are normally used as exosome markers. A family of transmembrane proteins called tetraspanins (e.g. CD63, CD81, CD9) cluster into microdomains at the plasma membrane; these proteins are abundant in exosomes and considered to be markers as well (Raposo and Stoorvogel 2013b; van der Pol et al. 2016). On the other hand, microvesicles (MV) and apoptotic bodies are vesicles generated by particles blebbing off the plasma membrane that do not necessarily follow the endocytic pathway of biogenesis and their size may vary between 50nm to 1,000nm. Common protein markers used to define these vesicles are selectins, integrins and the CD40 ligand (EL Andaloussi et al. 2013). Confusion on the origin and nomenclature of EVs exists because vesicles with the size of exosomes that bud at the plasma membrane have also been called exosomes (Booth et al. 2006).

As this plethora of terms is based on different criteria, *in vitro* studies, and outdated isolation and detection techniques, a generic term ‘extracellular vesicles’ was introduced to resolve the confusion and improve the exchange of information between researchers and societies. In 2014, the International Society on Extracellular Vesicles (ISEV) released a position statement to address the discrepancies by recognising tetraspanins to identify EV subpopulations. **Table 1.1** essentially describes three types of membrane bound EVs: exosomes, microvesicles, and apoptotic bodies, as classified by their pathway of origin, size and biogenesis (**Figure 1.2**). Although the statement advocates the use of ‘EVs’ as an umbrella term to include all secreted vesicles, by research societies, as of 2018, it requests researchers to report further specifics and fulfil criteria as outlined by ISEV, while documenting their work on EVs (Théry et al. 2018).

A single cell type can release both exosomes and MVs. For example, this phenomenon has been observed for platelets (Heijnen et al. 1999), endothelial cells (Deregibus et al. 2007), and breast cancer cells (Muralidharan-Chari et al. 2009). Hence, a major on-

going challenge is to establish methods that will discriminate exosomes from MVs. Only when we are equipped with the knowledge of molecular machineries required for EV formation and cargo sequestration will their origins be optimally determined. Such knowledge will also open new avenues to resolve their respective functions.

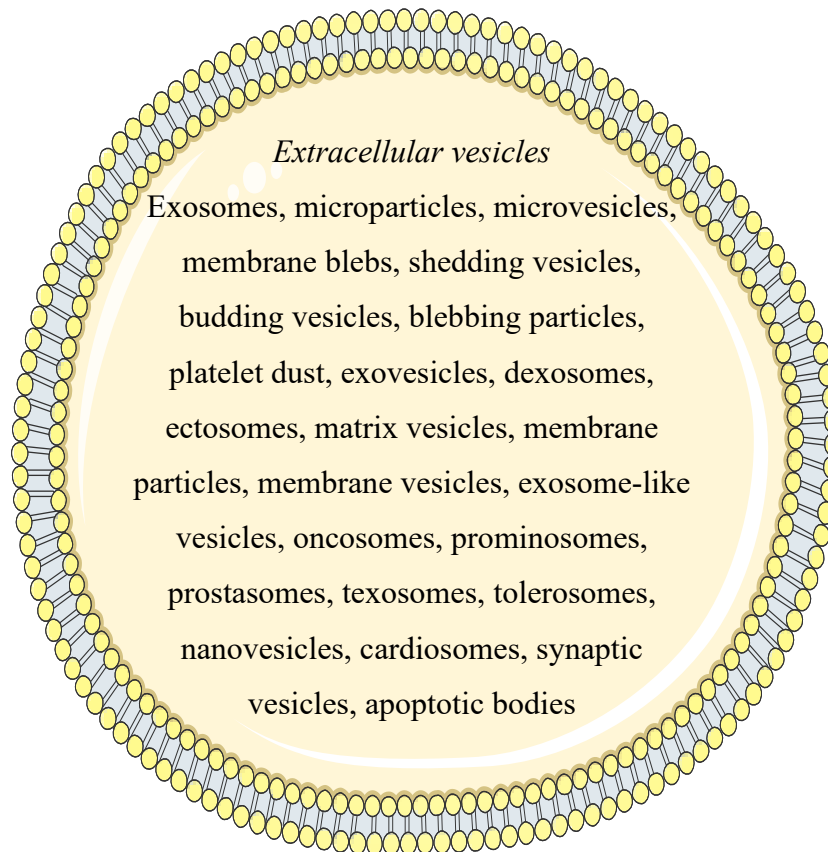


Figure 1.1 Nomenclatures of EVs. Different terms used to address EVs or particles released by cells, used by medical and scientific societies.

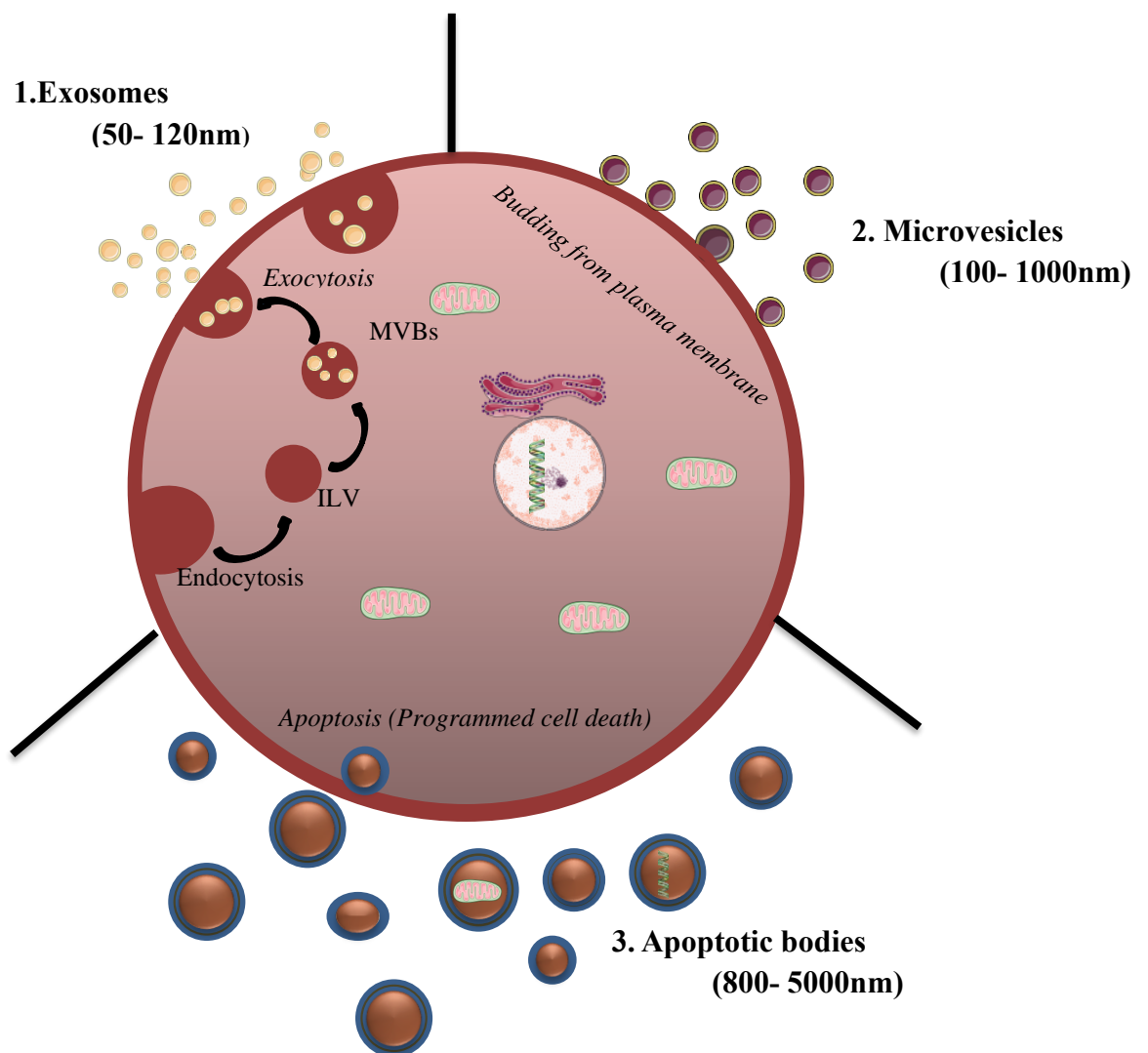


Figure 1.2 Types of EVs released from a cell. 1. Exosomes are 50-120nm vesicles, formed as the intraluminal vesicles, budding into MVBs. They are released by fusion of MVEs with the plasma membrane. 2. MVs are formed by direct blebbing from the plasma membrane and size range from 100-1000nm. 3. Apoptotic bodies are vesicles of size 800-5000nm, secreted during apoptosis or programmed cell death. ILV = intraluminal vesicles, MVB = multivesicular bodies, MV = microvesicles.

	Exosomes	Microvesicles	Apoptotic Bodies
<i>Origin</i>	Endocytic pathway	Plasma membrane	Plasma membrane
<i>Size</i>	40 -120 nm	50 - 1000 nm	500 - 2000 nm
<i>Function</i>	Intercellular communication	Intercellular communication	Facilitate phagocytosis
<i>Markers</i>	Alix, TSG101, tetraspanins (CD9, CD81, CD63,), flotillin	Integrins, selectins, CD40	Annexin V, phosphatidylserine
<i>Content</i>	Cytoplasmic and membrane proteins and nucleic acids (mRNA, miRNA and other non-coding RNAs), MHC molecules	Cytoplasmic and membrane proteins, and nucleic acids (mRNA, miRNA and other non-coding RNAs)	Nuclear fractions, cell organelles

Table 1.1: Classification of EVs based on key characteristics. Ambiguity remains in the literature, with overlap in characteristics between EV subsets. Essentially, these are membrane-bound vesicles of cellular origin that carry protein-lipid cargo. CD = cluster of differentiation, TSG = tumour susceptibility gene

1.1.2 Molecular composition

EVs carry a cargo of soluble and membrane-bound proteins, lipids, metabolites and nucleic acids comprising of DNA and RNA (mRNA, miRNAs, and other small regulatory RNAs). This bioactive cargo is contained within a protective lipid bilayer. They are enriched in proteins such as integrins, MHC molecules and cytoskeletal proteins that are regularly used as EV markers (EL Andaloussi et al. 2013). The specific molecular load of EVs is likely to reflect the cell of origin or reveal the metabolic condition for its release. **Figure 1.3** summarises the overall composition of a typical EV.

Proteins: Protein remains the key content and has been extensively studied as identification markers of exosomes or shed membrane vesicles and relate to the mode of biogenesis. Exosomes are enriched in major histocompatibility complex class II (MHC class II) and tetraspanins including CD63, CD81, CD37, CD53, CD9 and CD82, since their production involves the endolysosomal compartment (Heijnen et al. 1999; Tauro et al. 2012). Exosomes carry ESCRT proteins which is integral for the formation of MVBs and these include Alix, TSG101, and chaperones, such as Hsc70 and Hsp90, irrespective of cell type (Morita et al. 2007). Exosomes are augmented with glycoproteins and transmembrane proteins, when compared to their parent cells (Sinha et al. 2014; Zaborowski et al. 2015). Owing to their origin from plasma membrane, MVs are enhanced in a different repertoire of proteins as compared with those included in exosomes namely, integrins, glycoprotein Ib (GPIb), and P-selectin (Heijnen et al. 1999). Proteins with post-translational modifications such as glycoproteins or phosphoproteins, are realised more in MVs as opposed to exosomes (Larsen et al. 2012).

Some of these proteins especially MHC II, tetraspanins, ESCRT proteins, Alix, TSG101, and heat-shock chaperones, can be used as a general marker to identify EVs when isolating from biological fluids, as they are present in EVs sourced from all cell types. For example, a study by Bobrie et al., (2012) found that inhibiting Rab27a led to decreased exosomal markers (CD63, Alix and TSG101) but not as much for CD9. Large vesicles that were produced exhibited CD9, suggesting that CD9 is probably more ubiquitous among other tetraspanins in EVs (Bobrie et al. 2012). On the contrary, EVs are devoid of those proteins associated with cell organelles, namely mitochondria

(e.g., aconitase), the Golgi apparatus (e.g., GM130), the endoplasmic reticulum (e.g., calreticulin), and some cytoplasmic proteins (e.g., α -tubulin). Hence, their absence could be considered as a negative control for EV origin (Belting et al. 2013; Sinha et al. 2014).

Lipids: Studies have implicated an enriched presence of sphingomyelin, gangliosides and cholesterol in EVs with reduced proportion of phosphatidylcholine and diacylglycerol (Laulagnier et al. 2004; Llorente et al. 2013). Unlike cell membranes, EVs contain increased phosphatidylserine in the outer layer, that aid in their internalisation by recipient cells (Fitzner et al. 2011). Placental EVs have been found to contain an elevated level of sphingomyelin and cholesterol compared to that normally observed in cells (Baig et al. 2013). Interestingly, the lipid composition of reticulocyte-derived exosomes shows no particular enrichment in phosphatidylinositol or sphingomyelin, and lipid composition is similar to the producing cells (Carayon et al. 2011). As reticulocyte maturation into red blood cells causes enrichment in ceramide, it indicates a modification of the intracellular mechanisms of exosome biogenesis (Carayon et al. 2011). Lipid sorting into EVs is a carefully crafted process with membrane tightly packed within lipid rafts and lipids (e.g. cholesterol, ceramide) themselves playing a role in regulating EV release (Del Conde et al. 2005; Salzer et al. 2008; Yáñez-Mó et al. 2015). Increased lipid content lends EV a structural rigidity and stability under conditions of physiochemical changes. Lipid-enriched EVs can also cause functional effects in the recipient cell; for instance, contributing to apoptosis of cells which was positively used in treating tumour cells (Beloribi et al. 2012). Overall, studies strongly suggest that EVs differ in lipid composition according to their source cells and thus, marks a mechanism to allow sorting of these specific lipid species into the vesicles to cause changes in recipient cells.

RNA: RNA-enclosed in EVs were first noticed in murine mast cell derived EVs. Studies have reported EVs containing mRNA, miRNA, rRNA and fragments of t-RNA with an average size of <700 nucleotides. EVs were reported to contain an enriched source of 3'UTR mRNA fragments that contain multiple binding sites for regulatory miRNA, suggesting the cellular RNA might compete with EV RNAs, in order to regulate stability and translation (Batagov and Kurochkin 2013). The release of RNA molecules might cause intrinsic effects in the gene regulation of parental cells. Some EVs have been found to contain miRNA-induced silencing complex (miRISC),

required for processing precursor microRNAs (pre-miRNAs) into mature miRNAs, generating cell-independent microRNA biogenesis (Melo et al. 2014). Heterogeneous nuclear ribonucleoproteins (hnRNP) A2B1 are a family of proteins involved in RNA trafficking and regulating functions. hnRNPA2B1 controls the loading of miRNA into EVs suggesting RNA loading is not passive. An active sorting mechanism ensures a specific repertoire of miRNA is exported into EVs to cater for particular functional effects (Zhang et al. 2010; Villarroya-Beltri et al. 2013; Villarroya-Beltri et al. 2014). Similarly, mRNA is also selectively enriched in EVs where a consensus sequence within the 3'UTR acts as a zip-code sequence that targets distinct mRNAs into EVs (Bolukbasi et al. 2012).

Human mesenchymal stem cell-derived EVs contained mRNAs, which are involved in cell differentiation, transcription, cell proliferation and immune regulation (Collino et al. 2009). Treatment of mice with mRNA-containing EVs enhanced cell survival and repair of tissues (Bruno et al. 2012). mRNA content in EVs is significantly altered by the metabolic state of the cell under normal and stressed conditions where some functional effects were hampered with modulated mRNA (Eldh et al. 2010). Cross talk between large and small adipocytes in fatty acid esterification and lipid droplet biogenesis has been demonstrated to be mediated by transfer specific mRNAs (Müller et al. 2011a). Selective release of miRNA load in EVs has been linked to inducing metastatic properties during tumour progression or lymphocyte activation, by vaccination (de Candia et al. 2013). miRNAs- containing EVs released from immune cells (Mittelbrunn et al. 2011), adipocytes (Müller et al. 2011a) and blood cells (Hunter et al. 2008) have physiological roles that are mediated by the carrying miRNAs. EV-mediated transfer of miRNA has immunological significance. For example during immune synapses formation, there occurs an antigen-driven unidirectional transfer of some miRNAs from T-cell to antigen-presenting cells mediated by EVs (Mittelbrunn et al. 2011). Human breast milk EVs contain immune-related miRNAs, which are transferred from the mother's milk to the infant for the immune development (Zhou et al. 2011).

Therefore, the ability of EVs to harbour RNA material and induce functional effects is remarkable. However, it has been challenging to distinguish between coding and non-coding RNAs and measure the extent of their contribution to these effects. Nevertheless, such RNA-loaded EVs can be used as biomarkers and for targeted

therapy (Huang et al. 2013). Thus, the composition of an EV greatly influences its functional drive.

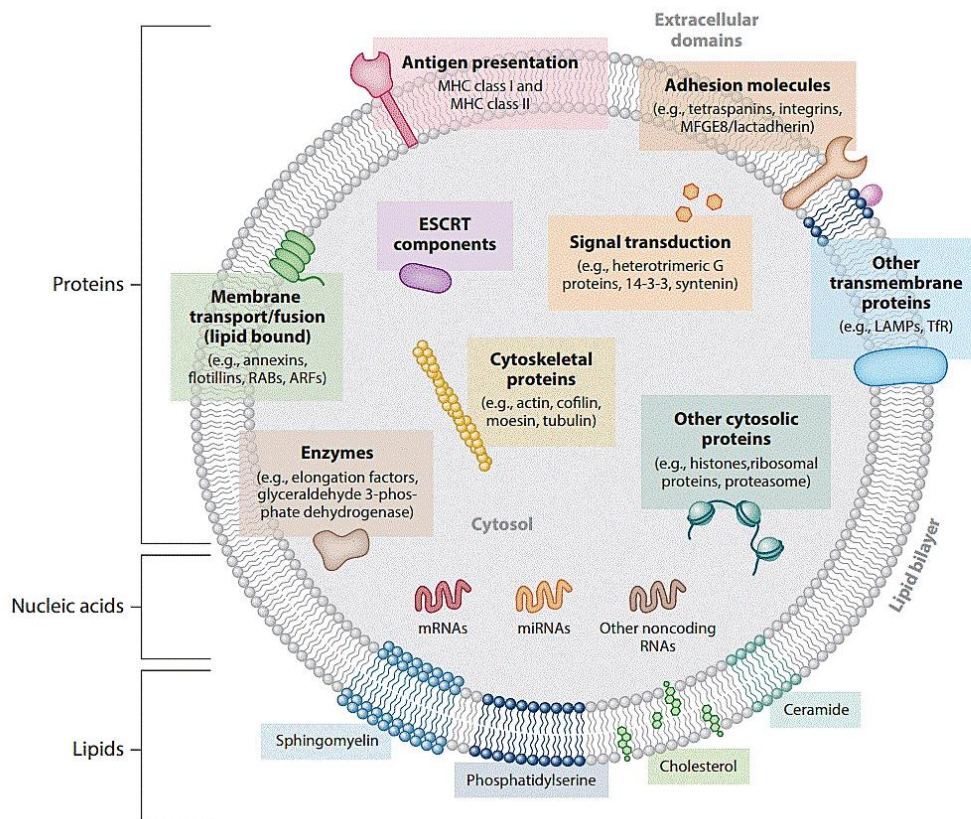


Figure 1.3: Molecular composition of extracellular vesicles EVs. Schematic representation of the EV content (proteins, lipids, and nucleic acids) and membrane orientation of EVs. Abbreviations: ARF = ADP ribosylation factor, ESCRT = endosomal sorting complex required for transport, LAMP = lysosome-associated membrane protein, MHC = major histocompatibility complex, MFG8 = milk fat globule–epidermal growth factor–factor VIII, RAB, Ras-related proteins in brain, TfR = transferrin receptor (*Adapted from Colombo, Raposo and Théry, 2014*).

1.1.3 Biogenesis of Extracellular vesicles

The endocytic pathway involves highly dynamic membrane compartments for the internalisation of extracellular ligands or cellular components, their recycling to the plasma membrane, and/or their degradation (Gould and Lippincott-Schwartz 2009; Klumperman and Raposo 2014). The genesis of an exosome begins with the creation of intraluminal vesicles formed when proteins, lipids, and cytosol are sequestered by the inward budding of endosomal membrane. During the maturation of early endosomes into late endosomes they accumulate intraluminal vesicles (ILVs) in their lumen (Stoorvogel et al. 1991). By virtue of their morphological features, they are generally referred to as multivesicular endosomes or multivesicular bodies (MVBs). In most cells, the content of MVBs is subjected to degradation after fusion with lysosomes, acidic compartments that contain lysosomal hydrolases. Organelles with hallmarks of MVBs, that bear the tetraspanin CD63, lysosomal-associated membrane proteins LAMP1 and LAMP2, and other molecules of late endosomes (eg: MHC class II in antigen-presenting cells), can fuse with the plasma membrane, releasing their content into the extracellular milieu (Raposo et al. 1996; Jaiswal et al. 2002). However, in reticulocytes, MVBs that fuse with the plasma membrane bear markers of early endosomes, such as RAB4 or RAB5, rather than late endosome markers (Vidal & Stahl 1993). These observations suggest that different subpopulations of MVBs coexist simultaneously in cells, with some being destined for the degradation pathway, whereas others are exocytosed.

Cells host morphologically different subpopulations of MVBs, identified based on size and appearance of the ILVs that are present in their lumen. In EBV-transformed B cell lines, cholesterol-positive and -negative MVBs coexist, where cholesterol-containing MVBs undergo an exocytic manner of fusion with the cell surface, in agreement with the finding that exosomes are enriched in cholesterol (Mobius et al. 2003). In HeLa cells, two distinct populations of MVBs have been observed after stimulation with EGF (White et al. 2006). The EGF-receptor reaches CD63- positive endosomes, whereas another subset of MVBs contains LBPA (lyso bisphosphatidic acid) and CD63 but no EGF-receptor. Those MVBs containing LBPA are likely destined for degradation, as exosomes are not enriched in LBPA (Wubbolts et al. 2003). Epithelial cells host morphologically different MVBs at the apical and basolateral sides of the cells. The cellular machinery responsible for MVB manufacture and subsequent fate

decisions is not well understood; the cell type differences that exist create a major challenge in the field.

1.1.3.1 Mechanisms of intraluminal vesicle formation in MVBs

The endosomal sorting complex required for transport (ESCRT) drives the mechanism for the formation of MVBs and ILVs. The pathway involves approximately thirty proteins that assemble into four complexes (ESCRT-0, -I, -II and -III) with associated proteins (VPS4, VTA1, ALIX also called PDCD6IP) conserved from yeast to mammals (Hanson and Cashikar 2012). The secretion of EVs is a process that appears to be conserved throughout evolution (Raposo and Stoorvogel 2013a). The ESCRT-0 complex functions to recognise and sequester ubiquitinated transmembrane proteins in the endosomal membrane, whereas the ESCRT-I and -II complexes facilitate membrane deformation into buds with sorted cargo; subsequently vesicle scission is driven by ESCRT-III components (Hanson and Cashikar 2012).

HRS (hepatocyte growth factor–regulated tyrosine kinase substrate, official gene symbol HGS) and STAM (signal transducing adaptor molecule) are the key components of ESCRT-0 complex that recognises the monoubiquitinated cargo proteins and associates with two non-ESCRT proteins namely Eps15 and clathrin. HRS recruits TSG101 of the ESCRT-I complex, and ESCRT-I then engages ESCRT-III via ESCRT-II or ALIX. Finally, the interaction of the ESCRT machinery with the AAA-ATPase VPS4 effects dissociation and recycling. The mechanisms of inclusion of soluble cytosolic proteins into ILVs are poorly understood, but a role for HSC70 has been proposed (Sahu et al. 2011): the chaperone binds to soluble cytosolic proteins containing a KFERQ sequence and to PS on the MVB outer membrane and thus enters ILVs formed in a TSG101- and VPS4-dependent manner.

TSG101 and ALIX are the principle ESCRT proteins in exosome biogenesis and are present in exosomes originating from different cell types (They et al. 2001). The role of ALIX in exosome biogenesis was demonstrated in reticulocytes, where its binding to the cytoplasmic domain of Transferrin receptor (TfR) was proposed to compete with binding to HSC70 and promote TfR sorting onto ILVs (Géminard et al. 2004). A study by Baietti et al. (2012) showed that tumour cell exosomes contain syndecan, syntenin and ALIX (Baietti et al. 2012). Overexpression of syntenin induced an increase in the

ALIX-dependent release of exosomes (as evidenced by an increase in exosomal markers CD63 and HSP70), whereas exosome release was impaired by the downregulation of syndecan, syntenin or ALIX. ESCRT-II, ESCRT-III and VPS4 functions play a role in the biogenesis of syndecan-, syntenin-, and ALIX-containing exosomes. These data support a role of ALIX in exosome biogenesis and exosomal sorting of syndecans via an interaction with syntenin. In dendritic cells, the decreased exosome secretion was observed only after incubation with an antigen and not in a steady-state situation, thus suggesting an alternate mechanism of exosome secretion under different cellular physiological states (Tamai et al. 2010). The ESCRT-0 protein HRS is also linked to exosome secretion as established by reduced exosome release in HRS-deficient DCs (Tamai et al. 2010) or HGS-depleted HEK293 cells (Gross et al. 2012) and tumour cells (Hoshino et al. 2013). Interestingly, the relationship between ESCRT-dependent formation of exosomes and their cargo load has not yet been clearly determined. The incorporation of MHC class II molecules into the ILVs are linked to the display of an ubiquitination sequence (Van Niel et al. 2006), but a mutant MHC class II β -chain deficient in the ubiquitination site is still recovered in exosomes by means of detergent-resistant membranes containing CD9 (Buschow et al. 2009). Decreased amounts of CD63 and MHC class II were observed on EVs recovered from TSG101- or STAM1- knockdown HeLa cells (Colombo et al. 2013), indicating that TSG101 and STAM1 participate in transmembrane cargo inclusion in EVs. Another proposed mechanism involves the chaperone HSC70, whose binding to the cytosolic tail of the TfR has been shown to allow targeting of this transmembrane protein to exosomes (G eminard et al. 2004).

1.1.3.2 ESCRT-independent manner of MVB formation

There is evidence to suggest that MVBs and ILVs can form in the absence of ESCRT function. The concomitant inactivation of four proteins of the four different ESCRT complexes does not abrogate MVB formation (Stuffers et al. 2009). For example, in melanocytic cells, the sorting of premelanosomal protein PMEL to the ILVs of MVBs is promoted by the tetraspanin CD63 which accumulates in ILVs even in the absence of ESCRT function (Stuffers et al. 2009; van Niel et al. 2011). The pathway occurs in the absence of ubiquitination, ESCRT-0, ESCRT-II (Theos et al. 2006) and ESCRT-III components (Colombo et al. 2014). Consistently, CD63 was recently shown to be instrumental in the formation of small (<40nm) ILVs, independently of HRS, in MVBs

of HeLa cells (Edgar et al. 2014). Two independent studies have shown two lipid metabolism enzymes generating lipids in the limiting membrane of MVBs, which instigate inward budding and thus formation of ILVs in an ESCRT-independent manner: neutral sphingomyelinase (nSMase) causing hydrolysis of sphingomyelin into ceramide (Trajkovic et al. 2008), and phospholipase D2 responsible for hydrolysis of phosphatidylcholine into phosphatidic acid (Ghossoub et al. 2014). Therefore, there exist both ESCRT-dependent and -independent mechanisms of MVBs and ILVs biogenesis relevant to the cargo that is sorted within a given cell (Carayon et al. 2011). A small integral membrane protein of lysosomes and late endosomes, called SIMPLE, has been associated with exosome secretion. Fibroblasts expressing its mutant form (found in Charcot-Marie-Tooth disease patients), CMT1C, secreted less CD63- and ALIX-containing exosomes (Zhu et al. 2013). SIMPLE contains a binding domain for two proteins namely TSG101 and Nedd4 type-3 ubiquitin ligase but regulation of exosomes secretion remains to be understood. A transmembrane protein has been shown to promote exosome secretion by binding to Nedd4, Nedd-family interacting protein 1, hence an interaction between SIMPLE and Nedd4 could potentially be relevant to exosome biogenesis (Putz et al. 2012).

1.1.3.3 Biogenesis and Release of Plasma Membrane-Derived Vesicles

Components of the ESCRT machinery, including TSG-101 and VPS4, are involved in the formation of EVs budding from the plasma membrane; however, the ESCRT-0 proteins HRS and STAM are not involved in the case of membrane fission during cytokinesis or plasma membrane repair (Henne et al. 2011, Jimenez et al. 2014). Hence, a requirement for ESCRT-0 proteins strongly suggests an MVB formation and exosomal nature of EVs. Oligomerisation of cell surface receptors can promote PM-derived EVs from T lymphocytes (Fang et al. 2007) by antibody-mediated crosslinking. In a study involving Jurkat cells, the release of EVs from plasma membrane was induced by the interaction between domains of PM that are enriched for exosomal and endosomal proteins (e.g.: TSG-101) with a PXAP sequence present in the gag protein of retroviruses (Booth et al. 2006), directing an outward blebbing of EVs instead of MVB lineage.

In platelets, elevated levels of intracellular Ca^{2+} ions activate the protease calpain that remodels the cytoskeleton. Cleavage of cytoskeletal proteins and modulation of the

activities of flippase, floppase, and scramblase, cause the loss of membrane asymmetry and leads to budding of EVs from the PM (Hugel et al. 2005). An overexpression of the small GTPase ARF6 depolymerises the actin cytoskeleton which results in release of large PM-derived oncosomes from tumour cells (Muralidharan-Chari et al. 2009). During the degranulation of mast cells an increase in EV release is accompanied by overexpression of phospholipase D2 (Laulagnier et al. 2004a). Sphingomyelinases particularly acid sphingomyelinase originating from lysosomes contributes to the release of large vesicles from the PM of astrocytes upon receptor triggering (Bianco et al. 2009), whilst neutral sphingomyelinase is involved in ILV formation and exosome secretion by oligodendrocytes (Trajkovic et al. 2008). Thus, like ESCRT, the same machinery can play a role in two compartments either at the PM or intravesicular bodies. RAB protein RAB22 is found to play a role in MV shedding especially under physiological conditions of hypoxia (Wang et al. 2014).

1.1.4 Techniques for the isolation and characterisation of EVs

In order to gain an in-depth understanding of EVs and their potential application in therapy, it is essential that the techniques employed in the isolation of exosomes exhibit high efficiency, in terms of yield and quality, and are competent in isolating from various sample matrices. With the advancement in science and technology, techniques have been specifically tailored for the isolation of EVs to obtain optimal quantity and purity. Characteristics of EVs such as their density, shape, size and surface proteins may be exploited to surmise an isolation technique. Each technique has its own set of advantages and limitations. In the following sections, popular and established techniques are discussed.

1.1.4.1 Ultracentrifugation-based isolation techniques

EV isolation by ultracentrifugation (UC) is considered the gold standard technique and is one of the most commonly used and reported approaches for EV isolation. The technique is easy to operate, requires minimal technical expertise, is affordable, requires minimal sample preparation and is only moderately time consuming. For these reasons, UC-based techniques have become popular, accounting for nearly 60% of all EV isolation techniques employed by users in exosome research (Zarovni et al. 2015; Konoshenko et al. 2018). Differential ultracentrifugation and density gradient ultracentrifugation are the types of preparative UC used in the isolation of EV.

Differential ultracentrifugation consists of a series of centrifugation steps of varying centrifugal force and duration to isolate EVs based on their differences in density and size among the components in a sample. The technique is popular for isolation from biological fluids (human plasma/urine). The centrifugal force used typically ranges from $300 \times g$ to $100,000 \times g$ and is performed in a series of steps to successively remove large bioparticles (cell debris/dead cells/proteins). In some cases, the sample is supplemented with protease inhibitors to prevent the degradation of exosomal proteins (Rechavi et al. 2009). At the end of the UC process, EV particles are sedimented to a pellet, which is resuspended in suitable buffer before storing the sample (Li et al. 2017b). A typical workflow of differential ultracentrifugation is presented in **Figure 1.4**.

In density gradient ultracentrifugation, separation of EVs involves a density gradient medium (e.g. sucrose cushion) constructed in a centrifuge tube with incremented density from top to bottom. The sample is layered onto the top of the density gradient medium and subjected to an extended round of ultracentrifugation, where sample solutes (including EVs) move through the density gradient and form discrete solute zones. The fraction containing the separated EVs is recovered from the density region between 1.10 and 1.21 g/ml. This allows for efficient separation of EVs with high purity from other non-specific proteins and nucleoproteins (Van Deun et al. 2014; Miranda et al. 2014). Unlike differential UC, a downside of density gradient UC is that its capacity is largely limited by the narrow load zone.

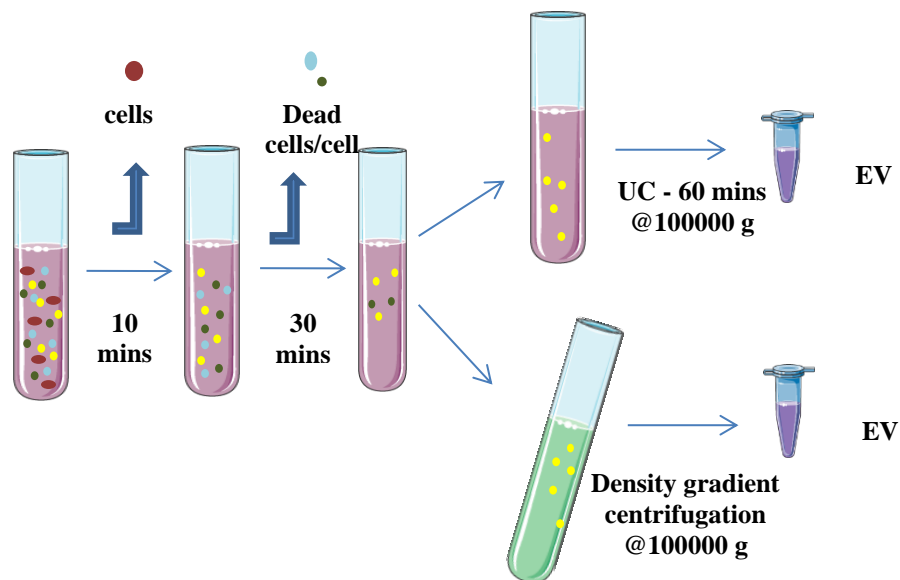


Figure 1.4 EV isolation by ultracentrifugation. Plasma sample are subjected to two low speed spins to remove dead cells, debris and large proteins. Differential UC at 100000 g leaves an EV pellet while density gradient UC has a fraction containing EV that is selectively harvested.

1.1.4.2 Size-based isolation techniques

The technique of ultrafiltration uses the size and molecular weight characteristic of EVs for isolation with membrane filters with size exclusion limits. It is simple to operate with no requirement for sample pre-treatment, however, the use of force in some instances can deform large vesicles potentially skewing downstream analysis (Batrakova and Kim 2015; Zeringer et al. 2015). It involves a series of filtration steps where floating cells and large cell debris are removed first with selective filters. Following this, free proteins are filtered out and subsequently, with filters of pore size 0.22 and 0.1 μm are used to filter out EV particles with occasional application of transmembrane pressure, illustrated in **Figure 1.5**. This approach of isolation has been used effectively to isolate urinary EVs (Tataruch-Weinert et al. 2016) as well as for the isolation of therapeutic exosomes for clinical trials (Escudier et al. 2005). Nanomembrane concentrators along with centrifugation has been effective in enriching exosomes from biological fluids, with working volume as low as 500 μl (Cheruvanky et al. 2007).

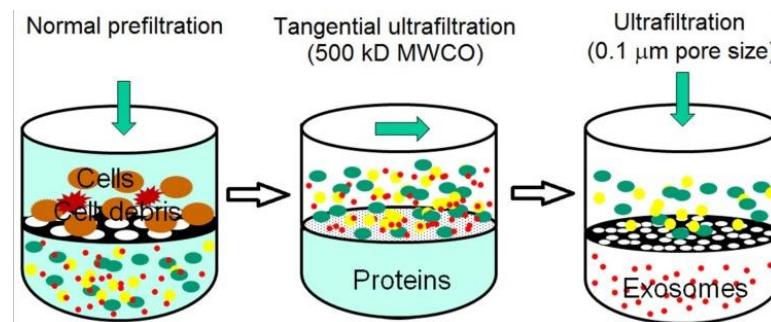


Figure 1.5 Schematic illustration of sequential filtration. Firstly, cells and cell debris are trapped leaving behind the EV in solute. Following, the use of different pore size filters, free protein is filtered out and the sample is concentrated. (*Adapted from Li et al. 2017*)

Yet another size-based separation technique that's been gaining popularity is size exclusion chromatography (SEC). Typically, this involves Sepharose CL-2B (or similar matrix) columns through which the sample is run. Particles with large hydrodynamic radii (that includes EVs/exosomes) are eluted first and those with smaller radii as well as the majority of free protein elute in later fractions after passing through the Sepharose pores (Feng et al. 2014; Li et al. 2017b). SEC has also been standardised in protocols to enrich EVs from plasma or serum samples (Böing et al. 2014; Hong et al. 2014b; Welton et al. 2015); researchers have also employed SEC to collect EVs from conditioned culture media (Lai et al. 2010). Studies have reported that SEC may be more efficient than UC and density gradients to remove contaminant proteins and lipoproteins from plasma and urine samples (Lozano-Ramos et al. 2015; Gámez-Valero et al. 2016). The technique benefits from high EV yield, purity and scalability while preserving vesicle integrity and biological activity. Commercially available pre-made columns (Sigma, USA Cell Guidance systems, UK; IZON Science, UK) offer a quicker and convenient method for vesicle enrichment.

1.1.4.3 Immunoaffinity capture-based techniques

The presence of unique surface proteins on EVs offers opportunity to develop highly specific techniques for the isolation of EVs. The principle is based on the immunoaffinitive interaction between the EV marker protein and target antibody. This technique demands the identification of unique and stable EV proteins expressed in high concentration. The concept led to the development of an immuno-plate and immuno-beads for the capture of EVs from biological samples by means of immunoaffinity (Zarovni et al. 2015). It provided a quantitative analysis of the captured EVs as well as offering the advantages of high EV and RNA yield with intact biological activity. Another success story refers to isolating exosomes from plasma of acute myeloid leukaemia (AML) patients by coating antibody directed against CD34 (biomarker of AML blasts) on magnetic beads (Hong et al. 2014a). Commercially available ExoTEST™ (HANSABIOMED, Tallinn, Estonia) are ELISA plates coated with CD9 antibody, enabling specific capture of exosomes from biofluids and culture supernatants. The immunoassay technique was coupled with mass spectrometry where CD9+ EVs were captured from clinical samples and subject to proteome-wide mass

spectrometric profiling, using CD91 as a biomarker for lung cancer (Ueda et al. 2014). Large volumes of EV source samples are a limitation of this technique; however, a pre-concentration step can be considered to reduce sample volume.

Over the past decade, EV isolation techniques have seen significant progress. Approaches may be combined in order to achieve an efficient, rapid and high yield, while preserving the integrity of EVs during harvest from biofluids.

1.1.5 Characterisation of EVs

With the growing interest in EVs as signalling mediators and biomarkers of disease in pathological conditions, methods are constantly being developed, or the current ones adapted, towards reliable and comprehensive measurement and characterisation of EV properties.

1.1.5.1 Microscopy

EV sizes range from 50nm-1000nm, typically small for the diffraction limit of visible light and cannot be resolved by standard optical microscopy. Hence, electron microscopy techniques, namely scanning electron microscopy (SEM) and transmission electron microscopy (TEM), have been used to visualise EVs for structural and morphological investigation. Samples containing EVs are required to be conductive for SEM and biological samples are typically coated with a thin film of conductive material (e.g. gold) prior to imaging. While there are reports on the use of SEM and variants thereof for the characterization of EVs, TEM is most commonly used (Sharma et al. 2010; Sokolova et al. 2011). TEM does not require the sample to be conductive; however, standard TEM is performed in a vacuum which means that biological samples need to be fixated and dehydrated prior to imaging. TEM can perform immuno-electron microscopy which allows the detection of a specific biomolecule of interest present on the outer surface of a vesicle using gold-conjugated antibodies. This labelling method opens the possibility for searching subpopulations of vesicles exhibiting a pre-defined biomolecular identity and consequently categorising specific size and morphology. To investigate the nature of EV populations from body fluids, TEM-based approaches in combination with immunostaining have been widely used (Klang et al. 2013; Lässer 2013). In an attempt for biomarker discovery, immunoelectron microscopy was used to characterise aquaporin 2-containing small EVs in urine, to confirm their endosomal origin and to characterise the size of this subpopulation (Pisitkun et al. 2004). In the context of neurodegenerative diseases such as Alzheimer's disease, immunoelectron microscopy was used to demonstrate that a fraction of beta-amyloid peptides is released in association with small EVs, leading to new hypothesis on the spreading mechanism of the disease (Rajendran et al. 2006). Microscopy studies on blood plasma samples, for example, illustrated the existing heterogeneities in lamellarity, size and morphology

of the EVs, exhibiting either spherical or tubular morphologies (Yuana et al. 2013; Rupert et al. 2016). The bilayer of EVs observed with cryo-TEM reflects characteristics of cellular membranes it originates from, and their bilayer thickness is likely to be in the order of about 5 to 8 nm (Agarwal et al. 2015).

1.1.5.2 Dynamic light scattering

Dynamic light scattering (DLS) is a widely used optical technique to determine the size distribution of nanometre-scale objects in solution (Berne and Pecora 2003; Rupert et al. 2016). Its working principle involves measuring the fluctuations (Brownian motion) in the intensity of light scattered by nanoparticles in solution upon illumination with a laser beam. Since the Brownian velocity of the particles is proportional to their hydrodynamic radius (also temperature and viscosity), the DLS technique utilises a mathematical model and applies the Stokes-Einstein equation to extract the particle's size distribution down to a couple of nanometres, a size detection limit well-suited for the detection of exosomes and other small EVs.

DLS has been utilised in a number of studies for the characterisation of EVs extracted from cell culture (Atay et al. 2011; Palmieri et al. 2014) or from fresh plasma samples (Lawrie et al. 2009). To improve the performance of DLS whilst dealing with complex samples, conventional DLS may be coupled with either size exclusion chromatography (Varga et al. 2014) or field flow fractionation (a method where nanoparticles are separated according to their size in a laminar velocity gradient) (Agarwal et al. 2015). While DLS provides an accurate size determination of monodispersed samples, the scattering data becomes ambiguous in the case of polydispersed samples. Furthermore, the presence of a few strongly scattering particles can affect the results, whereby small objects are hidden in the ensemble-averaged data. Mathematical modelling may also be a source of uncertainties as particles are assumed to be dense spherical objects, in contrast to the shell-like geometry of vesicles. Considering these glitches, Palmieri et al.,(2014) proposed a hollow shell geometry form factor to increase the accuracy of vesicle size determination using DLS (Palmieri et al. 2014).

1.1.5.3 Nanoparticle tracking analysis

Nanoparticle tracking analysis (NTA) is a widespread and popular alternative method to DLS for determining the size distribution and particle concentration of vesicles, exosomes and other small EVs in particular. Using a conventional microscope, NTA allows for the direct visualisation of individual particles illuminated by a laser beam. The hydrodynamic radius of a single particle is determined after tracking its Brownian motion and quantifies the number of particles in solution, after estimating the sample volume (Dragovic et al. 2011).

NTA is better suited for polydisperse samples than DLS, since the particles are individually visualised under NTA without using an ensemble-averaged signal. The relatively weak scattering properties of nano-sized vesicles challenges NTA in the context of the analysis of small EVs such that the detection sensitivity is limited to diameters larger than approximately 50 to 70 nm (van der Pol et al. 2014; Shang and Gao 2014). NTA, being a label-free technique, may not allow vesicles present in complex biological suspensions to be distinguished easily from other types of particles and in particular from protein aggregates (Van Der Pol et al. 2010). Nevertheless, NTA remains a quick and convenient sizing technique in the context of the characterisation of EVs. The technique has been used to assess vesicle sample quality and stability, to characterise EVs associated with Parkinson's disease (Tomlinson et al. 2015) or those found in blood samples of cancer patients (Gercel-Taylor et al. 2012). With technological advancement, including the use of antibody-mediated fluorescent labels that specifically bind to the antigen of interest on the EV surface, NTA enables the detection of EV subpopulations (Dragovic et al. 2011). This feature enables users to detect, analyse, and count only the selective nanoparticles to which the fluorescently labelled antibodies are bound, with background non-specific particulates being excluded through the use of appropriate optical filters.

1.1.5.4 Antibody-Based Assays

Immunoassays are paramount for profiling the protein composition of EVs. The availability of specific antibodies that bind their target with high affinity is the key step for development of robust antibody-based assays, providing greater sensitivity and a larger dynamic range of the assays. The ability to perform multiplexed phenotyping of EVs is another advantage of this technique. Multiplexed protein profiling of EVs discriminates multiple protein biomarkers in a single setting generating data of diagnostic and prognostic value. However, multiplexed assays may be distorted because of false positive signals generated by non-specific binding of antibodies (cross-reactivity) (Juncker et al. 2014). Western blot and enzyme-linked immunosorbent assay (ELISA) remain the two predominant and established EV characterisation techniques. Western blotting provides an indication about the presence of protein of interest based on its molecular weight by gel electrophoresis and subsequent labelling of the target antigen (Harshman et al. 2016). The ELISA method is a standard technique for quantitation of antigens in solution. It involves immune-mediated EV capture and quantified detection through a secondary labelling procedure (Zarovni et al. 2015). This technique forms the basis of different immunoassay variants, namely fluorescent immunosorbent assay (FLISA), time-resolved fluorescent immunoassay (TRFIA) and immunomagnetic beads in a microchip ELISA (IMEAP), where the capture surface has been mobilised onto immunomagnetic beads (Coumans et al. 2017).

Flow cytometry (FC): Flow cytometry is a commonly used technique for the phenotyping of EVs. In FC, the EV sample is hydrodynamically focussed to enable single particle illumination by several lasers and the measure of scattered light is detected to obtain EV size distribution and enumeration. Although the technique is established and robust for cellular analysis, the use in EV investigation is challenging. Their nanometric size and low refractive index subjects them to low detection sensitivity (Chandler et al. 2011; Jenster et al. 2019). The size detection limit of many conventional FC is curbed at size <300nm, but exosomes typically are a population of EVs falling below 300nm. Another limitation is the low signal-to-noise ratios generated by EVs in the relevant detection area. A low antigen density can cause reduced detectable fluorescence signals (Baumgarth and Roederer 2000). Therefore, it

is essential to minimise background from non-vesicular contaminants, as well as performing strict gating.

Phenotyping of these vesicles is achieved by fluorochrome-conjugated antibodies that target antigens on the EVs (Van Der Pol et al. 2010). FC methods have been modulated for their use in clinical setting when analysing EVs (Dragovic et al. 2013; Inglis et al. 2015). EVs can nevertheless be phenotyped after preabsorption onto antibody-coated beads to elevate them to the detection range (Nielsen et al. 2014). FC can analyse 6 - 11 markers simultaneously in a routine multiplex biomarker analysis, with high throughput where each sample is stained and analysed individually. Plasma has been a regular sample on FC for EV phenotyping (Orozco and Lewis 2010; Dragovic et al. 2013; Inglis et al. 2015), in addition to cell culture supernatant (Johansson et al. 2008; Hoen et al. 2012; van der Vlist et al. 2012), urine (Jayachandran et al. 2015) and cerebrospinal fluid (Verderio et al. 2012). With the development of the next generation of flow cytometers facilitating submicron analysis, the size limit of detection has been lowered to 150 - 190 nm (Welsh et al. 2017a). The need for specialised sensitive and nano-FC will enable identification of novel EV markers, ultimately applicable in a clinical setting.

EV Array: The EV Array, conceptually based on protein microarray, is capable of detecting and phenotyping EVs from impurified starting material with remarkable sensitivity and high throughput (Jørgensen et al. 2013; Jørgensen et al. 2015). Protein microarrays are recognised as powerful tools to search for antigens or antibodies in a multiplexed platform (Melton 2004; Jørgensen et al. 2013) . The principle advantage of such a microarray is that large numbers of proteins can be tracked in parallel; it is a rapid and highly sensitive method requiring only small quantities of samples and reagents.

The EV Array consists of standard epoxysilane coated microarray slides where spots of capturing antibodies are printed using microarray printing technology. Following the addition of EV-containing samples, the captured EVs are detected using a cocktail of biotinylated antibodies against the tetraspanins CD9, CD63 and CD81 that are specific antigens present on EVs. Fluorescently-labelled streptavidin is subsequently used to determine the amount of EVs captured on each individual microarray spot. The fluorescence signals are detected by a microarray scanner or high resolution gel

scanner with a microarray adaptor (**Figure 1.6**) (Jørgensen et al. 2013; Martins-Marques et al. 2016).

A research group under Dr Jørgensen has published and developed extensive work with EV microarrays. The EV microarray platform can detect up to 60 protein markers simultaneously enabling molecular profiling of EV surface proteins. Currently, the method is optimised to be a high throughput analysis with 20 samples analysed simultaneously on each microarray slide. Plasma is the most common sample type used for the EV Array, but EVs from CCS, urine, ascites, and cerebrospinal fluid have also been employed for phenotyping of EVs (Pugholm et al. 2015; Bæk and Jørgensen 2017). With only 10 µl of plasma, fresh or frozen samples can be analysed directly without pre-analytical purification steps. For each microarray spot (~1 nl), only 2.5×10^4 exosomes were required for a detectable signal (Jørgensen et al. 2013). The technology of the EV Array opens the possibilities to alter the detection antibodies in order to investigate other populations or subpopulations of EVs, for example, tissue-factor-bearing vesicles.

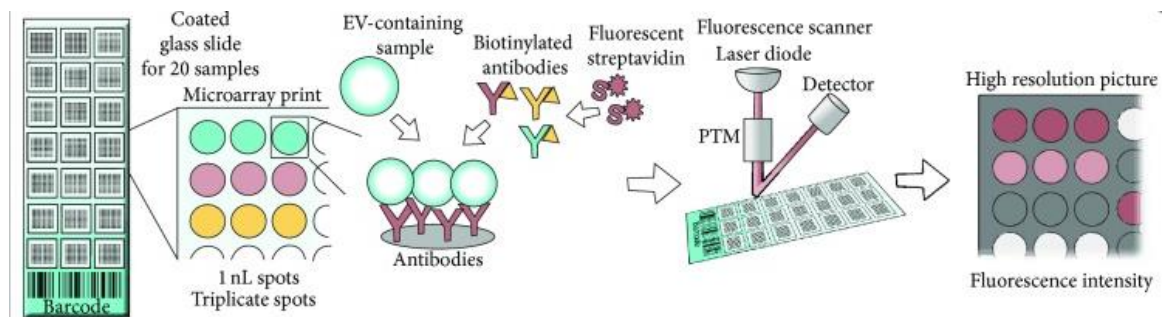


Figure 1.6 Schematic view of the EV Array. A basis for the procedure is epoxy-silane coated slides printed with 21 identical antibody microarray prints (for 20 samples and one control). Each antibody is printed in triplicate. EV-containing samples are applied and the EVs are captured onto the slides depending on the presence of surface antigens. Detection is performed by biotin-labelled detection antibodies against the exosomal markers CD9, CD63, and CD81 followed by fluorescently labelled streptavidin and fluorescence read through a high-resolution scanner (Imported from Pugholm et al. 2015)

Detection of analytes with high sensitivity and specificity is key for applications analysing proteins in biological samples, for example disease diagnosis. Generally, immunoassays use antibodies labelled with radioisotopes, luminophores, or enzymes to generate signal in response to the concentration of analyte present. However, the sensitivity and dynamic range of all immunoassays can be affected by the issue of the background signal observed under very low amounts or absence of the analyte. Samples can contain a multitude of proteins and detecting one intended protein can be challenging especially if their copy number is low. A potential approach of minimising background signals in immunoassays involves the use of lanthanide chelate labels. Luminescent lanthanide complexes have remarkably long-lived luminescence in comparison with conventional fluorophores, enabling the short-lived background interferences to be removed via time-gated acquisition and delivering greater assay sensitivity and a broader dynamic range. The lanthanide ion europium (Eu^{3++}) is most commonly used in bioanalytical applications (Enomoto et al. 2002; Soukka et al. 2003; Zuchner et al. 2009; Webber et al. 2014a).

Luminescence from conventional fluorescent dyes and sample interferences occurs on a nanosecond scale whereas lanthanide ions luminesce in the microsecond to millisecond range. Lanthanide luminescence can be selectively detected by time-gating the signal, even in the presence of other luminescent substances. It can be achieved by marking the acquisition cycle after the more rapid background fluorescence has decayed (**Figure 1.7**). Lanthanide-based time-resolved luminescence immunoassays have been commonly used in solid phase microtitre plates. The most successful and commercially available lanthanide-based immunoassay is the dissociation-enhanced lanthanide fluorescence immunoassay (DELFI A). The DELFI A assay works with four of the luminescent lanthanides (Dy, Eu, Sm, Tb), but due to the differences in the emissive levels of the different ions, it requires different ligands and a single specific enhancement solution (Hemmilä et al. 1984; Hagan and Zuchner 2011).

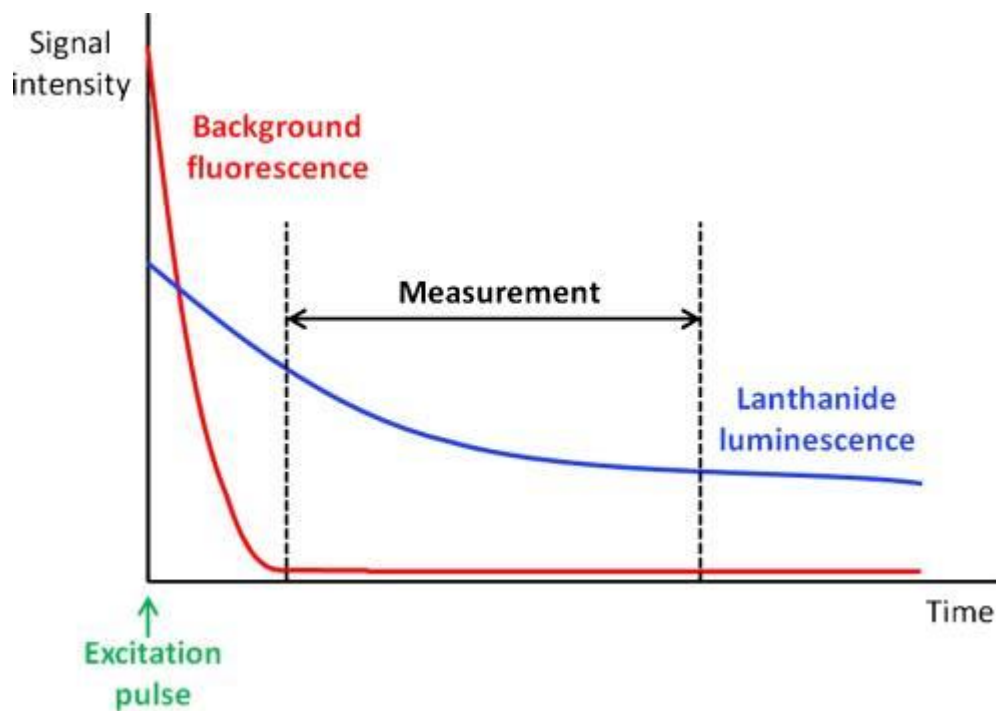


Figure 1.7 Principle of Lanthanide luminescence measurements. Lanthanide ions have long-lived luminescence as compared to conventional fluorescent dyes and can be time gated for an effective measure to avoid background noise. *Illustration adapted from Hagan and Zuchner (2011)*

1.1.6 Functional Role of EVs

1.1.6.1 EVs in body fluids

Body fluids contain a mixture of vesicles originating from different sources such as the cells in circulation and cells lining the cavities of extruded body fluids. The biological contents encapsulated in the EVs are protected by the lipid membrane from degrading enzymes secreted by body fluids, thus protecting them as a source of physiological and pathological information which can be sent over a distance.

Blood: The first report of the existence of EVs in blood was described as platelet “dust”. Later the release of EVs with transferrin receptor during the maturation of reticulocytes was yet another significant find (Wolf 1967; Pan and Johnstone 1983). Plasma-derived EVs are a mixture of vesicles from the cells lining the blood vessels and sourced from different cells found in blood. The largest individual population of EVs in plasma is positive for platelet specific markers (such as, CD41a, CD61 and GPIb) and are considered to be ~25-70% of the total blood EVs as examined by flow cytometry (Caby et al. 2005; Arraud et al. 2014). However, it has also been suggested that the platelet-marker-positive EVs in plasma from healthy subjects are mostly derived from megakaryocytes. The different activating mechanisms by which EVs may be generated suggests a versatile way for the platelet to participate in various physiological maintenance functions from haemostasis to immunity and development (Aatonen, Gronholm and Siljander, 2012). Besides platelet derived EVs, the peripheral blood also harbours EVs derived from blood cell population, that is leukocytes, endothelial cells and red blood cells that mediate several metabolic functions (Menck et al. 2017).

The protein and RNA content of plasma-derived EVs, as well as the number of EVs present, has been shown to be altered by several pathological states, suggesting that blood can also harbour an EV population derived, for example, from tumours (Colombo et al. 2014; Miyazaki et al. 2018). In addition, altered physiological status (such as pregnancy or pathological condition) is reflected in the number and molecular composition of circulating EVs (Agouni et al. 2008; Nardi et al. 2016; Pomatto et al. 2018). The physiological function of plasma-derived EVs, in association with vascular biology, coagulation and the immunological response, is discussed in later chapters.

Urine: About 3% of the total urinary protein content has been estimated to be derived from EVs (De Palma, Sallustio and Schena, 2016). Urinary EVs are collectively released by the cells lining the renal epithelium, extending from the glomerular podocytes through the proximal tubule, the thick ascending limb of Henle, the distal convoluted tubule and the collecting duct (Dear et al. 2013; Prunotto et al. 2013). CD24, expressed both by tubule cells and podocytes, has been identified as a suitable urinary EV marker. Most of the RNA within urinary EVs is rRNA, while only 5% of the total RNA is aligned to protein coding genes and splice sites. A role for urinary EVs in intrarenal signalling has been suggested, representing a mechanism for cell-to-cell signalling along the nephron, through secretion and reuptake of their content such as proteins, mRNAs and miRNAs that can affect the function of the recipient cell (Knepper and Pisitkun 2007). The vasopressin-regulated water channel aquaporin-2 (AQP2), an apical Na⁺ transporter protein, is predominantly excreted via urinary EVs from renal collecting duct cells. Thus, EVs apparently trigger AQP2 trafficking towards the apical plasma membrane where they fuse, thereby increasing water permeability across the nephron. Urinary EVs are described as enriched in innate immune proteins, such as antimicrobial proteins and peptides and bacterial and viral receptors. This suggests a new role for urinary EVs as innate immune effectors that contribute to host defence within the urinary tract (Hiemstra et al. 2014). On the other hand, urinary EVs has proven to be an excellent source of biomarkers for disease progression and non-invasive liquid biopsy for the detection of prostate and bladder cancer (Woo et al. 2019).

1.1.6.2 EVs in vascular biology

EVs enhance coagulation and participate in haemostasis. EVs generated by cancer cells have procoagulant capacity amplified in several pathological processes (Cocucci et al. 2009). The physiological significance of EVs in coagulation is supported by clinical disorders in which microvesiculation is impaired resulting in bleeding tendency. Scott syndrome is a severe bleeding disorder with reduced procoagulant effect of platelets, whereby an impaired phospholipid scramblase activity leads to reduced phosphatidylserine (PS) exposure, decreased release of procoagulant vesicles and low prothrombinase activity (Weiss et al. 1979; Toti et al. 1996). The physiologically relevant procoagulant role of EVs is illustrated by a study of sedentary men in which increased formation of procoagulant platelet-derived EVs during hypoxic exercise training enhanced *in vitro* thrombin generation (Chen et al. 2013). Furthermore, the addition of exogenous platelet EVs to a flow model of circulation induced thrombosis (Suades et al. 2012). The procoagulant activity of EVs seems to be predominantly exerted by the larger-sized EV populations from different cellular sources rather than exosomes (Heijnen et al. 1999).

In addition to platelets, various leukocyte populations, red cells, ECs and even megakaryocytes may participate in forming procoagulant EVs (Owens and MacKman 2011). Smooth muscle cells may also act as a source of procoagulant EVs. Activated monocytes shed TF+ EVs and neutrophils may also contribute; the presence or absence of TF in EVs can be regarded as the major determinant of the procoagulant potential of an EV-population (Egorina et al. 2008; Owens and MacKman 2011). EV-mediated transfer of TF in the circulation may also be relevant. Monocyte-derived TF+ EVs were reported to bind activated P-selectin-expressing platelets via PSGL-1 and to fuse with them, leading to enhanced TF-FVIIa activity (Del Conde et al. 2005). Increased circulating levels of TF+ EVs with procoagulant activity have been associated with pathological states. In diseases such as cancer or acute coronary heart syndrome, the thromboembolic risk mediated by EVs may be enhanced (Matsumoto et al. 2004; Geddings and Mackman 2013). The exact role of EVs in the balance between coagulation and anticoagulation remains unclear, as the predominantly procoagulant role of EVs has been challenged by observations that EVs may also harbour anticoagulant and fibrinolytic properties. ECs, as well as monocytes, express tissue

factor pathway inhibitor (TFPI) and TFPI+ EVs have been detected in normal pregnancies, but their presence was found to be increased in gestational vascular complications (Colombo et al. 2014).

The delivery of pro-angiogenic factors at sites of angiogenic sprouts are believed to be mediated by leukocyte- and platelet-derived EVs (Rhee et al. 2004). EVs derived from mononuclear blood cells are reportedly involved in horizontal mRNA transfer and induce pro-angiogenic effects *in vitro* and *in vivo*. Human endothelial cell (EC) network formation was improved by supernatants derived from T cells and monocytes co-cultured under pro-angiogenic conditions (Rohde et al. 2007). EC stress influenced the EVs in terms of protein and RNA content, and these EVs interact with macrophages in vascular niches to promote vascular growth. Hypoxia-cued EVs from multiple myeloma cells were identified to accelerate angiogenesis by targeting the FIH-1/HIF-1 signalling pathway via miR-135b (Umezu et al. 2014). EV-mediated protection against endothelial apoptosis depended on annexin-I/PS receptor function in target ECs, and the transfer of miRNA-126 promoted endothelial repair. EV-mediated cross-talk between ECs depends on miR-214 and was shown to activate an angiogenic programme in target cells, while EC senescence was suppressed (Balkom et al. 2013; Colombo et al. 2014). Increased understanding of the role of EVs in vascularisation has opened the potential use of EVs in therapeutics, with emerging concepts focused on the development of EVs for pro- or anti-angiogenic therapies used for organ regeneration or cancer treatments, respectively.

Recent studies have associated EVs with cardiovascular related effects. EVs derived from stressed smooth muscle cells can cause endothelial dysfunction modulated by dysregulated EV release with altered profile (Jia et al. 2017). Endothelial cells generate EVs with altered protein cargo that contribute to the pathogenesis of atherosclerotic disease (Goetzl et al. 2017). EVs sourced from adipose tissue carry miRNA that can regulate systemic glucose tolerance at local and distal tissues (Thomou et al. 2017). Studies in mice have shown a role of EVs in improving muscle damage and vascular remodelling, that relies on the presence of certain enzymes within EVs (Cavallari et al. 2017).

1.1.6.3 Role of EVs in the Immune system

EVs act as paracrine messengers building on the innate immune system and have been mainly described as pro-inflammatory mediators inducing or propagating inflammatory signals during infections and metabolic disorders. EVs released from macrophages and dendritic cells predominantly exert pro-inflammatory effects. EVs released from monocytes/macrophages are known to cause inflammation-induced programmed cell death in vascular smooth muscle cells via transfer of functional pyroptotic caspase-1 (Sarkar et al. 2009). It was shown that macrophage-derived EVs could induce differentiation of naive monocyte recipient cells to macrophages (Ismail et al. 2013), which is accounted by the high levels of the miRNA molecule miR-223, which is an important regulator of myeloid cell proliferation and differentiation. Microbial infection of macrophages was also shown to modify their EV content and promote the release of EVs that stimulate pro-inflammatory responses in resting macrophages (Bhatnagar and Schorey, 2007; O'Neill and Quah, 2008). The macrophages infected with *Toxoplasma* or *Mycobacterium tuberculosis* release characteristic EVs that induce immune cell recruitment and secretion of pro-inflammatory cytokine RANTES and TNF- α (Bhatnagar et al. 2007; Anand et al. 2010). Intranasal injection of mice with infected-macrophage EVs led to increased secretion of pro-inflammatory cytokine mediators (TNF- α and IL-12) along with an influx of neutrophils and macrophages into the lungs of mice (Bhatnagar and Schorey 2007). EVs released from stimulated macrophages are capable of triggering F- κ B signalling pathway, to amplify inflammation (McDonald et al. 2014; Zhang et al. 2017).

Besides promoting inflammation, polymorphonuclear neutrophils (PMN) a cell type involved in innate immunity, generate large EVs, termed ectosomes, at the plasma membrane that have immunosuppressive effects. PMN-derived EVs induced the secretion of the anti-inflammatory cytokine TGF β from monocytes or DCs and decreased the release of the inflammatory cytokines IL-8, IL-6 and TNF α . They also promoted the phagocytosis of apoptotic PMN and the release of pro-resolving mediators from macrophages (Dalli and Serhan 2012). *In vitro* studies have shown that antigen presenting cells (dendritic cells/macrophages)-released EVs activate CD8⁺ and CD4⁺ T cells by delivering MHC-I, MHC-II and T cell co-stimulatory molecules

(Utsugi-Kobukai et al. 2003). In addition, B-cell line released EVs can also cause direct stimulation of CD4⁺ T cell lines (Raposo et al. 1996). Immune cell-derived EVs can mediate the transfer of antigen-MHC complexes between immune cells by the process called cross-dressing. The dendritic cell-secreted EVs are captured and internalised by APC, containing antigen-MHC complexes. Subsequently, the APC presents the internalised antigen-MHC complex to activate T-cells instead of EVs (Montecalvo et al. 2008). During autoimmune diseases, patients are detected with increased levels of EVs that are associated with complement activation, bearing complement components. An anti-inflammatory therapy in such instances, suppressed inflammation but didn't affect the number of EVs (associated with complement activation) secreted, suggesting that inflammation may not be the underlying driver of EV release (Yin et al. 2008; van Eijk et al. 2010).

Immune cell-derived EVs can also induce immunosuppressive effects. Thymic-derived EVs play a role in regulatory T-cell selection and the induction of central tolerance (Skogberg et al. 2013). Peripheral immune tolerance effects were effected by immune cell-derived EVs following a genetic modification or IL-10-treatment in DCs (Cai et al. 2012). Furthermore, activated T-cell-secreted EVs diminished the immune response by blocking cytotoxicity of natural killer cells, inhibiting T-cell stimulation and inducing T-cell apoptosis (Wen et al. 2017). T-cell derived EVs were found to mediate anti-tumour activity, a potential target for therapeutic design (Zhang et al. 2011). Therefore, EVs from immune cells can modulate as well as aggravate the immune response.

1.1.6.4 Role of EVs in cancer

Secretion of EVs by tumour cells is understood to play a major role in intercellular signalling to neighbouring tumour cells and to distant tissues via blood or other biological fluid. Tumour derived EVs (TDEs) impact tumour stroma, including fibroblasts, endothelial cells, and immune cells.

Tumour stroma has fibroblasts as a major constituent cell type. TDEs are able to induce a phenotype change, transforming normal fibroblast into cancer-associated fibroblasts (CAFs) (Paggetti et al. 2015; Song et al. 2017). TDEs from prostate cancer were found to contain TGF β that facilitate fibroblast transformation (Webber et al. 2015). The extent of CAF activation correlates with the aggressiveness of the tumour cells. EVs from an aggressive cell line were marked with elevated CAF marker expression, proliferation rate, and enzyme release compared to EVs from a less aggressive cell line (Giusti et al. 2018). Upon activation CAF also release EVs that elicit metabolic changes in tumour tissue to promote tumourigenesis (Donnarumma et al. 1959; Richards et al. 2017). An intriguing role of TDEs is in inducing resistance to chemotherapy (Au Yeung et al. 2016). For instance, a study demonstrated that carcinoma cells pre-conditioned with pancreatic fibroblast media gained resistance to gemcitabine (Richards et al. 2017). Another key role for TDEs lies in the movement of pro-angiogenic molecules from tumour to endothelial cells, thus inducing angiogenesis (King et al. 2012; Umezu et al. 2014). TDEs released from hypoxic tumour cells had a profound effect in promoting angiogenesis, whilst a hypoxic environment elevates the production of TDEs with altered EV cargo. TDEs also affect immune cells to promote tumour associated inflammation. TDEs can activate the NF κ B pathway in macrophages to release pro-inflammatory cytokines IL-6, TNF α , GCSF, and CCL2 (Chow et al. 2014; Minciacchi et al. 2017).

1.2 Adipose Tissue

Obesity is a serious and growing epidemic over the past decade. Worldwide, the prevalence of obesity has tripled since 1975 with nearly 650 million adults currently described as obese (WHO). In England, about two-thirds of adults are classified as obese and it costs the national health service an estimated £27 billion (Public Health England 2017). Obesity represents a major global concern as it is a significant risk factor for the development of numerous chronic conditions including cardiovascular diseases, diabetes, cancer, musculoskeletal disorders and other associated syndromes. Cardiovascular diseases (CVDs) are the leading cause of death globally (approx. 31%) with an estimated 17 million people dying of CVD in 2015 (World Health Organization 2015). The alarming increase in obesity and associated cost of treatment has led to calls for intense research to understand the underlying pathophysiology and development of therapeutics. Over the past two decades, there has been a surge in research into adipocyte biology and adipogenesis, functional pathways, metabolic and homeostatic regulation, and how adiposity can lead to disease conditions. Adipose tissue, once thought of as just an energy depot storing fat, is now recognised as an endocrine organ with adipocytes capable of secreting hormones, cytokines, adipokines, extracellular vesicles and growth factors that not only affect the neighbouring cells but also impact target tissues involved in energy metabolism and influencing physiologic and pathologic processes (Rosen and Spiegelman 2006; Gao et al. 2017). Adipocytes are developed from pre-existing pre-adipocytes which are fibroblast-like cells that upon appropriate conditions (adipogenic stimuli) undergo adipogenesis to form mature adipocytes. In addition to mature adipocytes, adipose tissue also comprises stromal-vascular cells such as fibroblasts, smooth muscle cells, pericytes, endothelial cells, and adipogenic progenitor cells or preadipocytes (Miettinen et al. 2008).

Adipose tissue/adipose depots (AT) are present throughout the body; that which is found in loose association with the skin is classified as subcutaneous adipose tissue (SAT) whilst depots within the body cavity, surrounding the heart and other organs are referred to as visceral adipose tissue (VAT). Intra-abdominal visceral fat drains into the portal circulation; excess VAT in particular has been linked to morbidities associated with obesity such as type-2 diabetes and CVD (Giorgino et al. 2005; Rosen and Spiegelman 2006). Hence, those individuals with preferential accumulation of

adiposity around the visceral/ abdominal region carry more risk of disorders and certain cancers when compared to those individuals where adiposity is distributed to the subcutaneous regions. Adipocytes and precursor cells from different depots have different replicative potential, different developmental attributes and different responses to hormonal signals, although the mechanistic basis for these distinctions is under investigation (Kershaw and Flier 2004). Compared to SAT, VAT is more vascular, innervated and contains a larger number of inflammatory and immune cells. Adipocyte characteristics in the two depots also vary, whereby VAT adipocytes are metabolically active, sensitive to lipolysis and more insulin-resistant than SAT adipocytes. Furthermore, while SAT is more active in uptake of circulating free fatty acids and triglycerides, VAT has a greater capacity to generate free fatty acids and uptake glucose, and is more sensitive to adrenergic stimulation (Ibrahim 2010; Stephens 2012).

1.2.1 Types of adipose tissue

Two predominant types of adipose tissue with distinct characteristics have been defined: white adipocyte (WAT) and brown adipocyte tissue (BAT). White adipocytes, constituting WAT, are characterised by a single large lipid droplet occupying about 90% of the cell volume, squeezing the nucleus to the periphery and cytoplasm forming a thin rim. The organelles are not well developed, with mitochondria being small, elongated with short, randomly organised cristae. These cells are also referred to as unilocular adipocytes. In contrast, brown adipocytes making up BAT, are comparatively smaller in size, their cytoplasm contains several lipid droplets, a round nucleus and numerous, large, generally spherical mitochondria with lamellar cristae, and hence referred to as multilocular adipocytes (Smorlesi et al. 2012; Giordano et al. 2014). BAT is evolved to regulate thermal homeostasis at the expense of glucose and lipids. Exposure to low temperatures/cold induces the development of brown adipocytes within the tissue to meet the increasing thermal demand. This metabolic function is mediated by the presence of a unique protein called uncoupling protein-1 (UCP-1) (Cannon and Nedergaard 2004; Sidossis and Kajimura 2015). In humans, BAT is seen surrounding the heart and great vessels (Giordano et al. 2014). **Table 1.2** gives an overview of the types of adipose tissue.

WAT demonstrates plasticity and can undergo “browning” whereby some white adipocytes can turn into brown-like adipocyte within the tissue and referred to as beige adipocytes (also called brite adipocytes). They are sparsely found within WAT and found to occur in response to cold exposure, chronic endurance exercise or β 3-adrenergic stimulation. They are characteristically similar to brown adipocytes in expressing UCP-1, contain multiple lipid droplets and large numbers of mitochondria. This phenomenon is thermogenically competent where energy is consumed within the depot while limiting the substrate for WAT, thus expanding the energy- dissipating ability of the organism (Harms and Seale 2013; Sepa-Kishi and Ceddia 2018).

These tissue types do not show anatomical boundaries but are found as a continuum in all depots. The relative amount of WAT and BAT varies across the adipose organ depending on several factors including age, diet, environment and physiology. The functional role of white adipocytes lies in storing energy in the form of a lipid droplet. They release fatty acids into the circulation which serves as an energy substrate for other organs when glucose availability is limited. The breakdown of triacylglycerols generates fatty acids which contain more energy per unit mass than carbohydrates. They also secrete endocrine hormones which regulate metabolic functions. On the other hand, brown adipocytes burn lipids to generate heat; the multilocularity maximises the cytoplasmic-lipid interface making a large amount of fatty acids readily available for mitochondrial coupling and consequently thermogenesis. Under light microscopy the adipose organ shows ‘brownish’ areas corresponding to brown adipose tissue, which is predominantly a parenchymal cell type, richly innervated and vascularised. ‘White’ areas, of predominant white adipocytes, show fewer nerves and a lower number of blood vessels (Vitali et al. 2012; Giordano et al. 2014). Depot colour is determined by the relative amount of the two cell types and the degree of vascularisation (Schulz and Tseng 2013).

Adipocytes with intermediate morphology between white and brown have been identified, designated as paucilocular adipocytes found in all adipose depots (Giordano et al. 2014). They exhibit the phenomenon of transdifferentiation whereby they show great affinity to turn into brown adipocytes upon environmental or pharmacological stimulus. There has been evidence to support the fact that fully differentiated adipocytes can undergo genome reprogramming to change morphology and serve a physiological role (Cousin et al. 1996; Himms-Hagen et al. 2000; Smorlesi et al. 2012;

Giordano et al. 2014; Pellegrinelli et al. 2016). White-to-brown transdifferentiation, also referred to as ‘browning’ is essential to meet increased heat production requirements during chronic cold exposure. β 3-adrenoceptors (AR) are specifically expressed by brown adipocytes and under circumstances of cold exposure, they are activated by noradrenaline to drive brown adipocyte thermogenic function mediated by sympathetic nervous fibres (Giordano et al. 1998; Foster and Bartness 2006). The tissue remodelling constitutes recruitment of precursor cells, especially in interscapular and inguinal subcutaneous depots, as well as direct conversion of a subpopulation of unilocular/paucilocular adipocytes (Barbatelli et al. 2010; Rosenwald et al. 2013; Wang et al. 2013). The two processes, which most likely coexist, are driven by the same physiological stimulus through β -AR activation. In a study involving mice, those that lacked beta-3 adrenergic receptor (β 3-AR) did not undergo browning on exposure to cold, but endure precursor development, probably driven by beta-1 adrenergic receptor (β 1-AR) (Barbatelli et al. 2010). Preadipocyte development was observed after administration of β 1-AR agonists, simultaneously, administration of β 3-AR agonists led to a lack of development. Thus, *in vivo* findings suggest that β 3-AR could be responsible for white-to-brown transdifferentiation and β 1-AR for precursor proliferation and differentiation. The remarkable plasticity of adipose tissue is of pathophysiological interest, because it could be harnessed to tackle obesity and metabolic syndrome (Bartelt et al. 2011; Nedergaard et al. 2011). It is interesting to note that human white adipocyte precursors can be induced *in vitro* to express UCP1 through administration of drugs (Elabd et al. 2009; Beranger et al. 2013). A study by Yang et al. (2003), suggested that insulin resistance is associated with a reduced brown adipose phenotype and that a basal brown adipose phenotype may be essential for maintaining normal insulin sensitivity (Yang et al. 2003). The plasticity of the adipose organ could potentially be explored for future treatment, or prevention, of obesity and type-2 diabetes. White-to-brown transdifferentiation involves a reduction in adipocyte size and an increase in their mitochondrial content. Thus, ‘mild’ white-to-brown transdifferentiation could render white adipocytes less prone to death and turn the adipose organ parenchyma into a ‘healthier’ tissue. The **Table 1.2** summarises the three types of adipose tissue.

Adipocytes	Appearance	Function	Location	Developmental origin
White	Unilocular fat droplet, low mitochondrial density	Storage of lipids, endocrine functions, tissue regeneration, cardiovascular function, inflammation	Subcutaneous, intra-abdominal	Potentially within tissue depot
Brown	Multilocular fat droplets, high mitochondrial content	Thermogenesis, endocrine functions	Supraclavicular area, axillary, paravertebral region	Myf5 ⁺ /Pax7 ⁺ precursor
Beige	Multilocular fat droplets, very high mitochondrial content	Thermogenesis, regulation of nutrient homeostasis	Spread among brown and white adipocytes, supraclavicular area, axillary, paravertebral region	Smooth-muscle-like origin

Table 1.2 Overview of the types of adipocytes found in human adipose tissue

Myf5 = myogenic gene, Pax7 = Paired box gene 7

1.2.2 Function of Adipocytes

The classical function of adipocytes is storage and release of energy, serving as an energy bank. When excess energy is generated, free fatty acids (FFAs) enter adipocytes following the hydrolysis of triglycerides from triglyceride-rich lipoproteins and chylomicrons. FFAs are then re-esterified into triglycerides through the sequential actions of multiple enzymes, including glycerol-3-phosphate acyltransferase (GPAT), 1-acylglycerol-3-phosphate acyltransferase (AGPAT), phosphatidic acid phosphatase (PAP), and diacylglycerol acyltransferase (DGAT) (Gupta 2014). Lipids can also be synthesised from carbohydrates through *de novo* lipogenesis by the adipocytes. When energy levels are low, adipocytes activate the enzymatic machinery comprising adipose triglyceride lipase (ATGL), hormone-sensitive lipase (HSL), and monoglyceride lipase (MGL) required to hydrolyse triglycerides and release FFAs back into the circulation (Ameer et al. 2014). Lipid trafficking in adipocytes constitutes an element of its function that has been extensively studied for the past decade (Thompson et al. 2010; Pilch et al. 2011).

Adipocytes have endocrine properties. Perilipins, a family of proteins associated with the lipid droplet, play an important role in regulating lipolysis and lipid metabolism in adipocytes. Perilipins are found in both white and brown adipose tissue (Blanchette-Mackie et al. 1995; Tansey et al. 2004). The discovery that adipose tissue in obesity produced tumour necrosis factor (TNF- α), a pro-inflammatory cytokine involved in insulin resistance, provided the first link between adipose-secretory products and insulin resistance in obesity (Hotamisligil 1999). The discovery of the hormone leptin was a pivotal point in the field of energy metabolism. Leptin is produced and secreted by adipocytes, predominantly WAT, and functions centrally to regulate eating behaviour (Allison and Myers 2014; Sáinz et al. 2015). Food intake and energy expenditure are regulated endocrinologically by leptin, thus modulating adiposity. Leptin receptors are expressed highly in the mediobasal hypothalamus, and leptin-dependent effects commence from the central nervous system (CNS) (Rosen and Spiegelman 2006; Sáinz et al. 2015). The control centre in the CNS orchestrates responses in glucose homeostasis and energy control (Morton and Schwartz 2011). This adipostat has been found to increase insulin sensitivity in the liver and muscles. Leptin also acts on peripheral tissues to control nutrient homeostasis and inflammation (Kang et al. 2016c).

Two other ‘adipokines’ namely adiponectin and adipisin, are primarily produced by adipocytes. Adiponectin exerts pleiotropic effects on glucose and lipid metabolism, thus providing cardioprotection through direct actions on the heart as well as on several types of vascular cells (Nedvídková et al. 2005; Lin et al. 2013; Gupta 2014). Adiponectin has been considered a potential therapeutic agent after a study conducted in mice demonstrated decreased hyperglycaemia, reversed insulin resistance, and sustained weight loss without affecting food intake (Xu et al. 2003a). Other profound beneficial effects include alleviating insulin resistance and adipose tissue inflammation. Adipisin acts at the adipose–pancreas interorgan axis to regulate the insulin secretory capacity of β -cells (Lo et al. 2014). Mice lacking this adipokine had reduced glucose-stimulated insulin secretion and thus glucose intolerance. In a similar vein, T2DM patients with β cell failure have been found to be deficient in adipisin. Visfatin, another key adipokine, has insulin-mimetic effects: it stimulates glucose uptake and promotes insulin sensitivity, as well as exerting proadipogenic and lipogenic effects (Sidossis and Kajimura 2015).

Adipocytes also play a role in glucose homeostasis and exert a significant effect on global glycaemic control. Alterations in adiposity, in cases of obesity or lipodystrophy, have profound effects on glucose homeostasis. Leptin exerts a notable effect by reversing hyperglycaemia and increasing insulin sensitivity (Sadaf Farooqi et al. 2002). In muscles, leptin aids in reducing hepatic intracellular triacylglycerol levels. A functional ‘adipo-insular axis’ has been proposed with insulin promoting leptin secretion and leptin inhibiting insulin release (Kieffer and Habener 2000). The hormone adiponectin has been found to stimulate AMP kinase activity in the liver and skeletal muscle, with profound effects on fatty acid oxidation and insulin sensitivity, as observed in obese/diabetic mice. The loss-of-function models of adiponectin have reported reduced insulin sensitivity on high-fat diets (Kubota et al. 2002; Maeda et al. 2002). The adipokine visfatin has a salutary effect on glucose uptake mediated by direct binding and activation of the insulin receptor, not directly involved in insulin resistance. Serum levels of visfatin do not correlate with type-2 diabetes or insulin resistant states (Rosen and Spiegelman 2006; Stephens and Vidal Puig 2006).

Brown adipocytes are another means by which adipocytes can modulate whole-body energy balance. Brown adipocytes have been deemed as thermogenic cells that perform uncoupled respiration and which function to dissipate chemical energy in the

form of heat with their abundant presence of mitochondria. The mitochondria in BAT contain uncoupling protein 1 (UCP1) that supports the thermogenic function by performing uncoupled respiration. UCP-1 aids in the dissipation of proton gradient across the mitochondrial membrane without concomitant ATP synthesis, resulting in the dissipation of chemical energy into heat. In rodents, brown adipose tissue makes a substantial contribution to whole-body energy metabolism (Harms and Seale 2013). Mice lacking brown adipose tissue exhibit reduced energy expenditure and are prone to diet-induced obesity. Interestingly, mice lacking UCP-1 are cold-sensitive but not obese. In addition, beige adipocytes also have a thermogenic function in addition to their role in glucose homeostasis and energy balance.

1.2.3 Process of Adipocyte differentiation

When the growth arrested pre-adipocytes embark on cell cycle to complete rounds of clonal expansion, it marks the beginning of adipogenesis. The tumour suppressor retinoblastoma protein (Rb) is key in the initiation of adipogenesis and further plays a pivotal role in adipocyte differentiation. In a study undertaken by Hensen et al., the mouse lung embryonic fibroblasts (MEFs) failed to undergo adipocyte differentiation after a targeted disruption in Rb gene coding (Chen et al. 1996; Hansen et al. 1999). The phosphorylation of Rb drives cell-cycle progression, where Rb is hypophosphorylated in growth-arrested preadipocytes and hyperphosphorylated in proliferating cells. Rb in the hypophosphorylated state complexes with transcription factor E2F and coincides with an inhibition of E2F-dependent transcriptional activity (Hiebert et al. 1992). Upon addition of adipogenic hormones, Rb rapidly undergoes hyperphosphorylation by cyclin-dependent kinases (CDKs) leading to dissociation of Rb and E2F. The unoccupied E2F progresses the cell-cycle through to S-phase. Prior to the terminal differentiation state, Rb is restored to a hypophosphorylated state by binding with E2F and thus, impeding cells from the cell cycle expansion (Camp et al. 2002). Cell-cycle-associated proteins including CDKs and their inhibitors, p18, p21 and p27, essentially mediates the advancement of cell cycle followed by its entry into the terminal stage of differentiation (Morrison and Farmer 1999; Reichert and Eick 1999).

The process of adipogenesis is regulated by a set of transcription factors that steers a series of gene expressions. The key catalyst for the activation of terminal adipocyte differentiation is determined by two transcription factor families, namely the CCAAT/enhancer-binding proteins C/EBP α , - β and - δ , and peroxisome proliferator-activated receptor γ (PPAR γ) (Darlington et al. 1998; Rosen and Spiegelman 2000). With the onset of adipogenic signals, the differentiation process begins by the rapid induction of C/EBP β and - δ expression and these proteins subsequently bind to the promoter region of the gene encoding p21 stimulating CDK inhibitor p21 expression. The CDK-mediated Rb phosphorylation is inhibited with increased expression of p21 (Elberg et al. 2000). The significance of C/EBP β and - δ during adipogenesis was demonstrated by genetic studies in mice. Adipogenesis was augmented as a result of an overexpression of either C/EBP β or - δ in preadipocytes, whereas MEFs lacking either C/EBP β or - δ reported reduced levels of adipogenesis compared with the wild

type (Yeh et al. 1995; Tanaka et al. 1997). Reduced white adipose tissue mass and limited lipid staining in interscapular brown adipose tissue were characteristic of MEFs derived from mice with impaired C/EBP β and - δ expression. Furthermore, with C/EBP β and δ -double-knockout mice, harvested MEFs completely failed to differentiate. These studies thus indicate that adipocyte differentiation and maturation is achieved through the synergistic roles of C/EBP β and - δ .

C/EBP α is a pre-requisite in adipogenic induction; hence, this protein is expressed slightly before most adipogenic genes are initiated (Lekstrom-Himes and Xanthopoulos 1998). PPAR γ 2, a ligand-dependent nuclear receptor transcription factor is another important regulator of adipogenesis whose secretion is induced by C/EBP β and - δ expression (Elberg et al. 2000). C/EBP- β and C/EBP- δ are involved at an earlier stage than PPAR γ in adipogenesis, and the promoter region of the PPAR γ gene has binding sites for C/EBP (Lin and Lane 1992; Camp et al. 2002). The induction of C/EBP β and - δ follows an increase in PPAR γ and C/EBP α expression. The transcription factor PPAR γ , expressed substantially in adipose tissue, exists in two isoforms, PPAR γ 1 and PPAR γ 2, derived from the same gene by alternative promoter usage and RNA splicing. While PPAR γ 2 is exclusively expressed in adipocytes, detectable levels of PPAR γ 1 are reported in other tissues, including liver, muscle and macrophage (Camp et al. 2002). A study by Ren et al. underlined the significance of PPAR γ 2 over PPAR γ 1 in 3T3-L1 adipogenesis, where artificial zinc finger repressor proteins selectively decreased the expression of that isoform by specifically binding to the PPAR γ 2 promoter region (Ren et al. 2002). The extent of lipid accumulation is associated with the level of PPAR γ 2 expression. Cells failed to undergo adipogenesis with a depletion in PPAR γ 2 expression whereas adipogenesis was restored when PPAR γ -deficient cells were treated with exogenous PPAR γ 2 and no significant effect as observed with overexpression of PPAR γ 1. Thus, the two isoforms interact differentially with the coactivators and corepressors to mediate PPAR γ transcriptional activity. PPAR γ 1 being expressed in preadipocytes, could act as a priming factor to produce PPAR γ 2 along with C/EBP- β and C/EBP- δ . The cell-cycle is also regulated by PPAR γ 1, feasibly by modulating E2F or its dimerisation partners (the DP proteins). During the later stages of adipogenesis, it's been proposed that endogenous production of PPAR γ ligands are mediated by PPAR γ 1 (Altiok et al. 1997; Morrison and Farmer 1999; Camp et al. 2002).

As differentiation progresses, a role for C/EBP α comes to play post PPAR γ 2 expression and studies have established co-regulating expression between the two. A targeted gene-knockout strategy in mice help understand the degree of PPAR γ and C/EBP α in adipose development. Homozygous knockout of either gene resulted in embryonic lethality and poor development of normal AT in mice (Barak et al. 1999; Kubota et al. 1999). Under heterozygous gene knockout, mice with diminished PPAR γ expression, also expressed a reduced level of C/EBP α and no functional PPAR response element was identified in the enhancer region of C/EBP α (Barak et al. 1999). Similarly, in another study, mice with disrupted C/EBP α expression had a low level of PPAR γ (Wu et al. 1999). In C/EBP α -null MEF cells, where adipogenesis is blocked, an overexpression of PPAR γ 2 was able to restore the process. The PPAR γ gene transcription is activated by the binding of C/EBP α to the promoter region of PPAR γ 2. The PPAR γ 2 promoter region carries a binding site for C/EBP α and C/EBP δ , but not C/EBP β (Elberg et al. 2000). The intricate roles of PPAR γ and C/EBP α were revealed when non-adipogenic cells converted from fibroblasts into adipocytes by the overexpression of either transcription factor, as seen in NIH3T3 cells (Freytag et al. 1994; Tontonoz et al. 1994b). Likewise, in PPAR γ -null MEFs, adipogenesis could not be restored even after forced C/EBP α expression (Rosen et al. 2002). Thus, it leads us to believe that PPAR γ 2 is the fundamental player in adipogenesis while C/EBP α takes an accessory role for PPAR γ 2 and regulates PPAR γ 2 expression. C/EBP α is actively involved in the regulation of genes involved in the metabolic actions of insulin, such as glucose transporter 4 (Glut4). Evidently, the synergistic act of the transcription factors PPAR γ and C/EBP α are key in adipogenesis to generate fully differentiated, insulin-responsive adipocytes (Wu et al. 1999; Camp et al. 2002).

Activated PPAR- γ induces exit from the cell cycle and triggers the expression of adipocyte-specific genes, resulting in increased delivery of energy to the cells. Adipocyte determination- and differentiation-dependent factor-1/sterol regulatory element-binding protein-1 (ADD-1/SREBP-1) is involved in adipogenesis as well as lipogenesis through gene expression as demonstrated *in vivo* (Kim and Spiegelman 1996). Steroid receptor coactivator-3 (SRC-3) impacts white adipocyte formation, where it acts synergistically with the transcription factor C/EBP to regulate the gene expression of PPAR γ 2 (Louet et al. 2006).

An enzyme prominently found in adipose tissue is lipoprotein lipase (LPL), which catalyses the hydrolysis of triglyceride (TG) molecules. Lipid accumulation in mature adipocytes is controlled by LPL; thus, the presence of LPL mRNA is considered as a marker of terminal adipocyte differentiation (Miettinen et al. 2008). A transmembrane protein, preadipocyte factor-1 (pref-1), is an indicator of a preadipocyte phenotype as it's involved in maintaining the cell (preadipocyte) character. During adipocyte differentiation, the expression level of pref-1 dwindles and *in vivo* studies have demonstrated its inhibitory effect on adipogenesis (Wang et al. 2006; Connolly et al. 2015).

On approaching the terminal phase of differentiation, adipocytes *in vitro* sensitise to insulin and increase *de novo* lipogenesis. Additionally, the proteins and mRNA coding for enzymes including adenosine triphosphate (ATP) citrate lyase, malic enzyme, glycerol-3-phosphate dehydrogenase and fatty acid synthase, that are involved in TG metabolism are escalated (Gregoire et al. 1998; Miettinen et al. 2008). Furthermore, adipocytes nearing maturation, synthesise an adipocyte-specific fatty acid binding protein (ap2/FABP4) known as a transitional marker regulating adipocyte differentiation. FABP4 is principally located in adipose tissue controlling intracellular metabolism and transport of fatty acids. A study by Garin-Shkolnik et al., (2014) demonstrates that FABP4 can downregulate PPAR γ whilst terminating the adipocyte differentiation process, thus regulating adipogenesis (Garin-Shkolnik et al. 2014). FABP4 attenuates PPAR- γ to interfere with the insulin responsiveness. In visceral fat depot, the inhibition of PPAR γ by FABP4, indicates FABP4 in the progression of obesity-related morbidities, such as insulin resistance, diabetes, and atherosclerosis (Moseti et al. 2016). Adipocytes also secrete other adipokines namely adiponin, angiotensinogen II and leptin, indicators of the terminal stage of differentiation (Jones et al. 1997). A late marker of adipogenesis significantly induced is acyl-coenzyme A (CoA)-binding protein (ACBP) that modulates the availability of acyl-CoA esters for metabolic and regulatory purposes during adipocyte differentiation (Hansen et al. 1991).

The transcription factors C/EBP α and PPAR γ establish the mature adipocyte phenotype by inducing adipocyte-specific genes. Adipocytes at the terminal differentiation stage are established with mechanisms that are important for insulin

action, lipid synthesis and transport, as well as secretion of adipocyte specific protein factors (Farmer 2006). Sustained expression of C/EBP α maintains terminal differentiation by activating various adipocyte genes. To ensure continued expression of C/EBP α throughout the differentiation process, C/EBP α contains a C/EBP binding site to allow for auto-activation of its own expression, located within its proximal promoter (Moseti et al. 2016). To conclude, adipocyte differentiation is a very complex process that involves the coordinated expression of a host of growth factors, hormones and transcription factors. Comprehending the complexities of adipogenesis process is of prime importance when understanding metabolic disorders and related diseases.

1.2.4 Models to study adipocytes and adipogenesis

Adipocyte differentiation and cellular metabolic functions are complex processes, which can be studied owing to the development of diverse *in vitro* cell models and molecular biology techniques that allow for a better understanding of adipogenesis and adipocyte dysfunction associated with obesity. This section discusses the different animal and human cell culture models available for studying the *in vitro* adipogenic differentiation process related to obesity and its co-morbidities.

1.2.4.1 Animal models

Preadipocytes and mature adipocytes have been explored and studied from different animal sources over the past years. Although rodents have been the traditional source, feline and porcine cells have also been used to a lesser extent. Although studies in animal models of obesity and related metabolic diseases offer significant insights, their applicability to humans is limited by differences in their metabolism and physiology. **Figure 1.8** gives an overview of mouse models available in the field.

Primary preadipocytes are fibroblast-shaped cells that, under appropriate conditions, can differentiate into mature adipocytes. Adipogenesis consists of two main phases: commitment and terminal differentiation. Committed preadipocytes express markers that include the PPAR γ and C/EBP family of regulators prior to differentiation induced by adipogenic stimuli. Once preadipocytes have committed to the adipocyte lineage, a transcriptional cascade induces the expression of metabolic genes and adipokines associated with the adipocyte phenotype, such as fatty acid-binding protein 4 (FABP4, also known as AP2), glucose transporter 4 (GLUT4, also known as SLC2A4), leptin and adiponectin (Cristancho and Lazar 2011).

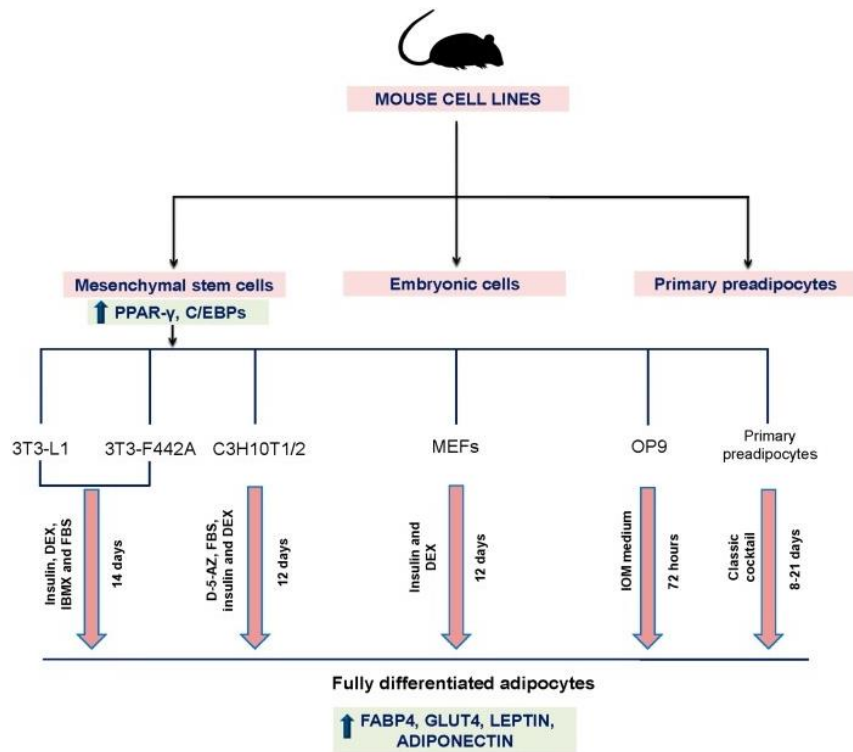


Figure 1.8: Overview of the mouse models used in the study of adipogenesis.

The media requirements and the maturation time are indicated over/below the arrows. The fully differentiated cells display increased concentration of FABP4, adiponectin and leptin. (*Adapted from (Ruiz-Ojeda et al. 2016)*)

Murine preadipocytes have been extensively used to study various aspects of adipocyte biology and adipogenesis. Primary cultures have advantages that they can be obtained from various locations or depots and from animals of different ages to examine depot- or age-dependent adipogenic or secretory mechanisms, whereas preadipocyte cell lines are incapable of addressing these aspects (Hausman et al. 2014). However, these models have several limitations such as inadequate propagation in culture; troublesome DNA transfection; huge triacylglycerol stores that interfere with biochemical and microscopy analyses; extent of variation owing to genetics and source conditions; and the tedious isolation procedure (Ruiz-Ojeda et al. 2016a).

3T3-L1 Mouse Cell Line

In the study of adipogenesis and obesity-related pathologies, the most popular and well-established cell line is the preadipocyte 3T3-L1 cell line derived from murine Swiss 3T3 cells (Green and Meuth 1974). The 3T3-L1 cells are sourced from 17-19-day-old Swiss 3T3 mouse embryos, that display a fibroblast-like morphology and under appropriate treated conditions, procure an adipocyte-like phenotype (Green and Kehinde 1976; Aoki et al. 2007).

Development of 3T3-L1 fibroblast cells into an adipocyte phenotype requires treatment with adipogenic agents, such as insulin, dexamethasone (DEX), and 3-isobutyl-1-methylxanthine (IBMX), which under defined concentrations and along with foetal bovine serum (FBS) elevates the intracellular cAMP levels. 3T3-L1 cells differentiate within 10 to 12 days and are able to maintain their phenotype as far as passage 10 using additional adipogenic agents such as rosiglitazone (2 μ M) (Caprio et al. 2007; Zebisch et al. 2012). Moreover, Vishwanath *et al.* published a novel method that uses a combination of DEX and troglitazone to achieve differentiation in a shorter order of time compared to the conventional protocol of IBMX and DEX. The accumulation of lipid droplet increased by 112% and glucose uptake by 137% compared to cells differentiated using the traditional method (Vishwanath et al. 2013). The straightforward procedure of cell culture, the homogeneous cell population, ability to maintain identity through several passages and cost effectiveness are some of the key advantages in the use of this cell line (Poulos et al. 2010).

Research using 3T3-L1 cells have helped in a better understanding of the underlying molecular mechanisms of adipogenesis as well as in evaluating the effects and potential application of compounds on adipogenesis for obesity treatment (Kang et al. 2016b; Lai et al. 2016). Compounds such as quercetin and resveratrol have been examined in the 3T3-L1 cell line as adipogenesis inhibitory factors (Chang et al. 2015; Eseberri et al. 2015). Moreover, the effect of melatonin (Kato et al. 2015), reactive oxygen species (ROS), or antioxidants on adipogenic differentiation have been studied through these cell lines (Calzadilla et al. 2013). Adipogenic differentiation can be inhibited by some androgens, such as testosterone by activation of the androgen receptor/ β -catenin/T-cell factor 4 interaction as examined

in 3T3-L1 adipocytes (Singh et al. 2003). The role of different functional genes has been investigated through genetic procedures conducted in 3T3-L1 cells. Gene silencing techniques such as siRNA and shRNA, and transfection procedures (virus transfection and plasmid electroporation) have been applied to investigate the function of enzymes, adipokine synthesis and inflammatory pathways.

Investigating the proliferation and differentiation of 3T3-L1 cells revealed the biological role of miRNA-195a in various cellular processes (Ruiz-Ojeda et al. 2016a). Convincingly, this cell line has been constructive when used in co-cultures and 3D cell cultures, as well as high-throughput screening of compounds (Turner et al. 2015).

However, the adipogenic 3T3-L1 cell line model has its limitations. The cells require at least two weeks for adipogenic differentiation and prone to losing their ability to differentiate under extensive passage. The process of transfection has been challenging and in certain circumstances fails to restate all the characteristics of primary cell culture models as this cell line originated from a single clone (Wolins et al. 2006; Ruiz-Ojeda et al. 2016a).

3T3-F442A Mouse Cell Line

3T3-F442A is another significant cell line derived from murine Swiss 3T3 cells that display an enhanced commitment in the adipocyte lineage than 3T3-L1. These clones of cells are characterised by increased size and differentiation at a higher frequency; capable of accumulating more lipids than the 3T3-L1 cells. Initiating the adipogenic differentiation does not necessarily require exposure to glucocorticoids (Green and Kehinde 1976). This cell line has been used in adipogenesis research to study compounds that affect differentiation. The role of alkaline phosphatase in lipid metabolism, adipokine secretion and gene expression has been explored through siRNA gene silencing technique (Hernández-Mosqueira et al. 2015). Desarzens et al. (2014), employed the 3T3-F442A cell line to investigate the effects of drugs on adipocyte differentiation (Desarzens et al. 2014). Others have used this model to report the effects of different receptors and transcription factors during adipogenic differentiation (Scroyen et al. 2015). Despite some limitations, these Swiss murine

obtained cell lines have been well- established cell models in the study of adipogenesis *in vitro* since 1974 and on-going.

OP9 Mouse Cell Line

The OP9 mouse stromal cell line is a bone marrow-derived adipocyte cell culture model established from the calvaria of new-born mice. The cell line is genetically deficient in functional macrophage colony-stimulating factor and provides a tractable alternative for adipogenesis studies. OP9 cells accumulate large triacylglycerol lipid droplets within seventy-two hours of significantly expressed adipogenic stimuli bestowing a suitable cell model (Wolins et al. 2006; Lane et al. 2014). OP9 cells significantly express adipocyte specific proteins namely PPAR- γ , CEBP α , CEBP β , perilipin 1 (PLIN1), and PLIN4 proteins and adipogenic differentiation is particularly driven by PPAR- γ . These cells are capable of retaining their identity through a number of passages and potent in protein expression following transient transfection in fully differentiated adipocytes (Wolins et al. 2006).

With these advantages in mind, OP9 cells have been used in research to examine the effect of compounds in adipogenesis, for example whereby the mechanism of quercetin as an anti-adipogenic agent was established as well its ability to effect lipolysis in these cells (Seo et al. 2015). The inhibitory effects of *Pericarpium zanthoxyli* extract on the adipogenic differentiation of OP9 cells has been reported (Kim et al. 2014a). Adipogenesis have been found to be repressed in OP9 cell lines by ascorbic acid, an adenylate cyclase inhibitor (Rahman et al. 2014). Furthermore, the role of oxidative stress on the process has been studied using this cell model (Xiao et al. 2011; Saitoh et al. 2012). OP9 cells offer a potential model for drug screening and gene knockout experiments. OP9-K was developed from a clonal population of OP9 with an enhanced rate of differentiation and reproducibility, in addition to an increased transfection rate of 80%, rendering it a high-end adipocyte model for research into the differentiating transcriptome (Lane et al. 2014).

On the other hand, OP9 cells need optimisation for adipocyte differentiation and requires maintaining in high cell density, which otherwise alters the morphology of

the cells and impairs differentiation. Overall, OP9 offers a promising model for study of adipogenesis.

Primary Mouse Embryonic Fibroblasts (MEFs)

Sourced from totipotent cells of early mouse mammalian embryos, primary mouse embryonic fibroblasts (MEFs) are capable of differentiating and maturing into adipocytes, with limited addition of external pro-adipogenic transcription factors (Rosen and MacDougald 2006). Ease of establishment and maintenance, rapid proliferation, ability to endure several passages and large numbers of cells produced from a single embryo are the advantages provided by MEFs, making it an attractive cell culture model. Owing to cellular heterogeneity of the embryonic tissue, there is variable efficiency in differentiation (10 - 70 %) and tissue homogeneity (Garfield 2010). *In vitro* studies on MEFs have implicated several genes or transcription factors implicated in obesity-related adipogenesis mechanisms and associated signalling pathways. A study was conducted that signified the role of fat mass and obesity-associated (*FTO*) protein and its gene in adipogenic differentiation. Overexpression of *FTO* in mice is associated with increased affinity for adipogenic differentiation, while MEFs derived from *FTO* knockout mice showed repressed adipogenesis. Thus, fat pads isolated from *FTO* mice fed on a high-fat diet showed an increased number of adipocytes (Merkestein et al. 2015).

Unfolded protein response (UPR), a protein associated with oxidative stress, has been implicated in adipogenesis and UPR expression confirmed in adipose tissue (Han et al. 2013). Kim et al. (2014) conducted a study with MEFs to establish Makorin Ring Finger Protein 1 (MKRN1), a negative regulator of PPAR- γ 2 in obesity, as a potential therapeutic target in PPAR- γ related diseases (Kim et al. 2014b). A novel paracrine role for *Fst* in regulation of lipid metabolism and modulation of brown adipocytes has been shown by Braga et al. (2014), using MEFs harvested from *Fst*-KO mice (Braga et al. 2014).

Therefore, MEF cells appear to be a good *in vitro* model to study adipogenesis. However, the key limitation lies in different physiological characteristics in terms of species/origin (mouse embryos) as compared to human adipocytes.

1.2.4.2 Human Cell Models

Animal cell models have been the conventional choice for *in vitro* adipogenesis studies; however, human cells have been gaining popularity and actively explored in the current research setting. The conducted experiments and results thus obtained from human cells are of greater significance and reliability than animal models because they closely mimic the human tissue (*in vivo* conditions) and display improved applicability towards human diseases such as obesity and its derived metabolic dysfunctions. The stromal vascular fraction (SVF) serves as a source for the development of human cell models, a collection of cells including preadipocytes, stem cells, endothelial cells, as well as immunological cells such as macrophages, neutrophils, and lymphocytes (Esteve Ràfols 2014). **Figure 1.9** provides a summary of human models used to study adipocyte tissue and adipogenesis.

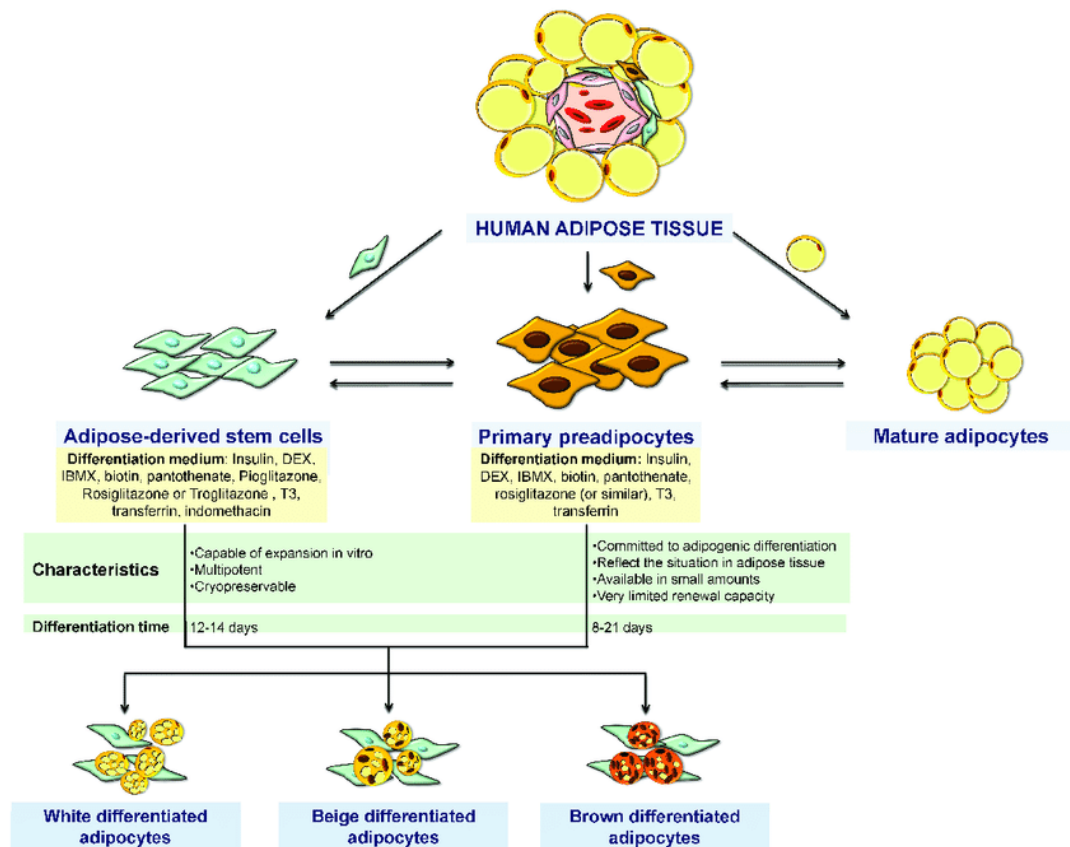


Figure 1.9 Overview of Human models to study the adipogenesis process.

(Adapted from (Ruiz-Ojeda et al. 2016))

Adipose-Derived Stem Cells (ASCs)

Adipose-derived stem cells (ASCs) is one of the major constituent cell types within the SVF of the adipose tissue. These perivascular cells are multipotent and can differentiate into numerous cell types (adipocytes, chondrocytes, osteocytes, and myocytes) given appropriate cell culture conditions (Cawthorn et al. 2012; Huang et al. 2012). They are characteristically distinguished from adherent bone marrow adult stem cells, known as MSCs or multipotent mesenchymal stromal cells (MMSCs) and their culture habits and routine are well-documented (Bunnell et al. 2008; Lee and Fried 2014). Besides their nature of multipotency ASCs possess a high expansion rate, ability to withstand a good number of passages and subject to cryopreservation for considerable period of time are their key benefit (Lee and Fried 2014). Since they reflect donor- and depot-specific characteristics, one can explore the variation in adipose tissue proliferation or differentiation. With the critical addition of cAMP-elevating agents such as IBMX, ASCs differentiate into adipocytes exhibiting true adipocyte phenotypic markers. Hormones such as insulin and β -adrenergic agonists, also cause physiological changes in the cells phenotype (Jia et al. 2012; Ruiz-Ojeda et al. 2016a).

Research exploring ASCs in human adipocyte differentiation in recent years has focused on the mechanisms, protein molecules and transcription factors involved (Higuchi et al. 2013; Narvaez et al. 2013). The effect of external factors and different compounds has been studied using this cell model (Kang et al. 2016a). Rouiz Odeja and colleagues have investigated the role of different genes involved in human adipogenic differentiation and adipose tissue inflammation (Ruiz-Ojeda et al. 2016b). One of the interesting features of ASCs is their ability to convert from white to brown adipocytes, which has led to further exploration of certain molecules such as p53 in differentiation (Pisani et al. 2011; Molchadsky et al. 2013).

Primary Preadipocytes

A novel model that contributes to the study of adipogenesis is primary preadipocytes, which are easily harvested from the SVF of adipose tissue and differentiated into mature adipocytes under appropriate culture conditions. ASCs and preadipocytes have

similar surface markers but the latter express a higher proportion of PPAR- γ . Multilineage-differentiation capacity is limited in this cell types because the preadipocytes in the SVF are already committed to an adipocyte lineage (Cawthorn et al. 2012).

Human primary preadipocytes provide an ideal model to study adiposity and obesity-related complications as they closely manifest the adipose tissue characteristics, especially when isolated from subcutaneous and visceral sources. The isolated cells exhibit depot-specific properties and thus, aids in evaluating differences between individuals (obesity, weight-loss, age, etc.) (Lessard et al. 2014; Michaud et al. 2014). With their ability to differentiate efficiently under serum-free conditions, it allows their study with compounds that are otherwise sensitive to serum components (Armani et al. 2010). One of the major disadvantages is their very limited passaging capacity and low yield in the cell number compared to other cell models.(Ruiz-Ojeda et al. 2016a). The proliferative capacity of human SVF derived preadipocytes was successfully expanded when telomerase activity was induced through the co-expression of the h-TERT and E7 oncoprotein from the human papillomavirus type 16 (HPV-E7) (Darimont and Macé 2003; Church et al. 2015). With increasing passage numbers, preadipocytes required the addition of PPAR- γ agonists to counter the declining adipogenic potential to accumulate lipids.

Different methods of lentiviral gene transfection, adenoviral delivery, and plasmid transfection have been able to induce gene expression in primary human preadipocytes, whereas siRNA delivery has facilitated gene silencing (Divoux et al. 2014; Lee et al. 2014b). A crucial process of precursor cell commitment and differentiation is altered during hypertrophic obesity. Human preadipocytes have proven useful in comprehending the mechanisms involved in adipogenic capacity (Fenech et al. 2015; Gustafson et al. 2015a). The role of miRNAs on adipogenic differentiation and proliferation have also been investigated by virtue of these preadipocytes. Thus, human preadipocytes have contributed to our understanding of the function and formation of adipose tissue as well as potential therapeutic targets against obesity-related diseases (Ruiz-Ojeda et al. 2016a).

In addition to these aforementioned models, there are other recognised models used in the study of adipogenesis and associated metabolism. These include models to study

brown adipose, namely murine primary brown preadipocytes and brown/beige differentiated adipocytes (ASANO et al. 2014; Nam et al. 2015). There also exist cell lines representative of selected diseases such as Simpson-Golabi-Behemil syndrome cells and LiSa-2 cells (Wabitsch et al. 2000; Wabitsch et al. 2001). Researchers have also co-cultured adipocytes with cell types (i.e., endothelial cells, macrophages, muscle cells.) to create 3D cell cultures. These have the potential to gain insight into the metabolic connections between adipose and other tissues (Ruiz-Ojeda et al. 2016a). Although recently the focus has shifted to human primary cell lines/explants, the 3T3-L1 cell line remains the most popular and best-established model to study adipogenesis.

1.2.5 Adipocyte-derived Extracellular vesicles (ADEVs)

Adipose tissue releases EVs which act as endocrine mediators and signalling molecules for the routine function of adipose tissue as well as during pathological conditions (such as metabolic syndrome). Exploring ADEVs is a very new field and hence still under development, but numerous studies have already implicated ADEVs as the link between obesity and metabolic dysfunction (Ferrante et al. 2015; Hubal et al. 2017; Wadey et al. 2019)

1.2.5.1 Composition

Adipocyte-derived EVs were first isolated and characterised from the mouse 3T3-L1 cell line by Aoki et al. in 2007. They were called adiposomes and validated by an exosomal marker protein, Milk fat globule-epidermal growth factor 8 (MFG-E8) (Aoki et al. 2007). EVs secreted by cultured adipocytes comprised heterogeneous sized particles ranging from small exosome-like to large membrane vesicles as revealed by electron microscopy. Several integral, cytosolic, and nuclear proteins such as caveolin-1, c-Src kinase, and heat shock protein 70 were also found to be microvesicle components along with substantial amounts of adiponectin.

The physiological state of the adipocyte is an important regulatory factor in the production of ADEVs. The production of ADEVs from 3T3-L1 cells was increased in response to elevated levels of insulin and TNF- α . This study also confirmed increased secretion of MFG-E8 under oxidative stress conditions (Aoki et al. 2007). In addition to MFG-E8, adiponectin was identified as a potential marker for the adiposome. Connolly et al., in our own group, more recently characterised 3T3-L1 derived EVs pre- and post-adipogenesis, observing that EV production per cell was greater at a pre-adipocyte stage. This might relate to a role in promoting adipocyte differentiation as intercellular communicators (Connolly et al. 2015). Their sizes ranged from 50-1000nm as measured by nanoparticle tracking analysis, and size increased by three times as compared to their pre-adipocyte stage. However, when comparing the differentiation process from pre-adipocytes to mature adipocytes (i.e. from day 0 through to day 15), there were changes noted in several fatty acids and in protein content at different stages. FABP4 and PREF-1 EV expression decreased with differentiation, while adiponectin increased and PPAR- γ showed no significant change. These observations agreed well with the corresponding protein content in the

cell during the stages of differentiation (Connolly et al. 2015). 3T3-L1 adipocyte exocytosis has been shown to be stimulated by cAMP via a PKA-independent pathway and this was regulated via both calcium-dependent and -independent processes (Komai et al. 2014). The long chain omega-3 fatty acid docosahexaenoic acid has an escalating effect in exosome release from 3T3-L1 cells (Declercq et al. 2015). Potential hypoxia in adipose tissue resulting from adipocyte hypertrophy, has a profound effect on 3T3-L1 differentiated adipocyte exosome production (Sano et al. 2014). 3T3-L1 adipocytes exposed to hypoxia had a different exosome proteomic profile compared to control adipocyte exosomes. In particular, exosomes produced under hypoxic conditions were enriched in enzymes involved in *de novo* lipogenesis and these exosomes were able to promote lipid accumulation in recipient 3T3-L1 cells. Preliminary evidence for the presence of ADEVs in the circulation has emerged from the observation that perilipin-A-positive EVs were upregulated in obese mice as well as in human patients with metabolic syndrome (Eguchi et al. 2016).

A study by Durcic et al. 2017, distinguished two subsets of adipocyte-derived EVs from 3T3-L1 cultured cells, namely large extracellular vesicles (IEVs) and small extracellular vesicles (sEVs) (Durcic et al. 2017). These two EV subpopulations had significant differences in their size, morphology and electron density as observed from nanoparticle tracking analysis (NTA) and transmission electron microscopy (TEM). Although IEVs were secreted at lower concentration compared to sEVs, a greater diversity of proteins was identified in the IEV fractions, especially cytosolic proteins. This could be a consequence of specific sorting of exosomes from MVBs, which is known to be controlled by Rab GTPases and other ESCRT proteins (Ostrowski et al. 2010; Colombo et al. 2013). Upon proteomic analysis, the IEVs were enriched in membrane, organelle and cell part components in comparison with sEVs, in agreement with membrane-derived shedding of microvesicles, whereas the sEV fraction was specifically enriched in extracellular matrix and macromolecular complex components. The sEV fraction was also specifically enriched in proteins related to cell adhesion as well as in macrophage activation. The EV sub-populations were also distinguished based on their cholesterol content and externalised PS. The high sterol content was a characteristic of the sEVs, whereas the IEVs carried a greater amount of externalised phosphatidylserine than the sEV fraction (Durcic et al. 2017).

Adipose tissue explants from visceral and sub-cutaneous regions have been compared with respect to EV production. Kranendonk *et al.* characterised EVs isolated from *ex vivo* subcutaneous and visceral adipose tissue explant cultures by differential ultracentrifugation and from human adipocytes differentiated *in vitro* from Simpson Golabi Behmel Syndrome (SGBS) pre-adipocytes (Mariette E G Kranendonk et al. 2014). EVs generated from differentiated human adipocytes contained presumed adipose-specific markers FABP-4 and adiponectin as well as several inflammatory adipokines, including MIF, TNF α , MCSF, and RBP-4 as distinguished from other stromal cells, when isolating from whole adipose tissue. The adipokine profile differed between subcutaneous adipose tissue EVs and visceral adipose tissue EVs, with concentrations of IL-6, MIF, and MCP-1 significantly higher in visceral adipose tissue EVs compared to those from subcutaneous adipose tissue (Kranendonk et al. 2014a)

1.2.5.2 Functional effects

The study conducted by Kranenedock *et al.*, (2014) established a paracrine signalling crosstalk between adipocytes and macrophages. Explant adipose tissue from subcutaneous and visceral depots as well as SGBS-derived adipocytes secreted EVs with immunomodulatory effects, promoting the differentiation of primary monocytes into macrophages of pro-inflammatory (M1) and anti-inflammatory (M2) phenotype. Adiponectin-positive EVs were much more effective than adiponectin-negative EVs in effecting monocyte transformation into macrophages, as were EVs derived from visceral rather than subcutaneous tissue explants (Mariette E G Kranendonk et al. 2014). The differentiation of monocytes into pro-inflammatory macrophages contributes to AT inflammation (Xu et al. 2003b). Human adipocytes, both *in vitro* and *ex vivo*, secrete EVs with immunomodulatory properties, which can cause the development of local insulin resistance (IR), a key element in the mechanistic link between obesity and adverse metabolic complications (Dandona et al. 2004). Monocytes, in contrast to other immune cells, actively consumed AT-EVs, as observed when injected into mice; these then differentiated into macrophages secreting TNF α and IL-6 (Deng et al. 2009). Wild-type mice developed IR when injected with exosome-like vesicles containing high RBP-4 content produced by ob/ob mice; however, this response was less marked in TLR4 knockout mice. Taken together,

these data provide evidence that EVs produced by adipocytes may communicate with immune cells and influence whole body IR. Stimulated macrophages impair insulin signalling in adipose tissue, hence one can postulate that adipose tissue inflammation can secrete ADEVs to mediate/aggravate the development of IR (Olefsky and Glass 2010). A further study demonstrated that differentiated 3T3-L1 adipocytes, when stressed by exposure to palmitic acid produced microparticles which could act as chemo-attractants for monocytes and primary macrophages (Eguchi et al. 2016). When hepatocyte cells were incubated with subcutaneous and visceral ADEVs, there was a negative association between Akt signalling and glucose-6-phosphatase gene expression (Kranendonk et al. 2014a). Exosomes isolated from visceral AT were found to integrate into HepG2 cells and hepatic stellate cell lines, induce metabolic disruption in TGF β signalling pathways and dysfunctional extracellular matrix regulation in HepG2 cells, as indicated by genetic profiling (Koeck et al. 2014). The researchers hypothesised that these changes may induce liver fibrosis and may link obesity to non-alcoholic fatty liver disease. Our study group under Dr Wadey, demonstrated that inflamed and hypoxic adipocytes released characteristic EVs that promote endothelial dysfunction by enhancing the leukocyte attachment on the endothelial surface (Wadey et al. 2019). This was also supported by a study that observed an exchange of EV particles between endothelial cells and adipocytes within the adipose tissue that regulated the metabolic state of the tissue (Crewe et al. 2018). EV release from adipocytes is also governed by the systemic nutrient state.

The tumour microenvironment can harbour adipocytes and promote tumour progression (Dirat et al. 2010). Obesity is a risk factor for melanoma and its malignant progression, where a correlation between adipose tissue exosome shedding and donor BMI was demonstrated after isolation from subcutaneous adipose depot (Lazar et al. 2016). When used at equal concentrations, exosomes from overweight and obese donors increased melanoma migration more than exosomes from lean individuals. This effect was thought to be mediated via fatty acid oxidation as the effect was reversed by inhibition by etomoxir. Interestingly, mass spectrometry analysis of 3T3-F442A derived exosomes showed an abundance of proteins involved in lipid metabolism, particularly those involved in fatty acid oxidation (Gao et al. 2017).

ADEVs mediate local cell–cell communication within adipose tissue as observed by a series of studies conducted by Muller and his team (Müller 2011). Secretion of CD73-

bearing EVs from adipocytes was induced using lipogenic stimuli (e.g. palmitate, the antidiabetic sulfonylurea drug glimepiride, phosphoinositolglycans (PIG), and H₂O₂). Upon incubation of these CD73-bearing EVs with adipocytes, the recipient cells imbibed CD73 which was translocated into cytoplasmic lipid droplets and consequently up-regulated esterification (Müller et al. 2011b). Interestingly, the large adipocytes showed greater efficacy in releasing CD73 into the microvesicles and lower affinity in translocating the CD73 into lipid droplets as compared to the small adipocytes. These EVs held transcripts and miRNAs involved in upregulation of lipogenesis (e.g., diacylglycerol acyltransferase-2) and lipid droplet assembly (e.g., caveolin-1 and perilipin-A) and, when applied to adipocytes in culture, had a greater effect on small than on large adipocytes. This secretion and translocation of CD73 predominantly from large to small adipocytes could be a model of cell- to- cell interaction mediated by EVs. The regulation (and dysregulation) of adipocyte size and lipid droplet assembly is a likely key determinant of adipose and metabolic health (Virtue and Vidal-Puig 2008). Further exploration of this exchange between adipocytes may help contribute to our understanding of how hyperplasia and hypertrophy is regulated within calorically challenged adipose tissue (Müller 2011).

1.3 Obesity and Cardiovascular disease

1.3.1 Vascular Endothelium

The vascular endothelium is an organ lining the entire circulatory system. It acts as a selectively permeable barrier between extravascular and intravascular compartments. It carries out important functions in providing a non-thrombogenic lining, regulating vascular tone, molecular exchange between blood and tissue compartments, immune signal regulation, inflammation and haemostasis. The endothelium releases a repertoire of coagulation inhibitors as well as prothrombotic molecules according to different condition in the body and includes tissue factor pathway inhibitor (TFPI), thrombomodulin, heparin-like proteoglycans, and endothelial cell protein C receptor. Anticoagulant substances including prostaglandin I₂ (PGI₂), nitric oxide, and ectonucleotidase CD39/NTPDase1 are also produced by the intact endothelium. As thrombomodulin binds to thrombin, it activates protein C and along with protein S inactivates clotting factors Va and VIIIa. Heparin cofactor II (HCII) and antithrombin found in the circulation bind to heparin proteoglycan on the normal vascular endothelial glycocalyx that inhibit thrombin. Platelet adhesion is controlled at the endothelial surface by secretion of a disintegrin and metalloprotease with a thrombospondin type 1 motif member 13 that cleaves large von Willebrand factor multimers that also play a role in blood haemostasis. Thus, an intact healthy vascular endothelium is a powerful regulator of the dynamic haemostatic system (Nguyen and Coull 2017).

The endothelium releases various vasoactive factors that are vasodilatory or vasoconstrictive in function. Vasodilators include nitric oxide (NO), prostacyclin (PGI₂) and endothelium derived hyperpolarizing factor (EDHF) whereas thromboxane (TXA₂) and endothelin-1 (ET-1) are vasoconstrictors. Basal vasodilator tone of the blood vessels is maintained by NO. Endothelial NOS (eNOS) produces nitric oxide in the vasculature from the amino acid L- arginine. The production of NO is regulated by the levels of intracellular Ca²⁺ in the endoplasmic reticulum as well as the influx of Ca²⁺ into the cell from extracellular stores (Fleming and Busse 1999; Moncada and Higgs 2006). NO production is increased due to shear stress as well as when blood-borne agonists attach to endothelial cell receptors and increase intracellular Ca²⁺ that

results from increased blood flow in the vessel (Tran et al. 2000). NO can diffuse across the endothelial cell into the adjacent smooth muscle to stimulate production of cyclic guanosine-3', 5-monophosphate (cGMP) that eases muscle tension (Jones et al. 1999). Besides vasodilatation, NO is also involved in preventing platelet activation and leukocyte adhesion to the vessel wall (Kubes et al. 2006).

The vascular function is also regulated by synergistic actions of two prostanoids, prostacyclin (PGI₂) and thromboxane (TXA₂). Cyclooxygenase (COX) enzymes are the primary enzymes involved in their production. While COX-1 is continuously expressed on endothelial cells, COX-2 is activated when the endothelium is exposed to damage and inflammatory cytokines (Flavahan 2007). COX-2 along with prostacyclin synthase catalyses the conversion of arachidonic acid to PGI₂. PGI₂ binds to the prostacyclin receptors (IP) found on platelets and smooth muscle cells. In platelets, the receptor binding inhibits platelet aggregation meanwhile binding to the smooth muscle cell IP receptor directs the synthesis of cAMP which allows relaxation of the smooth muscle (Corsini et al. 1987; Sandoo et al. 2015). In contrast, COX-1 synthesises TXA₂ from arachidonic acid by thromboxane synthase. TXA₂ causes platelet aggregation and vasoconstriction in smooth muscle cells with increasing intracellular Ca²⁺ levels in the smooth muscle (Thomas et al. 1998). Thus, the homeostasis in the healthy vessel is maintained by the balance in the activity of PGI₂ and TXA₂.

Endothelial cells also release a vasoconstrictor, endothelin-1 (ET-1). Receptors for ET-1 have been identified both on smooth muscle cells (ETA and ET-B2) and endothelial cells (ET-B1) (Alonso and Radomski 2003). Inflammatory mediators such as interleukins and TNF- α cause an increased production and release of ET-1 and decreased by NO and PGI₂. On smooth muscle, ET-1 opens Ca²⁺ channels and allows extracellular Ca²⁺ into the cell, causing vasoconstriction. Activation of ET-B1 receptors on the endothelium induces the release of NO and PGI₂, causes vasodilatation (Cardillo et al. 2000). In totality, the endothelium forms an important part of the vasculature and promotes an atheroprotective environment by the balanced production of endothelial cell-derived vasoactive factors.

1.3.2 Endothelial Dysfunction

Dysfunction in the health of the vascular endothelium contributes to the pathogenesis of a broad spectrum of vascular disease that includes CVD, atherosclerosis, stroke, diabetes, insulin resistance, chronic kidney failure, thrombosis, tumour growth and viral diseases. A host of risk factors and lifestyle choices subjects an individual to endothelial dysfunction (ED). Family history of CVD (genetics), obesity, ageing, smoking, mental stress, hypertriglyceridemia, elevated LDL and reduced HDL cholesterol, patients with insulin resistance, hypertension, etc. are some of the broad classes of risks (Hadi et al. 2005; Huang et al. 2012). The progression of the ED hinges on the intensity and extent of proven risk factors and total risk of the individual subject.

An imbalance in the NO production or metabolism leads to a dysfunctional endothelium. Under these conditions, cytokines are activated that increase the permeability of the vessel lining to lipoproteins, immune cells and inflammatory mediators as well as increase in platelet activation and leukocyte adhesion. This leads to a structural damage of the endothelium and smooth muscle proliferation that develops into atherosclerotic plaque.

Hyperglycaemia induces intracellular changes in the redox state depleting the cellular NADPH pool and increasing non-enzymatic glycation of proteins and macromolecules. Diabetes has been associated with overexpression of growth factors advancing neovascularisation, the proliferation of endothelial cells and vascular smooth muscle (Calles-Escandon and Cipolla 2001). The diabetic state is characterised by an increased oxidative stress and high levels of oxidised lipoproteins (low-density lipoprotein) and fatty acids. Consequently, escalating prothrombotic tendency and platelet aggregation. The pro-inflammatory cytokine TNF- α plays a critical role and provides a link between diabetes, insulin resistance and endothelial dysfunction (Hadi et al. 2005). *In vitro* studies have demonstrated that endothelial cells in a diabetic environment exhibit a diminished capacity of NOS to generate NO (Hattori et al. 1991; Avogaro et al. 1999; Salvolini et al. 1999). Individuals with insulin resistance resulting from obesity exhibit impaired vasodilation with high levels of ET-1 in plasma (Steinberg et al. 1994; Ferri et al. 1997).

Cholesterol is one of the well-established risk factors for premature coronary artery disease (Kjelsberg 1982). High levels of cholesterol (hypercholesterolaemia) confers

impaired endothelium-dependent vasodilation (Steinberg et al. 1997). Studies have concluded that cholesterol levels even in the normal range can induce endothelial dysfunction and impaired vasodilation. The lipotoxicity is mediated through oxidative stress and proinflammatory responses, and effects are magnified in patients with obesity, metabolic syndrome, and diabetes (Steinberg et al. 1996; Berg and Scherer 2005). Interventions that reduced lipid load in plasma ameliorate endothelial dysfunction and significantly modify metabolic and CV risk

The pathogenic effect of obesity in ED and vascular disease are the culmination of several metabolic syndromes (insulin resistance, dyslipidaemia, hyperoxidative stress, and hypertension) on the biology of endothelium-derived NO. A state of increased oxidative stress is expressed by non-adipocyte tissue (muscles, liver and pancreatic β -cells) by means of elevated cytosolic triglyceride (Bakker et al. 2000). It is accompanied by high concentrations of cytosolic long-chain acyl-CoA esters that stimulate production of mitochondrial oxygen free radicals. Likewise, enhanced production of oxygen free radicals in endothelial cells, or vascular smooth muscle cells, leads to the increased sub-endothelial oxidation of LDL and atherosclerosis, a factor in endothelial breakdown. Chronic inflammatory state of the adipose tissue during obesity, dysregulation in the endocrine and paracrine actions of adipokines, NO bioavailability, insulin resistance and oxidised LDL, disrupt vascular homeostasis and contribute to endothelial dysfunction (Iantorno et al. 2014; Engin 2017).

1.3.3 Endothelial Dysfunction and Atherogenesis

Atherosclerosis is a disease condition of the vascular intima characterised by the formation of intimal plaques as a result of hyperlipidaemia and lipid oxidation. The term, atherosclerosis is of Greek origin and can be broken into two parts; atherosis referring to accumulation of fat accompanied by several macrophages and sclerosis indicating a fibrosis layer comprising smooth muscle cells [SMC], leukocyte, and connective tissue. The pathogenesis of atherosclerosis begins with the appearance of fatty deposits called atheromatous plaques in the intimal layer of the arteries. The plaque grows with the continuous deposition of cholesterol crystals coupled with the proliferation of fibrous tissues and the surrounding smooth muscle cells, pushing the plaque towards the lumen of arteries and consequently restricts the blood flow. Subsequently, hardening of the arteries or sclerosis ensues with connective tissue production by fibroblasts and deposition of calcium in the lesion. Finally, the irregular surface within the arteries results in clot formation and thrombosis, which leads to the sudden obstruction of blood flow (Rafieian-Kopaei et al. 2014, Falk, 2006). Endothelium is considered to be the stimulus for the migration of leukocytes, classifying atherosclerosis as an inflammatory disease. Immune and inflammatory systems act in tandem for a sequential development of the atherosclerotic lesion. Leukocyte migration is resolved as a combined consequence of the inflammatory response as well as accumulation and modification of the lipoproteins.

A study conducted by Ganz and colleagues, using coronary angiography demonstrated the clinical relevance of NO in atherosclerotic cardiovascular disease (Ludmer et al. 1986). The arteries of individuals with advanced stenosis showed dose-dependent vasoconstriction in response to acetylcholine while individuals with normal coronary arteries recorded dose-dependent vasodilation to acetylcholine. Hypercholesterolemia has been established to impair endothelium-dependent vasodilation as documented in animal models of atherosclerosis (Freiman et al. 1986; D'Uscio et al. 2001). Hampering the production or bioavailability of endothelial NO precedes the formation of clinically significant atherosclerotic lesions.

The key stages in the progression of atherogenesis include (i) initiation of atherosclerotic plaque by low density lipoprotein-cholesterol (LDL-C) trapping, activation of endothelial cells, role of immune cells and leukocyte attachment,

formation of foam cells, (ii) progression of the plaque by smooth muscle cell migration and extracellular matrix deposition and finally the (iii) plaque rupture.

Fatty streak formation marks the beginning of the atherosclerotic process, characterised by the focal increase in the lipoproteins at the lesion of the intimal layer of the arteries. Lipoproteins particularly, cholesterol-rich low-density lipoprotein (LDL), are the central particles involved in atherogenesis. When the equilibrium between the plasma LDL and intracellular LDL concentration is disturbed, LDL particles become trapped in the intima encouraged by the extracellular proteoglycans. It begins to accumulate in the vascular intima either by adhering to the proteoglycan component of the extracellular matrix or by permeating into the endothelium. This delays the process of exiting from the intima leading to their accelerated accumulation (Rafieian-Kopaei et al. 2014) and leads to spontaneous oxidation and cell oxidation of the trapped particles (Tavafi 2013).

This stage of early atherosclerosis also sees the infiltration of monocytes and T-lymphocytes into the vascular intima. The oxidised LDL also acts as an antigen for T-cells causing its activation to secrete cytokines. These cytokines activate the macrophages that leads to further activation of the endothelial and smooth muscle cells. The oxidised lipids (oxidised LDL) and cytokines cause monocyte-to-macrophage differentiation to form damaging foam cells.

Oxidised LDL stimulates the vascular endothelial cells to synthesise a chemoattractant cytokine, monocyte chemokine protein (MCP-1). MCP-1 initiates monocyte recruitment to the arterial wall and is believed to amplify the recruitment and formation of macrophages (Molestina et al. 2000; Romano et al. 2000). Leukocyte recruitment to the site of lesion is also augmented by the expression of the adhesion molecules VCAM-1 (Vascular cell adhesion molecule-1), ICAM-1 (Intercellular Adhesion Molecule-1) and P-selectin on the surface of the arterial endothelial cells (Langer and Chavakis 2009). Cytokines IL-1 and TNF- α also induce the expression of the adhesion molecules (VCAM and ICAM) on the endothelial surface. In patients with peripheral ischaemic arterial disease, the plasma harbours the soluble form of VCAM-1, ICAM-1 and E-selectin and serves as mediators of angiogenesis (Hwang et al. 1997; Blann et al. 1999). These adhesion molecules allow cell to cell adherence in addition to binding other extracellular matrix molecules. Elevated endothelial ICAM-1 expression

promotes fibrinogen deposition and monocyte attachment, followed by subendothelial migration, a crucial event in the pathogenesis of atherosclerotic lesions (Engin 2017). Yet another inducer of MCP-1 and ICAM-1 are platelets. The transcription of genes involved in the elaboration of MCP-1 and ICAM-1 is regulated by the transcription factor, NF- κ B and its activation is affected by cytokine IL-1. This promotes the development of atherogenesis by venture of monocyte chemotaxis, adhesion and transmigration into the intima of the arterial wall (Gawaz et al. 2000). Certain chemokines are released during this stage that have a pivotal role in leukocyte activation and migration, as well as causing endothelial and smooth muscle cells to migrate. The macrophages produce a considerable amount of MCP-1 and causes monocytes to move toward the vascular walls and infiltrates them into the lesion, thus inflating the endothelial dysfunction (Aiello et al. 1999). Studies have also supported that oxidised LDL can up-regulate the expression of adhesion molecules (Erl et al. 1998).

In an effort to clear the LDLs, monocyte turned macrophages phagocytose the accumulated oxidised LDL by their scavenger receptors and convert to foam cells. During differentiation of monocytes to macrophages, the expression of these receptors increases. Accumulation of these yellow foam cells on the arterial walls form the lipid streaks. Some foam cells in the developing intimal lesion undergo apoptosis and this lipid rich necrosing hub becomes the centre of more developed atherosclerotic plaque (Suzuki et al. 1997; Singh et al. 2002). In patients with familial hypercholesterolaemia, an abundance of arterial lesions and multiple xanthomata containing foam cell-rich lesions were observed and this was attributed to the lack of the LDL receptors (Holven et al. 2003). The leaking monocytes release cytotoxic factors such as TNF- α , growth factors, pre-coagulation substances (including tissue factors), and free radicals, which further injure endothelium and propagate more LDL oxidation, leading to more metabolic dysfunction

At the site of a lesion, adjacent endothelial cells and smooth muscle cells secrete inflammatory cytokines IL-1, and TNF- α which severely damages the vascular tissue. The balance between inflammatory and reparative processes relate to the stability of an atherosclerotic lesion or plaque. The dynamics of this balance relies on the vascular smooth muscle cells that undergo migration, proliferation and phenotypic modulation under the effect of cytokines, metalloproteinases, growth factors and matrix proteins.

Eventually, the smooth muscle cells migrate towards the luminal side of the vessel wall and synthesised matrix deposition forms a fibrous cap. The cap is composed of collagen-rich fibre tissues, SMC, macrophages and T lymphocytes and forms the mature atherosclerosis plaque that bulge into the lumen and reduces the blood stream in the vessels (Steinbrecher et al. 1984; Singh et al. 2002; Libby 2012).

A thick fibrous cap lends stability to the plaque by reducing the tensile stress and obstructing contact between the lipid-rich necrotic core and the blood. The lipid core in the plaque is thrombogenic in nature. On the contrary, a thin cap is predisposed to rupture while experiencing a tensile stress. Macrophages and T lymphocytes found at the borders of developed plaque contribute to the lysis of extracellular matrix and prevent the collagen synthesis in the SMC. This can weaken and break the fibrous cap (Libby and Aikawa 1998). With the passage of time, the reparative character of smooth muscle cells is lost and onsets early apoptosis, thereby increasing the chances of plaque rupture. Rupture of the fibrous the cap releases collagen and lipids to the blood stream which contributes to accumulation and adhesion of platelets and blood clot formation. These clog the circulation and have detrimental effects to the health of the individual.

Atherosclerosis is a complex disease involving the cardiovascular system, the inflammatory and immune systems, LDL handling mechanisms and thrombotic mechanisms. Deep understanding about the pathogenesis of atherosclerosis will help outline the causes and contribute to the improvement of therapeutic and management options. Biological integrity of the endothelium is crucial to maintain vascular homeostasis and prevent atherosclerosis.

1.3.4 Obesity and Atherosclerosis

Obesity is a well-established risk factor for development of cardiovascular disease. A multitude of factors have been proposed to link obesity with vascular diseases, especially atherosclerosis. The adipose tissue being an endocrine organ releases a host of adipokines that modulate the atherogenic environment of the arterial wall. As studies indicate, as the adipose tissue mass increases, the serum levels of adipokines are either elevated or dysregulated during obesity.

Adiponectin promotes oxidation of fatty acids, regulates insulin sensitivity and lowers plasma glucose levels. Hypoadiponectinaemia has been marked as an independent risk factor for type 2 diabetes and cardiovascular syndromes (Choi et al. 2004; Ouchi et al. 2006). The anti-inflammatory and antiatherogenic property of adiponectin was demonstrated when it suppressed the transcription of NF- κ B to induce TNF- α as well as arresting the TNF- α induced expression of adhesion molecules on endothelial cells (Ouchi et al. 2000). The cardio-protective role was also reported when serum adiponectin levels had a significant negative correlation with vascular inflammation (Choi et al. 2011). It is to be noted that adiponectin levels in plasma are inversely associated with obesity and its effects are markedly decreased during atherosclerosis (Kawano and Arora 2009).

The adipokine resistin showed a possible link between obesity and insulin resistance in rodents; however, in humans, inflammatory cells primarily express resistin and have been implicated in obesity-related subclinical inflammation and atherosclerosis (Steppan et al. 2001; Filková et al. 2009). Resistin induced the expression of adhesion molecules, such as VCAM-1 and ICAM-1 in vascular endothelial cells, meanwhile adiponectin controlled the effect of resistin in vascular endothelial cells (Kawanami et al. 2004). Lee *et al.*, (2009) observed that resistin mediated the dysregulation of scavenger receptors in macrophages that encouraged lipid accumulation and foam cell formation (Lee et al. 2009). A study by Choi *et al.*, (2011) showed a positive correlation between vascular inflammation and serum resistin levels, thus providing a linkage of obesity, inflammation, and atherosclerosis (Choi et al. 2011).

Adipocyte fatty acid binding proteins (FABPs) are synthesised in the cytoplasm and secreted into serum to control the distribution of fatty acids in various inflammatory responses and metabolic pathways (Xu et al. 2006). In prospective studies, the

development of metabolic syndrome and type 2 diabetes has been associated with circulating FABPs independent of adiposity (Xu et al. 2007). Studies through animal models have reported FABPs as a major mediator of vulnerable plaque formation whereas apoE^{-/-} mice (null for FABP) have higher survival rates due to increased stability of atherosclerotic plaques (Boord et al. 2004). Macrophages of FABP^{-/-} character significantly decreased intracellular LDL accumulation and production of inflammatory cytokines, such as TNF- α , MCP-1, and IL-6 was suppressed, compared with wild-type controls (Makowski et al. 2001). Circulating serum levels of FABPs were elevated as the number of stenotic coronary arteries increased, thus closely related to the progression of atherosclerosis (Rhee et al. 2009). Moreover, FABP4 was found in substantial amount within the atherosclerotic lesions, risking cardiovascular events (Peeters et al. 2011). Thus, this fat protein crosslinks adiposity and endothelial dysfunction through inflammation.

Omentin is an adipokine with roles in improving insulin sensitivity. Omentin hosts a positive role in energy homeostasis while being negatively correlated with metabolic risk factors, including obesity and hyperglycaemia (Yang et al. 2006). In endothelial cells, omentin significantly attenuated C-reactive protein and TNF- α -induced NF κ B and abated arterial calcification in OPG^{-/-} mice, indicating that omentin-1 might play a beneficial anti-inflammatory role in protecting the arterial wall (Tan et al. 2010; Yamawaki et al. 2011). Omentin-1 isolated from visceral adipose tissue has been found to contribute independently to endothelial dysfunction (Moreno-Navarrete et al. 2011).

Chemerin is expressed by adipocytes and their circulating levels are significantly higher in obese subjects. Loss of chemerin expression worsened adipogenesis in 3T3-L1 cells, and diminished the expression of genes involved in glucose and lipid metabolism (Goralski et al. 2007). In a clinical study conducted by Sell et al., patients having undergone bariatric surgery had their serum chemerin levels significantly reduced after surgery, suggesting that chemerin might mediate the metabolic alterations during obesity (Sell et al. 2009; Sell et al. 2010). They also reported that chemerin activated the NF κ B pathway and impaired glucose uptake in primary human skeletal muscle cells. Separate studies have proposed that chemerin might affect early atherosclerotic plaque development by stimulating macrophage adhesion to endothelial cells and up-regulation of chemerin receptor 1 in human endothelial cells by pro-inflammatory cytokines (TNF- α , IL-1 β , and IL-6)(Hart and Greaves 2010;

Kaur et al. 2010). With reference to its role in the atherosclerotic process, circulating chemerin level was found to be associated with atherosclerotic plaque burden and arterial stiffness (Kim et al. 2011). In totality, research studies have provided a novel link between obesity and arteriosclerosis through AT-released adipokines.

Impaired autophagy is another contributing factor to atherosclerosis that progresses from obesity. Identifying autophagosomes in the atherosclerotic plaque, initiated the idea that macrophage autophagy might be beneficial in limiting atherosclerosis (Martinet and De Meyer 2009). A study conducted by Razani et al., (2012) used Atg5-macrophage knockout mice to test if autophagy contributed to progression of atherosclerosis (Razani et al. 2012). Deficiency of macrophage autophagy induced a state of inflammation and increased plaques. In addition, there was a surge in cholesterol crystals in Atg5-m ϕ KO plaques and inflammasome activation, suggesting dysfunctional autophagy is characteristic of atherosclerosis. Atg7 is an essential autophagy gene. Furthermore, when mice with global haploinsufficiency of Atg7 (Atg7^{+/-} mice) were crossed with ob/ob mice, metabolic syndromes were absent however, exacerbated insulin resistance with increased lipid content and inflammatory changes were observed. These results suggest that systemic autophagy haploinsufficiency impairs the adaptive response to metabolic stress, and that aids in the progression of a pro-atherogenic state (Lim et al. 2014).

With obesity, the AT undergoes alterations in its systemic metabolism. A state of local inflammation arises by the secretion of proinflammatory factors (TNF- α , IL-6) by the accumulating macrophages; higher in obese individuals as compared to lean (Fried et al. 1998; Weisberg et al. 2003). Influx of macrophages and subsequent local inflammation are believed to result in endothelial dysfunction that follows obesity, including systemic inflammation and atherosclerosis. Visceral fat is credited with more cytokines than subcutaneous AT. Transplantation of visceral AT from genetically obese mice into *ApoE*-deficient mice accelerates atherosclerosis in the recipient animals, suggesting that inflamed adipose tissue triggers vascular effects, presumably through inflammatory cells such as macrophages resident within the visceral AT (Rodriguez et al. 2007; Öhman et al. 2008).

In vitro and clinical studies have confirmed endothelial dysfunction in obesity (Karaca et al. 2014). Decreased expression of eNOS leads to limited production and availability

of NO. Obese patients have elevated levels of dimethylarginine (ADMA) which serves as a stoichiometric inhibitor of eNOS, thus reducing the bioavailability of NO (Krzyzanowska et al. 2004; Sansbury et al. 2012). Alterations in endothelium derived prostacyclin and thromboxane has also been reported in obesity, and is conceived to promote the development of vascular disease, hypertension and thrombosis (Traupe et al. 2002). Endothelial expressed vasoconstrictor ET-1 is found in raised levels in obese individuals. ET-1-mediated vasoconstriction therefore promotes hypertension, atherosclerosis, and thrombosis, in addition to augmented leukocyte and platelet activation; prothrombotic and proatherogenic conditions, commonly observed in obese patients (Van Guilder et al. 2011; Cecala, 1995). Clinical studies have advocated that obese patients see a progressive decline in vascular functions characterised by impaired endothelium-dependent relaxation and marked endothelial dysfunction on macrovascular and microvascular beds as a result of oxidative stress along with reduced NO reach (Steinberg et al. 1996; Perticone et al. 2001; Grassi et al. 2010).

Therefore, to sum up, obesity pre-disposes an individual to a risk of developing CVD. However, it is impractical to indicate a single mechanistic contribution but should be defined by the culmination of several metabolic alterations including changes in adipokine profile in AT, impaired autophagy, systemic inflammation, and endothelial dysfunction. The central mechanism is inflammation and signalling via the NLRP3 inflammasome, that ties all the factors together.

1.3.4 Role of EVs in atherosclerosis

Obesity and CVDs have been associated with increased levels of EVs in the circulation (Eguchi et al. 2016). A clinical study involving morbidly obese subjects, has reported significant elevation in EVs derived from platelets, endothelium and erythrocytes. Moreover, these EVs have been found to contain increased levels of FABP4, TNF- α and interferon- γ , suggesting a likely role for EVs in the development of CVDs (Witczak et al. 2017). Cell activation and risk of thrombotic complications have also been observed with the circulating EVs in obese populations (Goichot et al. 2006). The secreted EVs comes in direct contact with vessel wall and give rise to inflammation and activation of endothelial cells, which further cause a steep increase in the release of EVs from cells.

EVs are a risk factor for the development of obesity-associated CVDs while mediating endothelial dysfunction. EVs collected from adipose tissue explants can alter the TGF- β signalling pathways, disrupting the inflammatory regulation (Ferrante et al. 2015). AT-derived EVs could potentially impair insulin signalling as concluded from an *in vitro* study (Kranendonk et al. 2014b) as well as induce a pro-inflammatory state characterised by higher TNF- α and IL-6, glucose intolerance, and insulin resistance (Deng et al. 2009). Uptake of AT-derived EVs by mononuclear cells induces activation towards a M1-phenotype macrophage (Eguchi et al. 2015). The increase in lipid accumulation within AT results in generation of M1 macrophages. Activated macrophages can further elicit infiltration of leukocytes into the tissue and evokes inflammation and insulin resistance, as seen in lean mice (Deng et al., 2009; Eguchi et al., 2015). Collectively, these phenomena accounts for obesity-related vascular dysfunction. In addition, a study has demonstrated platelet -EVs were able to alter gene expression in HUVECs through their miRNA cargo.

EVs also play a role in microcalcification, a process involved in the pathogenesis of atherosclerosis whereby, the protein sortilin, a key regulator of smooth muscle cell calcification, was packaged and delivered by EVs (Goettsch et al. 2016). Moreover, macrophage-derived EVs exhibited high calcification and aggregation potential, providing an alternative mechanism for microcalcification in atherosclerotic plaques (New et al. 2013). Leukocyte-derived EVs have also been implicated in the pathogenesis of atherosclerosis (Chironi et al. 2006). In an extensive study by Amabile

et al. (2014), several cardiometabolic risk factors including higher triglyceride levels and hypertension, were correlated with endothelial-derived EVs in the circulation (Amabile et al. 2014). Individuals subject to cardiovascular risk had EVs sourced from smooth muscle cells and hematopoietic cells that were clear predictors of CVD (Chiva-Blanch et al. 2016).

1.4 Thesis aims and objectives

1.4.1 Hypothesis

Adipocytes release EVs that bear proteins that relate to their cell of origin as well as reflect the physiological state of cell. In obese conditions, where the AT is hypoxic and inflamed, the released EVs have altered protein profile compared to those EVs secreted from healthy AT, which could render them pathological mediators of endothelial dysfunction and contribute to risk events related to cardio-vascular disease. In essence, ADEVs could be potential biomarkers of AT health.

1.4.2 Overall aim

To establish if adipocyte-derived EVs exists in human circulation and mediate in the pathogenesis of obesity-associated diseases.

1.4.3 Specific objectives

- To gain insight into EV processing techniques and develop an approach to optimally isolate an EV population from human plasma.
- To identify a population within plasma-derived EVs selective for adipocyte character.
- To examine pathologically relevant effects of circulating ADEVs obtained from healthy and obese subjects, using leukocyte attachment to endothelium as a model for atherosclerosis.

2. Methods

2.1 3T3-L1 cell culture

2.1.1 Cell Culture and cell counting

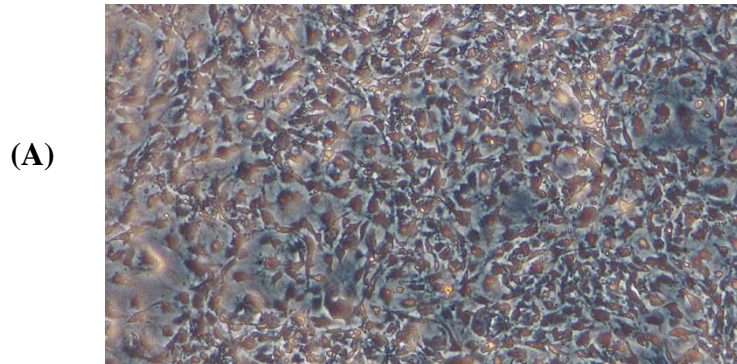
The murine fibroblast cell line 3T3-L1 was grown from pre-adipocyte to a mature adipocyte stage through induced differentiation within a span of 14 days. The cells were cultured in appropriate media namely control media (CM), differentiation media (DM) and maintenance media (MM), containing inducers of adipogenesis, specific to their stage of differentiation and detailed in **Table 2.1**.

Media Component	CM (per 100ml of media)	DM (per 100ml of media)	MM (per 100ml of media)
DMEM (high glucose 4.5 g/L)	45 ml	45 ml	45 ml
Ham's F12 nutrient mix	45 ml	45 ml	45 ml
FCS	10 ml	10 ml	10 ml
Penicillin/Streptomycin	1 ml	1 ml	1 ml
Insulin	-	100 µl (10 µg/ml)	100 µl (10 µg/ml)
Indomethacin	-	100 µl (50 µM)	-
Dexamethasone	-	10 µl (1 µM)	-

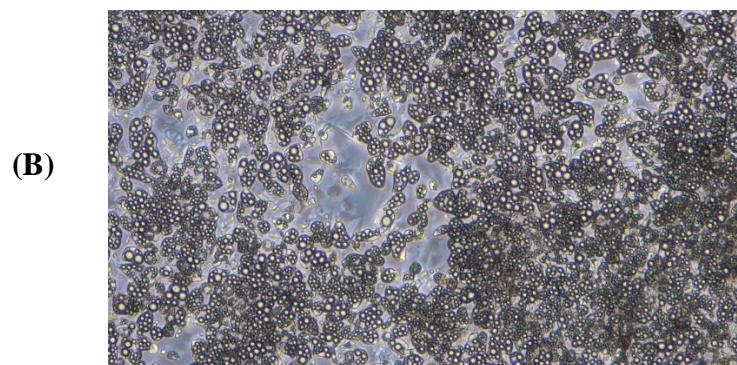
Table 2.1: Media used in the culture of 3T3-L1. Compositions of media used throughout 3T3-L1 experiments. CM = control medium; DM = differentiation medium; DMEM = Dulbecco's Modified Eagle Medium; FCS = foetal calf serum; MM = maintenance medium

As the pre-adipocyte (fibroblasts) cell culture attained confluency, the control media were replaced by differentiation media to induce differentiation and marked Day 0. On Day 2 through to Day 14, the maintenance media was used for the maturation of the adipocytes with a media change every 3 days (**Figure 2.2**). The cells used in this study were passaged less than 15 times. Images (5X) were obtained on Day 0 and Day 14 by inverted microscopy (Leica DM IL LED), **Figure 2.1**.

Confluent pre-adipocytes were trypsinised using 1X 0.05% Trypsin-EDTA (Life technologies) and spun at 1000 x g for 5 minutes to obtain a pellet which was re-suspended in 1ml of media. The cells were carefully divided for counting on a haemocytometer (Neubauer, 0.0025mm², 0.100 mm depth) and further passage.



Day 0 Pre-adipocytes



Day 14 Mature adipocytes

Figure 2.1 Microscopic images of 3T3-L1 on Day 0 and Day 14. (A) Confluent 3T3-L1 pre-adipocytes on Day 0, (B) following differentiation to mature adipocytes at the end of Day 14.

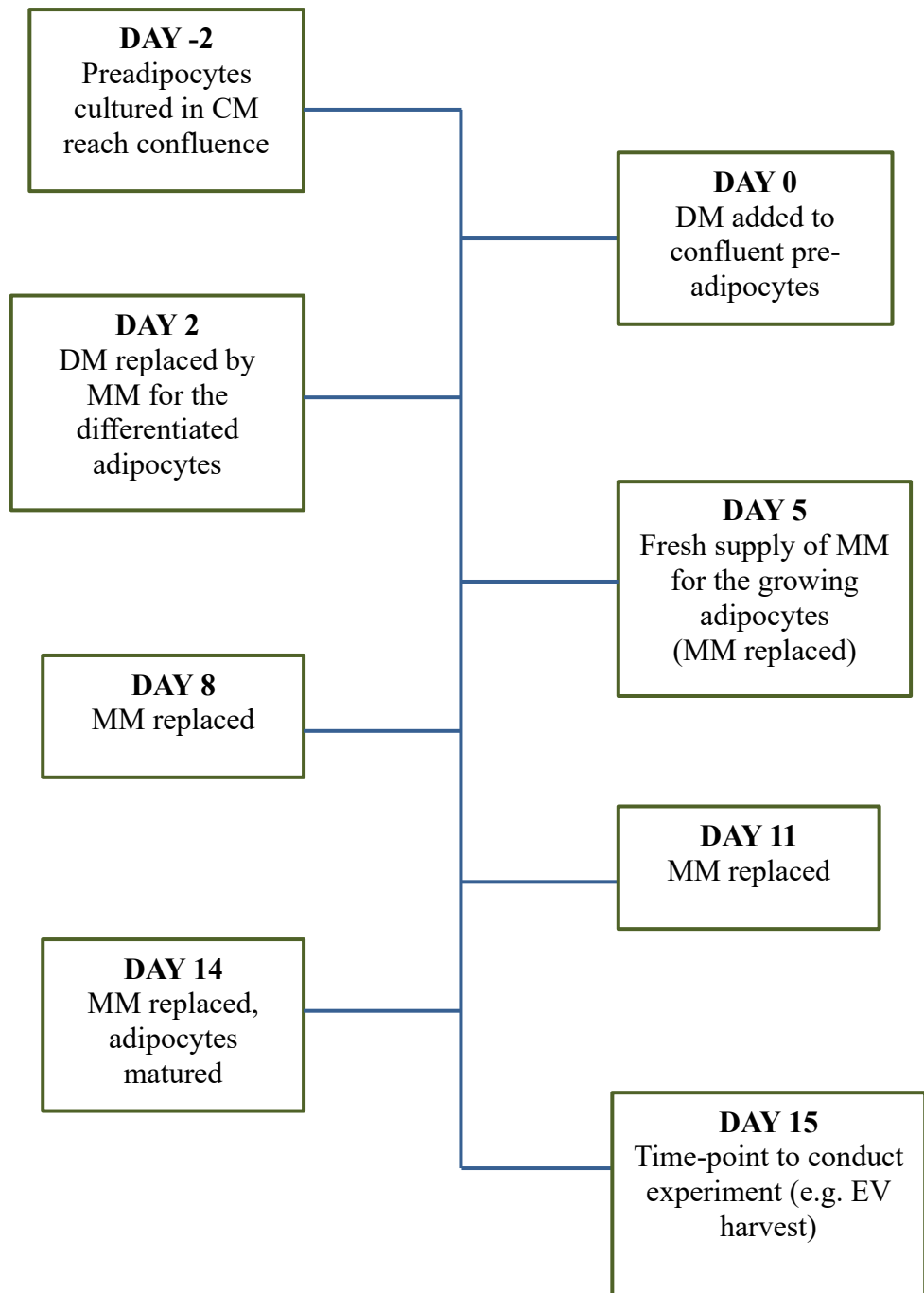


Figure 2.2 Representative Timeline for growth of 3T3-L1. Confluent pre-adipocytes have their media changed from CM to DM on Day 0 to facilitate differentiation and maintained in MM for 14 days until they grow into fully matured adipocytes (Day 14). On Day 15, cells or their growth media are subjected to experimental procedures. CM = control medium, DM = differentiation medium, MM = maintenance medium

2.1.2 Oil Red O-staining

The Oil red O working solution was freshly made from 0.5% oil red O stock solution (w/v in isopropanol) on diluting with dH₂O in a ratio of 3:2 (v/v). The solution was left at room temperature for 15 minutes and then filtered through Whatman filter paper to remove precipitates. 3T3-L1 cells cultured in 12-well plates were washed in sterile PBS prior to staining. They were then fixed in cold 4% formaldehyde (v/v in PBS) for 15 minutes at room temperature and washed with sterile PBS. Next, the cells were stained with the Oil Red O working solution for 15 minutes at room temperature. The excess stain was removed with 60% isopropanol (v/v in PBS) and washed twice with PBS before cells were imaged (Nikon Diaphot microscope, Nikon) at 10X magnification using ViewFinder™ software (version 3.0.1., Better Light Inc., USA). A volume of 100% isopropanol was used to extract the intracellular stain after the cells were washed twice with PBS and the optical density calculated at 490 nm (Multiskan EX, MTX Lab Systems, Inc., USA).

2.2 Extracellular Vesicle Isolation

2.2.1 Isolation of Extracellular vesicles from 3T3-L1 (Cell-derived EVs)

EV isolation was conducted as per ISEV criteria and as developed by senior researchers in our group (Lötvald et al. 2014; Connolly et al. 2015). Ideally, EVs were harvested on Day 15 as the adipocytes matured and the cells were incubated in serum-free media a day prior to isolating the EVs by differential ultracentrifugation. The conditioned media was first centrifuged at 1000 x g for 5 mins to remove floating/dead cells in suspension. Following this, the supernatant was centrifuged again at 15000 x g for 15 minutes at 4°C to remove the cell debris and larger vesicles. Finally, the supernatant was subjected to ultracentrifugation at 100,000 x g for 1 hr at 4°C to pellet the EVs. Sterile 1X PBS was used to re-suspend the pellet in 100ul volume per 25 ml of media spun (**Figure 2.3 (A)**). The EV samples were stored at 4°C and used within a week of isolation. This cell-derived EV preparation was referred as ‘crude prep’.

2.2.2 Isolation of EVs from human blood plasma (Plasma-derived EVs)

Following informed consent from healthy volunteers, blood was collected by venepuncture into sodium citrate vacutainers (BD Vacutainer® Citrate Tubes with 3.2% buffered sodium citrate solution) to process for plasma-derived EVs. Whole blood was immediately centrifuged at 2500 x g for 15 minutes at 21°C to collect the platelet-poor plasma (PPP). The PPP was spun again to obtain platelet-free plasma and then ultracentrifuged at 100,000 x g for 1 hr at 4°C to pellet the EVs, which were subsequently resuspended in 1X PBS for further experiments (**Figure 2.3 (B)**). EV samples were stored at 4°C and ideally used within 48 hrs. The ethics for the study was approved from Cardiff Metropolitan university with Project Reference no:7774.

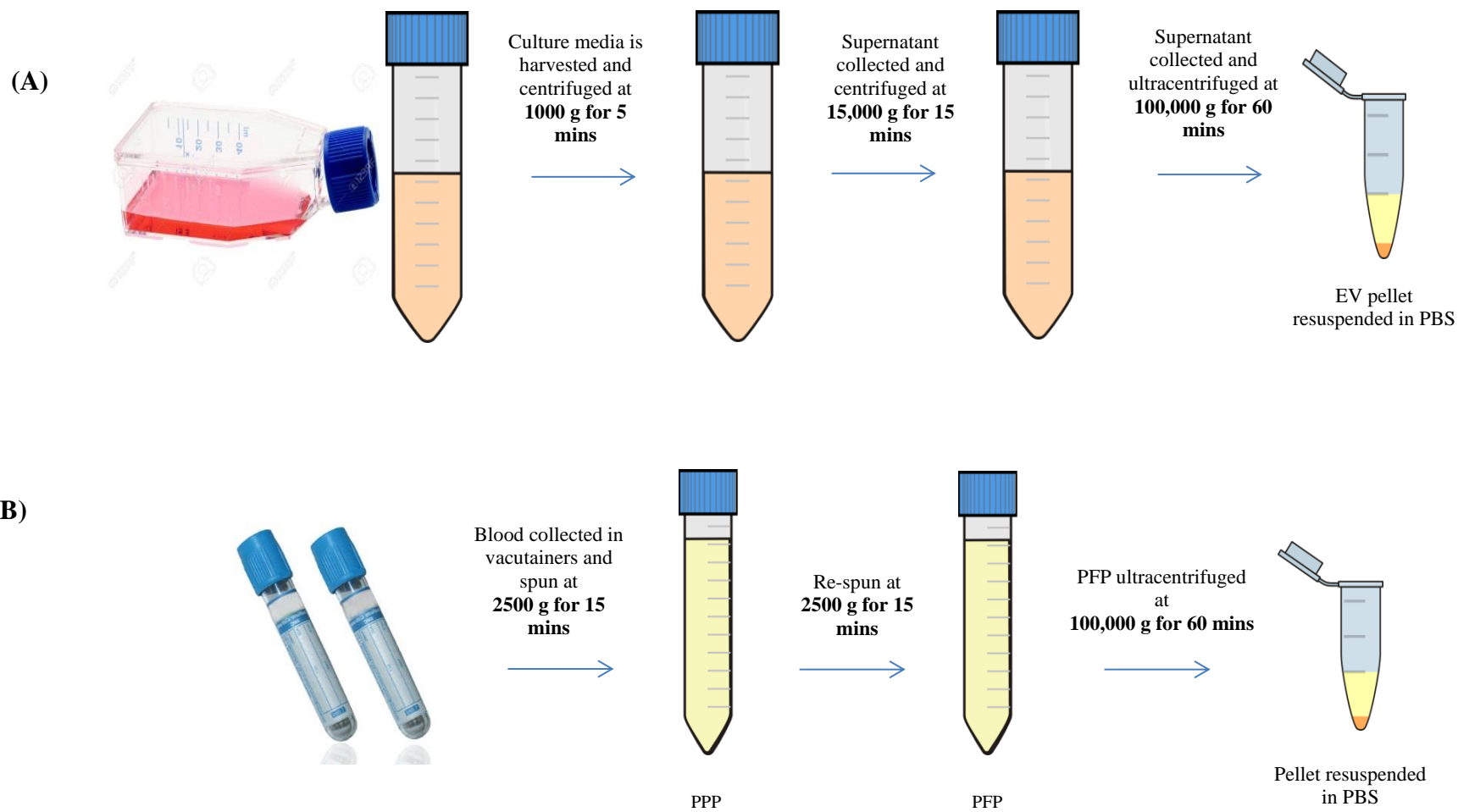


Figure 2.3 Isolation of EV Schematic diagram of EV isolation from 3T3-L1 cells (A) and human plasma (B).

PPP = platelet-poor plasma, PFP = platelet-free plasma

2.3 Nanoparticle Tracking Analysis

2.3.1 Working principle

Nanoparticle Tracking Analysis (NTA) involves assessing the Brownian motion of nanoparticles in liquid suspension on a particle-by-particle basis and correlates this movement to an equivalent hydrodynamic diameter. Subsequently, particle size distribution and concentration can be derived by the application of the Stokes-Einstein equation. The NTA software registers the movement of a single particle in two dimensions (x,y). It tracks the movement of a nanoparticle over a time interval t (~30 ms) and quantifies the displacement as diffusion coefficient D determined by

$$D = \frac{(x,y)^2}{4t}$$

The particle diameter d can be calculated by the Stokes-Einstein equation as a function of diffusion coefficient D at a temperature T and viscosity of the liquid η with Boltzmann's constant k_b as:

$$D = \frac{4k_B T}{3\pi\eta d}$$

A 488nm laser beam illuminates the chamber loaded with the sample containing particles and the light scatter is recorded with a scientific digital camera, arranged at 90° angle to the irradiation plane. In-built software captures the movement of a particle frame by frame which can be observed through a microscope and computer screen (**Figure 2.4**).

2.3.2 Experimental method

The NanoSight LM10 (Malvern Panalytical) was used for all the NTA analyses. Polystyrene beads of 100nm were examined on the Nanosight prior to sample analysis to validate the size and concentration determined by the system. A dilution of the EV sample was prepared with sterile water to achieve a concentration in the range of 1×10^8 and 1×10^9 particles/ml and injected into the sample chamber by means of a syringe pump. The working sample was run to measure for 60 secs with 5 replicates per sample to account for technical repeats. Measurements were conducted at room temperature and the sample chamber thoroughly washed with sterile water prior to,

and after a sample run. The mean of the population (nm) corresponded to the EV size whereas the concentration of the EV stock was determined by multiplying the given concentration of the working sample with the dilution factor. The analytical settings on the NTA pre- and post- experimental run are detailed in **Table 2.2**.

A detailed NTA calibration experiment was conducted once at the initial operation of the device using the standard sized beads of 100nm, 200nm and 400nm, provided by the company, Nanosight (discussed in Chapter 3). Subsequently, calibration beads of 100nm size was run every time through the NTA device on the days of its application, to verify the reproducibility of the technique.

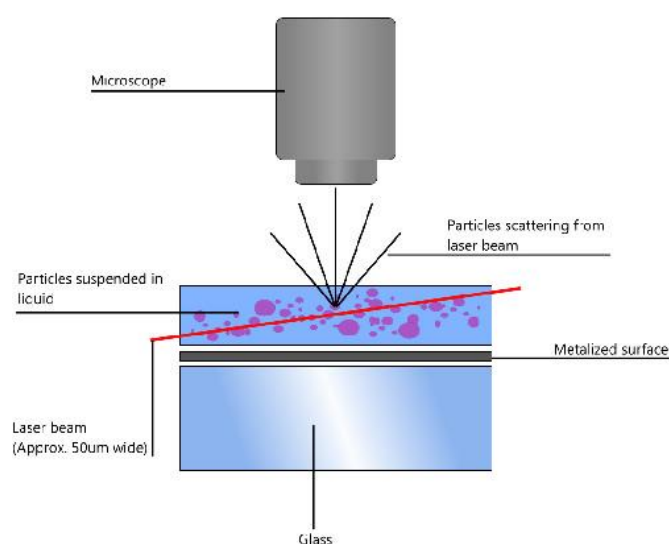


Figure 2.4. Principle of Nanoparticle Tracking Analysis. NanoSight laser illumination module where EVs in a suspension are illuminated by a laser refracted into the fluid via a glass prism, causing the EVs to scatter light. This light scattering is then visualised by a microscope with a video camera attached, allowing the tracking of illuminated EVs to determine the particle size. Image cited from ©Malvern Instruments Ltd.

	Setting	Value
Pre-analytical	Camera shutter	450
	Camera level	12-15
	Camera gain	200-300
	Syringe pump speed	20
Post-analytical	Temperature	22-25° C
	Screen gain	10-12
	Detection threshold	5-6

Table 2.2: Pre- and post-analytical settings used for NTA experiments. Details of all pre- and post-analytical settings used when analysing EV samples using NTA.

2.4 Time resolved Fluorescence (TRF)

2.4.1 Assay design

A modification of traditional immunoassay (ELISA) in the use of lanthanide chelates rather than typical fluorophores led to the development of dissociation-enhanced lanthanide fluorescence immunoassay or DELFIA, which is a time resolved fluorescence (TRF) technology. More recently, this was developed by Professor Aled Clayton to evaluate the protein content in EVs. The presence of a biomolecule is detected using lanthanide chelate labelled reagents with wash steps to remove the unbound reagent. TRF immunoassays use the ‘europium’ fluorophore that exhibits a high signal-to-noise ratio because of its large Stokes’ shift (difference between excitation and emission wavelengths) and the narrow emission peaks. The long fluorescence decay time and high signal sensitivity ensures strong detection of proteins even the less abundant ones. The EVs are adhered to high-affinity binding 96-well ELISA plates and probed for antigen of interest by specific antibody. The primary antibody is then detected using biotin-labelled secondary antibody and a streptavidin-europium conjugate. **Figure 2.5** illustrates the conceptual binding of EVs with antibodies.

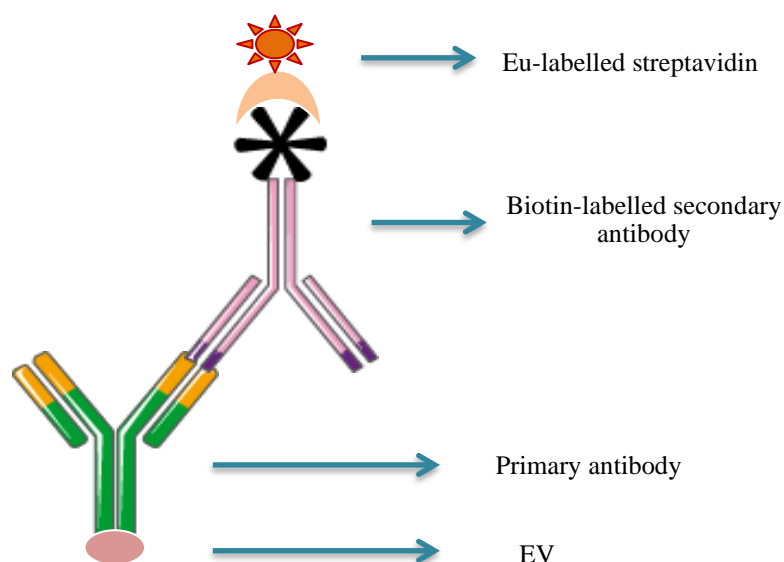


Figure 2.5: Concept of TRF assay to detect EVs. The primary antibodies that bind to the EV antigens are detected by biotin labelled secondary antibody. The high affinity between streptavidin and biotin, facilitates detection of secondary antibody and with Eu conjugate, the signal is enhanced and lasts longer.

2.4.2 Experimental method

The collected EVs (cell- and plasma- derived) of defined concentration 5×10^{10} EV/well were plated on a “sticky” ELISA plate (Grenier Bio-one Germany) and incubated overnight at 4°C . On the following day, unbound particles were washed, and non-specific sites were blocked by BSA (1% wt/vol) for 2 hrs. The EVs were permeabilised using RIPA (radioimmunoprecipitation assay) buffer (Santa Cruz, CA), prior to the addition of antibodies, for 1 hr at room temperature. Primary antibodies at a concentration of $3 \mu\text{g/ml}$ for plasma EVs and $1 \mu\text{g/ml}$ for 3T3 (cellular) EVs were incubated overnight with the EVs. The antigen markers were detected by addition of secondary antibody (anti-rabbit IgG biotin-labelled) and streptavidin-europium conjugate (Perkin Elmer) for 1 hour each at room temperature. DELFIA® wash buffer (Perkin-Elmer) was used to remove any unbound biomolecules between each step with three washes. The time resolved fluorescence (TRF) was read by spectrometer (FLUOstar OPTIMA plate reader, BMG Labtech, UK). Each well received 400 flashes, with the measurement beginning at $400 \mu\text{s}$ after the last flash and recorded for $400 \mu\text{s}$. Gain adjustment was achieved using a set of europium standards, allowing for comparison between multiple plate reads. Data were analysed using MARS software (BMG Labtech, UK) and presented as arbitrary fluorescence units (a.u). A negative control (EVs with no primary antibody) was included to adjust for background fluorescence. The list of antibodies used in TRF assays are recorded in **Table 2.3**. The secondary antibody used in the detection of EV-bound primary was donkey anti-rabbit IgG-HRP (GE Healthcare, # NA934V).

(A) Monoclonal Antibodies with reactivity against **mouse** antigens raised in **rabbit** used particularly to detect 3T3-L1 derived EV proteins.

Antibody	Manufacturer
CD9	Cell signalling (#13403)
FABP4	Cell signalling (#3544S)
Adiponectin	Cell signalling (#2789S)
PPAR-gamma	Cell signalling (#2443S)

(B) Monoclonal Antibodies with reactivity against **human** antigens raised in **rabbit** used particularly to detect plasma-derived EV proteins.

Antibody	Manufacturer
CD9	Cell signalling (#13403)
FABP4	Abcam (ab92501)
Adiponectin	Abcam (ab75989)
PPAR-gamma	Abcam (ab191407)
CD41	Abcam (ab134131)
CD11b	Abcam (ab52478)
CD144	Abcam (ab33168)
CD235	Abcam (ab129024)

Table 2.3 List of primary antibodies used in TRF assays

2.5 Bicinchoninic acid protein assay

2.5.1 Principle

The bicinchoninic acid (BCA) protein assay detects and measures the amount of protein by a colorimetric reaction. The assay combines the biuret reaction, the reduction of Cu^{+2} to Cu^{+1} by protein in an alkaline medium with the selective colorimetric detection of the cuprous cation (Cu^{+1}) by a reagent containing BCA. The chelation of two molecules of BCA with one cuprous ion results in a purple-coloured water-soluble complex that exhibits a strong absorbance at 562nm. It's a highly sensitive technique that is nearly linear with increasing protein concentrations with a detection range of 20-2000 $\mu\text{g}/\text{ml}$. The assay was performed prior to Western blotting and immunophenotyping to measure the protein concentration in EV and cell lysates.

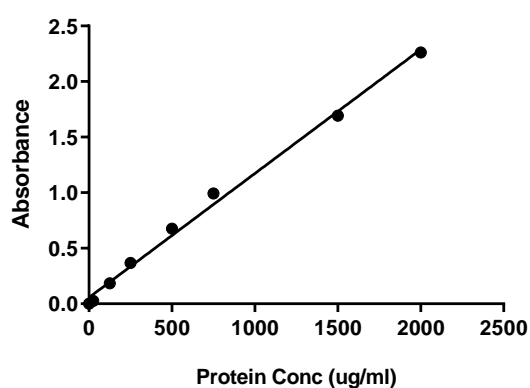


Figure 2.6: BCA assay standard curve. A typical 6-point standard curve generated from a BCA assay. BSA concentration standards range from 0-2000 $\mu\text{g}/\text{mL}$.

2.5.2 Experimental procedure

The BCA assay was performed using Pierce™ BCA protein assay kit (Thermo Scientific, UK) according to the manufacturer's instruction. Firstly, a set of albumin standards were prepared with protein concentration ranging from 0 - 2000 $\mu\text{g}/\text{ml}$ to generate a standard linear curve while the samples were diluted in PBS to a volume of 25 μl . The standards and the samples were then supplemented with the 200 μl BCA working reagent and incubated for 30 minutes on a plate shaker at 37°C. Absorbance was subsequently read at 562nm and protein concentrations ($\mu\text{g}/\text{ml}$) determined from

the standard curve. A typical absorbance standard curve plotted against protein concentrations is demonstrated in **Figure 2.6**.

2.6 NanoDrop Spectrophotometer

The NanoDrop® ND-1000 Spectrophotometer (Thermo Fischer Scientific, UK) was used to measure the protein concentration that uses a patented sample retention technology. It involves two fibre optic cables that are brought in contact by means of liquid source. A sample volume of 1µl is loaded onto the base measurement pedestal containing a fibre optic cable. The arm containing the second fibre optic cable holds the sample in place by means of its surface tension. A xenon flash lamp illuminates the sample and the extent of absorption at 280nm is recorded. Protein concentration is determined according to the Beer-Lambert law: $A = \epsilon \times l \times c$, where A is absorbance, ϵ is the molar absorption coefficient, l is the cell path length and c is the molar concentration. The working principle of NanoDrop is schematically represented in **Figure 2.7**. The device requires no cuvettes or any sample containment, and readings are obtained in matters of minutes.

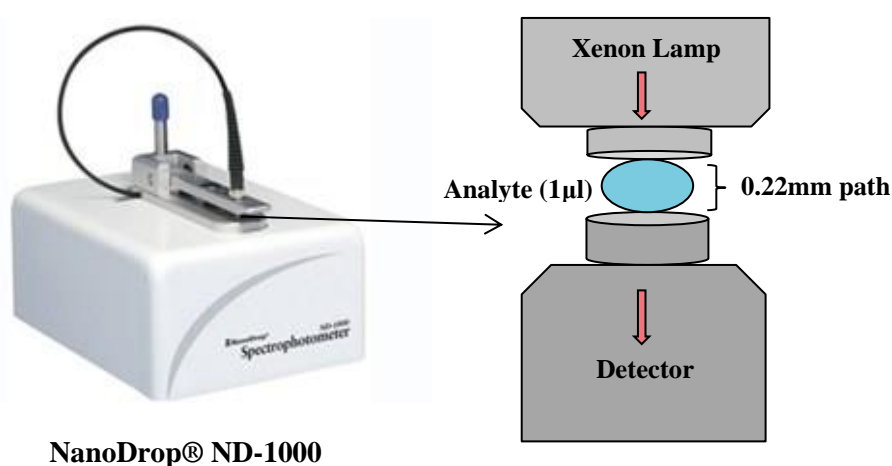


Figure 2.7 NanoDrop spectrophotometer. The protein sample is sandwiched between the two pedestals containing fibre optic cables. Protein concentration of the sample is measured the detector following the absorbance of UV at 280nm.

2.7 Western blotting

Western blotting or Immunoblotting is a protein analysis technique which involves gel electrophoresis for the separation of proteins in a sample based on molecular weight, followed by nitrocellulose membrane transfer. The trapped proteins on the membrane are probed for specific antigens and detected using chemiluminescent methods.

2.7.1 Sample preparation

The protein concentrations of EV samples were measured by NanoDrop 1000 Spectrophotometer (ThermoFisher Scientific, UK). A defined amount of protein (10 - 15 µg) was made up to 30µl volume by NuPAGE® Sample Reducing Agent 10X and NuPAGE® LDS Sample Buffer 4X in eppendorf tubes. The tubes were left on a heat block at 90°C for 5 mins to unwind/denature proteins, centrifuged at 12,000 x g for 5 mins at 4°C and left on ice until further loading onto the gel.

For cell lysate preparation, flask culture media was removed and cells washed with ice cold 1X PBS 3 times before the addition of chilled lysis buffer at a volume of 10µl per cm². The cells were then gently removed with a cell scraper, collected and centrifuged at 12,000 x g for 20 minutes at 4°C to sediment cell debris. The supernatant was taken for analysis on ice or stored at -20°C until further loading onto the gel.

2.7.2 Protein Separation by SDS-PAGE

Protein samples ranging from 10-15ug were loaded onto precast polyacrylamide NuPAGE Bis-Tris protein gels (ThermoFisher Scientific) along with a pre-stained protein ladder (3.5–260 kDa, ThermoFisher Scientific, UK) for molecular weight reference. Protein separation was achieved after sodium dodecyl sulphate polyacrylamide gel electrophoresis (SDS-PAGE) in 1X NuPAGE™ MOPS SDS Running Buffer (ThermoFisher Scientific, UK), run at 180 volts for 1 hour or until the stained protein bands reached the end of the gel.

2.7.3 Electroblothing

The gel was subjected to wet electroblotting to transfer the separated trapped proteins onto a PVDF membrane of 0.45 µm (Amerhsam Hybond P, GE Healthcare, UK). The membrane was activated by briefly soaking in methanol and washing with sterile water before laying it on the gel. The gel-membrane system was sandwiched between

blotting paper and secured with foam pads before encasing into a cassette (**Figure 2.8**). This was immersed in a tank of 1X NuPAGE™ Transfer Buffer (ThermoFisher Scientific, UK) and electro transfer occurred with the current passing in the direction from gel to the membrane for 1 hr at 80 volts.

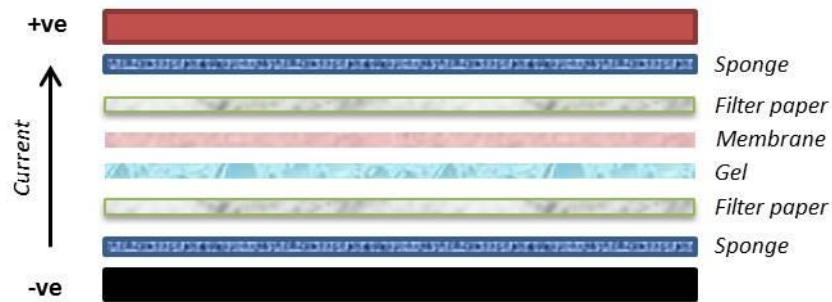


Figure 2.8 Electroblotting stack. The arrangement of components during electroblotting to facilitate the transfer of proteins from the gel to the membrane.

2.7.4 Antibody Incubation

Following protein transfer onto the membrane, the membrane was washed with Tris-buffered Saline with Tween 20 (TBS-T) thrice for 5 minutes. Prior to antibody incubation, the membranes were blocked with milk 5% w/v in blocking buffer for an hour at room temperature on an orbital shaker. Membranes were then incubated overnight with rabbit anti-mouse or anti-human monoclonal primary antibodies. On the following day, the membranes were washed with TBS-T before being left in horseradish peroxidase-labelled donkey anti-rabbit secondary antibody (GE healthcare) or goat anti-mouse IgG-HRP (Santa Cruz Biotechnology; sc-2302) diluted 1:2500 in blocking buffer for 1 hour at room temperature. Finally, the membranes were thoroughly washed (x 6 times for 5 mins each) before developing. The antibodies used in Western blot experiments are given in **Table 2.4**.

2.7.5 Detection

Amersham ECL Western Blotting Detection Reagent (GE Healthcare) at 0.125 ml/cm² membrane was loaded onto the membrane in order to detect the protein bands. The

membrane was then exposed to photographic film (Amersham™ Hyperfilm ECL, GE Healthcare) in a dark room for different time periods depending on the antibody/ detecting protein. Following exposure, the film was developed, fixed, washed and left to air dry.

Antibody	Manufacturer	Reactivity	Host species	Molecular weight
CD9	Cell signalling (#13403)	Mouse & Human	Rabbit	22 kDa
CD81	BioRad (MCA1847)	Human	Mouse	22-26 kDa
CD63	Santa Cruz Biotechnology (sc-15363)	Human	Rabbit	25 kDa
Alix	Santa Cruz Biotechnology (sc166952)	Human	Mouse	110 kDa
FABP4	Cell signalling (#3544S)	Mouse & Human	Rabbit	15 kDa
Adiponectin	Abcam (ab75989)	Human	Rabbit	27 kDa
PPAR-gamma	Cell signalling (#2443S)	Mouse & Human	Rabbit	53/57 kDa
Perilipin	Cell signalling (#9349)	Human	Rabbit	56 kDa

Table 2.4 List of primary antibodies used in western blotting experiments

2.8 Size-Exclusion chromatography

An alternative approach to the traditional isolation of EVs by ultracentrifugation was adopted using Exospin™ midi-columns (Cell Guidance systems).

2.8.1 Column preparation

The columns were supplied pre-equilibrated with sterile water containing 20% ethanol. Prior to their use, the preservative buffer was drained, and the columns were rinsed with 2 x 10ml PBS and re-equilibrated.

2.8.2 EV isolation

1ml of platelet-free-plasma (obtained as described in 2.2.2) was loaded onto the column in increments of 500µl and two column fractions (eluate) were drained. Thirty subsequent repeats of 500µl PBS were added on the column and each fraction collected in an Eppendorf tube. A validation experiment was undertaken on each fraction to confirm the presence of EVs which concluded that fractions 5 through to 10 contained the highest concentration of EVs (demonstrated in chapter 4). Hence, fractions 5-10 were pooled and spun at 100,000 x g for 1 hour at 4°C to concentrate the EV sample.

In the case of 3T3-L1 cells, a starting EV sample was prepared as described in 2.2.1 with the pellet obtained re-suspended to a final volume of 1ml in PBS, and subsequently loaded onto the column. Fractions were analysed to find the highest EV concentration from fractions 4 through 10, which was pooled, spun and resuspended to concentrate the EV sample.

2.9 Adipokine array

A commercially available Proteome Profiler Human Adipokine Array Kit (R&D Systems, Bio-Techne, UK) was used to analyse 58 adipocyte-related proteins in selected EV samples.

2.9.1 Assay principle

An adipokine array is designed with control- and capture- antibodies against selected human adipokines and fixed in duplicates on nitrocellulose membranes. Biological test samples are diluted, blended with a cocktail of biotinylated detection antibodies and incubated overnight with the adipokine array. The detection antibody complexes with the target antigen and is immobilised by its cognate capture antibody on the membrane. Any unbound material is washed with suitable buffer. Chemiluminescent detection reagents are added that generates signal with interaction between trapped complexes and streptavidin-horseradish peroxidase and is developed as described in the Western blot section. Signal (chemiluminescence) generated at each spot is proportional to the amount of protein bound.

2.9.2 Experimental procedure

The assay was performed as per manufacturer's instruction. The EV samples were mixed and adjusted to a volume of 1.5ml with given buffers, to which 30 µl of human adipokine detection antibody cocktail was added and incubated for 1 hour at room temperature. Meanwhile, the membrane was blocked for an hour at room temperature with specific blocking buffer. Then, sample-antibody mixture was incubated with the membrane overnight at 2-8°C on a plate rocker. On the following day, the membrane was washed three times for 10 minutes. 2ml of Streptavidin-HRP was loaded on the membrane and left on a plate rocker for 30 minutes at room temperature, after which it was washed to remove unbound protein. Detection reagents were added and detected using Amersham ECL Hyperfilm to capture the chemiluminescence following 15- and 30-minute exposures. The blots were scanned and pixel density at each spot was analysed using HLIImage++ (Western Vision Software, USA) software (**Figure 2.9**).

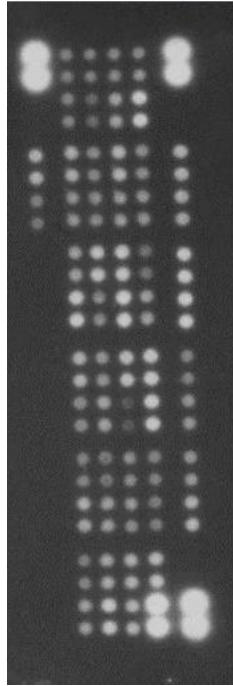


Figure 2.9: Representative blot of the adipokine array post development on film.

2.10 Immunoassay

2.10.1 Magnetic bead capture using Dynabeads

The Dynabeads® M-280 Sheep anti-Rabbit IgG are uniform, superparamagnetic, polystyrene beads of 2.8µm in size. They bind all rabbit IgG via the sheep anti-rabbit IgG covalently bound to the bead surface. They are kept at a concentration of $6 - 7 \times 10^8$ beads/mL (~10 mg/mL) in phosphate buffered saline (PBS) pH 7.4 with 0.1% bovine serum albumin (BSA) and 0.02% sodium azide.

Washing the beads: A selected volume of 50µl was taken in a flask with 1ml of wash buffer (1X PBS) and gently vortexed for >30 sec for a uniform resuspension. The vial was placed on the magnetic stand (DynaMag™-2, Life Technologies, UK) for 1 minute until the beads were captured on the side of the vial in contact with the magnet. The supernatant was subsequently discarded, and the beads resuspended again in PBS to repeat the wash twice. Finally, the beads were resuspended in 50µl of PBS.

Experimental procedure: During the magnetic bead capture experiment, first, a sample of plasma EVs was incubated with 3 µg/ml primary antibody for two hours. Then, 50µl of pre-washed magnetic beads were introduced to the EV/antibody mix and incubated for another 30 minutes at room temperature. The mixture was then placed on the magnet to separate the bound EV-antibody-anti-rabbit IgG complex and the supernatant collected for further study analysis and compared with the pre-capture sample for the loss/reduction of certain EV-associated protein markers. **Figure 2.10** demonstrates the principle of magnetic bead capture to exclude specific population of EVs while others remain.

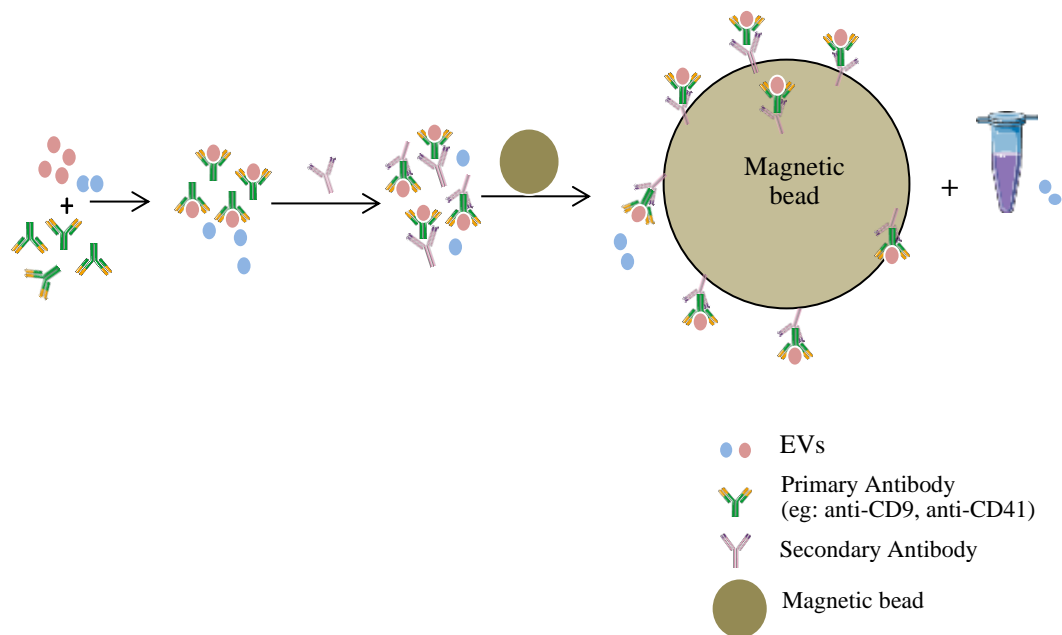


Figure 2.10: Principle of magnetic bead capture. EVs are incubated with desired capture antibody and identified using secondary antibody leaving unbound EVs in the solution. The addition of magnetic beads arrest EV-bound secondary antibodies and the free EVs are collected for downstream analysis. The magnetic beads are trapped by a bigger magnet.

2.10.2 Solid-phase capture of EVs

Rabbit monoclonal antibodies were diluted in PBS at a final concentration of 3 $\mu\text{g/ml}$ and coated in triplicates at the bottom of high binding ELISA plates (Greiner Bio-One Ltd, UK) by laying them overnight at 4°C. EV samples at a concentration of 1×10^{11} particles/ml from plasma were incubated in the well coated with specific antibodies for 2 hours. This enabled the capture of EVs with the desired antigen within the well and depleted supernatant was removed for analysis.

2.11 Human Umbilical Vein Endothelial Cell isolation

Human umbilical cords were provided from the Maternity ward at University hospital of Wales, with ethical approval from the North West-Lancaster Research Ethics Committee (REC reference 14/NW/1459), applied under Dr Rebecca Wadey (*Cardiff Metropolitan University*). The umbilical cord was cut from the placenta and examined for blood clots and damage from clamping during delivery. These sections were eliminated, and fresh cuts were made on both ends with a scalpel. The tools, glassware and trays used in the cell extraction process were washed in detergent and sterilised. The cord was washed with 0.9% saline solution to remove blood stains. The vein was distinguished from the other two thick walled arteries in the cord and saline solution was flushed through the vein until the effluent ran clear, to rinse out any remaining blood. One end of the cord was clamped and approximately 10ml of collagenase (1mg/ml) was slowly injected into the vein using a syringe; once the vein was taut, it was clamped at the injecting end (**Figure 2.11**). The cord with collagenase was incubated for 15 minutes with occasional massaging to aid digestion of cells. At the end of the incubation time, one end of the cord was unclamped, and the collagenase solution collected into a Falcon tube and topped with equal volume of HUVEC media to neutralise the collagenase. The cells were centrifuged at 300 x g for 10 minutes to form a pellet that was resuspended in HUVEC media in the desired volume. The cells were cultured in gelatine-coated 6- and 96- well plates and left for two hours before replacing the media to reduce erythrocyte contamination. Growth media was replaced every 2-3 days and cells grew to confluence in 5-6 days. The composition of the HUVEC media is detailed in **Table 2.5**.

Reagent	Supplier, code	Storage	Final (volume/conc)
M199 medium	Invitrogen, 3150-022	+4°C	500 ml
Gentamycin	Sigma, G1272	+4°C	35 µg/ml
Amphotericin B	Sigma, A2942	-20°C	2.5 µg/ml
FCS	Pan Biotech, P40-37500	-20°C	50 ml
hEGF	Invitrogen, 10533084	-20°C	1 ng/ml
Hydrocortisone	Sigma, H0888	-20°C	1 µg/ml

Table 2.5 HUVEC media constituents. Details of reagents and volumes/concentration required to prepare 500 ml of HUVEC culture medium. hEGF = human Epidermal growth factor, FCS = Fetal calf serum.



Figure 2.11: Isolation of HUVECs from human umbilical cord. The above shows a taut cord where the umbilical vein was filled with approximately 10ml of collagenase solution (1mg/ml) and incubated for 15 minutes to allow for endothelial cell digestion.

2.12 Leukocyte adhesion assay

2.12.1 Isolation of leukocytes

The leukocyte isolation protocol was primarily derived from the method of Pettit and Hallett (Pettit and Hallett 1998). Fresh human blood (approximately 10mls) was collected by venepuncture from healthy individuals into a universal container (UC) containing 100 μ l of Heparin (5000 I.U/ml). Dextran (2.5ml, 6 % (w/v), Sigma) dissolved in 1 \times balanced salt solution (BSS; 0.13 M NaCl, 2.6 mM KCl, 8.0 mM Na₂HPO₄, 1.83 mM KH₂PO₄, pH 7.4) was added and then mixed by gentle inversion. The complete solution was then transferred carefully into a new universal container and was left undisturbed for 45 minutes at room temperature in order for the buffy coat to develop. As the blood separated into an upper plasma layer and a lower erythrocyte layer, the middle buffy coat layer of approximately 1.5ml was carefully extracted using a pipette into a fresh universal container. Cells, namely leukocytes and erythrocytes, were pelleted by centrifugation at 300 g for 2 minutes and resuspended in sterile H₂O (1ml) for 10 seconds to burst the membranes of any contaminating erythrocytes. It was supplemented with 20ml of BSS and the leukocytes were recollected as a pellet by centrifugation at 300 x g for 5 minutes. The pellet was re-suspended in 1.5 ml Krebs-BSA buffer (0.1 % (w/v) bovine serum albumin (BSA) in 1 \times Krebs (1.2 M NaCl, 0.48 M KCl, 0.12 M KH₂PO₄, 0.12 M MgSO₄, 0.13 M CaCl₂, 2.5 M HEPES, pH 7.4)). Leukocytes were collected fresh on the day of the experiment and not subjected to storage.

2.12.2 Leukocyte adhesion assay

A monolayer of HUVECs was grown to confluence in a 96-well plate as outlined in 2.9. Media was removed and wells were incubated with EVs from different sources/conditions ($n=3$) diluted with 100 μ l of serum-free media (specified in chapter 5) for 6 hours. In parallel, as a positive control, TNF- α was diluted in SFM with concentration ranging from (0-25 ng/ml) to a final volume of 100 μ l and incubated on HUVECs. As a negative control, wells consisted of serum-free media only, with no EVs present. Meanwhile, the freshly isolated leukocyte preparation in 1.5ml of KREBS-BSA (as detailed in 2.10.1) was incubated with 1.5 μ l of CellTrace™ calcein red-orange (1:1000 dilution; C34851, Invitrogen) in darkness at 4°C. After 10 minutes,

leukocytes were pelleted by centrifugation to remove excess dye, re-suspended in 1.5 ml Krebs-BSA buffer and left to settle on ice for 30 minutes. The volume of the leukocyte suspension was topped to 15ml with pre-warmed (37°C) Krebs-BSA buffer.

After the 6-hour EV incubation, the HUVECs were washed three times with KREBS and 150µl of fluorescently-labelled leukocyte suspension added to all working wells for 30 minutes. Non-adherent cells were subsequently removed with 3x rounds of KREBS washes before leaving the cells in buffer. Leukocyte adherence to the HUVECs was observed using an inverted fluorescence microscope. Five images were captured per well spanning the area covered by HUVECs. Images obtained were evaluated using ImageJ (version 1.49v; National Institutes of Health, USA) software where images were converted to “8 bit” and “binary”, and contrast set to nearly maximum, in order to distinguish between leukocytes and underlying HUVECs. The total image area covered by leukocytes was calculated and expressed as percentage of the total field of view.

2.13 Statistical analysis

GraphPad Prism 5 (version 5.01, GraphPad software Inc., USA) was used to analyse the data gathered in this thesis. Details of specific statistical analyses are given in the Methods section of each Results chapter.

2.14 Sample size

The experiments conducted throughout this study used at least 3 or greater number of biological samples, to assess biological variation, unless otherwise stated. The term ‘*n*’ used throughout the text in Chapter 3, Chapter 4 and Chapter 5 denotes biological replicates (distinct samples). Each sample was seeded in triplicates (technical replicates) while conducting an experiment to counter technical errors.

3. Results I: Isolation and phenotyping of adipocyte and plasma EVs

3. Perspective

At the outset of my studies I embarked on a series of experiments to acquire a comprehensive understanding of the techniques available to me and the current standards set out in the EV field. The International Society for Extracellular Vesicles (ISEV) had recognised the need for standardising methods and protocols, and especially the need to establish key characteristics of EV so as to allow true comparison of data and results between laboratories. Despite this, wide scale adoption had not occurred and it was important to get hands on experience in the techniques and methods available to me, not least because the main aim of my thesis, the characterisation of adipocyte-derived EV, would need to adopt robust methods that would stand the test of time. The work described in this chapter therefore represents early investigation into the various methods available to me, those developed and preferred at the laboratories of my supervisors and an evaluation of their potential for characterising EV from adipocytes.

Dr Aled Clayton and Dr Jason Webber had developed a TRF-based immunoassay to investigate EVs derived from body fluids of cancer patients (Webber et al. 2014; Welton et al. 2015; J L Welton et al. 2016) and my senior colleagues had calibrated a series of primary antibodies that allowed for detection of specific antigen based on a fixed number of EV- that were attached to an ELISA plate. This underlies much of the work presented in this chapter and thesis. EVs derived from 3T3-L1 adipocytes were investigated pre- and post- adipogenesis in the PhD studies conducted by Dr Katherine Connolly (Connolly et al. 2015) in which initial detection of certain adipocyte specific markers (including FABP4) had been accomplished. However, at the outset of this chapter, no standard EV isolation protocol or identifiable EV/exosome markers were defined per se. The isolation procedure adopted in this chapter was largely based on the work published by my fellow researchers (Willis et al. 2014; Connolly et al. 2015). As for plasma-derived EVs, the sample can now be considered a relatively crude preparation (lacking steps of current standard EV preparation) which at the time was widely accepted.

Constituent proteins are widely used to identify and characterise EV populations. Our group has characterised 3T3-L1 derived EV during the differentiation process and found that surface protein, protein and lipid content, EV number and size distribution vary. After careful review of the limited literature on adipocyte derived EV, selected

adipocyte specific proteins were chosen as potential markers for our studies (Aoki et al. 2007; Aoki et al. 2010). Of particular relevance to my project, 3T3-L1 EV exhibit FABP4 which seems to be in part accessible from outside EV and a large component within EV. Further evidence of adipocyte lineage is provided by the existence of adiponectin and PPAR γ 2 and set the scene for piloting the TRFIA by employing a combination of markers.

3.1 Introduction

In contrast to the rest of the EV field, the study of adipocyte-derived EVs (ADEVs) has gained limited momentum over the past decade. From largely *in vitro* studies, ADEVs have been implicated in various metabolic functions and obesity-related pathophysiology, attributed to their role in carrying signalling molecules or as communicators between cells (refer to Introduction, section 1.5). EVs carry a unique set of protein markers reflective of their phenotype and/or their cell of origin. In this chapter, a murine-derived cell line 3T3-L1 has been utilised as a model to generate standard EVs of adipocyte phenotype. These cells provide a useful model because they may be maintained in a pre-adipocyte stage or they may be induced to undergo differentiation to develop into mature adipocytes.

According to a study based on an extensive survey, ultracentrifugation (UC) of conditioned cell media remains by far the most widely used classical isolation method for EVs (Gardiner et al. 2016). Other well-used methods include density gradient centrifugation (DC), filtration and size-exclusion chromatography. The chosen isolation technique has substantial effect on the EV harvest, i.e., final sample volume, EV concentration and purity; estimating the purity of samples remains difficult, with inconsistent approaches across diverse studies (Andreu et al. 2016; Gardiner et al. 2016). EVs isolated by UC are often co-pelleted with non-vesicular macromolecules (Webber and Clayton 2013), which give a false representation of EV populations, particularly during subsequent downstream analyses including -omics-based analyses, RNA extraction and measurement, and functional assays. Meanwhile, EV isolation from biological fluids such as plasma, serum, urine or cancer-related effusions is more complex and requires a combination of isolation techniques (Szatanek et al. 2015). Ensuring purity in samples remains a challenge, and it should be understood that different types of EVs require unique isolation approaches depending on the nature and aim of the study.

Size exclusion chromatography (SEC) was first explored for EV isolation from biological fluids as a single-step protocol, by Boing et al., (2014) using sepharose CL-2B (Böing et al. 2014). With human platelet-free plasma as the starting material, SEC was able to efficiently isolate EVs and separate them from free lipoproteins and proteins. The minimal risk of protein complex formation and vesicle aggregation are

its advantages over UC and DC, besides the high EV recovery rate. Following on, several studies have confirmed the use of size exclusion columns for EV isolation to obtain a ‘cleaner’ working sample (Webber et al. 2014a; Welton et al. 2015; Welton et al. 2016; Mol et al. 2017; Welton et al. 2017). Application of SEC improves downstream analyses on the dimensional, structural and functional properties of extracellular vesicles.

Immunoassay is a commonly used diagnostic technique based on antigen-antibody interaction and researchers have successfully applied the technique to detect markers on plasma EVs; showed it to be reproducible and highly applicable in clinical evaluation (Logozzi et al., 2009; Wang et al., 2010; Higginbotham et al., 2011). Immunoassays are highly specific, have enhanced sensitivity, are cost-effective and are rapidly measured. By further combining an immunoassay with TRF detection methods (TRF-IA) the sensitivity is enhanced further due to the amplification and stability of the generated fluorescent signal. *In vitro* and *in vivo* samples have been tested by our group while addressing EVs (Webber et al. 2014a; Connolly et al. 2015; Welton et al. 2017). An immunoassay similar in principle to the TRF-IA has been developed by a research group in the Netherlands to capture EVs based on EV-specific markers and further detect other relevant protein epitopes on the EV using a second set of antibodies (Oliveira-Rodríguez et al. 2016). The authors used a lateral-flow immunoassay design to quantify EVs wherein anti-CD9 and anti-CD81 were used collectively as capture antibodies, and anti-CD63 labelled with gold nanoparticles was used as the detection antibody. This has a detection limit of approximately 8.54×10^5 exosomes/ μL of test sample (cell culture supernatants, human plasma and urine).

Currently, there is not one single/standard method that allows phenotyping, sizing, and enumeration of the whole range of EVs. To truly understand the biology of EVs, it calls for a combination of methods for an effective EV profiling.

3.1.1 Objectives:

The overall aim of this chapter was to gain insight into the various techniques available for EV analysis in order to appreciate the pros and cons of these methods, and how these may be adopted in the study of circulating adipocyte-derived EVs.

In order to address this, I had the following specific aims:

1. To isolate EVs from a standard adipocyte cell line and from human plasma, and to characterise these EVs in terms of size, concentration and protein content (using adipocyte and EV markers).
2. To validate NTA, TRF-IA and western blotting to identify EV and adipocyte markers on 3T3-L1 derived and plasma-derived EVs.
3. To validate TRF-IA as a possible tool for assessing EV lineage in plasma-derived EVs and to assess the relative EV populations in a plasma EV sample (based on platelet, endothelial, macrophage and erythrocyte markers as the main component populations).
4. To explore the utility of a commercially available size-exclusion chromatography column as a means to purify and enrich plasma EVs compared to plasma EVs isolated using UC.

3.2 Methods

3.2.1 Cell Culture and EV isolation

3T3-L1 cells were cultured as outlined in Chapter 2.1.1 and serum-free media was supplemented to the cells 24 hrs prior to EV isolation conducted as detailed in Chapter 2.2.1.

As for plasma EVs, the isolation was performed as detailed in Chapter 2.2.2.

3.2.2 Oil Red O staining

Confirmation of adipogenesis in 3T3-L1 cells culture was established by Oil Red o-staining, described in Chapter 2.1.2.

3.2.3 Nanoparticle Tracking Analysis

NTA was conducted to estimate the size and concentration of EVs obtained from 3T3-L1 culture media and plasma.

3.2.4 Western blotting

EV lysates were subjected for western blotting as described in Chapter 2.7. 10mg of protein was loaded into the gels after estimating the protein concentration by BCA assay outlined in Chapter 2.5.2. Antibody control experiment under the absence of a primary antibody was not conducted during the protein detection stage.

3.2.5 Time Resolved Fluorescence based Immunoassay (TRFIA)

3T3-L1- and plasma-derived EVs were probed for EV and adipocyte-specific proteins using an immunoassay as outlined in Chapter 2.4.2.

3.2.6 Column chromatography

SEC using Exospin™ midi-columns (Cell Guidance systems) was performed on EVs as described in Chapter 2.8.2.

3.2.7 Statistical Analysis

Unpaired t-test was used to compare means and $p < 0.05$ was deemed statistically significant.

3.3 Results

3.3.1 Measurement of size and concentration by NTA

The ability of NTA to discriminate and measure particles of different sizes was investigated using 100 nm, 200 nm and 400 nm sized polystyrene calibration beads provided by the manufacturer (Nanosight, Malvern). The experiment also studied the efficiency in the detection range of NTA (**Table 3.1**).

Bead size	Dilution	Concentration	Mean	Mode
100 nm	1:1000	$(1.8 \pm 0.1) \times 10^8$	113 ± 1.1	103 ± 08
200nm	1:1000	$(2.2 \pm 0.3) \times 10^8$	193 ± 1.8	198 ± 2.7
400 nm	1:1000	$(7.1 \pm 0.4) \times 10^8$	373 ± 11.1	374 ± 20.6
Mix (100, 200, 400nm)	1:1000	$(9.5 \pm 0.1) \times 10^8$	154 ± 2.5	109 ± 0.4

Table 3.1: Calibration beads evaluated by Nanoparticle tracking analysis. Polystyrene calibration beads of three different diameters were diluted 1:1000 and analysed using NTA to generate a measure of the machine's accuracy in calculating bead diameter and concentration, (n=3). A mix of the three beads in equal proportion was also analysed to test the capability of NTA in detecting individual populations in a polydisperse sample.

NTA was able to resolve and accurately measure different-size particles, in terms of diameter and concentration in monodisperse (single size) and polydisperse medium (mixed size) solution. Sharp defined peaks were observed when uni-sized beads were analysed using NTA (**Figure 3.1 (C), (D) and (E)**). In case of the polydisperse sample, made of the same individual calibration beads, although the peaks slightly overlap, NTA clearly discriminates three differently sized populations of beads

revealed by three peak maxima (**Figure 3.1 (F)**), which is an essential prerequisite for analysing extracellular vesicles in biological fluids. The slight overlap of the peaks in **Figure 3.1(F)** is a potential problem and an inherent limitation owing to measuring a stochastic process (Brownian motion) by sampling over a finite time period (the time for which each particle can be tracked). For the analysis of beads of a defined, narrow size range, the NTA software can correct for this and produce tighter peaks. However, when measuring EVs, we cannot make assumptions about the size distribution, resulting in the apparent poorer resolution and/or under estimation as seen. The concentration measurement is also less precise in polydisperse samples. This is due to the optimisation of the instrument settings (camera shutter speed and screen gain) to include smaller particles (e.g. 100 nm or less) for their effective analysis, thus, larger particles are either missed or there is increased uncertainty over their precise size (they appear over a broader range and the peak is lower in amplitude – **Figure 3.1(F)**). As an illustration of this, simple summing of the measured concentration of each individual size ($\sim 15.5 \times 10^8$ particles/ml) should yield the same total as the mixed sample ($\sim 9.5 \times 10^8$ particles/ml).

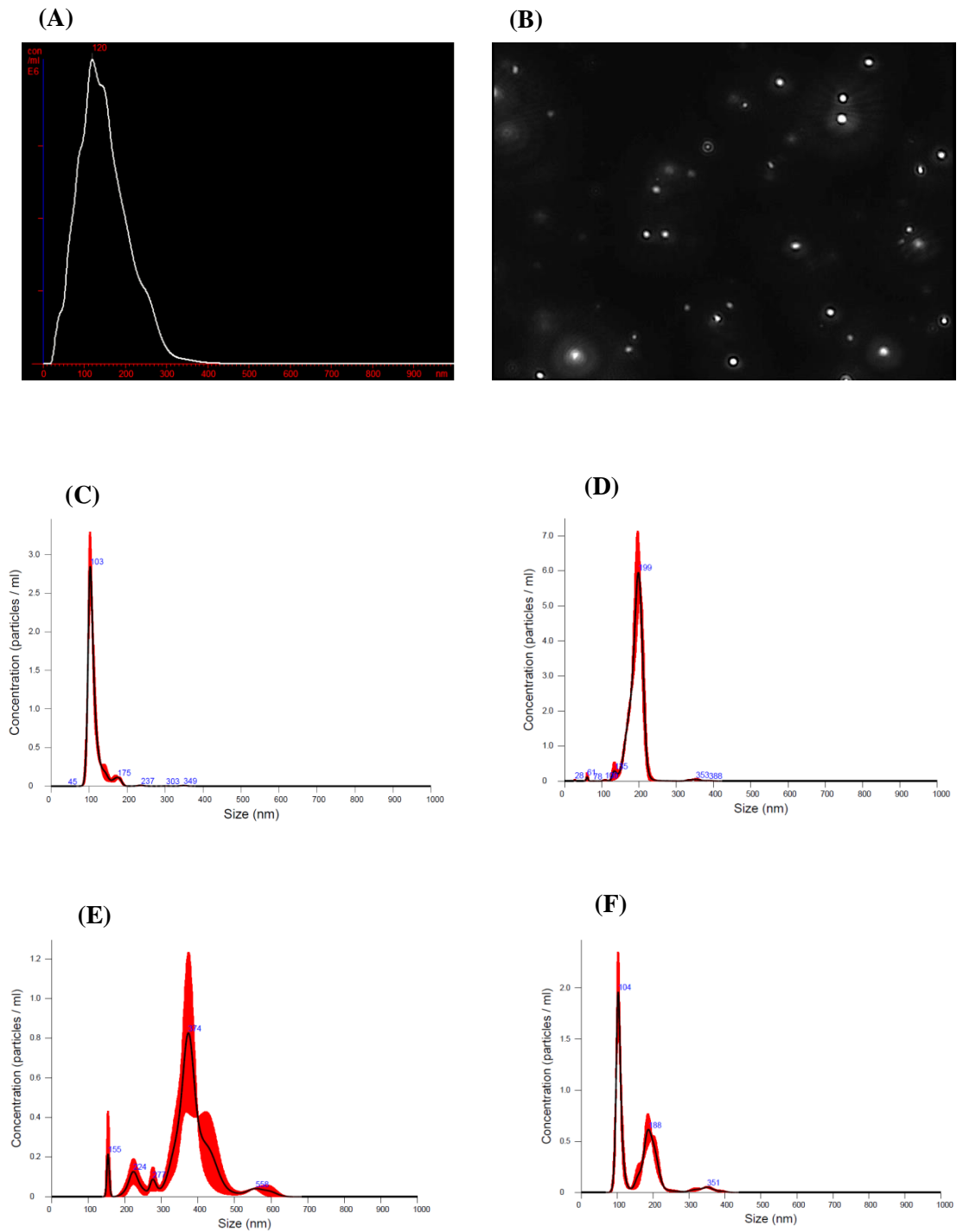


Figure 3.1: NTA analysis of size and concentration of polystyrene beads.

A typical trace generated by Nanosight (A) and a video screenshot from video of light scatter by beads (B). (C), (D) and (E) are plots generated of particle concentration versus size in monodisperse sample of bead size 100 nm, 200 nm and 400 nm respectively, and (F) represents polydisperse medium of beads, ($n=3$).

3.3.2 Confirmation of Adipogenesis

Oil red staining was used to qualitatively assess and confirm the maturation of 3T3-L1 cells from pre-adipocyte cells to mature adipocytes, by measuring the lipid accumulation within the cell. Microscopic pictures were taken at Day 0 and Day 14 for comparison (**Figure 3.2**) and showed clear accumulation of red-stained lipid droplets. The absorbance was also measured by spectrophotometer at 492 nm. Day 14 showed increased lipid accumulation indicating differentiation and maturation of 3T3-L1 cells. Statistical analysis was conducted using t-tests.

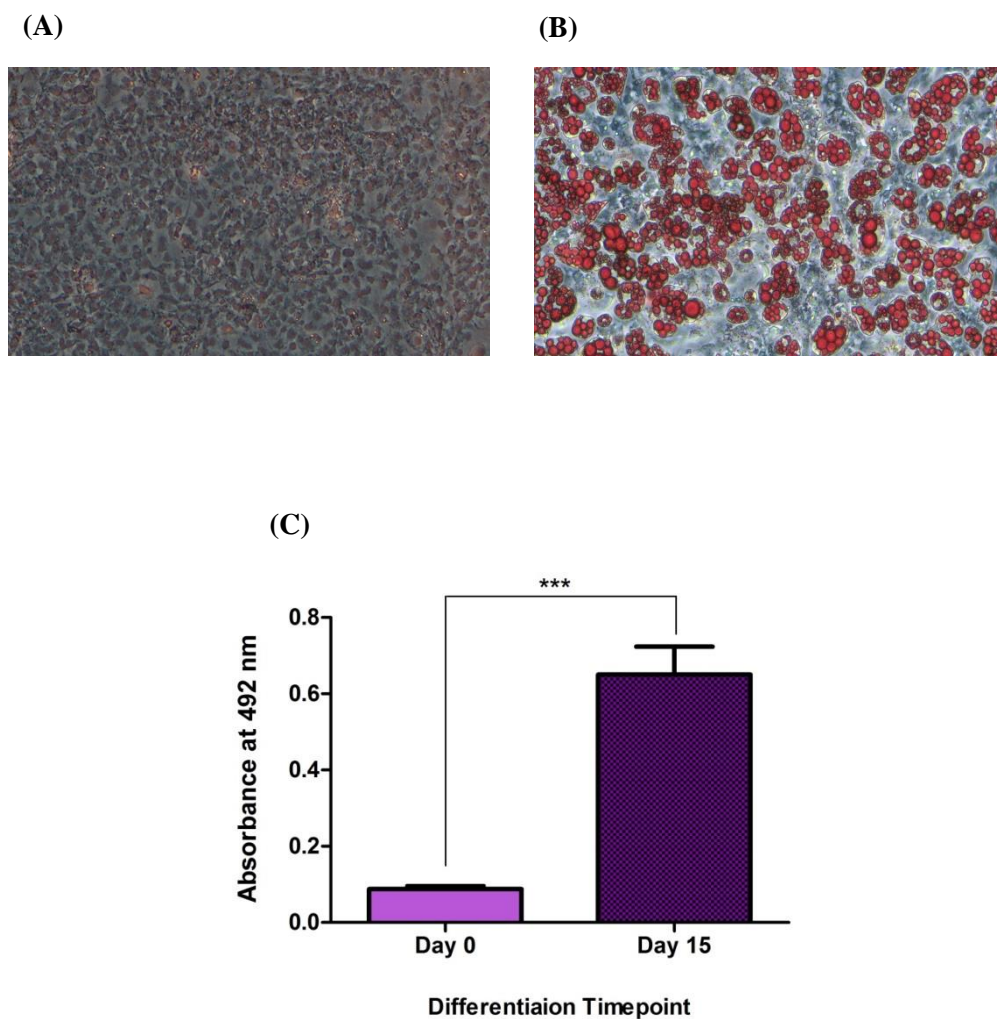


Figure 3.2: Evidence of Adipogenesis in 3T3-L1 cells. Lipid accumulation was visualised by Oil red O staining with light microscopy at Day 0 in preadipocytes (A) and at Day 14 in mature adipocytes (B). (C) The absorbance of Oil Red O at 492 nm was also quantified at each time point, $p < 0.001$, ($n = 6$).

3.3.3 Size and Concentration in cell and plasma derived EV sample

EVs collected from 3T3-L1 cell culture media were analysed by NTA to measure the size distribution, average particle size and total concentration of particles in the EV sample. The EVs collected from conditioned 3T3-L1 culture media yielded an average diameter of 163 ± 65 nm and an average concentration of 4.87×10^7 particles/ml of culture media (**Figure 3.3 (A)**). Similarly, plasma EVs were analysed for average size and concentration. The plasma EVs were calculated to have a mean diameter size of 95 ± 34 nm and concentration of 2.74×10^8 particles/ml of plasma (**Figure 3.3 (B)**). EVs from plasma exhibited a wider size distribution (10nm - 700nm) compared to 3T3-L1-derived EVs (30 nm - 500 nm).

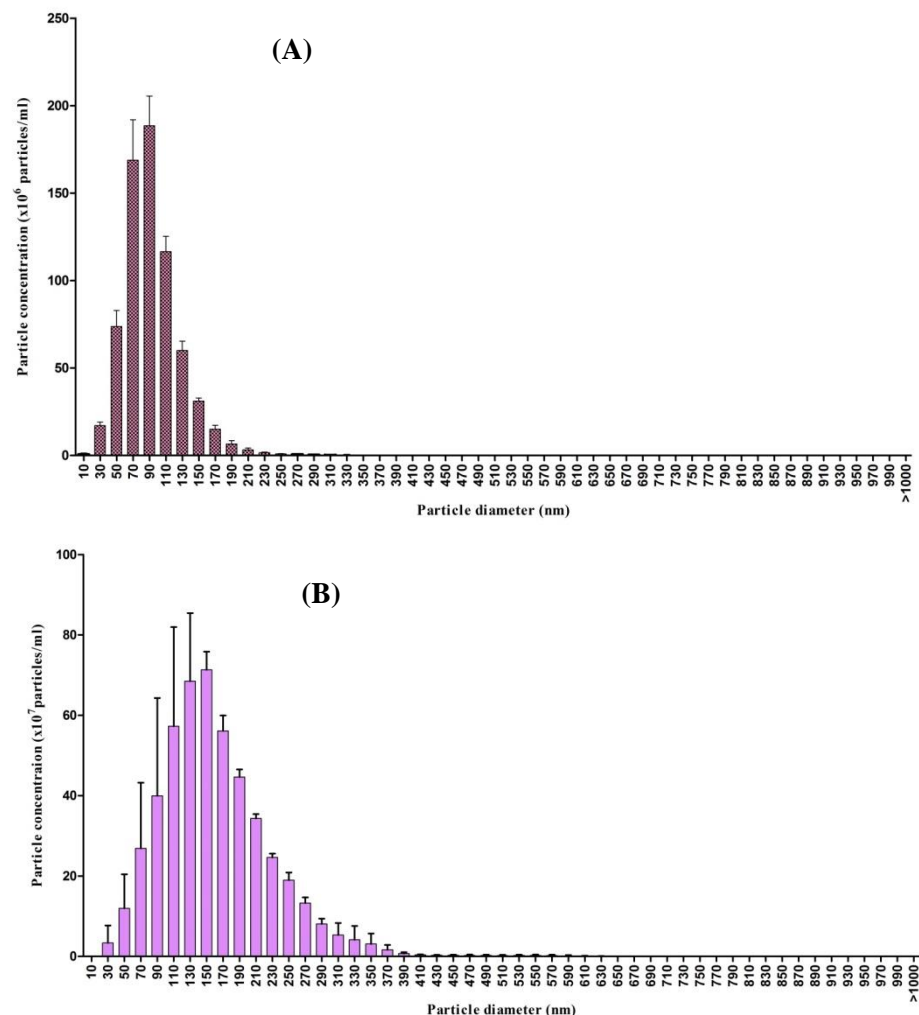


Figure 3.3: Measurement of the size and concentration of EVs. NTA analysis on 3T3-L1 derived EVs after maturation on Day 14 (**A**) and plasma-derived EVs (**B**) with mean diameter of 163 ± 65 nm and 95 ± 34 nm, respectively, ($n=3$).

3.3.4 Analysis of EV protein markers by Western blotting

The isolated EVs from mature 3T3-L1 cells were subjected to western blot analysis to identify EV markers (namely CD9 and CD63) and adipocyte-specific markers (namely FABP4, Adiponectin, PPAR- γ). **Figure 3.4 (A)** below clearly indicates the presence of a classic tetraspanin (CD9) in both 3T3-L1 and plasma-derived EVs as well as positivity for adipocyte specific markers, strongly confirming EVs derived from the adipocytes cell line. Hence, they are considered an appropriate positive control and model system for the remainder of the study described in this thesis.

Similarly, the plasma-derived EVs were also investigated for EV markers and adipocyte markers. The EVs stained positive for adipocyte markers FABP4, adiponectin and PPAR-gamma as well as CD9 (**Figure 3.4 (B)**)

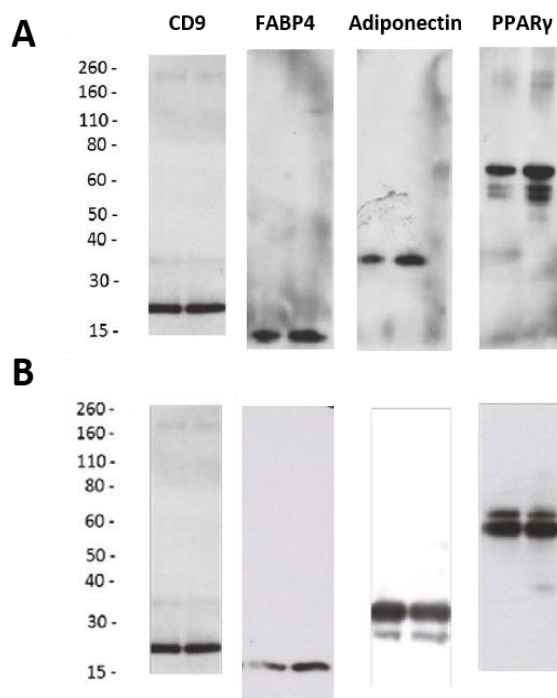


Figure 3.4: Western blot analysis of adipocyte markers in EV lysates. EV lysates collected from 3T3-L1 (**A**) and plasma (**B**) were evaluated for exosomal and adipocyte markers namely CD9 (25 kDa), FABP4 (15 kDa), Adiponectin (30 kDa) and PPAR- γ (53 kDa for PPAR- γ 1 and 57 kDa for PPAR- γ 2). Each blot shows 2 technical repeats ($n=2$)

3.3.5 Analysis of EV protein markers using a Time Resolved Fluorescence Immuno-Assay

Protein markers were also evaluated by immunoassay and **Figure 3.5** shows the profile of adipocyte markers measured in a defined EV population (5×10^{10} particles/mL). It shows the relative abundance of adipocyte-associated proteins in a controlled population of EVs (as opposed to the relative number of EV containing a particular marker). The EVs from 3T3-L1 cells and plasma were assessed for CD9 as well as FABP4, adiponectin and PPAR- γ (**Figure 3.5 A/B**). This generated a profile of the selected adipocyte markers in a defined population, where adiponectin and FABP4 protein markers were in relative abundance, compared to PPAR- γ . The abundance of adipocyte markers relative to CD9 was higher greater in plasma-derived EVs as compared to 3T3-L1-derived EVs (**Figure 3.5 (C)**).

In addition, plasma EVs were also probed for different protein markers to identify different populations of EV origin (CD41, CD11b, CD144 and CD235a; **Figure 3.5 (D)**). The component of each marker detected was expressed as a fraction of the total fluorescence of all markers and plotted as a pie chart.

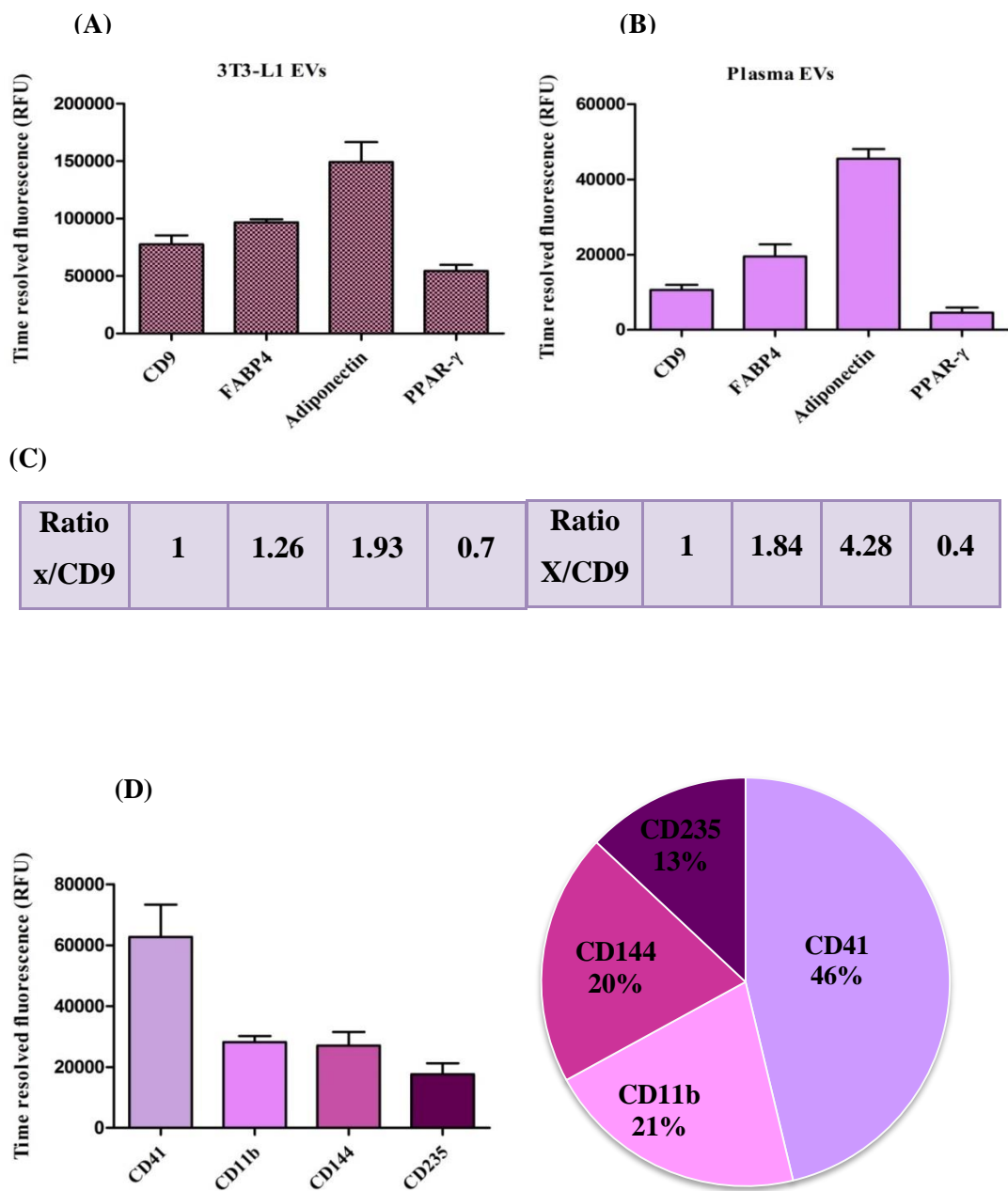


Figure 3.5: Measurement of EV protein content by TRF-IA. TRF-IA was used to measure exosomal (CD9) and adipocyte proteins (FABP4, adiponectin and PPAR- γ) in 3T3-L1 EVs (A) and plasma-derived EVs (B), ($n=3$). The relative abundance of adipocyte proteins compared to CD9 was calculated for both 3T3-L1 EVs and plasma EVs (C). The proportion of the four major EV populations in plasma-derived EVs was also measured by TRF-IA (D), ($n=3$).

3.3.6 Separation of soluble, free protein from EVs within a sample

Recognising that EV samples prepared by UC of cell supernatant or plasma likely contain free protein; initial studies were carried out on the utility of common laboratory separation techniques.

In an attempt to purify the EV prep, dialysis was employed with the use of appropriately sized membrane pores. The system was feasible with 3T3-L1 cell culture supernatant, but precarious with purifying plasma EVs, hence, this approach was discontinued. (Refer Appendix 1 for data)

3.3.6.1 Column purification of 3T3-L1 - derived EVs

3T3-L1-derived EVs were loaded onto size exclusion columns and fractions were collected as with plasma samples. Protein was prevalent in fractions 4 - 10 and the particle concentration increased from fraction 4 through to fraction 10 with subsequent fractions dwindling in number (**Figure 3.6 (A)**). Western blot analysis showed the expression of CD63 and FABP4 was limited to fractions 6-8 which corresponded with the peak in the particle-to-protein ratio (**Figure 3.6 (B), (C)**). This share of work was conducted with help of Dr Rebecca Wadey.

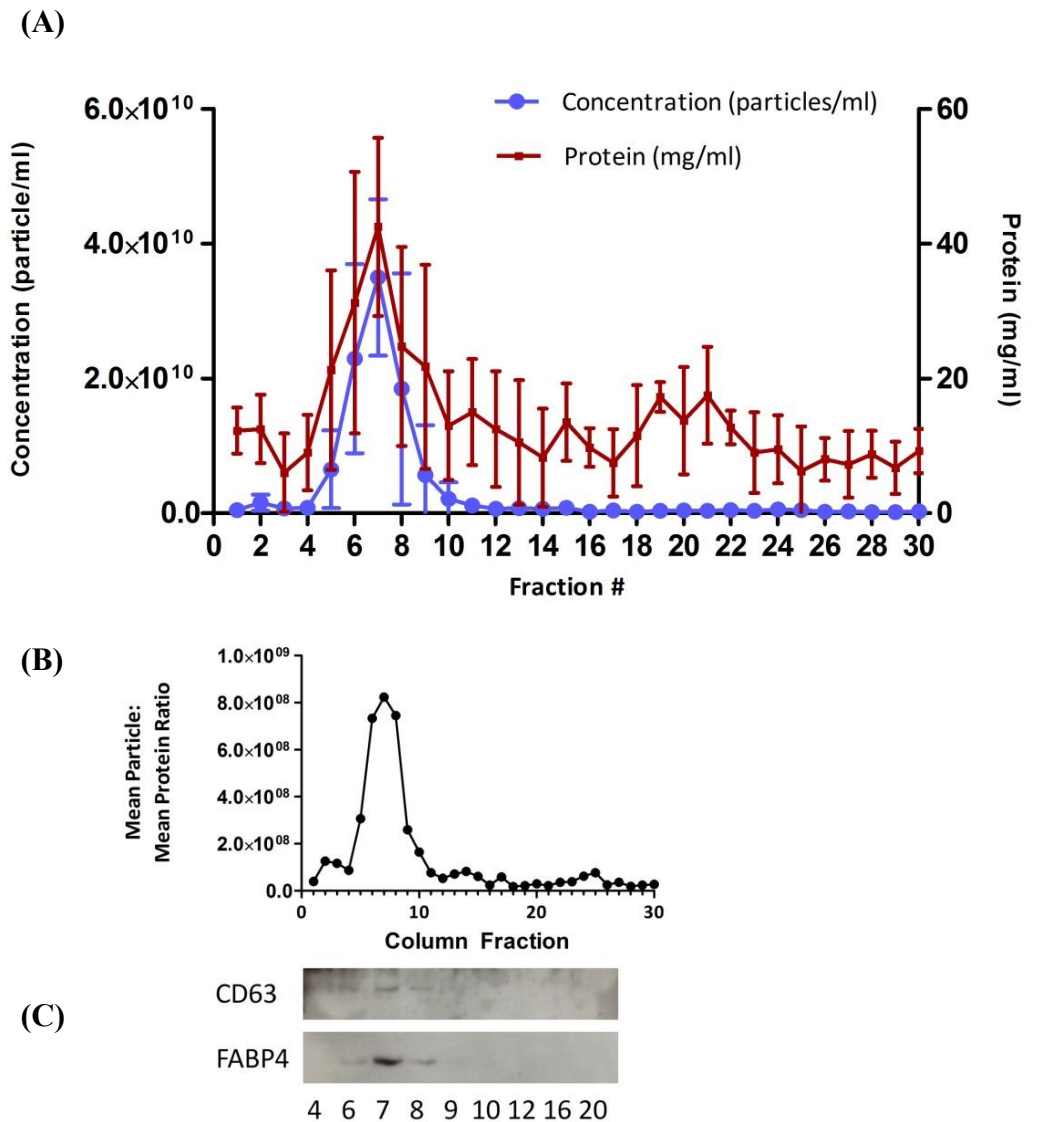


Figure 3.6: The elution of 3T3-L1 EVs through a size exclusion column. 3T3-L1-derived EVs isolated by ultracentrifugation (1 mL) were loaded onto size exclusion chromatography columns and 30 fractions were collected. Particle concentration (assessed by NTA) and protein content (assessed by Nanodrop) were plotted for each fraction (A), ($n=4$). The concentration of particles was divided by the protein concentration in each fraction to yield the particle-to-protein ratio (B). Samples between fractions 4 and 20 were tested for the presence of the exosomal marker CD63 and the adipocyte marker FABP4 using western blotting (C).

3.3.6.2 Column purification of plasma EVs

Size exclusion chromatography was tested for its ability to separate EVs from soluble protein. The particle concentration and protein content was measured in fractions 1-30 (**Figure 3.7 (A)**). The protein content showed a modest increase in fractions 5-10, which coincided with a minor peak in the particle concentration. A large peak in protein begins after fraction 10, which is accompanied by an increase in particle count. Fractions 2-28 were then assessed for EV markers (CD9, CD81 and ALIX) by western blot to verify the elution of EVs in the fractions (**Figure 3.7 (B)**). Fractions 5-10 revealed bands for the protein markers whereas the fractions 11-28 showed no indication of these proteins. Plotting the number of particles against the concentration of protein in each fraction revealed a peak in the particle-to-protein ratio from fractions 5-10 which aligns with fractions exhibiting positivity for the exosome markers (**Figure 3.7 (C)**).

A comparative study was undertaken of EV concentration and size by NTA, after isolation by either UC or SEC with starting volume of approximately 12-13 mL of plasma as illustrated in **Table 3.2**. EVs isolated by UC showed an average size of 255 nm whereas that of EVs eluted from the column was 180 nm. The apparent yield of EVs derived from the column is nearly 10x less than that obtained from UC. It should be noted that NTA will detect single particles with a diameter larger than 50 nm, which may not necessarily be extracellular vesicles, but could also include protein aggregates, lipoproteins and other serum particulates. Typically, column fraction 12 and above showed an increased protein content (**Figure 3.7 A**). Hence, these could account for increases in EV number observed by NTA with UC method of isolation, especially with no defined pre-purification step involved.

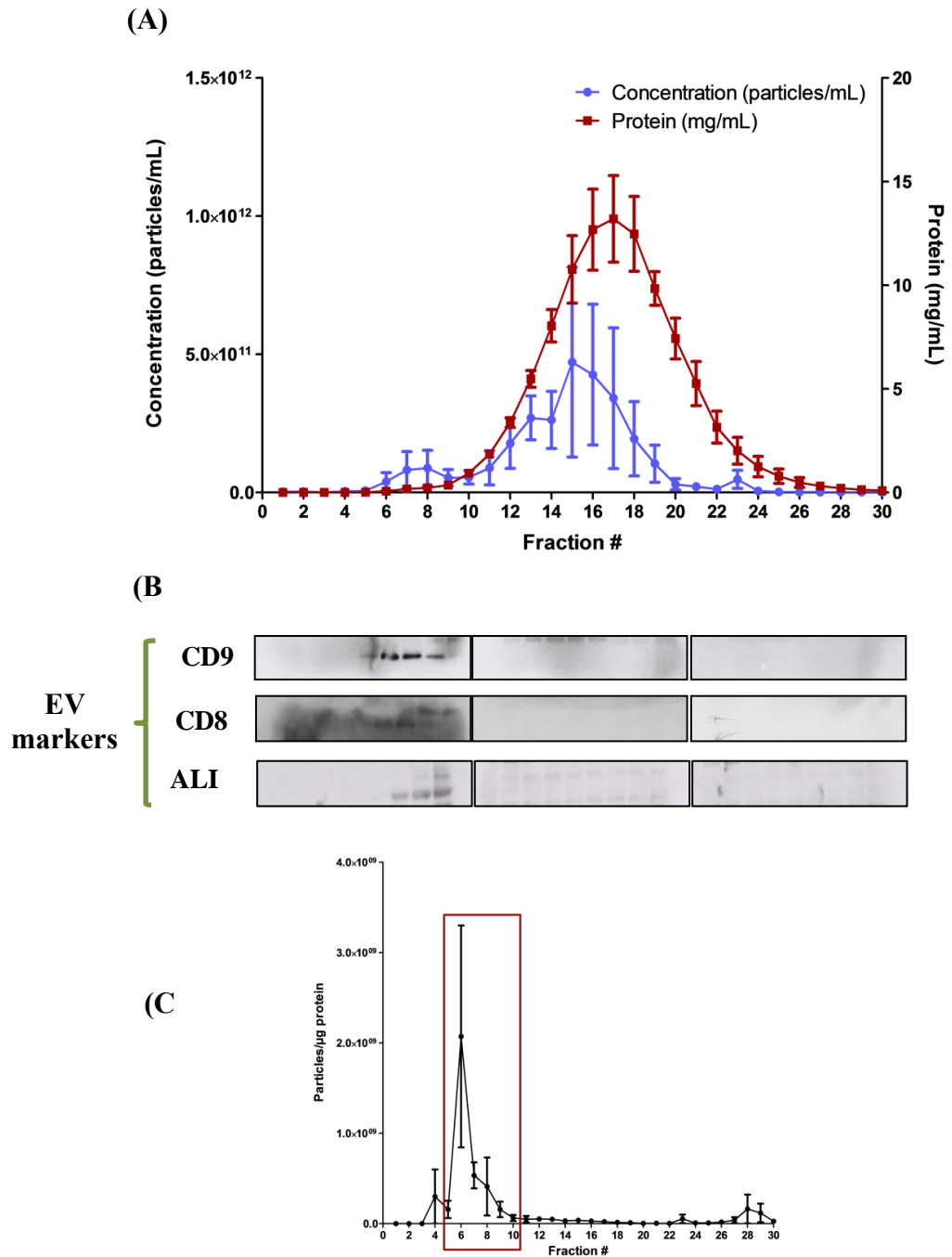


Figure 3.7: Evaluation of plasma eluent through a size exclusion column. Column eluent was collected over 30 fractions and the particle concentration (measured by NTA) was plotted against the protein content (measured by Nanodrop) of each fraction (A), ($n=3$). An equal amount of protein from fraction 2-28 was loaded for western blot analysis of exosomal markers CD9, CD81 and ALIX (B). The concentration of particles in each fraction was divided by the protein content of each fraction and plotted as the particle-to-protein ratio (C).

(A) NTA analysis of plasma-derived EVs isolated by direct ultracentrifugation (crude prep)

Sample Repeat	Concentration (particles/ml)	Mean diameter (nm)	Mode diameter (nm)
1	8.38×10^{11}	274	213
2	5.96×10^{12}	248	209
3	9.39×10^{11}	245	275
Mean	2.58×10^{12}	255.6±15	232.3±37

(B) NTA analysis of plasma-derived EVs isolated by size exclusion column chromatography (purified prep)

Sample Repeat	Concentration (particles/ml)	Mean diameter (nm)	Mode diameter (nm)
1	1.88×10^{11}	179	105
2	6.7×10^{10}	209	162
3	9.5×10^{10}	159	127
Mean	1.16×10^{11}	182.3±14	131.3±16

Table 3.2: Comparison of EV size and concentration of EVs following UC and SEC (A) NTA analysis of plasma-derived EVs isolated from direct ultracentrifugation of platelet-free plasma (crude prep). (B) EVs were isolated by SEC where 1 mL platelet-free plasma was loaded onto the column and fractions 5-10 were pooled and ultracentrifuged (purified prep).

3.4 Discussion

3.4.1 Main discussion

Key findings

- 3T3-L1 derived and plasma-derived EVs exhibit adipocyte and EV markers which were detectable by both western blotting and TRF-IA.
- TRF-IA was able to detect dual epitopes in the same EV sample posing the potential of double-labelling.
- Size-exclusion chromatography columns provide a convenient, reproducible and highly effective means of eliminating non-vesicular protein from complex bio-fluids such as plasma.

As discussed in detail in Chapter 1, adipocytes generate EVs as means of cellular communication for a range of metabolic functions. Adipocyte-derived EVs (ADEVs) were first characterised by Aoki et al. (2007) from 3T3-L1 adipocytes who reported the presence of several of integral, cytosolic and nuclear proteins as constituent components (Aoki et al. 2007). Their work formed the basis for identifying standard adipocyte EVs and to a lesser extent in the choice of adipocyte-specific protein markers to be tested in this thesis.

Extracellular vesicles are potential markers of human disease. To employ these vesicles in diagnosis, a simple and rapid method of simultaneously determining their size, concentration, and phenotype in bio-fluids such as plasma and urine is required. NTA was developed as an effective and efficient technique to serve this purpose. This technology, although relatively new, is well established in other fields including the measurement of engineered nanoparticles, protein aggregates, and viral particles. NTA offers distinct advantages over other methods EV quantification methods, such as flow cytometry (FC). The instruments for NTA are widely provided by the manufacturer NanoSight (Malvern UK) that states NTA can measure cellular vesicles as small as ~50 nm and there is broad agreement it more is sensitive than conventional flow cytometry, which typically has a lower limit of detection of ~300 nm. In this chapter, NTA analysis of plasma-derived EVs confirmed the presence of large vesicles with size >500 nm, but these were of a relatively low incidence compared to

the major population below 300 nm (**Figure 3.3(B)**). NTA has been reported to effectively categorise particle according to their size in a polydisperse sample with credible resolution (Gardiner et al. 2014; Vestad et al. 2017). EVs from plasma exhibited a wide distribution (50nm - 400nm) compared to 3T3-L1 EVs (50 - 270nm) indicated by a broader peak (**Figure 3.3**). It is important to recognise that the sample origin of 3T3-L1 derived EVs is a single cell type, hence exhibit tighter size range. On the other hand, the plasma EVs are sourced from different cells/tissues and thus, display a range of sizes and concentration that would depend on the plasma yield as well as the individual giving the blood sample (**Figure 3.3(B)**). As understood from the literature, much of the EV population from conditioned culture media and plasma fall within the size range of 50-300 nm and NTA has proven to be a useful tool in providing high resolution particle size and concentration distribution data by means of single particle (particle-by-particle) detection and analysis. Although the latest generation of high-resolution flow cytometers can detect beads as small as 100 nm and can discriminate these from 300 nm beads in a mixture, how these measurements relate to the minimum size of EVs that can be resolved must be interpreted with caution. FC relies on the refractive index of the analyte for accurate enumeration and sizing. EVs have a lower refractive index compared to latex or polystyrene beads, and this discrepancy could lead to an underestimation of their size and concentration (Dragovic et al. 2011). Because NTA determines particle size from Brownian motion, it is independent of the refractive index of the particle (Filipe et al. 2010). To overcome this challenge, tagging EVs with beads with a view to increasing its size for detection by FC has proved promising (Suárez et al. 2017; Volgers et al. 2017). Although NTA can analyse particles as large as 1 µm in diameter (above this the Brownian motion is too slow to measure), with large number of small vesicles in these preparations, the sample may require dilution prior to analysis. The effect of this is that the number of large vesicles analysed is significantly reduced, which means their concentration will be underestimated. Thus, studies of large vesicles (>500 nm) alone (e.g. apoptotic bodies) may be better carried out by flow cytometry than by NTA. The limitation of NTA lies in its inability to determine the phenotype of the vesicles. Biological fluids such as plasma and urine will inevitably contain mixtures of vesicles derived from different cell types. It is, therefore, crucial to be able to determine the cellular origin of the vesicles and, the molecules that they express on their surface to understand their biological function. Newer generation of NTA instruments allow the

use of 1–2 lasers for measuring fluorescence-antibody tagged vesicles (Backmark et al. 2013; Wang et al. 2016).

The immunoassay used in this study is based on time resolved fluorescence (TRF) which is highly sensitive in detecting even low concentration proteins (Hagan and Zuchner 2011). Especially, the use of europium lanthanide greatly amplifies the fluorescent signal and their lifetime is more protracted than the conventional fluorescent probes. The in-house developed TRF-IA was employed to analyse the proteins expressed on the 3T3-L1- and plasma- derived EVs based on earlier work by colleagues in cancer cell-derived EVs (Webber et al. 2014). CD9 and CD63 are tetraspanins frequently used to identify EVs. The detection of tetraspanins in an EV sample forms part of the guidelines for the minimal requirements for an EV population as set out by ISEV (Mateescu et al. 2017). Here, EVs collected from both 3T3-L1 cells and plasma showed the presence of these tetraspanins markers by both western blotting (**Figure 3.4 (A) & (B)**) and TRF-IA (**Figure 3.5 (A) & (B)**). As an endocrine organ, adipose tissue releases a host of hormones and signalling molecules, termed adipokines. A range of adipokines are expressed at different stages of adipogenesis (the transition from a pre-adipocyte to a mature adipocyte). Certain adipokines/adipocyte-associated proteins were selected as markers for adipocyte character on EVs as detected by TRFIA. FABP4 is predominantly expressed by adipocytes and has been implicated in obesity and associated co-morbidities, such as type-2 diabetes and cardiovascular diseases (Garin-Shkolnik et al. 2014; Rodríguez-Calvo et al. 2017). Adiponectin is also predominantly expressed in adipocytes and is strongly involved in lipid metabolism, glucose regulation and maintenance of insulin sensitivity (Robinson et al. 2011). The expression of both FABP4 and adiponectin increases as adipocytes undergo adipogenesis (Connolly et al. 2015). However, both FABP4 and adiponectin are released in a soluble form and can be detected in plasma. A small proportion also is derived from other cell types, namely macrophages /leukocytes (Furuhashi et al. 2008; Agardh et al. 2013; Steen et al. 2016) and therefore, although highly indicative of adipocyte character, these markers cannot be considered unique in isolation. PPAR- γ is an essential nuclear transcription factor in the initiation and maintenance of adipogenesis by activating key transcription factors associated with fat accumulation and a mature adipocyte phenotype. The level of PPAR- γ remains constant in the cells from the differentiating pre-adipocyte through

to maturation (Ahmadian et al. 2013; Connolly et al. 2015). There are two isoforms of PPAR γ , with PPAR- γ 2 being unique to adipocytes (Tontonoz et al. 1995). Western blot and TRF-IA analysis conducted on the EVs harvested from 3T3-L1 cells and plasma substantiates the presence of these adipocyte proteins in the EV sample (**Figure 3.4 and Figure 3.5**).

A typical plasma-derived EV sample contains vesicles primarily sourced from platelets, leukocytes, endothelial and erythrocytes (Orozco and Lewis 2010; Nielsen et al. 2014). The CD markers provide hallmarks in identifying populations of EVs from different cell sources. The chosen CD markers should be unlikely to exist as free proteins and ideally be definitive to the tissue/cell i.e.: CD41 for platelets, CD11b for monocytes, CD144 for endothelial cells and CD235a for erythrocytes. They are transferred to the corresponding EVs during their release from the cell; hence provide a unique tag to identify populations of EVs in a mixed isolate. The experiments performed in this study proved effective in the detection of classical blood component markers, CD41, CD11b, CD144 and CD235 in the plasma-derived EV prep, inferring the cellular source of EVs (**Figure 3.5 (D)**). The results also inferred that different markers on each EV can be detected in a mixed EV population. This could potentially lead to the development of an array-based system for the simultaneous isolation and detection of EVs from varying cellular origin. It also gives an indication of the ratio of the different EV source populations in a defined sample. The results obtained are in agreement with previous work from our laboratory (and that of others) in determining the primary EVs in plasma as being platelet-derived and erythrocyte-derived EVs being the least populous (Orozco and Lewis 2010; Nielsen et al. 2014; Willis et al. 2014; Witczak et al. 2017; Connolly et al. 2018).

The isolation procedure for EVs has been a long-debated issue and researchers have developed different approaches (Szatanek et al. 2015). At the outset of this study differential UC remained the standard and widely applied technique for the isolation of EVs from cell culture conditioned media. Some researchers had suggested using a combination of techniques coupling UC with filtration, density gradient separation or magnetic bead capture (Gardiner et al. 2016). However, an unfavourable aspect of UC is the contamination by non-vesicular particles or macromolecules, which may give false estimations of particle concentration in EV samples, contaminate further downstream analyses (e.g. analysis of protein, lipid mRNA, miRNA content of EVs)

and interfere with functional studies using EVs (Webber and Clayton 2013; Van Deun et al. 2014). UC can also cause aggregation of EVs which may reduce their overall concentration, epitope availability and functionality (Linares et al. 2015).

SEC was recently proposed as a novel method to purify EVs from blood plasma (Böing et al. 2014; Welton et al. 2015). Column chromatographic approaches offer a simple and efficient method for vesicle enrichment from complex biofluids. Pre-made commercially available columns offer the advantages of convenience and importantly, reducing variation between columns to provide consistency in EV separation. Following significant characterisation of the system, the rather arduous workflow of collecting multiple column fractions can be streamlined to collecting only the eluate fractions of interest. This can be achieved in around 10-15 minutes which makes this a viable method in the context of multiple clinical samples. Co-elution of plasma proteins and certain lipoproteins, some of which share the same physical properties as EVs, is a common trait in the processing of plasma-derived EVs (Yuana et al. 2014; Sódar et al. 2016; Simonsen 2017), thus, it was decided to perform the molecular characterisation of isolated vesicles by analysing total protein content, particle population profiles (NTA) and confirmation of EV markers by western blotting. The columns demonstrated good utility as a simple and rapid tool separating most plasma proteins in a single step. With plasma EV loaded on SEC, fractions 5-10 consistently contained the highest particle-to-protein ratio, expressed exosomal markers including CD9 and CD63, and were separate to the most abundant proteins peak (**Figure 3.7**). Hence, pooling fractions 5-10 yielded a selective vesicle-rich, low-contaminant sample of robust quality for downstream applications. Unlike the column elution of plasma, there was no additional peak to indicate the presence of substantial 'free' protein or particulates while purifying 3T3-L1 EV sample prepared after resuspending UC pelleted EVs. This suggests that the resuspended pellet after UC of cell supernatant predominantly contains EV and negligible amount of free protein contaminants. Thus, the mode of isolating EVs from 3T3-L1 culture media by ultracentrifugation was considered robust and was used throughout this thesis.

Research studies have demonstrated that SEC is a suitable option for obtaining purified vesicle preparations that retain morphology and phenotype (Muller et al. 2014a; de Menezes-Neto et al. 2015; Gámez-Valero et al. 2016). Importantly in the context of my research SEC was able to yield an EV sample exhibiting EV markers

and expressing epitopes that were highly characteristic of adipocyte character. In conclusion, SEC is in itself a method of EV isolation and sample purification.

The concentration of vesicles measured by NTA when isolated by UC shows a dramatic increase when compared to the isolate harvested from SEC fractions (**Table 3.2**). This could be because the UC co-pellets free circulatory proteins and lipoproteins with EVs, which was observed during SEC in the later fractions (past fraction 10). In addition, it appears that the greater EV number in UC as compared to SEC is because SEC has eliminated free proteins which are being counted by NTA in UC samples. Although the apparent yield of EVs from SEC is lower, it grants an effective means of isolating EVs from non-vesicular protein in biological fluids. It further highlights the importance for consideration of the method utilised for pre-analytical processing for EV isolation as each method gives varying purities of EVs.

Overall, the 3T3-L1 derived EVs showed heterogeneity in size and displayed the classical EV markers as well as protein markers consistent with an adipocyte origin. Thus, the data confirms the adipocyte cell line 3T3-L1 secretes a significant amount of EVs that can be considered to be a pure ADEV population for control experiments and comparison in future experiments. Importantly, blood plasma contains EVs from different tissue sources and yet it was possible to detect the same panel of adipocyte-specific markers that were found in 3T3-L1-derived EVs, implying the presence of adipocyte-derived EVs in circulating plasma. My results also confirmed that the TRF-IA was able to differentiate sub-populations of EV epitopes and pointed the way forward to specifically 'select-out' ADEVs from the mixed sample prep. The work therefore forms the basic groundwork for achieving the long-term objectives of the project.

3.4.2 Limitations and Conclusion

At this point of my studies, no primary (human) cell line had been used. 3T3-L1 cell line is derived from mouse but has been well characterised and has been an established model to study adipogenesis and adipocyte-related biology/disease. Hence, they are considered a positive control and an appropriate model system in this study. However, the adipocyte and exosomal markers used here are also present in primary adipocyte derived EVs (M. E. Kranendonk et al. 2014; M. E. G. Kranendonk et al. 2014).

Isolation of EVs has always been a cause for debate and regularly updated based on new evidence-based findings. Studies have argued large vesicle populations may be lost by differential centrifugation, which may lead to significant loss of target EVs (Aatonen et al. 2014; Livshits et al. 2015). Hence, further research is required to improve techniques for the isolation and the purification of EVs from different biological sources. In the case of EV isolation from blood/plasma, the basic techniques of UC are not efficient enough to deplete free proteins/contaminants. The EV prep can contain relatively large amounts of free protein/contaminant which can compromise the molecular detection-based techniques. Hence, the use of SEC columns provides a valuable tool in enriching the EV sample. A shortcoming of this technique in filtering out free proteins is the fact there is a considerable loss of particles when compared to isolation by UC. With the extent of EV size range, some EVs could be excluded along with the other contaminant proteins, thus compromising on EV concentration. It can be argued that the increased EV/particles in UC prep as counted by NTA could be free circulatory proteins that have compromised the purity. Whilst the column method is successful in significant clean-up of blood proteins, some optimisations are certainly still required to concentrate selectively, and to minimise vesicle losses during subsequent handling steps. Purification techniques prior to evaluating EVs by TRF-ELISA should be an integral step in the experimental set up, which has been addressed in the chapters following.

Another limitation lies in the TRFIA assay, wherein the assay does not confer an account on EV enumeration, rather gives a relative proportion of the protein markers in a defined number of EV. Thus, there has been no single standard technique for evaluating EVs of a unique source or character, and a combination of techniques may be the most appropriate approach.

NTA cannot discriminate vesicles from non-vesicular particulate material; and here we have assumed that all detected particles are vesicles. This assumption may be unfounded, as there may be protein aggregates, and large crystals of salts and other components present giving us an overestimation of the true number of vesicles present. We anticipate that as this technology platform evolves, particularly in relation to its capacity to measure fluorescent particles, future approaches will be able to discriminate vesicles from aggregated material, and aid in the refinement of our proposed method. These results stress that appropriate EV-isolation method should be considered and will vary depending on the intended application of the purified EV sample.

4. Results II: EVs with adipocyte character in circulation

4. Perspective

Development of an efficient methodology to specifically isolate adipocyte-derived EVs (*or EVs of adipocyte character*) from a mixed population is the primary focus. Hence, the strategic development of an EV purification technique will inform this overall goal directly. Clearly the greatest challenge is in ensuring the markers we have associated with adipocyte character are indeed bound to or within the EV, as opposed to free soluble protein being loosely associated or co-isolated in the preparation protocol. This is particularly important in the context of plasma that contains a large number of potential contaminant proteins.

Based on the findings of chapter 3, it was understood that the EV isolate obtained from ultracentrifugation was a ‘crude’ prep. Hence, SEC separation was necessary to remove much of the protein contaminants that infiltrated through the UC. Also, recognising that ultracentrifugation as a means of EV isolation from plasma would procure EVs from all cell types, it was then necessary to investigate ways to selectively gather adipocyte-derived EVs from the mixed population of EVs. Hence, I decided to employ two well characterised approaches based on immunoaffinity (antigen-antibody interaction), namely magnetic bead and solid phase capture technique, to selectively isolate and purify an EV sample to conclusively obtain semi-purified adipocyte-derived EV fraction from plasma.

4.1 Introduction

Ultracentrifugation is undoubtedly the favoured and commonly adopted technique for EV isolation. However, the drawback of the technique is that as it pulls down the total population of EVs, it cannot discriminate based on their size (exosomes (30-100 nm) and microvesicles (100-1000 nm)) or phenotype (EVs secreted by different cellular mechanisms) or particles other than EV. Antibody-based techniques could potentially overcome this limitation due to the principle of immunoaffinity where the antigen-antibody binding is highly specific. Isolation of EVs based on the principle of immunoaffinity has been an attractive strategy, also capable of characterising EVs in terms of size distribution, enumeration, protein composition, and intravesicular cargo (Li et al. 2017a). It can further provide information on EV functionality and their potential use as biomarkers for the identification of diseases. The technique recognises the surface antigen present on EVs typically using magnetic beads coated with an antibody against the target protein. Commercially available beads bound to specific exosomal markers (e.g., CD9, CD63, and CD81) allow the separation of subpopulations of EVs. Similarly, these antibody-bound immunomagnetic beads allow purification of EVs expressing cell-specific target markers, allowing the selective isolation of EVs derived from a single cell type. In other words, this design of the technique excludes the capture of those EVs that fail to express a particular surface protein/marker of interest. The advantage of this method lies in the EV yield being pure and homogeneous (Mathivanan et al. 2010; Tauro et al. 2012).

Antibody-coated magnetic bead isolation of EVs for antigen presenting cells has been shown by Clayton *et al.* (2001). Immunoaffinity capture microbeads was successfully used to capture exosomes from a tumour cell line and further utilised for proteomic studies (Mathivanan et al. 2010). Circulating tumour-derived EpCAM-positive EVs were isolated using magnetic beads coated with anti-EpCAM antibody (Taylor and Gercel-Taylor 2008). Antibody-coated magnetic beads are a promising strategy to isolate and characterise EVs; however, they cannot be utilised for the isolation of large amounts of EVs. Hence, a pre-concentration step is considered to scale down the initial sample (Momen-Heravi et al. 2013). Immunoaffinity based isolation of exosomes using antibody-coated magnetic beads against specific antigens offers the advantage of their further characterisation in flow cytometric, immunoblot, and electron microscopic analysis of bead-EV complexes. However, elution of the captured EVs

from the bead surface may distort their functionality in some instances (Théry et al., 2006).

Likewise, the immunoassay principle can also be applied in a 96-well immunoassay plate. Plates are typically pre-coated with a capture antibody to isolate EVs with the selected antigen and subsequent detection with another set of antibodies, executing a sandwich immunoassay mechanism. It facilitates an enrichment procedure for isolating subpopulations of EV in addition to providing a quantitative and qualitative analysis of captured EVs. ExoQuant™, ExoPure™ and ExoAssay™ (Biovision, USA) have developed kits that consists of ELISA plates pre-coated with exosome antibodies that enable specific capture of exosomes sourced from different biological samples, including cell culture supernatants and human biological fluids. Subsequently, quantification and characterisation of exosomal proteins is performed using appropriate detection antibodies against exosome associated antigens that can be for either generic or cell/tissue-specific exosomes (Zarovni et al. 2015; Brett et al. 2017). Hansabiomed (Lonza), a scientific company has designed different types of plates for capturing the overall or enriching specific exosome subpopulations (tumour, neural, glial, monocytes and platelets). Some of the advantages of using immunoplates are that the assay requires small amounts of sample (100-200ul); the setup is stable for a long period of time and further allows multiple profiling of EV markers from a single sample. They do not induce any molecular changes to the vesicles and the enriched sample can be processed for downstream analysis of RNA/protein. These immunoplates can be custom developed to cater for the capture of selective EV population based on their antigenic marker protein. Besides offering the advantage of high sensitivity and specificity, the antibody-based assay has been developed for its potential to perform multiplexed phenotyping of EVs.

There has been mounting evidence for the generation of EVs from adipocytes; most studies in this context are conducted using the 3T3-L1 cell line model. Recently, EVs have been isolated from human adipocytes and adipose tissue explants. Research studies have highlighted the endocrine and paracrine role of ADEVs in adipocyte metabolism, tissue inflammation, macrophage induction and insulin signalling. EVs originating from adipocyte or adipose tissue (AT) may mediate the promotion of tumour metastasis (Lazar et al., 2018), and may also be involved in angiogenesis since they carry bioactive molecules in their cargo and travel through the circulation to

induce signalling cascades in target/recipient cells. However, their presence in the human circulation has not yet been definitively established. There has been some preliminary evidence from flow cytometric analyses that plasma contains ADEVs, as evidenced by expression of FABP4 and PREF-1 (Gustafson et al. 2015b). Other studies have associated EVs with the presence of perilipin and PPAR- γ . Populations of EVs are pre-dominantly derived from platelets and leukocytes and to a lesser extent from endothelial cells and erythrocytes. Lack of a signature protein marker/markers and an optimal technique fail to distinguish ADEVs readily in plasma. Therefore, there is a compelling need to seek evidence for the presence of ADEVs in the circulation, in order to explore their potential as a novel biomarker in adipose tissue health.

This chapter explores two approaches, magnetic bead capture and solid phase immunoassay, to selectively enrich a population of particles positive for EV markers (CD9, CD81, CD63 or Alix) and adipocyte specific proteins (FABP4, adiponectin, PPAR- γ , perilipin and other relevant adipokines). Nanosight tracking analysis (NTA), Time resolve fluorescence immunoassay (TRFIA) and western blot are the underlying techniques used to assess EV characteristics.

4.1.1 Overall Aim:

To develop an approach to provide evidence for the presence of adipocyte -derived EVs in the human circulation.

Objectives:

1. Validation of magnetic bead capture and solid phase assay techniques to specifically deplete an EV population.
2. Sequential removal of EV populations (platelets-, leukocytes-, vascular endothelial- and erythrocyte-derived) by magnetic bead and solid phase capture methods to obtain a purified sample ('residual' sample).
3. Assess the purified (residual) sample for adipocyte markers (FABP4, adiponectin, perilipin and PPAR- γ) and exosomal markers (CD9, Alix, CD81, CD63).

4.2 Methods

4.2.1 Isolation of extracellular vesicles and plasma-derived EVs

3T3-L1 cells were cultured to mature adipocytes as described in Chapter 2.1.1 and EVs were isolated by differential UC as described in Chapter 2.2.1. In addition, SEC was also used in the isolation of plasma EV, as per the procedure outlined in Chapter 2.8.

Plasma-derived EVs were obtained from blood of healthy volunteers as described in Chapter 2.2.2 by differential UC. Additionally, in this chapter, EVs were isolated and purified from plasma by size exclusion chromatography, as per the procedure outlined in Chapter 2.8. EVs were resuspended in 100 μ l of 1X PBS.

4.2.2 Nanoparticle Tracking Analysis

The concentration of cell-derived and plasma-derived EVs were determined by NTA procedure as described in Chapter 2.3.2. Company (Nanosight)-provided 100nm sized beads were used as calibration beads and indicated a mean concentration of $1.77 \times 10^{11} \pm 0.06$ between the batches of experiments.

4.2.3 Selective capture of EV populations

Magnetic bead capture and solid phase immunoassay were used to selectively capture EVs positive for a protein marker. The procedures are detailed in Chapter 2.10. The magnetic bead capture technique to isolate EVs exhibiting a particular CD epitope/protein marker is an established method for isolation of specific cell types. The concept was of particular interest to us because it was hypothesized that the same primary antibodies used for TRF-IA could also be utilised in this capacity. To be noted, the term 'selective capture' is interchangeably used with the term 'selective depletion' or to understand the concept better under different contexts.

4.2.4 Detection of proteins in EVs

Protein markers in EVs were detected using TRF-IA and western blotting, conducted as outlined in Chapter 2.4 and Chapter 2.7, respectively. Antibody control experiment under the absence of a primary antibody was not conducted during the protein detection stage.

4.2.5 Adipokine array

Plasma EVs were probed for adipokines using a commercially available array kit, and protocol is outlined in Chapter 2.9.2.

4.2.6 Sequential depletion of EV population

Following SEC and UC of the pooled EV, they are diluted to a final concentration of 1×10^{11} particles/ml with 1X PBS. EVs were incubated with anti-CD41 for 2 hours at room temperature at a final concentration of 3µg/ml. 50µl of prepped Dynabeads (outlined in Chapter 2.10.1) were then added and incubated for a further 30 mins with gentle mixing. Samples were then placed on the magnet (DyanMag™, Life Technologies) to deplete the CD41+EV. The process was sequentially repeated with the addition of 3µg/ml anti-CD11b, anti-CD144 and anti-CD235a to consequently deplete EV population positive for these markers. Final supernatant, referred as the 'post-depleted sample' was examined for adipocyte and EV-specific markers.

4.2.7 Statistical Analysis

Statistical analysis was conducted by GraphPad Prism version 5.0 (GraphPad Software, San Diego, USA). Paired t-tests were used to compare means where significance was marked by * reflects $p < 0.05$, ** reflects $p < 0.01$ and *** reflects $p < 0.001$. One-way ANOVA with Tukey's Multiple comparison test was used to determine significant differences between groups. Data is expressed as mean \pm SD, where applicable.

4.3 Results

4.3.1 Magnetic bead capture of selective EV population

At this stage of the work, the EV sample was isolated by ultracentrifugation without column purification and herein referred to as 'crude' prep. The change in EV concentration after the bead capture was measured by NTA and the percentage decrease calculated from the total number of EVs in the original sample, i.e., the amount (expressed as percentage) EVs decreased following magnetic bead capture of a defined EV subtype. TRFIA experiments were also conducted on the sample prior (pre-) and after (post-) capture by the magnetic beads. Calibration beads of 100nm varied with

With respect to 3T3-EVs, the difference in the concentration of the sample was measured by NTA (**Figure 4.1 (A)**). There was a mean decrease of ~64% in EV concentration following bead capture based on CD9 as the primary capture antibody. FABP4 bead capture resulted in the loss of nearly ~60% EVs, compared to the starting concentration. Both the drop was deemed significant with $p < 0.0005$). The results are shown in **Figure 4.1(B)** also indicates a drop in protein signal readings.

As with plasma-derived EVs, the NTA readings indicated a ~62% capture for CD9+ve EVs and resulted in a ~35% capture when probed for FABP4+ve EVs with magnetic beads (**Figure 4.1 (C)**) which is also indicated by TRFIA (**Figure 4.1 (D)**).

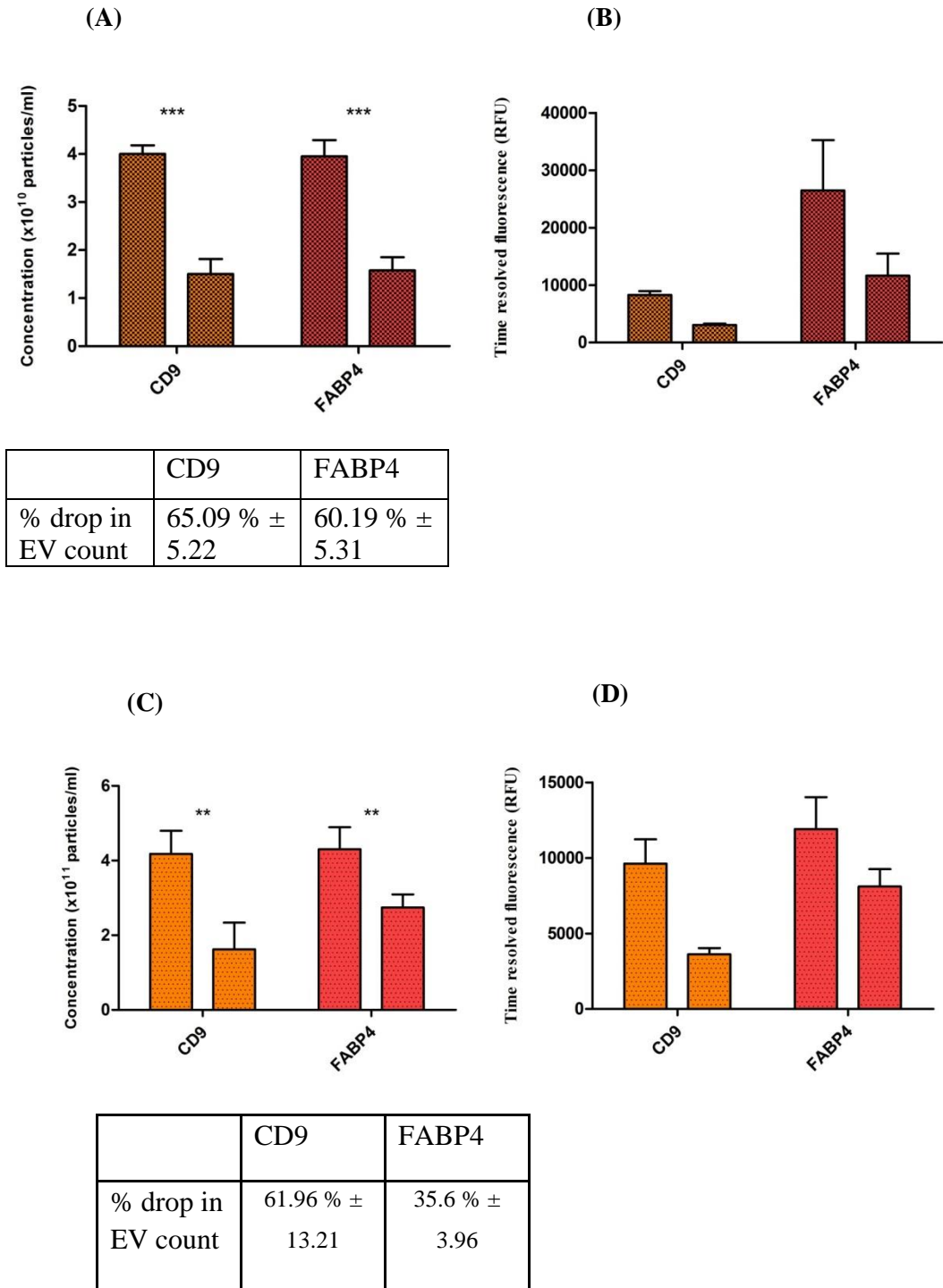


Figure 4.1: Analysis of magnetic bead capture by NTA and TRFIA in crude prep. In separate experiments, magnetic bead capture for CD9+ and FABP4+ EVs was conducted on 3T3-L1 EVs and plasma-EVs and examined for particle count and protein signal drop by NTA and TRFIA, respectively. **(A)** and **(C)** indicating change in EV concentration measured by NTA pre- & post- bead capture in 3T3-L1 and plasma-EVs respectively, significance marked by*** $p < 0.001$, ($n=5$). **(B)** and **(D)** show TRFIA conducted on pre- & post- bead capture with CD9 and FABP4 antibody in 3T3-L1 and plasma-EVs respectively, showing a change in fluorescence signal ($n=3$).

Further, to examine if the FABP4 capture affected other populations of plasma EVs, TRFIA probing for CD235, CD11b, CD144, CD41 was carried out pre- and post- bead capture (**Figure 4.2**). The graph shows a modest and consistent decline in all EV populations of ~10%. This could be the result of (a) free FABP4 from the circulation (plasma) contaminating the EV preparation or (b) free FABP4 in the circulation covalently binding to other EV species, causing them to be pulled out. Among the EV population, endothelial EVs (CD144) were found to visibly but not significantly, decreased ($p>0.05$). To test if this was the result of non-specific binding by magnetic beads, magnetic bead capture was carried out on 3T3-EVs using CD9 as a positive capture control followed by TRFIA (re-probed for CD9) on the residual sample to measure the loss. (**Figure 4.3**). Following a magnetic bead capture for CD9+ EVs, the residual EV samples were incubated with normal IgG, non-specific Ab and anti-CD9 (specific). The sample incubated with anti-CD9 showed a marked decrease whilst EVs with beads (no antibody) also showed a slight 10% decrease; this might be attributable to some non-specific binding taking place (**Figure 4.3**).

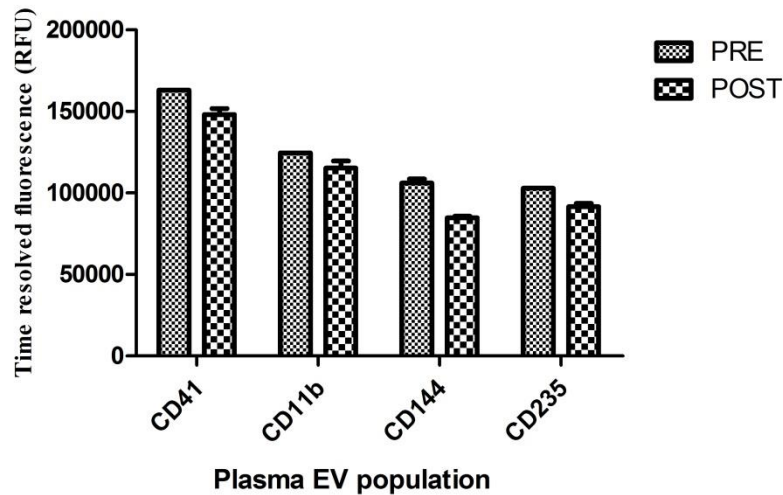


Figure 4.2: Effect of FABP4+ve EV pullout on plasma EV populations. Plasma derived EVs were subjected to a FABP4+ EV pull-out by magnetic beads and TRFIA was conducted on the initial and residual sample to observe any change in EV sub-population markers, $n=3$.

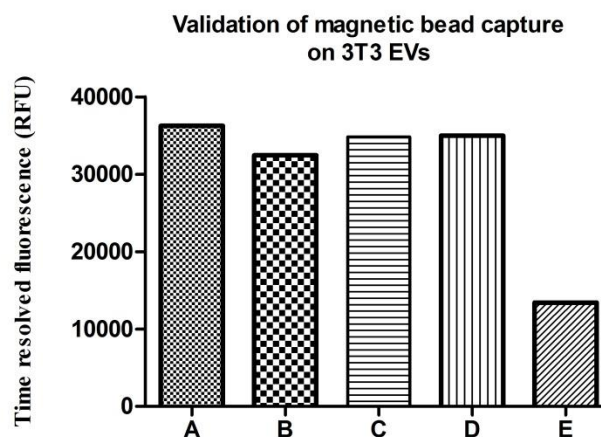


Figure 4.3: Control experiment of on 3T3-EVs through a CD9+ magnetic bead capture. The experiment was designed to validate non-specific binding by magnetic beads in the absence of an initial primary antibody interaction, by setting five conditions namely **A**: EV (control), **B**: EV+beads, **C**: EV+normal IgG+beads, **D**: EV+non-specific primary Ab+beads **E**: EV+specific anti-CD9+beads ($n=2$). **E** showed a visible decrease, indicating the system had successfully pulled out CD9+ EVs where a decrease in **B likely** reflects occurrence of non-specific binding. No statistical testing was undertaken due to the low number of biological replicates.

4.3.2 Effect of magnetic bead capture on column purified EV samples

In this section of work, the EV samples were isolated by SEC followed by UC as discussed in Chapter 3 (Section 3.3.6.2). EV sample obtained post SEC was subjected to magnetic bead capture for CD9+ and FABP4+ EVs in separate experiments, followed by TRFIA validation (**Figure 4.4 (A) and (B)**). Similarly, plasma EVs isolated by SEC was subjected to either CD9 or FABP4+ve capture. These results are shown below (**Figure 4.4 (C) and (D)**).

Interestingly, after the column purification the extent of CD9+EVs pulled out by the beads was shown to increase in the case of 3T3 EVs (**Figure 4.4 (A) and (B)**) from previously ~65% (**Figure 4.1 (A)**) in the “crude” preparation to ~72% in the post-column sample(* $p < 0.05$). Similarly, in the case of plasma EVs, there was an additional 6% increase in the pullout of CD9+ EVs to 66% when compared to the previous “crude” non-columned preparation at ~60% (**Figure 4.4 (C)**). However, the FABP4+ EVs captured in plasma EVs was drastically reduced to ~10% (**Figure 4.4 (C)**) in the columned prep when compared to a previous drop of 35% in the “crude” preparation (**Figure 4.1 (C)**). This could mean the additional EVs / particles captured in the crude sample were potentially free protein that contaminated the EV prep. While this part of the work was undertaken using the SEC purified EV prep, whether these EVs are purely adipocyte-derived or not requires further investigation by probing for other adipocyte markers on these captured EVs.

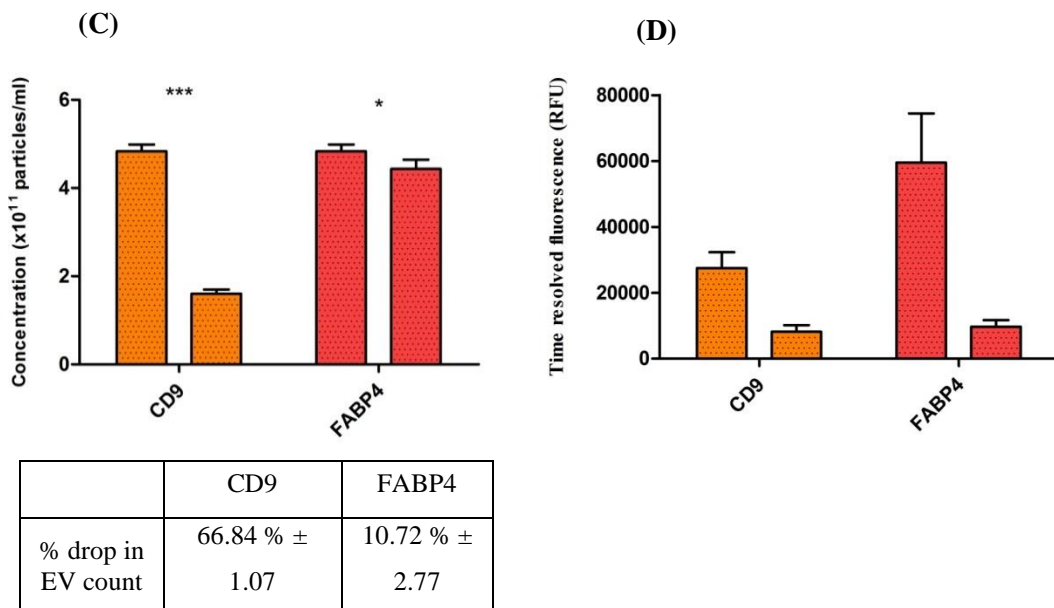
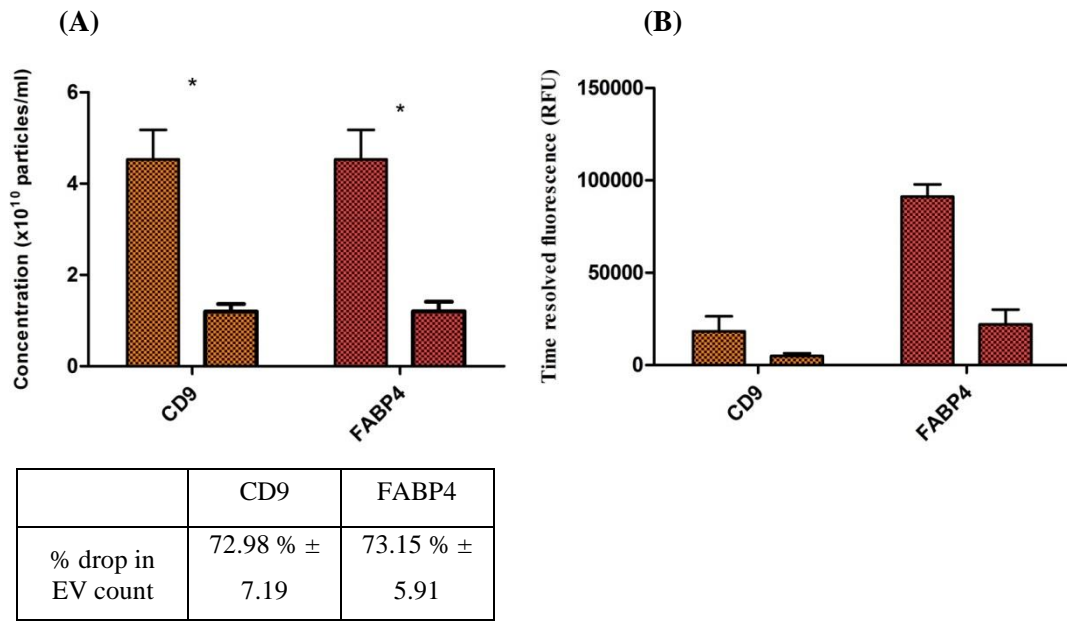


Figure 4.4: Evaluation of CD9+ve and FABP4+ve magnetic bead pullout on 3T3-derived and plasma-derived EVs post column (SEC) purification. Samples of EVs were incubated with anti-CD9 and anti-FABP4, pulled out with the secondary antibody bound-magnetic bead, and residual sample was reprobred for CD9 and FABP4 to evaluate the loss. The concentration of EV samples pre- and post- pull-out by was determined by NTA (A) and (C) for 3T3- and plasma- derived respectively whereas (B) and (D) shows TRFIA signal generated for CD9+ and FABP4+ in pre- and post- samples from 3T3- and plasma- derived respectively.

Although the adipokine FABP4 is pre-dominantly released by adipocytes, FABP4 expression has been demonstrated in several types of cells and tissues (Lee et al. 2014a; Fuseya et al. 2017). For example, FABP4 and FABP5 are expressed in macrophages and dendritic cells, though their concentration is much lower than in adipocytes (Furuhashi et al. 2014). Moreover, FABP4 exist in circulation and their levels are elevated in disease conditions.

Under these arguments, FABP4 alone cannot therefore confirm the EVs as adipocyte in origin. In addition, adiponectin and PPAR-gamma are not transmembrane proteins that can be probed by external antibody. Therefore, I employed a strategy to sequentially deplete the known major populations of circulating EVs (platelet-, endothelial-, leukocyte-, and erythrocyte- derived) in order to further purify the EV preparation for detection of ADEVs. A solid phase immunoassay was undertaken to capture a pool of EVs positive for certain markers using antibodies immobilised on an ELISA plate (detailed in Chapter 2.10.2).

The efficiency of the depletion process on individual markers was undertaken as an initial measure to validate how much of the target EV pool remained post-magnetic bead and post-solid phase removal. This was undertaken on a column-purified plasma EV sample. The expression of each marker used for depletion was reduced by both methods. With the magnetic bead-based approach, markers were depleted to beyond the detection limits of time resolved fluorescence (**Figure 4.5 (A) (B)**).

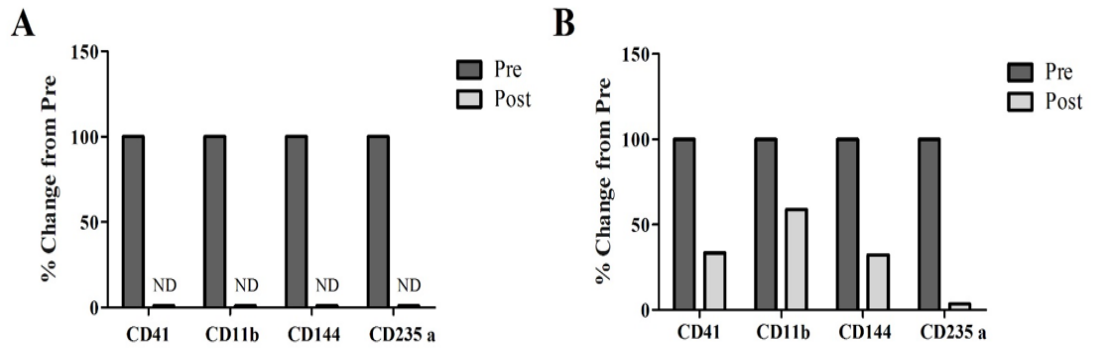


Figure 4.5: Validating efficiency of magnetic bead and solid phase assay in depleting EV-sub population. Equal numbers of EVs were immobilised onto ELISA plates pre- and post-CD41, -CD11b, -CD144 and -CD235a depletion using magnetic beads (**A**) and solid phase capture (**B**). Pre and post samples were assessed by TRFIA for the presence of the depleted marker and plotted as a percentage of the “Pre” sample fluorescence. ND = not detected, ($n=2$).

4.3.3 Analysis of plasma-derived EVs using size-exclusion chromatography

To address the issue of contamination by soluble free plasma proteins, platelet-free plasma was subjected to size exclusion column chromatography to obtain a more enriched EV sample. Although EV isolation by SEC was established earlier in Chapter 3.3.6.2, this further examined adipocyte specific proteins in column fractions.

NTA of column fractions showed a minor peak (expressed as concentration of particles/ml) between fractions 5-10, followed by a major peak in particle/ml and protein from fractions 11 through to 30. Western blot on all fractions detected the adipocyte-selective protein markers FABP4, adiponectin, PPAR- γ and perilipin in fractions 5-30, whereas both adipocyte and EV marker proteins were exclusively found in fractions 5-10 (**Figure 4.6**). EV markers CD9, CD81 and Alix were absent from fractions 11 to 30.

A plot of particle-to-protein concentration ratio was generated as previously described (Webber and Clayton 2013). This showed a high value in fractions 5-10 (**Figure 4.7 (A)**). The column eluents from these fractions (5-10) were thus pooled and centrifuged to pellet plasma-derived EVs (pooled EV prep). TEM on the pooled EV sample was conducted by my colleague Dr Katie Connolly, who also helped in part developing this chapter. **Figure 4.7 (B)** demonstrated the presence of EV structures. The pooled EV prep was then subjected to western blot analysis which indicated the presence of classical EV and adipocyte markers (**Figure 4.7 (C)**).

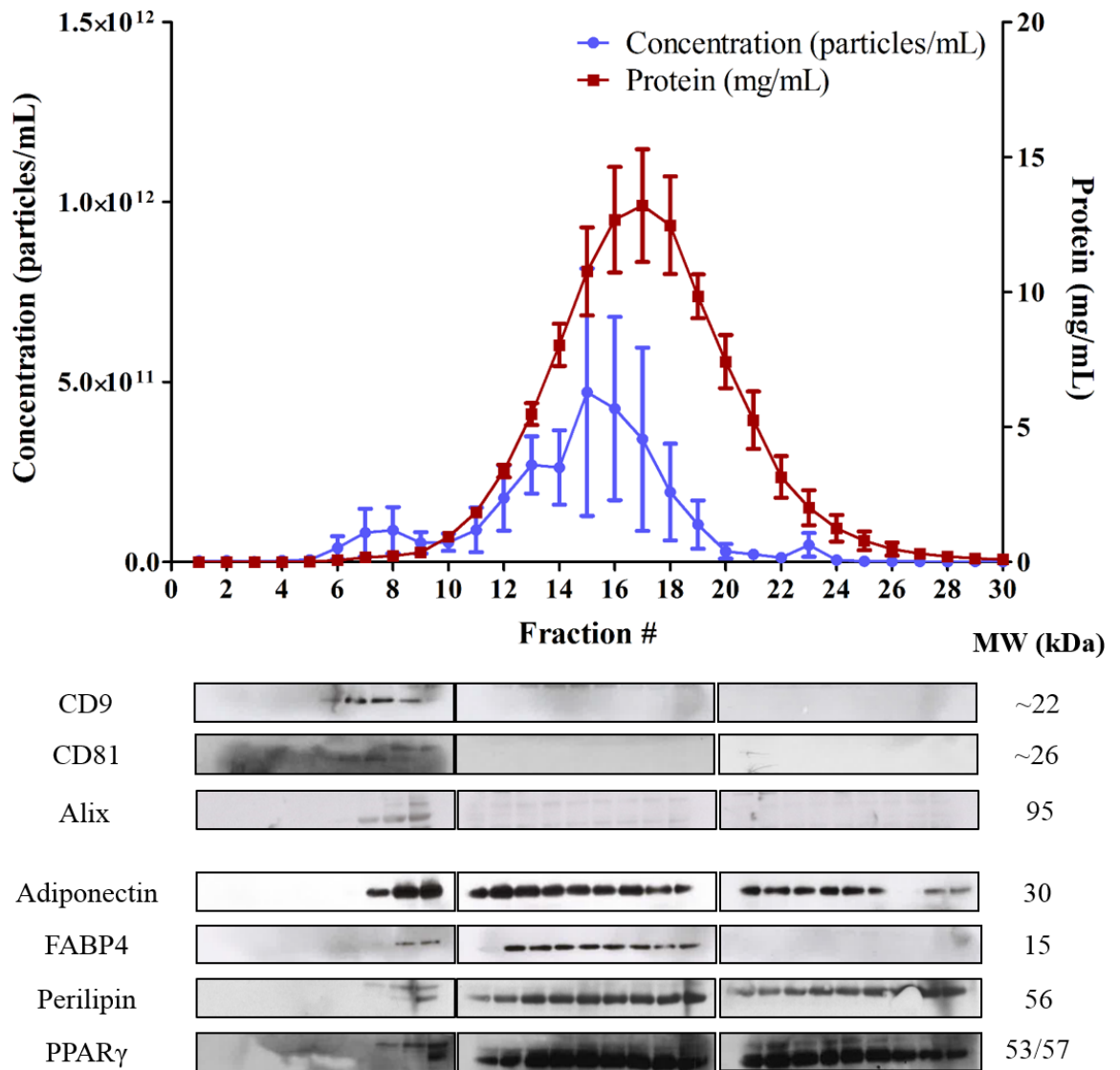


Figure 4.6: Evaluation of human plasma on SEC. Thirty of 500 μ l fractions were collected after loading 1ml plasma on SEC and these eluents were examined for particle concentration using NTA and the protein concentration measured using Nanodrop for each fraction. The fractions were then analysed by WB (8 μ g/lane) for the EV markers: CD9, CD81 and Alix, and the adipocyte markers: Adiponectin, FABP4, Perilipin and PPAR γ . The small peak in particle concentration from fraction 5-10 coincides with the presence of EV and adipocyte markers. The adipocyte markers begin to appear from fraction 5 through to fraction 28. However, fractions 11- 30 show absence of EV markers but presence of adipocyte markers ($n=3$). [Published image: (Connolly et al., 2018)]

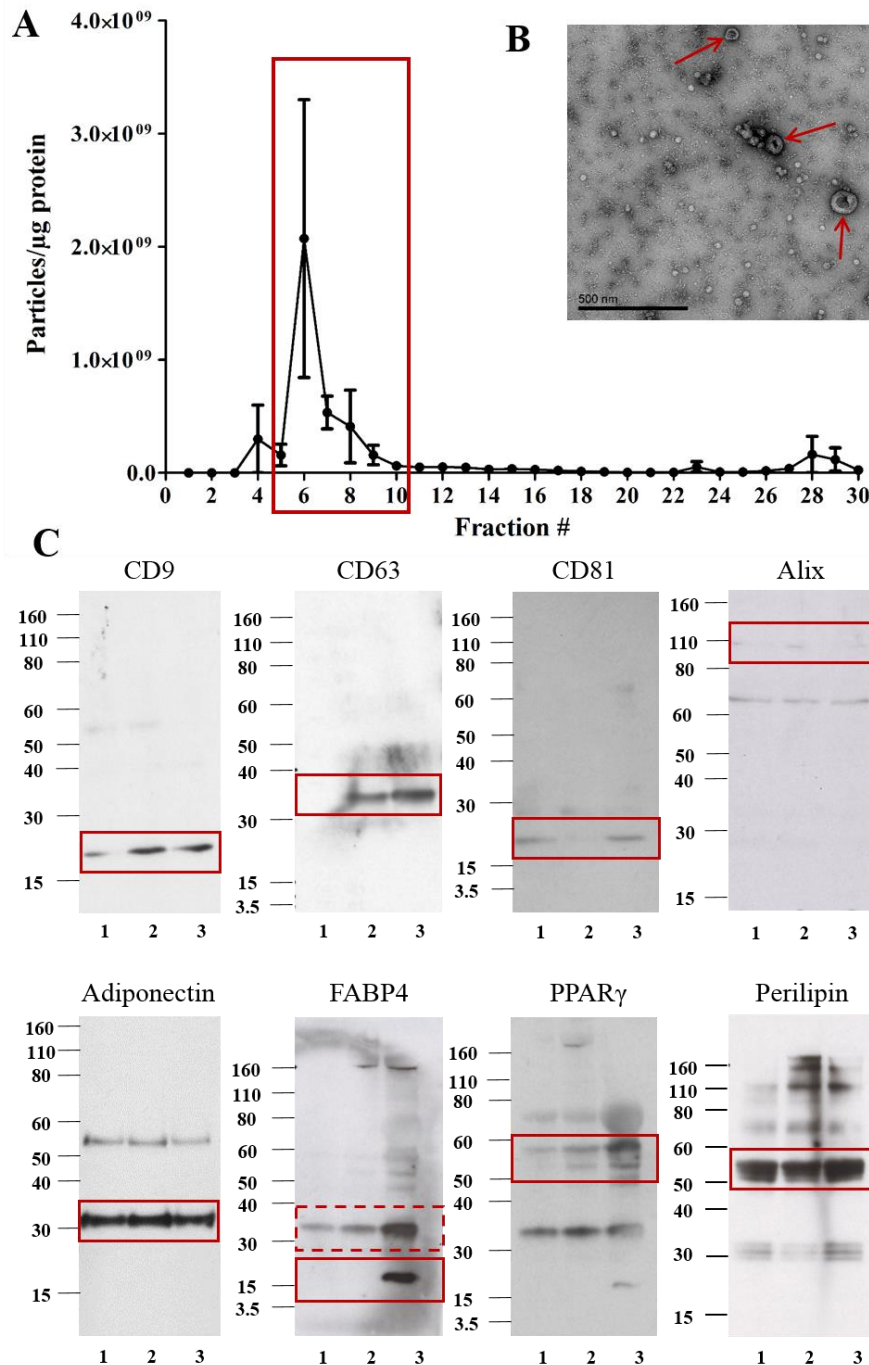
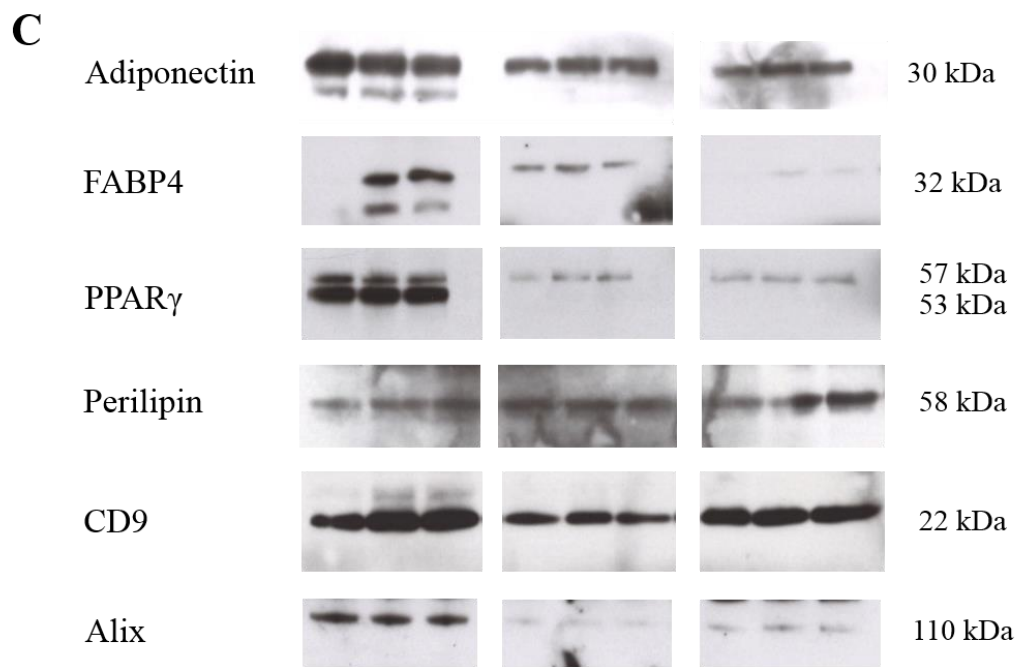
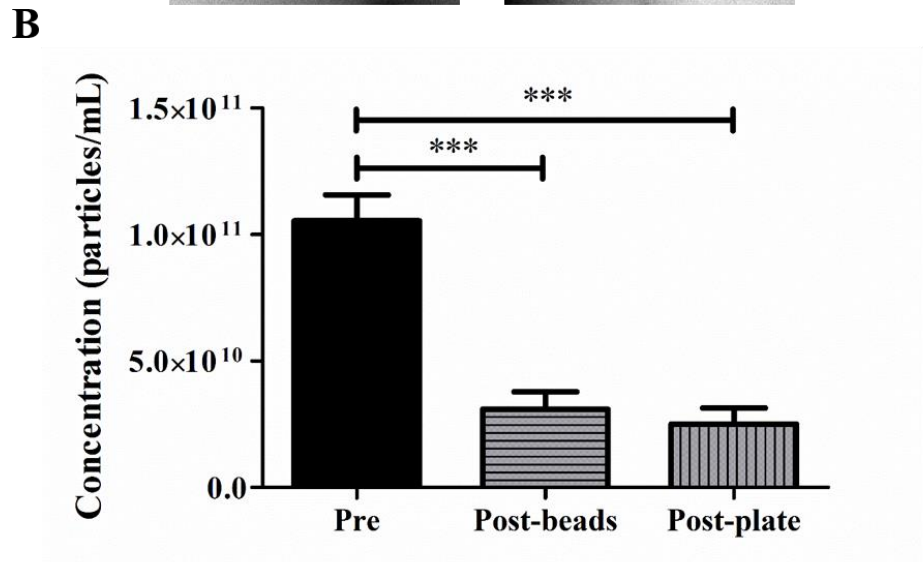
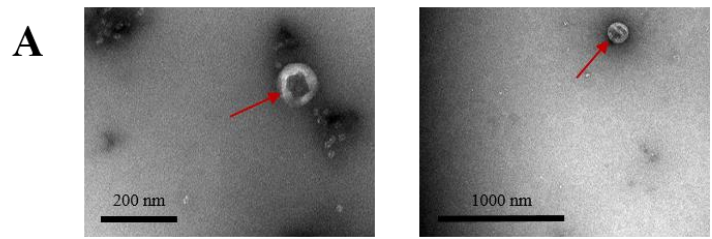


Figure 4.7: Investigation of pooled plasma EVs. (A) Plot of particle-to-protein concentration ratio showed the highest ratio in fractions 5-10 and the presence of EV structures by TEM (B, red arrows indicate EV structures) following ultracentrifugation. (C) Pooled EVs were then probed by western blot for EV markers: CD9, CD63, CD81 and Alix, and adipocyte markers: Adiponectin, FABP4, PPAR γ and Perilipin (1, 2, 3 refers to the replicates, $n=3$). Solid red boxes indicate the predicted molecular weight for each antigen; the dotted red box may indicate a FABP4 dimer ~32 kDa. [Published image: (Connolly et al., 2018)].

4.3.4 Sequential depletion of EV sub-populations with “column purified” plasma-derived EVs

Magnetic bead capture and solid phase-immunoassay were used to sequentially deplete EVs bearing markers of the four major EV populations in plasma (platelets: CD41, monocytes: CD11b, endothelial: CD144 and erythrocytes: CD235). EV structures were present in both post-magnetic bead and post-solid phase depletion samples as revealed by TEM (conducted by Dr Connolly) (**Figure 4.8 (A)**). EV concentration was reduced by a total of approximately 75% post-magnetic bead and post-solid phase depletion: $1.01 \times 10^{11} \pm 1.00 \times 10^{10}$ particles/ml to $3.10 \times 10^{10} \pm 6.90 \times 10^9$ particles/ml and $2.50 \times 10^{10} \pm 6.50 \times 10^9$ particles/ml respectively, $p < 0.001$, ($n=5$) (**Figure 4.8 (B)**). Adiponectin, FABP4, PPAR γ , perilipin, CD9 and Alix were detected in both pre- and post-magnetic bead and solid phase depleted samples (**Figure 4.8 (C)**). Interestingly, in post-depletion samples, only the adipocyte specific PPAR γ -2 isoform was retained. TRFIA provisionally indicated the presence of adipocyte markers post-solid phase depletion **Figure 4.8 (D)**.

Meanwhile, EV concentration using NTA was measured after each step during sequential depletion of EV populations by the two techniques of magnetic bead and solid phase; and represented graphically in **Figure 4.8 (E)** and **(F)**, respectively.



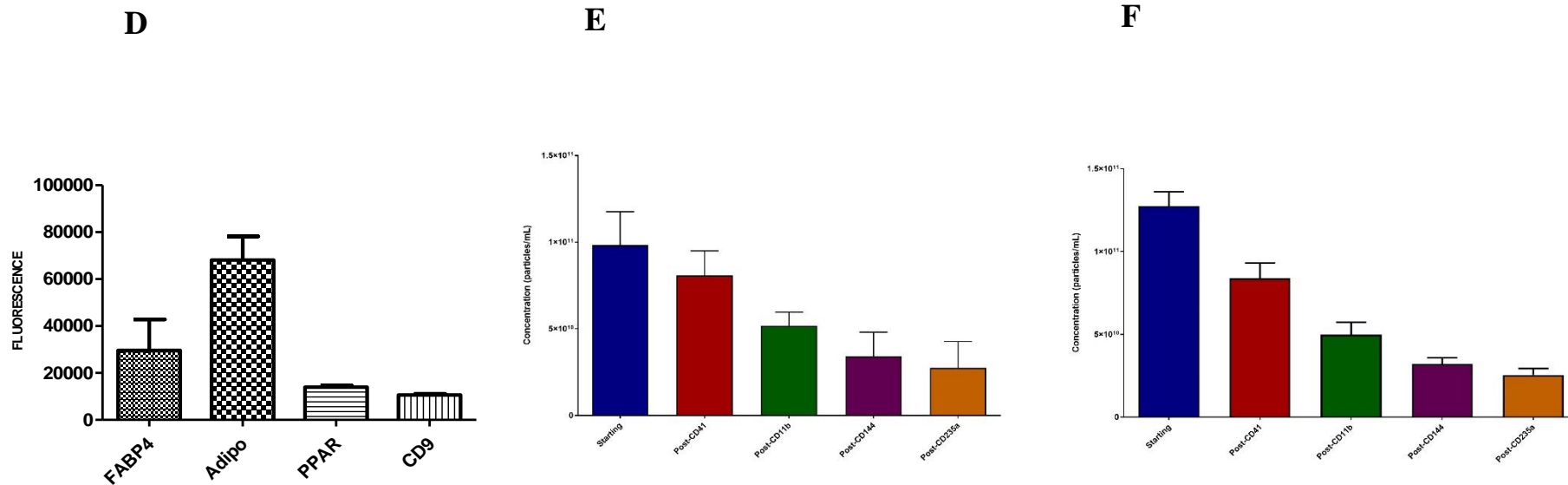


Figure 4.8: Evaluation of adipocyte and EV markers in the post-magnetic bead and solid phase depletion sample. The column purified plasma EV sample was subjected to sequential depletion of EV populations by magnetic beads and solid phase method using antibodies against the specific marker of an EV population. The retained EV sample (supernatant) was evaluated for EV and adipocyte character. (A) EV structures were visible by TEM in post-magnetic bead depletion (left, scale bar 200 nm) and post-solid phase depletion (right, scale bar 1000 nm) (figures provided by Dr Connolly). (B) EV concentration was reduced following sequential depletion of major EV families using magnetic beads or a solid phase method, *** $p = 0.005$ ($n=5$). (C) Adiponectin, FABP4, PPAR γ -2, Perilipin, CD9 and Alix were still present in post-depletion samples of three different individuals (D) Presence of adipocyte markers in the EV sample post solid phase depletion, detected by TRFIA ($n=3$). [Published image: (Connolly et al., 2018)]. (E) and (F) represents the concentration of EVs following each step of depletion by post-bead and post-solid phase method, respectively as measured by NTA.

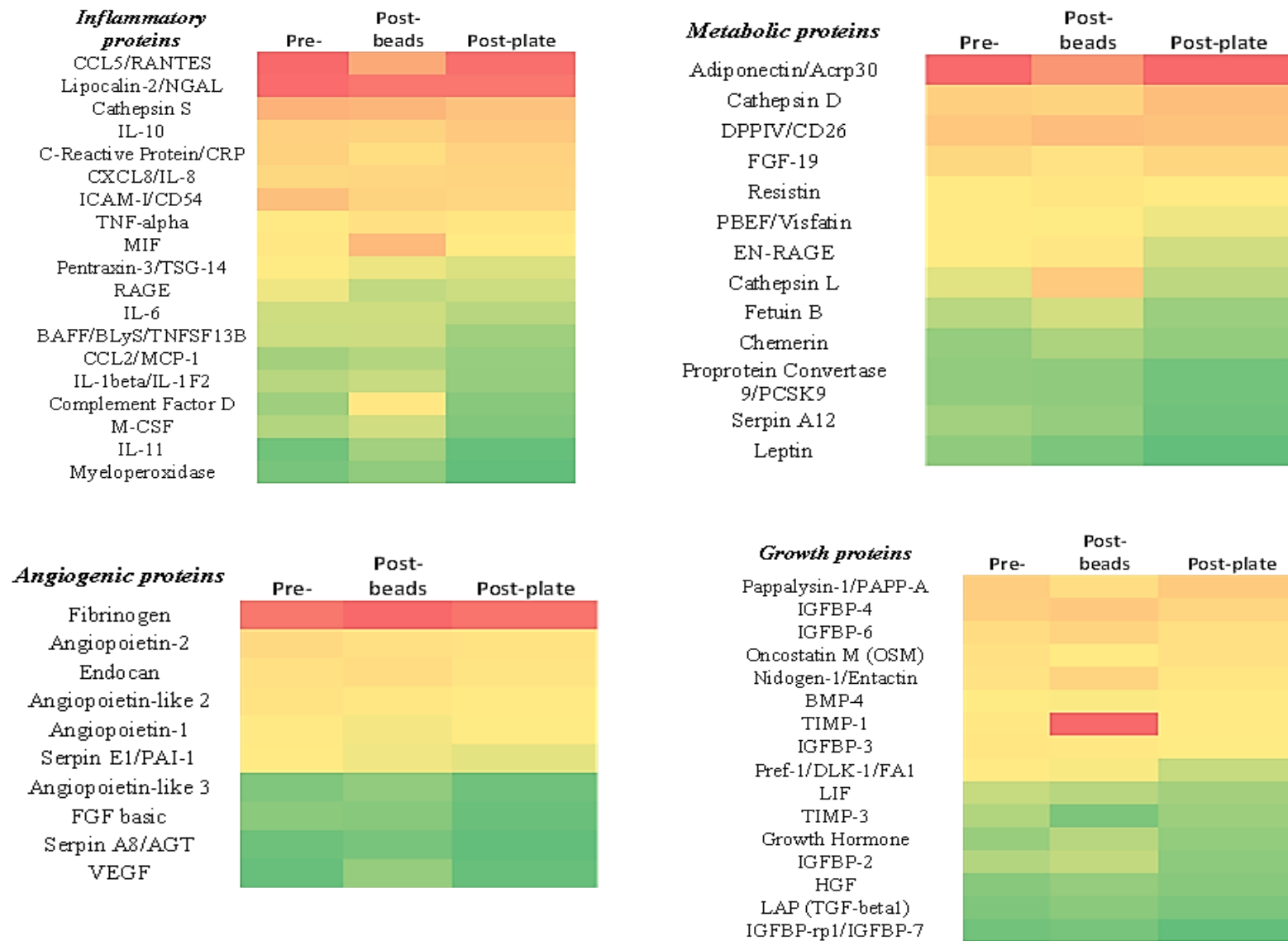
4.3.5 Measurement of adipokines in pre- and post-depletion samples

As an additional validation, I subsequently used a commercially available adipokine protein array to probe for 58 adipokines in pre-depletion, post-magnetic bead and post-solid phase depletion plasma EV samples. The list of adipokines assessed is tabulated in **Figure 4.9**. Adipokines were expressed at a consistent level in pre- and post-depleted samples, with no significant differences observed between samples. This is evidenced by the raw expression data, but perhaps more conveniently by the heat map analysis subsequently undertaken whereby the most and least abundant proteins are ascribed the colour red and green, respectively. The heat map analysis takes into account potential differences in sample loading. Results were subsequently grouped according to their functional role as shown in **Figure 4.10**. The inflammatory and metabolic category of proteins showed stronger expression compared to the other groups. Some of the key adipokines detected were adiponectin, resistin, lipocalin, RANTES and angiopoietin proteins (reflected by red or approaching red colour). There was a strong correlation between the two methods (magnetic bead versus solid phase). Correlation analysis also confirms the reliability of the results obtained across $n=3$ experiments (**Figure 4.10**).

Adipokines	Pre-	Post bead	Post plate	Adipokines	Pre-	Post bead	Post plate
Fibrinogen	35002.30	38828.37	36146.27	PBEF/Visfatin	4028.56	3819.79	3540.30
CCL5/RANTES	26495.39	15406.44	25518.39	IGFBP-3	4233.48	3944.95	3488.55
Adiponectin/Acrp30	24424.83	17417.31	24429.29	Pentraxin-3/TSG-14	3902.59	3638.66	3401.13
Lipocalin-2/NGAL	26196.83	24183.83	24199.73	RAGE	3676.08	3040.67	3193.67
Cathepsin S	13899.33	13171.52	11030.98	EN-RAGE	3845.86	4634.37	3032.56
Cathepsin D	8319.74	7733.59	11027.72	IL-6	3233.92	3238.41	2918.91
DPPIV/CD26	9590.78	11137.80	10305.98	Cathepsin L	3309.52	9065.20	2661.36
IL-10	8715.85	8237.28	10025.47	BAFF/BLyS/TNFSF13B	3181.60	3212.43	2584.02
Pappalysin-1/PAPP-A	8221.91	5699.47	8714.91	CCL2/MCP-1	2639.67	2864.04	2464.09
C-Reactive Protein/CRP	8584.86	6316.50	8281.09	IL-1beta/IL-1F2	2920.53	3149.47	2446.61
CXCL8/IL-8	7350.44	7811.21	8001.43	Pref-1/DLK-1/FA1	3525.18	3236.58	2324.70
ICAM-1/CD54	11422.10	8229.85	7768.31	Complement Factor D	2577.66	4493.91	2253.80
Angiopietin-2	9963.17	8095.09	7482.38	M-CSF	2847.02	3269.67	2160.51
Endocan	7882.17	9139.75	7220.83	Fetuin B	2619.78	3059.76	2104.09
FGF-19	6986.70	5403.05	7196.50	Chemerin	1999.87	2404.60	1963.85
IGFBP-4	7911.42	8848.39	6902.52	IL-11	1927.95	2621.63	1778.52
Angiopietin-like 2	7484.10	6259.68	5543.49	Angiopietin-like 3	2152.97	2581.56	1771.96
Angiopietin-1	5977.72	4961.13	5464.78	Myeloperoxidase	2034.63	2377.53	1726.93
IGFBP-6	5850.25	7141.42	5144.34	LIF	2309.85	2055.08	1704.48
Oncostatin M (OSM)	4983.73	3646.65	4960.57	FGF basic	2407.20	2355.44	1623.88
TNF-alpha	4260.46	5899.59	4942.25	TIMP-3	1932.06	1015.11	1557.41
Serpin E1/PAI-1	5613.21	4857.81	4560.42	VEGF	1541.17	2668.90	1555.16
Nidogen-1/Entactin	4819.65	7034.23	4173.26	Serpin A8/AGT	1712.30	1978.99	1436.52
MIF	4646.22	12565.70	4129.67	Proprotein Convertase 9/PCSK9	1934.60	1904.36	1422.87
Resistin	4120.89	4731.44	4023.87	Growth Hormone	1513.65	2059.59	1403.80
BMP-4	3402.76	3267.41	3564.52	Serpin A12	2215.42	1997.35	1327.15
TIMP-1	4024.13	24027.90	3550.11	IGFBP-2	1972.47	2242.84	1312.99
				HGF	1207.26	1433.42	1210.28
				Leptin	1901.92	1554.29	1116.38
				LAP (TGF-beta1)	1033.40	1254.15	1007.97
				IGFBP-rp1/IGFBP-7	804.82	937.23	527.49

Figure 4.9: Profile of adipokines in the pre- and post-depleted samples using a protein array kit. The pre- and post- depleted (by magnetic bead capture and solid phase immunoassay) EV samples were loaded on the nitrocellulose membrane fixed with appropriate antibodies. The amount of proteins bound was proportional to the signal generated. List of probed adipokines arranged in decreasing order of expression, represented as mean pixel density, $n=3$. Colour coded to match the intensity of strength, expressed as mean pixel density ($n=3$), red being the strongest and green the weakest.

(A)



(B)

Correlation Table	
post plate (N1) v/s post plate (N2)	0.86
post plate (N2) v/s post plate (N3)	0.73
post plate (N3) v/s post plate (N1)	0.51
post bead (N1) v/s post bead (N2)	0.89
post bead (N2) v/s post bead (N3)	0.86
post bead (N3) v/s post bead (N1)	0.72
post plate (N1) v/s post bead (N1)	0.85
post plate (N2) v/s post bead (N2)	0.83
post plate (N3) v/s post bead (N3)	0.89

Figure 4.10: Adipokine array results (A) Adipokines grouped in order of functionality. The adipokines detected in the pre- and post-depleted samples were categorised into groups of inflammatory, metabolic, angiogenic and growth proteins. The intensity of signal strength, expressed as mean pixel density ($n=3$), colour coded from red being the strongest and to the green the weakest. **(B)** Table indicative of correlation between the two methods and between the individual experiments of a technique ($n=3$).

4.4 Discussion

Key findings

- Magnetic bead technique and solid phase assay proved effective in depleting EV populations for a given marker.
- Adipocyte associated proteins, FABP4 and adiponectin do exist as free proteins and hence, not an exclusive marker to identify ADEVs
- Sequential depletion of major EV families recovered a sample of EV that expressed adipocyte specific proteins and contained a range of adipokines.

This chapter aimed to provide evidence for the presence of adipocyte-derived EVs in the human circulation. Demonstrating the existence of EVs in the circulation may be a key step in understanding and assessing the health of adipose tissue as well as employing them as a potential biomarker in the assessment of metabolic health. However, the presence of adipocyte-derived EVs in circulation has not been definitively confirmed. Owing to the lack of a unique adipocyte marker and the overwhelming presence of EVs from other sources, primarily from platelets and leucocytes (endothelial and erythrocyte-derived EV to a lesser extent), establishing the presence of ADEVs in circulation is a challenge. Flow cytometric detection of EVs has met with limitation in lower end detection size of ~300nm, resulting in an underestimation. As mentioned before, adipocyte proteins adiponectin, FABP4 and perilipin have been associated with plasma-derived EVs, though the EV-processing from plasma in such studies is questionable with soluble proteins not being distinguished, leading to false assessment. Given the lack of conclusive evidence, this study combines proficiency of sample processing techniques in accordance with ISEV guidelines, and validation using EV/adipocyte-specific markers to conclusively provide evidence for the presence of ADEVs in human circulation. Size-exclusion chromatography coupled with ultracentrifugation was employed for EV isolation from platelet-free plasma, whilst magnetic bead pull-out and solid phase immunoassay were the two techniques adopted to deplete EVs from major circulating sources (platelet, monocyte, endothelial & erythrocyte). The purified EV sample obtained was assessed for adipocyte origin by a selection of adipocytes markers and using an adipokine array.

When studying the magnetic bead capture in 3T3-EVs (**Figure 4.1 (A), (B)**), observation of similar percentage capture of CD9⁺ and FABP4⁺ was considered

conclusive, since the EVs used in this study were solely of adipocyte cell line origin, and all the sampled EVs potentially carry the adipocyte marker FABP4. It also convinces us that the magnetic bead technique works in selectively pulling out EVs with the desired antibody marker. The result was further supported by TRFIA pre- and post- bead capture.

In the case of plasma-EVs (**Figure 4.1 (C), (D)**), the results were intriguing when FABP4+ capture given that the proportion of adipocyte-derived EVs in the circulation is anticipated to be much lower than 35% (according to recent flow cytometry-based studies <1%) (Gustafson et al. 2015b) and suggested FABP4 might adhere to the surface of many EV types and therefore may not necessarily be specific to adipocyte-derived EVs (despite FABP4 protein being of adipocyte origin). This implied although FABP4 is produced exclusively by adipocytes, it may not represent a strong adipocyte marker or at least not exclusive to adipocyte cell origin. It is also noteworthy that FABP4 and adiponectin, circulate free in plasma in measurable concentrations whereas that contained on or within EV likely represents a relatively small proportion of the total. In the case of EVs derived from the 3T3 cell line, column separation did not improve the situation significantly, with both CD9 and FABP4 capturing similar amounts from the EV population comparing columned to non-columned samples (**Figure 4.1 (A), (B)** and **Figure 4.4 (A), (B)**). This agrees with very little contaminating protein being detected in later fractions when isolating the purified EV fraction by column (**Figure 3.6**). In the case of plasma-derived EVs, there was a significant reduction in the number of EVs captured by FABP4 as a result of removal of a significant amount of free FABP4 from the starting EV sample (**Figure 4.1 (C)** and **Figure 4.4 (C)**). Overall, it can be concluded that the magnetic bead capture technique works well to isolate EVs of a specific population, provided the purity of the EV sample is assured.

During the time of this study, no specific marker of adipocyte-derived EVs had been defined nor had a consensus EV cargo been identified; this was a challenge in pinning down ADEVs from plasma. However, based on previous studies, the adipocyte protein markers FABP4, adiponectin and PPAR-gamma were chosen to identify adipocyte character in isolated EVs (Looze et al. 2009; Siersbæk et al. 2010; Shan et al. 2013; Mariette E G Kranendonk et al. 2014; Connolly et al. 2015). Perilipin, a protein associated with lipolysis, has also been identified in circulating EVs and used as a

biomarker for ADEVs (Eguchi et al. 2016). FABP4 has been extensively used to characterise EVs from the adipocyte cell line 3T3-L1. FABP4 expression is almost exclusive to adipose tissue although macrophages have also been found to express this protein, albeit in restricted amounts. FABP4 is highly regulated during adipocyte differentiation (Furuhashi et al. 2008). *In vivo* studies on mouse serum have detected adiponectin in the exosomal fraction, rendering it a protein of interest to establish adipocyte lineage (Phoonsawat et al. 2014).

Isolation of pure EVs from human plasma faces considerable challenge largely related to potential “contamination” with larger vesicles, subcellular fractions, protein aggregates, protein-nucleic acid aggregates or plasma proteins. Contamination with high levels of protein in blood can mask significant vesicular-associated proteins and generate misleading/overestimated data. The conventional procedure of EV isolation by differential centrifugation or ultracentrifugation of plasma alone is not adequate to remove various “contaminants” or non- EV particles (Muller et al. 2014a). Several research studies have evaluated the efficiency of SEC in isolating EVs from biological fluids (e.g. human plasma, urine and CSF) and found it more effective in reducing the non-vesicular protein contaminants and lipoproteins than UC and density gradient methods. These commercially available columns have been shown to purify EVs with commendable yield and good reproducibility (Welton et al. 2015). A ‘cleaner’ EV preparation from plasma was obtained by subsequent application of a size-exclusion chromatography (SEC) column, critical for removal of plasma proteins and other soluble components.

Here, I adopted size-exclusion chromatography with platelet-depleted plasma to obtain a cleaner preparation of plasma EVs with the removal of non-specific proteins. This proved effective to eliminate free proteins (**Figure 4.6**). As discussed in the previous chapter, fractions 5-10 were observed to contain the tetraspanin-containing EVs with subsequent fractions containing abundant proteins. Column fractions 5 -10 exhibited the highest particle-to-protein ratio and tested positive for the EV markers CD9, CD81 and Alix. In addition to these EV markers, the pooled fractions also identified adipocyte markers FABP4, adiponectin, perilipin and PPAR- γ . Although the adipocyte proteins were detected in the EV-rich fractions 5-10, they were also detectable in subsequent fractions (**Figure 4.6**). This could imply that the adipocyte proteins previously detected in non-columned plasma EV preparations are free

proteins and less likely to be expressed by EVs themselves. Nevertheless, FABP4 and adiponectin are soluble and found freely in the circulation (Arita et al. 1999; Furuhashi et al. 2011), and thus, detected in the non-EV fractions 10 - 30. These later fractions carried no EV markers (CD9, CD81, ALIX) and their particle-to-protein ratio was lower. PPAR-gamma and perilipin were also detected in these later fractions, but negative for EV markers. This observation is of key significance when considering the measurement of these adipocyte markers in plasma EV preparations, where the SEC technique is crucial to exclude the majority of soluble proteins in order to avoid overestimations. The initial strategy of selectively obtaining adipocyte-EVs using FABP4 as a marker failed, due to the same reason that an un-columned EV preparation carries soluble proteins that cause erroneous capture with magnetic beads. Hence employing an adipocyte marker as a probe to select out ADEVs from a crude plasma EV preparation was unreliable. I, therefore, subjected EVs collected from plasma (platelet-free plasma) to column purification by SEC to obtain a working EV preparation/sample largely free from soluble proteins for subsequent experiments.

In the human circulation, whole blood carries EVs originating primarily from platelets, leukocytes, endothelial cells and erythrocytes (Orozco and Lewis 2010; Gustafson et al. 2015b). Adipose tissue is also capable of generating EVs which may be released into the circulation; however, their proportion in plasma is yet to be defined. Obesity, which is characterised by 'stressed' or inflamed adipocytes, is associated with elevated amounts of EV compared to those observed in healthy or lean individuals (Goichot et al. 2006; Agouni et al. 2008; Kranendonk et al. 2014c). Adiponectin, PPAR- γ , FABP4 and perilipin are secretory proteins predominantly produced in adipose tissue whose levels vary in the metabolic syndrome. EV preparations traditionally processed from platelet-free plasma by UC alone, can sediment these soluble proteins, thereby overestimating adipocyte character. In these studies, eluents from fraction 5-10 were pooled and ultracentrifuged; the obtained EV pellet tested positive for EV markers and adipocyte markers (**Figure 4.8**). Transmission electron microscopy further confirmed the presence of EV structures.

As discussed above, some of the adipocyte proteins chosen in this study (e.g. FABP4 and adiponectin) may also be associated with other cell types and readily secreted in the circulation. Ultracentrifugation might thus, co-pellet these soluble proteins leading to falsely attributed EV adipocyte expression. A study has shown exogenous FABP4

was internalised by endothelial cells, primarily through the plasma membrane proteins to subsequently mediate vascular functions (Saavedra et al. 2015). Similar FABP4-cell interaction could cause this protein to be packaged into other EV populations. Therefore, two separate techniques, magnetic bead capture and immuno-affinity on solid-phase, were employed to selectively remove/deplete the major populations in plasma-derived EVs (platelets, leukocytes, endothelial cells and erythrocytes) with a view to evaluating the ‘retained’ EV sample for adipocyte character. I hoped therefore to use this as a means of generating conclusive evidence for the presence of ADEVs in the circulation. Specifically, I hoped to evaluate whether the signature adipocyte markers were retained in the residual EV population after depletion of ‘non-adipocyte’ EVs.

Both the techniques of magnetic bead capture and solid phase immunoassay adopted for the depletion of selective EV populations showed significant reduction in marker expression, confirmed by TRFIA (**Figure 4.5**). Hence, these techniques proved effective in lowering the concentration of major circulating EV populations in plasma preparations. The NTA analysis from both techniques showed an overall drop of around 75% in the EV concentration post-depletion, which accounts for the proportion of other major EV populations in plasma (**Figure 4.8 (B)**). The post-depleted sample was positive for the classic adipocyte markers FABP4, adiponectin, perilipin and PPAR- γ (**Figure 4.8 (C)**). However, their expression was reduced. This could imply that these protein markers could perhaps be associated with EVs generated from non-adipocyte sources, i.e., loss of proteins with the pull-out of the other ‘non-adipocyte’ EV populations. Numerous studies have shown that FABP4 and PPAR- γ are produced by other cell types besides adipocytes, especially macrophages (Hertzel et al. 2017; Heming et al. 2018). Expression of FABP4 varied with individual donors, such that some were not readily detected by western blot, which advocates the use of multiple markers to affirm ADEVs in plasma. FABP4 can take a homodimeric configuration depending on ligand activation, thus explaining the detection at higher molecular weight than expected (Gillilan et al. 2007). PPAR- γ , a master regulator of adipogenesis, exists in isoforms namely PPAR- γ 1 and PPAR- γ 2 which were evidently seen in pre-depletion samples; however, only PPAR- γ 2 was retained in post-depleted samples. Interestingly, PPAR- γ 2 is an adipocyte-specific transcription factor and contributes a greater role in inducing adipogenesis (Tontonoz et al. 1994a; Mueller et

al. 2002), thus its presence in post-depleted EV samples is a strong indicator of adipocyte origin. Adiponectin and perilipin were also consistently expressed in pre- and post-depleted samples. The EV markers CD9 and Alix were present in post-depletion samples from both techniques, although the intensity of expression was reduced; this agrees with the decrease in the concentration of EVs (**Figure 4.8**).

An adipokine protein array evaluated the relative levels of other adipokines in the pre- and post- depletion (cleaner preparation) samples (**Figure 4.9 and 4.10**). Among the metabolic adipokines, adiponectin expression was abundant in the pre- and post-depleted samples, in addition to resistin, visfatin, cathepsin D and leptin. A study by Ogawa *et al.*, (2010) provided evidence for the presence of gene transcripts of adiponectin and resistin in microvesicles isolated from serum (Ogawa *et al.* 2010). These transcripts were transported into macrophages, mediating intercellular communication in a paracrine/endocrine manner.

Inflammatory adipokines demonstrated more intense expression compared to other protein groups, particularly RANTES, MCP-1, cathepsin S, lipocalin and cytokines such as TNF- α , IL-6, IL-10 and IL-8 in the EV sample post removal of major circulating EV populations. RANTES and MCP-1 have previously been reported to be packaged in plasma-derived exosomes of healthy individuals (Wahlgren *et al.* 2012; Kodidela *et al.* 2018), whilst the expression of inflammatory adipokines such as TNF- α , IL-6, IL-10 and IL-8 has been demonstrated within ADEVs (Mariette E G Kranendonk *et al.* 2014). These packaged proteins may potentially facilitate intercellular communication to induce inflammation in recipient cells and disease progression. RANTES is a chemokine secreted by adipocytes that has been shown to trigger leukocyte infiltration into adipose tissue to mediate a state of chronic immune activation. Mature adipocytes release RANTES particularly at higher concentration in obese individuals and under hypoxic conditions. It has been identified as an immune mediator for adipose tissue (Skurk *et al.* 2009). Expression of cathepsin S has been directly implicated in obesity through observations of increased expression by adipocytes in obese as compared to healthy controls. Macrophage-derived pro-inflammatory molecules, such as TNF α and IL-1 β , have been shown to cause a stimulatory effect in the release of cathepsin S by adipose explants (Naour *et al.* 2010). Owing to its selective increased secretion by adipocytes in obese individuals, cathepsin S has been considered a biomarker for adiposity and also been implicated in

atherosclerosis, dysregulated glucose metabolism and contribution to cardiovascular risks (Taleb et al. 2005).

The production of lipocalin by adipocytes up-regulates the production of adiponectin and PPAR- γ and suppresses TNF α -induced inflammation in adipose tissue, whilst also suppressing stimulation of cytokine expression in macrophages (Zhang et al. 2008). Lipocalin coupled with FABP4 modulates vascular function and mediates chronic inflammation (Wu et al. 2014). A study by Borkham-Kamphorst et al. (2018) showed compelling evidence for the trafficking of lipocalin 2 into the secreted exosome cargo from human carcinoma cell lines. Both glycosylated and non-glycosylated variants of lipocalin 2 were equally steered into membranous extracellular vesicles (Borkham-Kamphorst et al., 2018). Urinary exosomes secreted at different stages of renal disease carry lipocalin and its abundance correlates with kidney dysfunction (Alvarez et al. 2013). The presence of the angiopoietin family of proteins in post-depleted EV samples is also relevant. Angiopoietin-2 has a beneficial role in white adipose tissue depots by promoting vascular function or angiogenesis as well as reducing AT inflammation (An et al. 2017). It should be noted that SEC is efficient in clearing 95% of non-vesicular soluble/free proteins in a single step; hence the residual non-EV associated plasma proteins are likely to remain in the supernatant. The adipokine array was also undertaken on the supernatant obtained during EV pelleting; this also showed the presence of adipokines, whilst western blotting for CD9 showed its absence in the post-ultracentrifugation supernatant (non-EV segment) as compared to the pelleted EV prep (Connolly et al. 2018). Therefore, the proteins (including adipokines) found in the post-ultracentrifugation supernatant are not associated with EVs and can be referred as non-EV supernatant.

On the whole, the detection of major adipokines coupled with the presence of classical adipocyte and EV markers in the EV samples post-depletion of major circulatory EV populations by either magnetic bead capture or solid phase immunoassay technique, provides strong evidence for the presence of adipocyte-derived EVs within the human circulation. The work also emphasises the need to judiciously choose techniques for EV isolation and sample preparation, being particularly careful to avoid misinterpretation of adipocyte marker signal from the soluble protein fraction.

Although ADEVs have been comparatively well studied in terms of vesicle cargo, function and metabolic effects, their passage into the circulation through the endothelial barrier is still under study. In healthy individuals, lean AT is well vascularised by a capillary network through which EVs can be potentially trafficked. In obese AT, the tissue can be viewed as being closely related to a tumour environment, namely hypoxic and poorly vascularised. It has been found that tumour EVs can alter cellular physiology triggering vascular permeability (Zhou et al., 2014) or by conditioning pre-metastatic sites in distant organs (Costa-Silva et al., 2015; Hoshino et al., 2015). Adipokines have been implicated in the development of cancer (Ayoub et al. 2017). Similarly, the hypoxic environment and chronic inflammation of adipose tissue can cause continuous infiltration of pro-inflammatory cytokines and immune cells in addition to self-generated adipokines. This can cause oxidative stress on the endothelium, destabilising the junctions and increasing vascular permeability, thereby potentially providing an escape route for the ADEVs (Félétou and Vanhoutte 2006; Chistiakov et al. 2015; Rahimi 2017).

The ADEVs constitute a small proportion of circulating EVs but perhaps show major effects on vascular and adipose tissue health. The EVs produced from ‘unhealthy’ adipocytes tend to carry a different profile of proteins that can negatively impact on recipient cells or organs. Thus, ADEVs may have considerable potential as biomarkers in obesity-driven metabolic disease and cancer.

4.4.1 Limitations and Conclusion

The work produced in this chapter has some limitations. The number of experimental repeats for the pre- & post- depletion experiments was minimal at a number of 3. This can be scaled up in future studies to minimise any biological variation. TRF immunoassay confirmation could not be conducted for certain proteins namely perilipin and Alix. Furthermore, the EVs captured on the beads could not be effectively evaluated, although multiple attempts were made to release the bound EVs from the magnetic beads. In addition, studies on ADEV protein cargo in terms of RNA content were not undertaken and flow cytometric analysis was not undertaken to examine surface marker expression.

To summarise, my data, using a combination of methodologies including NTA, TRFIA and western blotting, provide convincing evidence for the presence of ADEVS in the human circulation. Adipocytes seem capable of secreting EVs loaded with adipokines and other adipocyte-specific proteins, lending a unique character. By employing two depletion methods (magnetic bead capture and solid phase immunoassay) to selectively remove four major circulatory EV populations from non-adipocyte sources (i.e., platelet-, leukocyte-, endothelial-, and erythrocyte-derived) in platelet-free plasma, a signature population of EV was established with adipocyte character.

5. Results III: Effect of circulating adipocyte-derived EVs on leukocyte attachment to endothelial cells

Perspective

Having provided evidence in chapter 4 for the presence of adipocyte-derived EVs (ADEVs) in the circulation, I thought it important to establish if circulating ADEVs isolated according to the protocol developed in the previous chapters elicited any functional effects, especially with respect to vascular homeostasis since cardiovascular disease is one of the major morbidities associated with obesity. Adipose tissue in obese individuals is often inflamed and hypoxic; this study thus, sought to establish if ADEVs derived from obese individuals could elicit changes in endothelial cells that resulted in the promotion of leukocyte adhesion. I focused on leukocyte adhesion since this is an early step in the development of atherosclerosis. Whilst this chapter presents early results, this might nevertheless prompt future studies in a larger patient cohort.

5.1 Background

The prevalence of cardiovascular disease has risen dramatically over the past decade. The state of obesity predisposes individuals to CVD mortality and morbidity, and poses a risk factor for a host of metabolic syndromes, insulin resistance, dyslipidemia, diabetes, hypertension, atherosclerosis, coronary heart disease, and stroke (Van Gaal et al. 2006; Ritchie and Connell 2007). Of note, visceral fat plays a key role in altering the physiological balance of adipose tissue and skewing the release of adipokines and EVs, rendering the AT hypertrophic and hypoxic. Although efforts are being made to understand the link between obesity and development of CVD, the molecular mechanisms that trigger the dysfunction of AT are still the subject of research.

AT is a heterogeneous tissue comprising pre-mature and mature adipocytes, a stromal fraction of inflammatory cells (predominantly macrophages and lymphocytes of various phenotype), fibroblasts, stem cells as well as vascular cells (Badimon and Cubedo 2017). As adipocytes expand, systemic metabolism of the AT is affected at the molecular and cellular level. Increased secretion of free fatty acids (FFAs) and glycerol has been reported in obese compared to lean individuals and subsequently promotes insulin resistance (Horowitz et al. 1999; Shulman 2000). Perilipin, a phosphoprotein that regulates the release of FFAs, was highly deficient in obese subjects with increased rate of lipolysis (Wang et al. 2003). AT produces several pro-inflammatory factors with increasing obesity. Higher expression of proinflammatory proteins in AT is observed in obese persons as compared to lean individuals, including TNF- α , interleukin 6 (IL-6), monocyte chemoattractant protein 1, inducible nitric oxide synthase (iNOS) and procoagulant proteins (Hotamisligil et al. 1993; Perreault and Marette 2001; Sartipy and Loskutoff 2003; Samad et al. 2018). Obese adipose tissue attracts and harbours increasing numbers of macrophages; this is associated with enhanced TNF- α expression and increased iNOS and IL-6 expression within the AT environment (Weisberg et al. 2003). Furthermore, adiponectin, a potent inhibitor of TNF- α -induced inflammation, is reduced in obesity (Bruun et al. 2003).

With the accumulation of macrophages, AT shifts to a state of inflammation and disrupts the normal metabolic state of the tissue. Preadipocytes residing within the

tissue have the potential to convert to a macrophage phenotype, emphasising the great cellular plasticity of adipose precursors (Charrière et al. 2003). Activated macrophages release cytokines and biologically active molecules such as NO, TNF- α , IL-6, and IL-1 (Duque and Descoteaux 2014). Supplemented with the escalation of pro-inflammatory molecules particularly TNF- α , this induces the activation of vascular endothelial cells to express adhesion molecules. Coupled with the low levels of adiponectin, the inflammatory process is amplified and leukocyte attachment to the vascular endothelium is heightened. This process leads to a chronic state of inflammation within the AT and with the absence of anti-inflammatory intervention, impairs the endothelium. Endothelial dysfunction is the hallmark for the subsequent development of CVD, especially atherosclerosis.

Adipocytes release EVs and moreover their presence has been established in the circulation. Since EVs carry characteristics from the source cell, ADEVs derived from inflamed and hypoxic AT may be different to that from lean AT. AT-derived exosomes from individuals of higher BMI exhibit atheroma-promoting properties by decreasing cholesterol efflux proteins and increasing LDL accumulation in macrophages, mediated through their miRNA cargo (Siegart et al. 2017). Depending on their adipokine content, ADEVs can affect insulin signalling in liver and muscle cells, contributing to systemic insulin resistance (Kranendonk et al. 2014). Also, EVs generated from stressed adipocytes have been identified as a chemoattractant *in vitro* and *in vivo* (Eguchi et al. 2015). They were shown to attract monocytes and macrophages by activation of caspase-3 signalling, thus contributing to macrophage infiltration in obesity.

The mechanism through which adipocytes elicit an endothelial inflammatory response and recruitment of monocytes and macrophages in atherosclerotic plaques is yet to be fully understood. It is likely that EVs can mediate the cross talk between tissues leading to plaque formation in atherosclerosis. Adipocyte EVs generated from obese AT could contain pro-inflammatory molecules to mediate an inflammatory response in vascular endothelial cells. Moreover, previous work from our group was able to establish that EVs from inflamed cultured 3T3-L1 adipocytes induced VCAM-1 expression on vascular endothelial cells that in turn increased leukocyte attachment to vascular endothelial cells (Wadey et al., 2019). Hence, I set out to test if ADEVs (isolated according to the techniques developed in Chapter 4)

from plasma of healthy and obese subjects could promote leukocyte attachment on endothelial cells, and thus, might be involved in mediating the pathogenesis of atherosclerosis. Primary vascular endothelial cells were obtained from human umbilical cords. Although not a true representation of adult endothelium, based on previous publications the HUVEC model was considered ideal for a pilot study on inflammation (endothelial activation) and leukocyte attachment (Makó et al. 2010; Onat et al. 2011; Zhang et al. 2014; Cao et al. 2017).

5.1.1 Aims:

To explore the effects of circulating ADEVs, obtained from healthy versus obese individuals, on leukocyte adhesion to endothelial cells (HUVECs).

Objectives:

1. To validate the leukocyte attachment assay using varying doses of TNF- α (0-50 ng/ml).
2. To study the effect of ADEVs from healthy and obese individuals on leukocyte attachment and endothelial adhesion molecule expression.

5.2 Methods

5.2.1 HUVEC isolation and culture

HUVECs were sourced from umbilical cords and cultured as per the procedure detailed in Chapter 2.11.

5.2.2 Recruitment of healthy and obese subjects

With ethical approval (REC approval number 16/EE/0342; East of England, Cambridge South Research Ethics Committee and local R&D (approval no: 16/JUL/6572) applied under Dr Justyna Witczak, along with Cardiff Metropolitan University ethical approval (CHS ethics no 8371)) and informed consenting, seven patients were considered as obese subjects for this study. Patients were recruited from Specialist Weight Management Service, conducted at University hospital Llandough under Dr Dev Datta.

The individuals for the 'obese' cohort were chosen with inclusion criteria of BMI > 40kg/m². The healthy cohort was limited to individuals with BMI ranging from 19-25kg/m², no history of illness and clear of medications. The women included in the study were not pregnant.

5.3.3 Isolation and purification of ADEVs from plasma

EVs were obtained from plasma of healthy ($n=7$) and obese subjects ($n=7$) as described in Chapter 2.2.2. Following, the EV samples were subject to sequential depletion of major EV populations derived with marker CD41-, CD11b-, CD144-, and CD235a-. The post depleted sample was considered the working stock and henceforth referred to as ADEVs, as established from previous Chapter 4.

The concentration of these plasma-derived EVs were determined by NTA procedure as described in Chapter 2.3.2. Company (Nanosight)-provided 100nm sized beads were used as calibration beads and indicated a mean concentration of $1.82e11 \pm 0.04$ between the batches of experiments.

5.2.4 Leukocyte Adhesion Assay

Leukocytes were freshly harvested on the day of the experiment and the steps involved in the isolation of leukocytes and assay as detailed in Chapter 2.12. In order to reduce variation, leukocytes obtained for the experiments were isolated from a single consistent source.

5.2.5 Western blot

HUVEC cell lysates were probed for endothelial markers using western blot as described in Chapter 2.7. Antibody control experiment under the absence of a primary antibody was not conducted during the protein detection stage.

5.2.6 Statistical analysis

GraphPad prism (Version 5) was used to generate graphical representation of data. One-way ANOVA was used to test for significance with Bonferroni's multiple comparison test significance where marked by * reflects $p < 0.05$, ** reflects $p < 0.01$ and *** reflects $p < 0.001$. Data were assessed for normality using the Kolmogorov-Smirnov test. Data is expressed as mean \pm SD, where applicable.

5.3 Results

5.3.1 Subject characteristics

Seven volunteers each were recruited from healthy and obese volunteers, with matching for gender. Average ages for the healthy and obese groups were 42.5 ± 8.5 and 44.7 ± 6.1 years, respectively. The difference in EV concentration between the two cohorts were significant with $*p < 0.5$ valued at 0.0262. By design, BMI was different between the two groups. **Table 5.1** summarises the characteristics of the subjects involved in this study.

Factors	Healthy	Obese
Gender	Female - 2	Female - 2
	Male - 5	Male - 5
Age Range (years)	42.5 ± 8.5	44.7 ± 6.1
BMI (kg/m²)	19 - 25	> 40
EV concentration (particles/ml)	$2.256e+011 \pm$	$4.267e+011 \pm$
	$9.802e+010$	$2.021e+011$
EV Size (mean/mode)	215.0 ± 15.68 nm /	200.7 ± 17.10 nm /
	180.6 ± 28.38 nm	166.4 ± 19.77 nm

Table 5.1: Summary of subject characteristics. Seven subjects each were chosen for obese and healthy cohort based on difference in BMI. Gender and age of the subjects were closely matched. SEC was used to isolate the EVs from the subjects' plasma. The size and concentration of the collected EVs were measured by NTA procedure and recorded. The EV concentration varied significantly between healthy and obese subjects, with $p=0.026$

5.3.2 Collection (Isolation) of Human umbilical vein endothelial cells (HUVECs)

In order to validate the protocol used to collect HUVECs, immunofluorescence was undertaken to establish the expression of endothelial markers. This showed that the cells collected from human umbilical cord veins exhibited a typical cobblestone-like appearance under bright-field microscopy. Strongly positive staining was observed for the endothelial cell markers CD144 (VE-Cadherin) and CD62E (E-selectin) (**Figure 5.1**). As anticipated, expression of CD144 was observed predominantly at the cell surface whilst CD62E expression was predominantly cytoplasmic/peri-nuclear, confirming an endothelial phenotype.

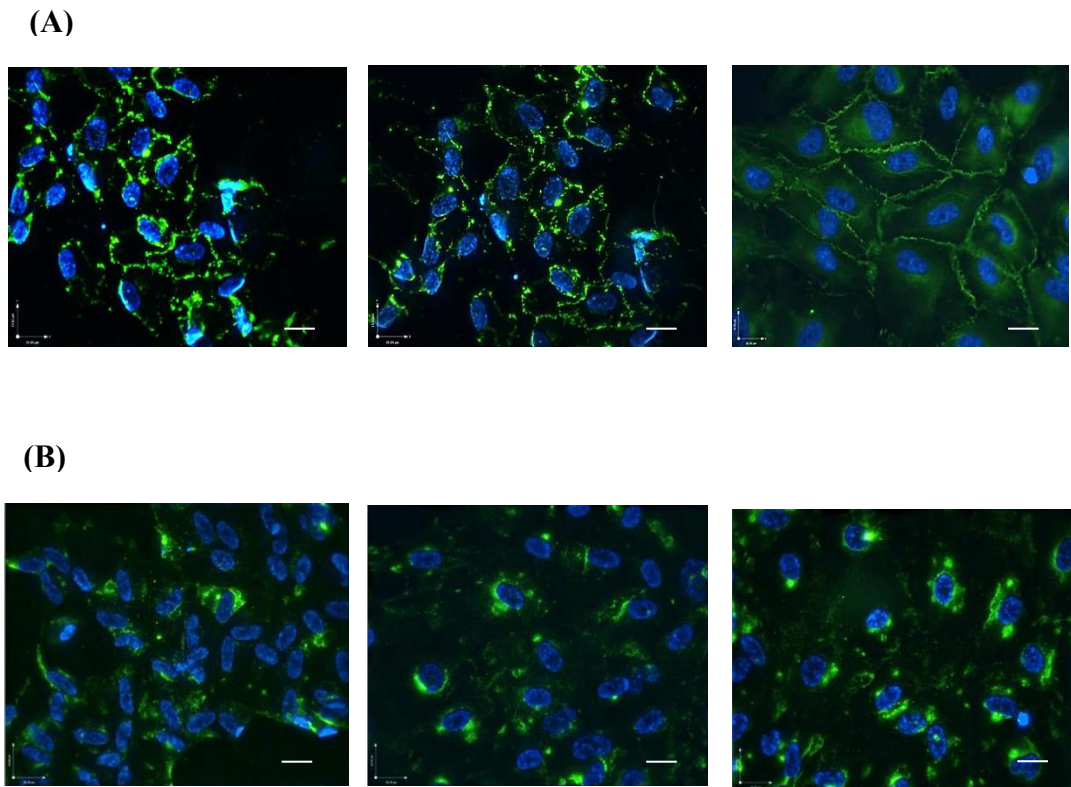
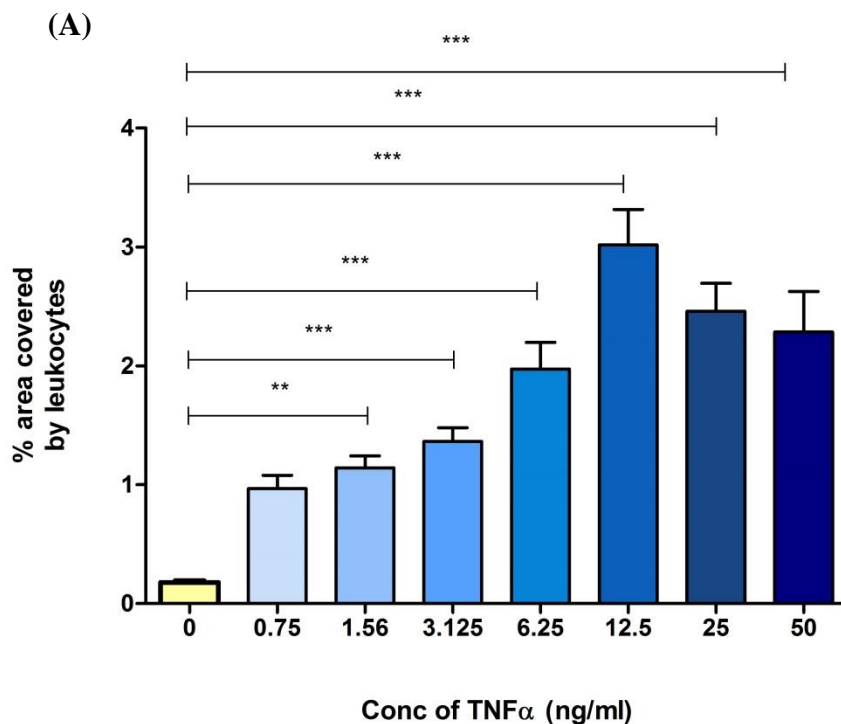


Figure 5.1: Immunofluorescence staining of HUVECs: HUVECs grown on coverslips, fixed with 4% paraformaldehyde, probed with primary antibodies (1:200) against CD144 and CD62E and stained with fluorescent secondary antibody (1:500). Nuclei were counterstained using DAPI. Images were captured using fluorescent microscope. (A) Indicates CD144 staining and (B) indicates CD62E staining. Scales bar: 20 μ m.

5.3.2 Effect of TNF- α on leukocyte-endothelial cell adhesion

A model for leukocyte adhesion to endothelial cells was developed by our research group (Wadey et al., 2019). TNF- α is known to increase leukocyte adhesion to HUVECs (Mackay 1993) and hence we sought to validate this model with varying doses of TNF- α . Increasing doses of TNF- α ranging from 0 to 50ng/ml was added to confluent HUVECs grown in 6-well plates, prior to the addition of leukocytes. Leukocyte attachment escalated with increasing dose of TNF- α (**Figure 5.2 (A) and (B)**). Maximal attachment was observed at TNF- α concentration of 12.5 ng/ml; beyond this, the percentage attachment reduced. **Figures 5.2 (A) and (B)** show the leukocyte coverage obtained expressed in quantitative and illustrative formats, respectively. Subsequently, expression of the cell adhesion molecule vascular cell adhesion molecule-1 [VCAM-1] was examined by western blotting. This confirmed an increase in expression in response to TNF- α at all concentrations used (**Figure 5.2 (C)**).



(B)

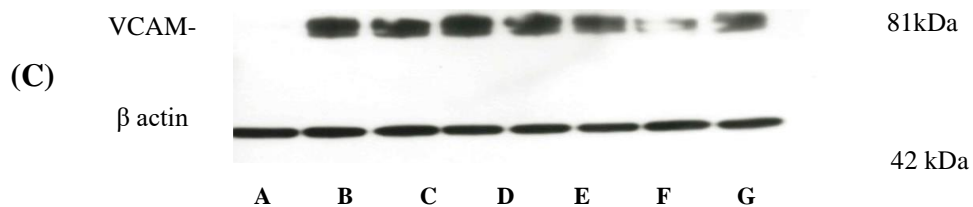
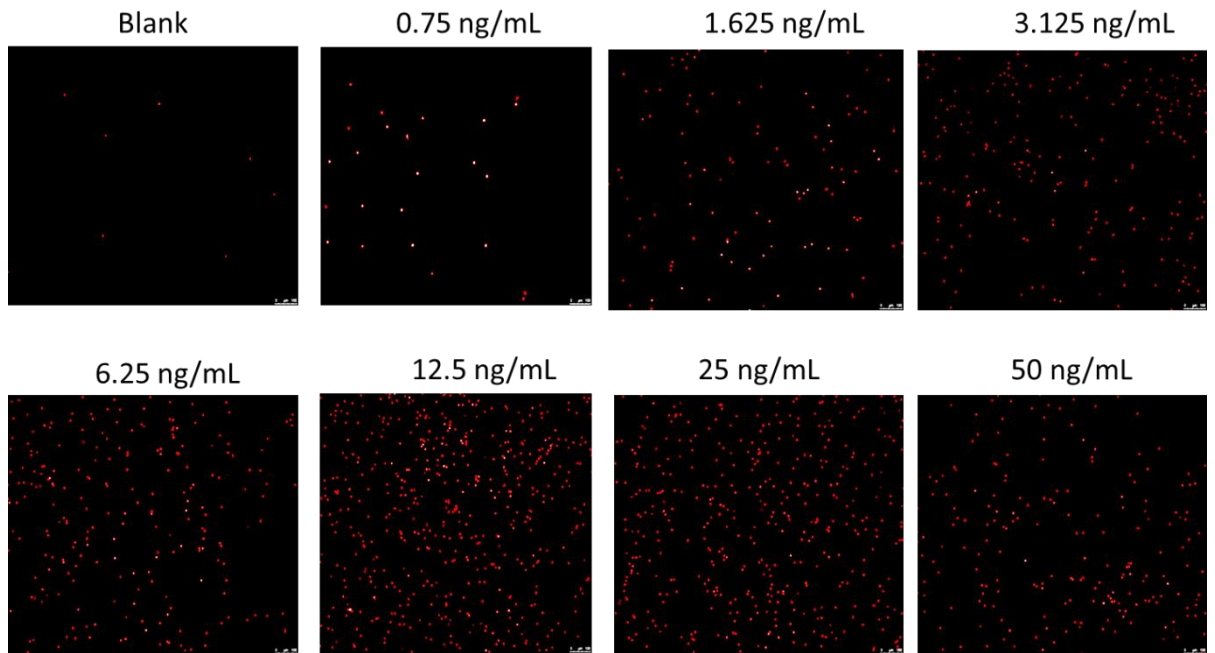
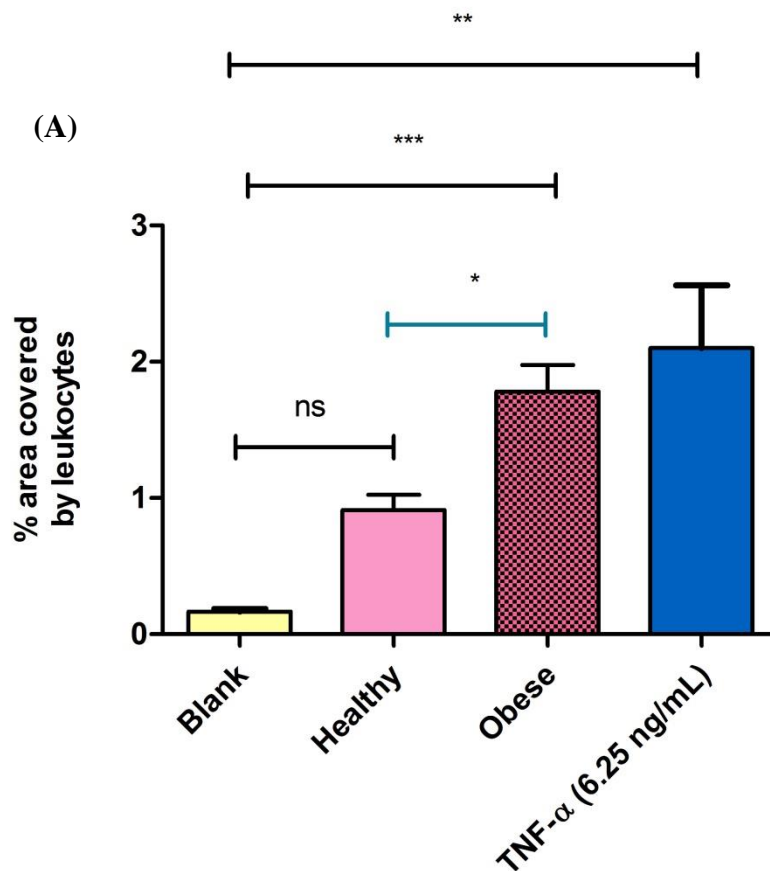


Figure 5.2: Effect of varying doses of TNF- α on leukocyte attachment to HUVECs. HUVECs pre-treated with TNF- α of varying doses from 0 (blank) to 50 ng/ml prior to the addition of CellTraceTM-stained leukocytes; the percentage leukocyte adhesion to HUVECs was subsequently investigated. (A) Denotes the percentage area covered by leukocytes to a confluent monolayer of HUVECs ($n=3$), ***, ** denotes $p<0.001$ and $p<0.01$, (B) corresponds to the representative fluorescent images of the percentage area covered ($n=3$), and (C) Western blot analysis of VCAM-1 expression in HUVECs where A = Blank, B = 0.75 ng/ml, C = 1.625 ng/ml, D = 3.125 ng/ml, E = 6.25 ng/ml, F = 12.5 ng/ml, G = 25 ng/ml, H = 50 ng/ml.

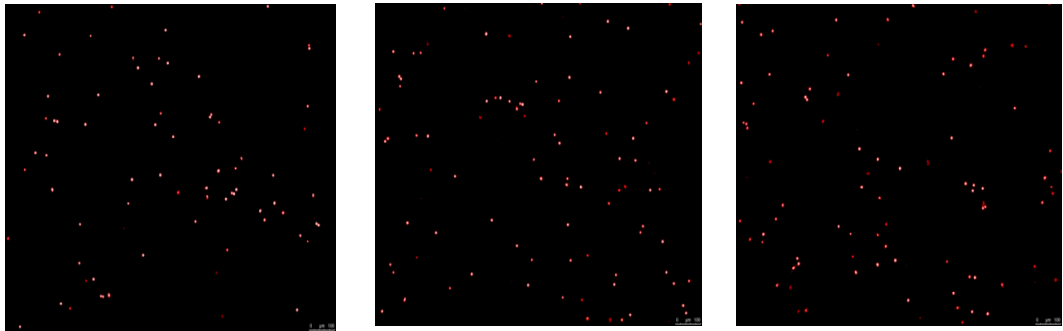
5.3.3 Effect of ADEVs (post-depletion) from Healthy and Obese subjects on leukocyte- endothelial cell adhesion

Following the validation of the leukocyte-endothelial cell adhesion model using TNF- α , I next sought to compare the effect of EVs, specifically ADEVs, obtained from healthy (n=7) and obese individuals (n=7) on leukocyte-endothelial cell adhesion. EVs obtained from plasma (of all subjects) were subjected to sequential purification by solid phase immunoassay to obtain a preparation of ADEVs, as described in the previous chapter (section). HUVECs were subsequently incubated with these purified ADEVs and leukocyte adhesion was evaluated. The mean percentage adhesion in the two groups was: healthy (0.91 ± 0.11 %) and obese (1.78 ± 0.20 %) that proved significantly different with $p < 0.05$



(B)

Healthy



Obese

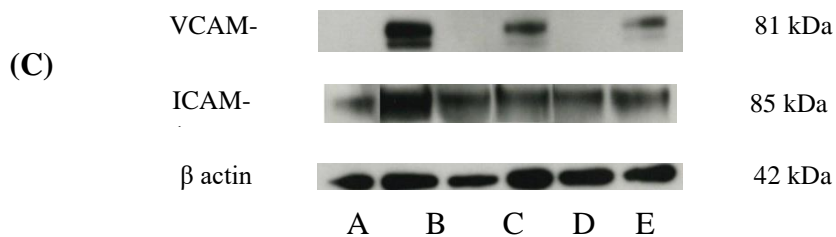
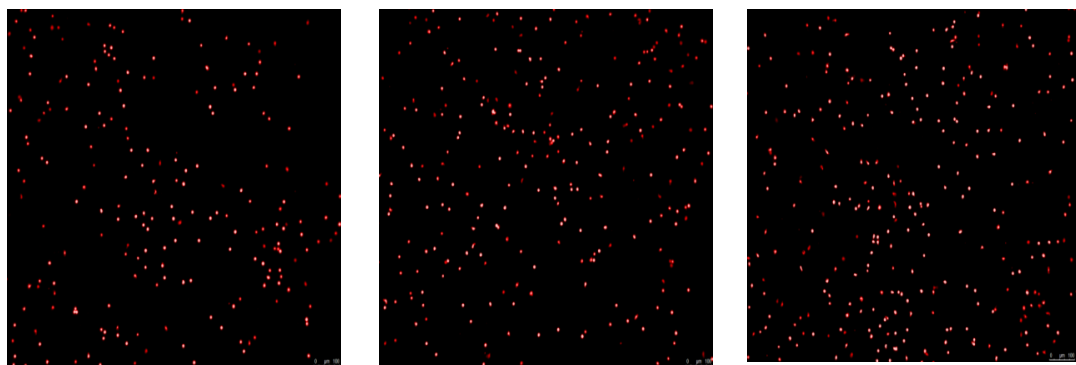


Figure 5.3: Effect of ADEVs from healthy and obese subjects on leukocyte attachment to HUVECs. ADEVs at a concentration of 3×10^9 particles/ml (absolute) obtained from both cohorts were incubated on HUVECs for 6 hours, followed by the addition of stained leukocytes. (A) Graphical representation of the mean of percentage leukocyte coverage in healthy (n=7) and obese (n=7) subjects, ***, **, * denotes $p < 0.001$, $p < 0.01$, $p < 0.05$ (B) three representative images of healthy and obese subjects ; (C) Western blot analysis of HUVECs treated with: A = Blank (no EVs), B = 10 ng/ml TNF (positive control), C and E = ADEVs from two healthy subjects, D and F = ADEVs obtained from two obese subjects.

5.4 Discussion

This chapter utilised the leukocyte adhesion assay to investigate the effect of ADEVs derived from two sample cohorts with characteristic differences in their BMI, in promoting the attachment of leukocytes to vascular endothelium. The sampled EVs (ADEVs) obtained from obese individuals elicited an increase in VCAM-1 on HUVECs that increased leukocyte attachment, when compared to EVs obtained from healthy individuals. Hence, it can be speculated that these ADEVs activate a pro-inflammatory response on HUVECs that mediates the recruitment of leukocytes. The crosstalk communication between leukocytes and endothelial cells plays a pivotal role in chronic vascular inflammation that hallmarks the development and progress of atherosclerosis, and consequently leads to CVD (Hosseinkhani et al. 2018). Thus, ADEVs are (or could be considered) potential mediators in the recruitment of leukocytes and contributing to vascular endothelial dysfunction.

HUVECs are a classic endothelial cell model used in scientific research to study aspects of endothelial function and pathways, under normal and disease-conditions. HUVECs were first cultured in the 1970s and soon were deemed a primary choice for vascular research (Jaffe et al. 1973). Their advantages include easy accessibility compared to other blood vessels, relative ease of culture, high proliferation rate, versatility and commercial availability. A standard laboratory protocol has been established for their isolation and maintenance with essential requirements, thus providing a fresh supply of primary cells (Marin et al. 2001; Baudin et al. 2007). HUVECs express characteristic endothelial markers, e.g. ICAM-1, VCAM-1 and selectins, and other signalling molecules associated with vascular physiology pathways (phosphorylation of VEGFR, Akt, MAPK, and expression eNOS) and dysfunction such as oxidative stress, hypoxia and inflammation (Boerma et al. 2006; Adya et al. 2008; Caniuguir et al. 2016). 3D culture models of HUVECs have been produced to gain better insights into the behaviour of ECs *in vivo* (Andrejcsk et al. 2013; Heiss et al. 2015). Furthermore, HUVECs are very responsive to physiological stimuli such as high glucose, TNF- α and lipopolysaccharide (Mackay 1993; Otu et al. 2005; Zhao et al. 2015b). HUVECs are harvested at an early developmental stage; a limitation may thus be that they are not truly representative of the *in vivo* condition as they derive from immune-privileged foetal tissue. Furthermore, some adult

endothelial markers may be absent. However, in this preliminary study I was able to demonstrate that the positive control TNF- α enhanced expression of VCAM-1.

TNF- α is a well-known pro-inflammatory cytokine that causes an increase in the expression of adhesion molecules on endothelial cells, thus inducing leukocyte attachment and a cascade of events (capture, rolling, migration) for their eventual entry into the vascular tissue bed (Muller 2003). Leukocytes, particularly monocytes, adhere poorly to ECs under normal conditions due to relatively low-level expression of adhesion molecules, whereas ECs can be activated by pro-atherogenic stimuli to release inflammatory mediators and express adhesion molecules to recruit monocytes. Numerous studies have been undertaken to show that ECs respond to several exogenous and endogenous pro-inflammatory stimuli; the three most recognised are lipopolysaccharide, TNF- α and interleukin-1 β . These proinflammatory factors differ in the pathways by which they bring about endothelial activation (Makó et al. 2010). HUVEC expression of TNF receptors TNF-R55 and TNF-R75 facilitate the binding of TNF- α on ECs, and the inflammation cascade is activated by the NF κ B (Mackay 1993). Studies have demonstrated different mechanisms through which TNF- α signalling can mediate endothelial breakdown and onset of vascular disease. TNF- α can induce gene expression of inflammatory cytokines and chemokines (Zhang et al. 2009), generate vascular oxidative stress by production of radicals (Picchi et al. 2006), decrease NO bioavailability (Gao et al. 2007), impair vasodilation, induce endothelial apoptosis and accelerate vascular atherothrombotic processes (Viridis et al., 2018). A study in mice with type-2 diabetes, inflammatory cytokines such as TNF- α and IL-6 were found to elicit endothelial dysfunction characterised by oxidative stress, reduced phosphorylation of eNOS and premature senescence (Khan et al. 2017; Lee et al. 2017). In this chapter of work, TNF- α in increasing dose was applied to examine its inflammatory effects on HUVECs (**Figure 5.2**). Western blotting confirmed the expression of VCAM-1 which is an indicator of endothelial activation. The leukocyte attachment reached a peak adherence at a concentration of about 12.5ng/ml and decreased thereafter. The decrease in leukocyte attachment with TNF concentrations above this critical point might reflect apoptosis or necrosis of HUVEC, but this was not investigated further. Others have also shown that a TNF- α concentration of 10ng/ml is optimal in inducing endothelial activation for leukocyte attachment (Turner et al. 2010).

EVs generated from various cell sources readily interact with endothelial cells (ECs). Besides cytokines and inflammatory molecules, studies have shown that EVs regulate activation of endothelial cells. Being the most exposed tissue, the endothelial surfaces come into contact with EVs released into the circulation. Studies have established their role in cell-to-cell communication, resulting in systemic effects by transferring their contents to recipient cells that differ from the cell of origin and transmitting metabolic signals from organ-to-organ (Tkach and Théry 2016, Thomou et al., 2017, Zhao et al., 2018). EVs shed by cancer cells (carcinoma cell lines) triggered HUVECs into a proangiogenic phenotype *in vitro*, by a defined CD147-mediated mechanism, promoting malignancy (Millimaggi et al. 2007). Tumour cell-derived EVs can carry oncogenes that switch the endothelial cells to an autocrine mode modulating angiogenesis via signalling receptors (Allison et al. 2009). ECs when pre-treated with EVs generated from infected macrophages, promoted macrophage migration through the monolayer as well as an upregulation of genes involved in cell adhesion and the inflammatory process (Li et al. 2018).

Our research group recently published a study culturing the preadipocyte cell line 3T3-L1 in different conditions of inflammation (TNF- α treated) and hypoxia that mimic the adipose tissue environment (Wadey et al., 2019) before the EVs were harvested. HUVECs were pre-treated with these EVs before measuring the extent of endothelial cell activation by leukocyte adhesion assay. EVs generated under TNF- α alone, and TNF- α plus hypoxia conditions showed significant activation of HUVECs and increased leukocyte adhesion when compared to EVs generated under normoxia. In my study, whilst ADEVs increased leukocyte attachment in both groups, this was significantly more marked in obese compared to lean subjects (**Figure 5.3**). This implies that obese ADEVs may elicit enhanced endothelial activation compared to lean ADEVs. Endothelial activation by these obese EVs was further reflected by the detection of VCAM-1 and ICAM-1, by western blot, taken to reflect an inflammatory character in obese-derived ADEVs. This preliminary observation could suggest a difference in the composition/nature of ADEVs derived from the two groups. However, this requires further investigation.

The EV samples used in the pre-treatment of HUVECs were obtained as developed in the previous chapter in order to comprise predominantly EVs of adipocyte character. The plasma collected from patients (healthy and obese) was column purified and

ultracentrifuged to obtain a preparation with maximum EV concentration. Subsequently, the major families of circulating EV populations were sequentially depleted to ensure an optimal isolation of ADEV. However, it should be acknowledged that the sample might still contain some trace amounts of other soluble particles and possibly other EVs that could have contributed to the activation of endothelial cells.

Obesity has been associated with increased levels of EVs in the circulation. An *in vitro* study revealed that stressed human primary adipocytes elicited a surge in EV production with a unique proteomic cargo following hypertrophy (Eguchi et al. 2016). During obesity, there is amplification in the release of EVs from adipocytes in the stromal fraction of AT which intensifies the vesicular effect in recipient tissue/organs (Stepanian et al. 2013; Lazar et al. 2016). This is exemplified in observations suggesting that ADEVs from obese subjects increase tumour metastasis, angiogenesis and AT inflammation. Lazar et al. demonstrated a positive correlation between BMI and EV shedding from AT and progression of exosome shedding with adipocyte maturation (Lazar et al. 2016). With the growth of adipose tissue in continuing obesity, the EVs generated are modified in a quantitative and qualitative manner. Metabolic changes in obese individuals were associated with differential expression of adipocyte-derived exosomal miRNAs between lean and obese individuals (Ferrante et al. 2015). Interestingly, miRNA expression profile of circulating ADEVs were also modified after bariatric surgery, correlating with improved insulin resistance (Hubal et al. 2017; Bae et al. 2019). Adipokine profiles differ between subcutaneous AT EV and visceral AT EV, with concentrations of IL-6, TNF- α , MIF and MCP-1 significantly higher in visceral AT EV compared to those from subcutaneous AT (Kranendonk et al. 2014a). A differential EV proteomic profile has also been observed between obese diabetic and obese non-diabetic rats (Lee et al. 2015).

A key aspect of obesity is the expansion in adipose tissue mass leading to adipocyte hypertrophy that directly correlates with BMI and metabolic dysfunction as studied in humans and mice (Cotillard et al. 2014; Rydén et al. 2014). In extreme obesity, as the hypertrophic threshold of adipocytes in AT is exceeded, it leads to ectopic lipid deposition in peripheral tissues (Muir et al. 2016). With adipocyte hypertrophy beyond a diameter of 100 microns, the effective oxygen supply to the tissue from the vasculature is compromised ensuing hypoxia (Muir et al. 2016). Hypertrophy coupled

with hypoxia within the AT instigates hypoxic-response genes, endoplasmic reticulum and oxidative stress, inflammation, and metabolic dysfunction, rendering the tissue inflammatory. Studies in *in vitro* cell culture systems and animal models have provided strong evidence for a role of hypoxia in modulating the production of several inflammation-related adipokines, including increased TNF- α , IL-6, leptin and macrophage migratory inhibition factor along with reduced adiponectin synthesis (Ye et al. 2007; Trayhurn 2013). Activated macrophages in inflamed AT also contribute to the production of TNF- α (Hagita et al. 2011) within adipose tissue. Interestingly, AT macrophages switch phenotype with increasing obesity. It has been observed in obese mice that a greater proportion of the macrophage population in AT are the classically activated M1 macrophages (Lumeng et al. 2008). On the other hand, the macrophage population in lean AT comprises the activated M2 phenotype that carries genes encoding anti-inflammatory proteins. *Weisberg et al.*, (2003) demonstrated that AT macrophages contribute almost all AT TNF- α expression as well as significant amounts of iNOS and IL-6 expression (Weisberg et al. 2003). This TNF- α could be packaged into EVs and released from AT into the circulation to elicit an inflammatory response in vascular endothelium.

EVs have been established as one of the key mediators in intercellular communication owing to their ability to traffic proteins, lipids and RNA between source and recipient cells. Inflammatory processes through endothelial cell activation have been propelled by EVs from various cell sources including leukocyte/monocyte adhesion and transmigration (Robbins et al. 2016). *In vitro* studies have shown that ECs and leukocytes release the pro-inflammatory cytokines IL-6 and IL-8 in response to EV signalling, promoting the expression of the adhesion molecules ICAM-1, VCAM-1 and E-selectin. This encourages monocyte adhesion onto vascular endothelium and subsequent transmigration, causing vascular inflammation and plaque development (Mesri and Altieri 1998; Mesri and Altieri 1999; Nomura et al. 2001). However, there has been limited work in understanding the role of ADEVs in endothelial activation in response to inflammation. An extensive study conducted by Crewe et al. (2018) unravelled a pathway of EV trafficking between adipocytes and endothelial cells influenced by the systemic nutrient state i.e. governed by fasting and obesity (Crewe et al. 2018). The extracellular molecules and signalling proteins were packaged into EVs by ECs for subsequent uptake in adipocytes. Conversely, adipocytes were seen

to release EVs that were taken up by ECs. EVs generated from a stressed adipocyte or an inflamed AT could pack itself with pro-inflammatory molecules like TNF- α , IL-1 β , IL-6, or leptin that are ubiquitously produced in AT and upon release into the circulation could induce an inflammatory response in vascular endothelium. The HUVECs in my studies demonstrated an inflammatory-like response as indicated in **Figure 5.3 (B)**, but investigation into the EV content, specifically for proinflammatory mediators such as TNF- α in healthy and obese derived EVs would have confirmed this.

In vitro studies conducted by our group under Dr Wadey's lead, were the first to show that adipocyte EVs (3T3-L1-derived) cultured in inflamed, TNF- α treated and hypoxic culture conditions, augmented the production of adhesion molecules on vascular endothelium and increased leukocyte attachment (Wadey et al., 2019). This model mimics the pathophysiological environment in extreme obesity, where AT is inflamed and hypoxic. These inflammatory adipocyte EVs significantly induced VCAM-1 expression, although other cell adhesion molecules including ICAM-1, E-selectin, P-selectin, PECAM and VE-cadherin was also detected. Similarly, in my work (**Figure 5.3 (C)**) ICAM-1 was expressed by HUVECs treated with EVs derived from both healthy and obese subjects, whereas VCAM-1 was selectively expressed by HUVECs treated with obese EVs and not detectable following exposure to lean EVs. The expression of VCAM-1 on activated endothelial cells is a strong indicator and critical for the development of atherosclerosis (Cybulsky et al. 2001). VCAM-1 mediates the firm adhesion to $\alpha 4\beta 1$ integrin which is constitutively expressed on leukocytes, especially lymphocytes and monocytes. Its expression is tightly regulated (Chen et al. 1999; Blankenberg et al. 2003). VCAM-1 is rapidly induced by pro-atherosclerotic conditions in rabbits, mice and humans, including in early lesions and not expressed under baseline conditions (Cybulsky and Gimbrone 1991; O'Brien et al. 1993; Nakashima et al. 1998). VCAM-1 and ICAM-1 participate in the pathogenesis of atherosclerosis by facilitating monocyte accumulation in the arterial intima. Expression is upregulated in atherosclerosis. However, VCAM-1 strongly induces the initiation of atherosclerosis and dominates at sites of lesion formation (Cybulsky et al. 2001). Antibodies targeting the blockade of VCAM-1 can be developed as a potential therapeutic agent. Anti-VCAM-1 antibody treatment in *ApoE*^{-/-} mice significantly reduced infiltration, adhesion and transmigration of immune cells into the

atherosclerotic plaques (Park et al. 2013). Reduced inflammation has proven to be an effective therapy to ameliorate and prevent CVD states such as atherosclerosis.

To summarise, if we extrapolate the results of my *in vitro* studies to the *in vivo* scenario, inflamed and hypoxic AT in obesity might release EVs with pro-inflammatory character that interact with the vascular endothelium. When released into the circulation, this subset of EVs with a proinflammatory character might prime the activation of endothelial cells in the peripheral vasculature to induce the expression of VCAM-1 that in turn increases leukocyte adhesion causing dysfunction of endothelial cells. The impaired endothelium subsequently leaks immune cells into the tissue, inducing a chronic state of inflammation that contributes to the progression of CVD notably atherosclerosis. The **Figure 5.10** demonstrates a conceptual representation of the role of ADEVs in endothelial dysfunction, as discussed above. This piece of work provides preliminary data to indicate a potential role of ADEVs in cascading the adhesion of leukocytes to vascular endothelium, which is a hallmark of inflammatory processes associated with obesity-related vascular disease.

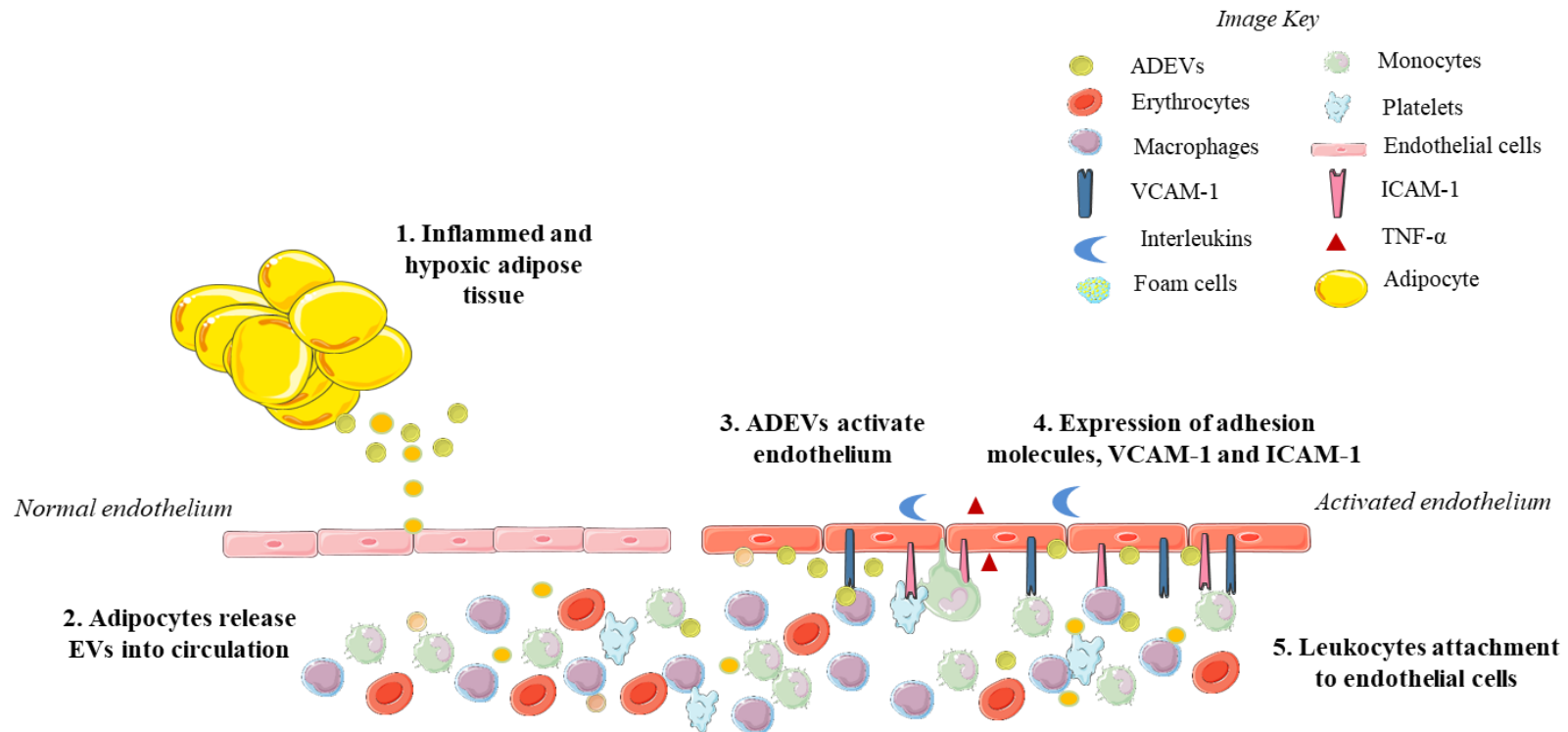


Figure 5.4: Conceptual illustration of the role of ADEVs in endothelial dysfunction. Under conditions of obesity where the adipose tissue is hypoxic and inflamed, it releases characteristic EV with altered profile. These ADEVs enter into circulation. Downstream, these ADEVs elicit an inflammatory response, potentially due to certain antigen present on them, inducing endothelial activation. Endothelial cells express adhesion molecules VCAM-1 and ICAM-1 that facilitate the attachment of leukocytes that otherwise travel through the circulation. ADEVs in circulation can also act as chemo-attractants. With increased attachment of leukocytes, a state of inflammation is intensified with presence of TNF- α and interleukins, eventually leading to endothelial dysfunction and vascular damage.

5.4.1 Limitations and future studies

This chapter comprises a pilot study into the role of circulating ADEVs in vascular endothelial inflammation. HUVECs provided an *in vitro* model to study interactions of ECs, whereas adult endothelial cells might offer a more relevant phenotype. The subject number in each cohort was also very limited; hence, although my results are compelling, a larger scale study with more detailed subject characterisation is still needed. In addition, a notable limitation of the study was that the comorbidities (including waist measurements) of the obese subjects could not be recorded during the time of this study. Based on earlier results, only two adhesion markers, VCAM-1 and ICAM-1, were examined, hence other adhesion molecules including PECAM-1 and E-selectin need to be evaluated. The key pro-inflammatory molecule delivered by ADEVs and the influence of EV content in leukocyte attachment also demands further investigation. Furthermore, elucidation of the pathway and mechanisms involved in the expression of adhesion molecules following incubation with ADEVs is required. Future studies should undertake more functional assays to delineate the role of ADEVs in tissue inflammation and progression of CVD. Indeed, the impact of ADEVs is likely not to be limited to vascular endothelium but may extend to other tissues and organs that orchestrate a systemic metabolic dysfunction. A better understanding of the effect of ADEVs on vascular endothelium may pave the way for the development of therapeutic targets for the diagnosis and treatment of obesity-associated CVD.

6. General discussion

6.1 Thesis summary

The overall aim of this research work was to establish techniques to obtain a purified EV population with a view to gathering evidence for the presence of adipocyte-derived EVs in the human circulation (plasma) and their potential functional impact on vascular endothelium.

Initially, I sought to gain an understanding in the relevant laboratory techniques for assessing EV concentration and character, in order to establish a footing for subsequent objectives. The well-established adipocyte cell line, 3T3-L1 was used as a comparative model to understand adipogenesis and establish adipocyte protein markers. Two approaches were considered while isolating EVs from plasma: ultracentrifugation of platelet-free plasma and size exclusion chromatography of platelet-depleted plasma. My results showed that the latter proved optimal for the isolation of plasma EVs with minimal protein contamination. After careful processing of the EV sample, magnetic bead capture and solid phase immunoassay was employed to deplete populations from major cell sources (non-adipocyte sources), leaving behind a portion of EV that was positive for a panel of EV- and adipocyte- specific markers along with certain adipokines, confirming a population of EVs sourced from adipocytes. This piece of work was novel in establishing that circulating human plasma contained adipocyte-derived EVs in healthy individuals. Furthermore, these ADEVs were examined for potential clinical implication, particularly in linking obesity and CVD. Samples containing ADEVs were procured by SEC followed by sequential magnetic bead depletion after collecting plasma from healthy and clinically obese individuals. The ADEV samples were used to pre-treat HUVECs before measuring the degree of leukocyte attachment on endothelial cells. An increased adherence was observed in ADEV samples obtained from obese subjects, accompanied by increased expression of VCAM-1 and ICAM-1 in HUVECs, when compared to healthy subjects. Leukocyte attachment on endothelium is an important initial event in atherosclerosis. This pilot study thus provided preliminary evidence of a functional effect of ADEVs which demands further in-depth investigation.

The potential of EVs as biomarkers is appreciable both in understanding physiological and disease states, since their protein content reflects information about the originating tissues, the pathophysiologic context and the severity of disease. EVs have also gained

interest as mediators in intercellular communication (Pitt et al. 2016). Notably, there are a growing number of studies examining their association with CVD (Zhao et al. 2015a; Lawson et al. 2016). However, if EVs are to be used as biomarkers of diseases, it is fundamentally important that the isolation technique ensures maximal vesicle yield in high purity while preserving biological structure. Since the field of EV research is relatively young, there are challenges in standardising EV isolation procedures, storage and analysis (Ramirez et al. 2018). However, during the course of this work, ISEV issued a statement with regards to the minimal requirements to identify EV populations as guidelines for researchers in the field (Lötvall et al. 2014). Although no gold standard isolation procedure was singled out, ISEV stated that the choice should depend on the downstream application and objectives in question. Due to their nanometric size and the complex composition of biological fluids, isolation of EVs at high yield is technically challenging. Therefore, methods and protocols to achieve this goal are under constant development.

The initial objective of Chapter 3 was to explore the principle techniques available in the research field for the phenotyping of EVs, as groundwork to achieve the aims of the subsequent chapters. NTA is a well-established method to estimate the concentration and particle size of EVs whereas TRF is a highly sensitive method of estimating the protein content in EVs by the principle of antigen-antibody binding and using lanthanide chelate-labelled reagents for an enhanced fluorescence detection (Webber et al. 2014b; Connolly et al. 2015; Szatanek et al. 2017). The presence of specific proteins was also detected by the well-established technique of western blotting. These techniques examined EV samples from 3T3-L1 cells and plasma for the adipocyte protein markers FABP4, adiponectin and PPAR- γ along with the classical EV marker CD9 (**Figure 3.4 & Figure 3.5**). SEC coupled with UC was assessed for the isolation of pure EVs from 3T3-L1 culture media (**Figure 3.7**) and similarly in plasma samples.

The initial section of this thesis included isolation of EVs through differential ultracentrifugation. Differential ultracentrifugation is a classical and common method of EV isolation. However, the efficiency of EV recovery from biological fluids is not fully optimised. Despite the advantages of the technique in handling large volumes of biological fluids, easy reproducibility, minimal use of reagents and chemicals, and cost effectiveness, the yield and purity of the EV isolate obtained through this protocol

is questionable (Lawson et al. 2016; Konoshenko et al. 2018). In downstream analysis (e.g., proteomic) which requires washing of the EV pellet, Webber and Clayton (2013) (Webber and Clayton 2013) demonstrated that washing reduced the EV yield (losses accounted by incomplete sedimentation and aggregation in the pellet); additional washing did not significantly improve the purity (the ratio of EVs to total protein) of the EV fraction as compared to the unwashed fraction. Parameters affecting the performance of UC include rotor type and sedimentation rate (Livshits et al. 2015). The buoyant density of EVs must be considerably different to other surrounding particles to enable isolation of pure fractions of particles. UC can sediment a mixture of particles with the same buoyant density if the sedimentation rates are not sufficiently different. Thus, during successive stages of differential centrifugation, a certain portion of small particles is sediment at earlier stages together with larger particles. In the meantime, a portion remains in the supernatant even after ultracentrifugation at 100,000 ×g. Such issues have been noted when processing urine samples for EV isolation (Musante et al. 2013). The UC pellet fraction contained large vesicles and protein aggregates, whilst the supernatant tested positive for EV markers. The authors concluded that nearly 40% of EVs were lost in the final UC supernatant. Furthermore, a longer centrifugation time increased the level of non-EV proteins in the EV preparation. Downstream EV protein analysis is thus compromised due to the formation of protein aggregates and co-sedimentation of non-EV particles. However, UC remains a favoured technique for EV isolation for *in vitro* studies (e.g. cell culture media-derived EVs) where the heterogeneity in particles is minimal, and samples are largely devoid of contaminating proteins or lipids. Ultracentrifugation can co-isolate plasma proteins, lipoproteins or RNP complexes that often contaminate EV working samples (Sódar et al. 2016; Takov et al. 2019). A one-step EV isolation method may thus, not ensure sufficient EV purification. This is especially important when considering purification from biological fluids that contain a mixture of particles, where UC cannot be used as a standalone technique for EV isolation. Under such circumstances, UC instead should be complemented by other isolation techniques. Novel strategies of coupling UC with ultrafiltration, dialysis and SEC are becoming increasingly popular and adopted in research studies involving biological fluids (Benedikter et al. 2017; Mitchell 2017).

SEC has become the method of choice for rapid isolation of relatively pure EVs from biological fluids, blood plasma, urine and CSF; SEC removes soluble proteins and lipoprotein impurities, which can be challenging, and where other methods fail (Muller et al. 2014b; Lozano-Ramos et al. 2015; Kreimer and Ivanov 2017). As demonstrated in **Figure 4.6** by western blotting and protein quantification, EVs and ‘free’ proteins are eluted in separate fractions which manifest a definite segregation of two populations by SEC. Although the later fractions (fractions 11 - 28) showed expression of the adipocyte marker proteins adiponectin, FABP4, perilipin and PPAR- γ , these were not associated with EVs. This observation has important implications in the evaluation of ADEVs in human plasma and underlines the importance of undertaking SEC prior to the analysis of adipocyte markers to avoid overestimations leading to flawed results. Thus, SEC ensures the isolation of EVs from biological fluids in an efficient, rapid, and almost loss-free method with a high reproducibility and reduced or absent contamination with non-EV proteins (Welton et al. 2015). In addition, since interaction with buffers and column fixed phase is minimal, the biological activity and integrity of the EVs (proteins and RNA) is preserved, which may be of particular value when undertaking downstream analysis for RNA profiling (Taylor et al. 2011; Taylor and Shah 2015; Gámez-Valero et al. 2016). The performance of column purification does, however, vary by commercial manufacturer. In a comparative study of columns from two manufacturers, SEC qEV (Millipore) showed enhanced performance in EV isolation from plasma with minimum protein contaminants and enriched identification of EV markers, as compared to the membrane affinity-based exoEasy kit (Qiagen) (Stranska et al. 2018). In another study, efficiency of SEC columns in EV isolation was evaluated based on albumin contamination (Baranyai et al. 2015). Sepharose CL-4B or Sephacryl S-400 columns eluted exosomes with significantly reduced albumin content whereas Sepharose 2B columns co-eluted albumin with exosomes. Therefore, it is critical to evaluate and validate such commercial columns prior to use in EV extraction from human plasma or urine samples.

The EVs found in the healthy human circulation are primarily derived from blood-borne and lining cells including platelets, leukocytes, endothelium and erythrocytes. Numerous *in vitro* studies have invoked evidence for the release of EVs from adipose tissue (Koeck et al. 2014; Mariette E G Kranendonk et al. 2014; Connolly et al. 2015).

Since adipose tissue comprises a mix of fibroblasts, leukocytes and endothelial cells, EVs released from the embedded adipocytes may be restricted in their entry into the circulation. Furthermore, ADEVs could be ingested by neighbouring cells before reaching the bloodstream (Crewe et al. 2018). For these and other reasons, ADEVs only form a small proportion of the totality of EVs present in human plasma. Based on some preliminary evidence gathered by our research group, Chapter 4 comprised an in-depth investigation into the presence of ADEVs in the human circulation. Two immuno-based techniques of magnetic bead capture and solid phase immunoassay were employed to sequentially deplete major circulating EV populations and establish if an adipocyte protein signature was retained in the post-depleted EV sample and verify if these adipocyte markers were reduced by the removal of non-adipocyte EV populations. The post-depleted EV sample tested positive for the expression of adipocyte-associated markers, namely FABP4, adiponectin, PPAR- γ and perilipin, as well as EV markers CD9 and ALIX (**Figure 4.8**). Also, the presence of major adipokines was recognised in the post-depleted sample, and TEM identified EV structures (**Figure 4.9**). Together, these findings confirm that an EV population derived from AT appears to exist in the human circulation. On the other hand, these proteins were also detected in the pre-depleted samples, indicating that these markers may also be associated with EVs from non-adipocyte origin. For example, macrophages are known to express FABP4 and PPAR- γ (Makowski et al. 2001; Furuhashi and Hotamisligil 2008).

Over the last decade, adipose tissue and adipocyte function have held the attention of the researchers due to its role in obesity and energy homeostasis, and potential role in the pathogenesis of diabetes, CVD and glucose metabolism (Rosen and Spiegelman 2006). AT is recognised as an endocrine organ that releases adipokines and cytokines, thus extending its role into metabolic regulation (Farmer 2006). More recently, it has become clear that ADEVs may contribute to AT dysregulation, insulin resistance and inflammation (Gao et al. 2017). Some studies have highlighted a paracrine role of ADEVs in the crosstalk between adipocytes and macrophages (Deng et al. 2009; Mariette E G Kranendonk et al. 2014). For example, differentiation of monocytes into macrophages of mixed phenotype (M1/M2) was induced by EVs derived from both subcutaneous and visceral adipose tissue explants (Mariette E G Kranendonk et al. 2014). Our group has previously shown that stressed 3T3-L1 adipocytes produce EVs

that act as chemo-attractants for monocytes and primary macrophages (Connolly et al. 2015). Furthermore, exosomes generated from AT explants was able to integrate into recipient cells and cause metabolic disruption. A study by Koeck et al. (2014) showed that AT-EVs can dysregulate TGF β signalling pathways in hepatocytes and impair the extracellular matrix, which in theory might contribute to liver fibrosis and link obesity to non-alcoholic fatty liver disease (NAFLD) (Koeck et al. 2014). A positive correlation has been established between ADEV shedding and BMI; moreover, EVs in overweight and obese individuals increased melanoma migration (Lazar et al. 2016). Adipocytes located in the tumour environment have been implicated in promoting tumour progression. EVs have been identified to modulate proliferation and survival of a tumour microenvironment by a signalling mechanism between tumour cells and stromal cells (Dirat et al. 2010). In the context of obesity, exosomes produced by mice adipose tissue explants exerted a pro-atherosclerotic role, by regulating macrophage foam cell formation and polarization, providing a link between AT and atherosclerosis (Xie et al. 2018). Of particular mention, the adipokine FABP4 has been implicated in the development of coronary atherosclerosis (Holm et al. 2011; Furuhashi et al. 2016). A study that investigated carotid atherosclerotic lesions of nearly 500 subjects recorded high levels of FABP4 in the plaque. FABP4 contributed to the instability of the plaque and increased risk of cardio vascular events (Peeters et al. 2011). With obesity-induced inflammation, FABP4 release is exaggerated in AT by adipocyte, inherent macrophages and recruited immune cells (macrophages, dendritic cells) and potentially harbouring in secreted EV load.

With this knowledge of a potential role of EVs in causing functional disruption and tissue damage, Chapter 5 investigated the role of circulatory ADEVs gathered from two cohorts (healthy and obese), in leukocyte adhesion, thus linking obesity and CVD. Recently, Crewe et al. (2018) established that EVs can signal between adipocytes and endothelial cells. They found that the systemic metabolic state was a regulating factor in the EV traffic from adipocytes and transfer of deprived proteins by packaged EVs from endothelial cells to adipocytes.

As discussed in Chapter 1, obese AT marked by increased adiposity and hypoxia, is associated with an increased infiltration of proinflammatory macrophages. This gives rise to tissue inflammation, predominantly via TNF- α secreted from large mature adipocytes and infiltrated or inherent macrophages (Thomas and Apovian 2017). Our

research group has recently shown that EVs generated from an inflamed and hypoxic AT model, can increase leukocyte adhesion accompanied by expression of endothelial adhesion molecules (Wadey et al., 2019). Connolly et al., (2015) found that hypoxic adipocyte (3T3-L1)-derived EVs are enriched in the monocyte chemoattractant protein, MCP-1, suggesting an aptitude of these EVs to communicate with monocytes and macrophages (Connolly et al. 2015). In the data I presented in chapter 5, ADEVs from obese subjects had a profound effect on leukocyte attachment compared to lean subjects (& control), established by the expression of VCAM-1 and ICAM-1 (**Figure 5.3**). Proinflammatory cytokines such as TNF- α , IL-1, IL-6 and MSP-1 could be contained in the EVs and mediate the activation of endothelial cells. I was careful to harvest and purify ADEVs as per protocols established in Chapter 4, by coupling SEC with UC and sequentially removing non-adipocyte EV populations. One of the limitations lies in the small subject numbers in each cohort and the practical difficulties in obtaining sufficient amount of plasma from clinics. Although this can be considered as a pilot study, the findings of increased leukocyte adhesion in ADEVs derived from obese subjects are nevertheless highly novel. As discussed in Chapter 5, this observation provides a new pathway linking obesity with vascular dysfunction, and is in agreement with a similar study conducted in mice where stressed AT released exosomes that had pro-atherosclerotic effects embodied through macrophage foam cell formation and M1 macrophage polarization (Xie et al. 2018). EV concentrations are known to increase in CVD and may contribute to atherosclerotic plaque formation and arterial stiffening (Rautou et al. 2011). However, further work is required to investigate these mechanisms further.

In summary, my data provide evidence for the existence of ADEVs in the human circulation, identified by adipocyte-specific proteins and adipokines, and their potential role in endothelial dysfunction. With EVs emerging as important mediators of intercellular communication, ADEVs are being recognised as novel markers of adipose tissue health and dysfunction. Adipocyte- and adipose tissue- derived EVs may be considered as active players in the pathogenesis of cardiovascular and metabolic diseases. On the other hand, they also hold promise as biomarkers and therapeutic targets with respect to AT function and obesity

6.2 Future directions

Research on EVs has seen unprecedented growth in recent years. This interest has arisen due to their potential roles as signalling molecules, pathogenic mediators, biomarkers and therapeutic vehicles. The EV research field is steadily growing, however, the isolation and measurement procedures have always been a topic of contention. ISEV has laid guidelines for the identification of EVs and defined standard procedures for isolation and characterisation (Lötvall et al. 2014). However, research studies that are designed under medical setting, it is essential that protocols are clinically approved and standardised in order for EVs to be considered as novel biomarkers or targets for therapeutic intervention.

Diagnostic tools for EV enumerations and characterisation are challenging and precarious when addressing plasma derived EVs, due to it containing a large number of proteins. The magnetic bead and solid phase capture techniques explored in this thesis could be developed as an immunoassay to selectively identify and quantify specific plasma EV populations by dual staining or testing positive for multiple markers (exosomal & cell-origin). This could be developed by adding a blend of carefully chosen antibodies to avoid cross-reactivity, which was attempted during early phases of this study but was met with limited success. A similar concept was used in the development of a one-step assay which was developed as a lateral flow immunoassay for the capture of exosomes with CD9 and CD81 (Oliveira-Rodríguez et al. 2016).

Given the evidence for a circulating population of ADEVs, it opens the door to several opportunities for research into identifying the types of EVs generated under varying systemic metabolic states, their protein signature, and functional role in the pathogenesis of metabolic disorders (Amosse et al. 2018). Another avenue for research is the pathway and mechanisms underlying the biogenesis of characteristic ADEVs under different physiological condition. Studies have established distinctive EV populations under pre- versus post adipogenesis, hypoxic versus normoxic, insulin-impaired EVs, inflammation induced EVs, etc in animal models and tissue explants and consequently, it would be interesting to investigate their existence in the circulation. With respect to obesity, inflamed AT and CVD has been linked based on clinical evidence from cohorts of different disease categories (Willerson 2004; Lopez-

Candales et al. 2017). EVs with pro-inflammatory character provide an alternative pathway for the propagation of endothelial dysfunction and breakdown, which could be the focus of further investigation. In parallel, this could also assist and benefit in the development of therapeutic strategies for the treatment of obesity driven CVDs (Welsh et al. 2017b). Furthermore, the function of ADEVs extends beyond vascular damage and my studies point to the potential in exploring other roles and functional impact of ADEVs.

References

- Aatonen, M. et al. 2012. Platelet-derived microvesicles: Multitalented participants in intercellular communication. In: *Seminars in Thrombosis and Hemostasis.*, pp. 102–113. doi: 10.1055/s-0031-1300956.
- Adya, R. et al. 2008. Visfatin induces human endothelial VEGF and MMP-2/9 production via MAPK and PI3K/Akt signalling pathways: Novel insights into visfatin-induced angiogenesis. *Cardiovascular Research* . doi: 10.1093/cvr/cvm111.
- Agardh, H.E. et al. 2013. Fatty acid binding protein 4 in circulating leucocytes reflects atherosclerotic lesion progression in Apoe^{-/-} mice. *Journal of Cellular and Molecular Medicine* . doi: 10.1111/jcmm.12011.
- Agarwal, K. et al. 2015. Analysis of exosome release as a cellular response to MAPK pathway inhibition. *Langmuir* 31(19), pp. 5440–5448. doi: 10.1021/acs.langmuir.5b00095.
- Agouni, A. et al. 2008. Endothelial dysfunction caused by circulating microparticles from patients with metabolic syndrome. *American Journal of Pathology* . doi: 10.2353/ajpath.2008.080228.
- Ahmadian, M. et al. 2013. PPAR γ signaling and metabolism: the good, the bad and the future. *Nature Medicine* 99(5), pp. 557–566. Available at: <http://www.nature.com/doi/10.1038/nm.3159>.
- Aiello, R.J. et al. 1999. Monocyte chemoattractant protein-1 accelerates atherosclerosis in apolipoprotein E-deficient mice. *Arteriosclerosis, Thrombosis, and Vascular Biology* . doi: 10.1161/01.ATV.19.6.1518.
- Allison, M.B. and Myers, M.G. 2014. 20 Years of Leptin: Connecting Leptin Signaling To Biological Function. *The Journal of endocrinology* 223(1), pp. T25-35. Available at: <http://www.pubmedcentral.nih.gov/articlerender.fcgi?artid=4170570&tool=pmcentrez&rendertype=abstract>.
- Alonso, D. and Radomski, M.W. 2003. The nitric oxide-endothelin-1 connection.

Heart Failure Reviews . doi: 10.1023/A:1022155206928.

Altiook, S. et al. 1997. PPAR γ induces cell cycle withdrawal: Inhibition of E2f/DP DNA-binding activity via down-regulation of PP2A. *Genes and Development* 11(15), pp. 1987–1998. doi: 10.1101/gad.11.15.1987.

Alvarez, S. et al. 2013. Urinary exosomes as a source of kidney dysfunction biomarker in renal transplantation. *Transplantation Proceedings* . doi: 10.1016/j.transproceed.2013.08.079.

Amabile, N. et al. 2014. Association of circulating endothelial microparticles with cardiometabolic risk factors in the Framingham Heart Study. *European Heart Journal* . doi: 10.1093/eurheartj/ehu153.

Ameer, F. et al. 2014. De novo lipogenesis in health and disease. *Metabolism: Clinical and Experimental* 63(7), pp. 895–902. doi: 10.1016/j.metabol.2014.04.003.

Amosse, J. et al. 2018. Phenotyping of circulating extracellular vesicles (EVs) in obesity identifies large EVs as functional conveyors of Macrophage Migration Inhibitory Factor. *Molecular Metabolism* . doi: 10.1016/j.molmet.2018.10.001.

An, Y.A. et al. 2017. Angiopoietin-2 in white adipose tissue improves metabolic homeostasis through enhanced angiogenesis. *eLife* . doi: 10.7554/eLife.24071.

Anand, P.K. et al. 2010. Exosomal hsp70 induces a pro-inflammatory response to foreign particles including mycobacteria. *PLoS ONE* . doi: 10.1371/journal.pone.0010136.

EL Andaloussi, S. et al. 2013. Extracellular vesicles: biology and emerging therapeutic opportunities. *Nature Reviews Drug Discovery* 12(5), pp. 347–357. Available at: <http://www.nature.com/doi/10.1038/nrd3978>.

Andrejcsk, J.W. et al. 2013. Paracrine exchanges of molecular signals between alginate-encapsulated pericytes and freely suspended endothelial cells within a 3D protein gel. *Biomaterials* . doi: 10.1016/j.biomaterials.2013.08.008.

Andreu, Z. et al. 2016. Comparative analysis of EV isolation procedures for miRNAs detection in serum samples. *Journal of Extracellular Vesicles* 1, pp. 1–10. doi: 10.3402/jev.v5.31655.

Aoki, N. et al. 2007. Identification and characterization of microvesicles secreted by 3T3-L1 adipocytes: Redox- and hormone-dependent induction of milk fat globule-epidermal growth factor 8-associated microvesicles. *Endocrinology* 148(8), pp. 3850–3862. doi: 10.1210/en.2006-1479.

Arita, Y. et al. 1999. Paradoxical decrease of an adipose-specific protein, adiponectin, in obesity. *Biochemical and Biophysical Research Communications* . doi: 10.1006/bbrc.1999.0255.

Armani, A. et al. 2010. Cellular models for understanding adipogenesis, adipose dysfunction, and obesity. *Journal of Cellular Biochemistry* 110(3), pp. 564–572. doi: 10.1002/jcb.22598.

Arraud, N. et al. 2014. Extracellular vesicles from blood plasma: Determination of their morphology, size, phenotype and concentration. *Journal of Thrombosis and Haemostasis* 12(5), pp. 614–627. doi: 10.1111/jth.12554.

ASANO, H. et al. 2014. Induction of Beige-Like Adipocytes in 3T3-L1 Cells. *Journal of Veterinary Medical Science* 76(1), pp. 57–64. Available at: <http://jlc.jst.go.jp/DN/JST.JSTAGE/jvms/13-0359?lang=en&from=CrossRef&type=abstract>.

Atay, S. et al. 2011. Morphologic and proteomic characterization of exosomes released by cultured extravillous trophoblast cells. *Experimental Cell Research* 317(8), pp. 1192–1202. doi: 10.1016/j.yexcr.2011.01.014.

Au Yeung, C.L. et al. 2016. Exosomal transfer of stroma-derived miR21 confers paclitaxel resistance in ovarian cancer cells through targeting APAF1. *Nature Communications* . doi: 10.1038/ncomms11150.

Avogaro, A. et al. 1999. Effect of acute ketosis on the endothelial function of type 1 diabetic patients: The role of nitric oxide. *Diabetes* . doi: 10.2337/diabetes.48.2.391.

Ayoub, N. et al. 2017. Analysis of circulating adipokines in patients newly diagnosed with solid cancer: Associations with measures of adiposity and tumor characteristics. *Oncology Letters* . doi: 10.3892/ol.2017.5670.

Backmark, A.E. et al. 2013. Fluorescent probe for high-throughput screening of

- membrane protein expression. *Protein Science* 22(8), pp. 1124–1132. doi: 10.1002/pro.2297.
- Badimon, L. and Cubedo, J. 2017. Adipose tissue depots and inflammation: Effects on plasticity and resident mesenchymal stem cell function. *Cardiovascular Research* . doi: 10.1093/cvr/cvx096.
- Bæk, R. and Jørgensen, M.M. 2017. Multiplexed phenotyping of small extracellular vesicles using protein microarray (EV array). In: *Methods in Molecular Biology*. doi: 10.1007/978-1-4939-6728-5_8.
- Baietti, M.F. et al. 2012. Syndecan–syntenin–ALIX regulates the biogenesis of exosomes. *Nature Cell Biology* 14(7), pp. 677–685. Available at: <http://www.nature.com/doi/10.1038/ncb2502>.
- Baig, S. et al. 2013. Lipidomic analysis of human placental Syncytiotrophoblast microvesicles in adverse pregnancy outcomes. *Placenta* . doi: 10.1016/j.placenta.2013.02.004.
- Bakker, S.J.L. et al. 2000. Cytosolic triglycerides and oxidative stress in central obesity: The missing link between excessive atherosclerosis, endothelial dysfunction, and β -cell failure? *Atherosclerosis* . doi: 10.1016/S0021-9150(99)00329-9.
- Balkom, B.W.M. va. et al. 2013. Endothelial cells require miR-214 to secrete exosomes that suppress senescence and induce angiogenesis in human and mouse endothelial cells. *Blood* 121(19), pp. 3997–4006. doi: 10.1182/blood-2013-02-478925.
- Barak, Y. et al. 1999. PPAR γ is required for placental, cardiac, and adipose tissue development. *Molecular Cell* 4(4), pp. 585–595. doi: 10.1016/S1097-2765(00)80209-9.
- Baranyai, T. et al. 2015. Isolation of exosomes from blood plasma: Qualitative and quantitative comparison of ultracentrifugation and size exclusion chromatography methods. *PLoS ONE* 10(12). doi: 10.1371/journal.pone.0145686.
- Barbatelli, G. et al. 2010. The emergence of cold-induced brown adipocytes in

mouse white fat depots is determined predominantly by white to brown adipocyte transdifferentiation. *AJP: Endocrinology and Metabolism* 298(6), pp. E1244–E1253. Available at: <http://ajpendo.physiology.org/cgi/doi/10.1152/ajpendo.00600.2009>.

Bartelt, A. et al. 2011. Brown adipose tissue activity controls triglyceride clearance. *Nature Medicine* 17(2), pp. 200–205. Available at: <http://www.nature.com/doi/10.1038/nm.2297>.

Batagov, A.O. and Kurochkin, I. V. 2013. Exosomes secreted by human cells transport largely mRNA fragments that are enriched in the 3'-untranslated regions. *Biology Direct* . doi: 10.1186/1745-6150-8-12.

Batrakova, E. V. and Kim, M.S. 2015. Using exosomes, naturally-equipped nanocarriers, for drug delivery. *Journal of Controlled Release* 219, pp. 396–405. doi: 10.1016/j.jconrel.2015.07.030.

Baumgarth, N. and Roederer, M. 2000. A practical approach to multicolor flow cytometry for immunophenotyping. *Journal of Immunological Methods* 243(1–2), pp. 77–97. doi: 10.1016/S0022-1759(00)00229-5.

Beloribi, S. et al. 2012. Exosomal Lipids Impact Notch Signaling and Induce Death of Human Pancreatic Tumoral SOJ-6 Cells. *PLoS ONE* . doi: 10.1371/journal.pone.0047480.

Belting, M. et al. 2013. Cancer cell exosomes depend on cell-surface heparan sulfate proteoglycans for their internalization and functional activity. *Proceedings of the National Academy of Sciences* . doi: 10.1073/pnas.1304266110.

Benedikter, B.J. et al. 2017. Ultrafiltration combined with size exclusion chromatography efficiently isolates extracellular vesicles from cell culture media for compositional and functional studies. *Scientific Reports* . doi: 10.1038/s41598-017-15717-7.

Beranger, G.E. et al. 2013. In vitro brown and 'brite'/'beige' adipogenesis: Human cellular models and molecular aspects. *Biochimica et Biophysica Acta - Molecular and Cell Biology of Lipids* 1831(5), pp. 905–914. doi: 10.1016/j.bbalip.2012.11.001.

Berg, A.H. and Scherer, P.E. 2005. Adipose tissue, inflammation, and cardiovascular

- disease. *Circulation Research* . doi: 10.1161/01.RES.0000163635.62927.34.
- Berne, B.J. and Pecora, R. 2003. *Dynamic Light Scattering: With Applications to Chemistry, Biology, and Physics*. doi: 10.1002/pi.4980090216.
- Bhatnagar, S. et al. 2007. Exosomes released from macrophages infected with intracellular pathogens stimulate a proinflammatory response in vitro and in vivo. *Blood* . doi: 10.1182/blood-2007-03-079152.
- Bhatnagar, S. and Schorey, J.S. 2007. Exosomes released from infected macrophages contain Mycobacterium avium glycopeptidolipids and are proinflammatory. *Journal of Biological Chemistry* 282(35), pp. 25779–25789. doi: 10.1074/jbc.M702277200.
- Blanchette-Mackie, E.J. et al. 1995. Perilipin is located on the surface layer of intracellular lipid droplets in adipocytes. *Journal of lipid research* 36(6), pp. 1211–1226.
- Blann, A. et al. 1999. Soluble intercellular adhesion molecule-1, E-selectin, vascular cell adhesion molecule-1 and von Willebrand factor in stroke. *Blood Coagulation and Fibrinolysis* . doi: 10.1097/00001721-199907000-00009.
- Bobrie, A. et al. 2012. Diverse subpopulations of vesicles secreted by different intracellular mechanisms are present in exosome preparations obtained by differential ultracentrifugation. *Journal of Extracellular Vesicles* . doi: 10.3402/jev.v1i0.18397.
- Boerma, M. et al. 2006. Comparative expression profiling in primary and immortalized endothelial cells: Changes in gene expression in response to hydroxy methylglutaryl-coenzyme A reductase inhibition. *Blood Coagulation and Fibrinolysis* . doi: 10.1097/01.mbc.0000220237.99843.a1.
- Böing, A.N. et al. 2014. Single-step isolation of extracellular vesicles from plasma by size-exclusion chromatography. *International Meeting of the of ISEV Rotterdam* 3, p. 118. doi: 10.3402/jev.v3.23430.
- Bolukbasi, M.F. et al. 2012. MiR-1289 and ‘zipcode’-like sequence enrich mRNAs in microvesicles. *Molecular Therapy - Nucleic Acids* . doi: 10.1038/mtna.2011.2.
- Boord, J.B. et al. 2004. Combined adipocyte-macrophage fatty acid-binding protein

deficiency improves metabolism, atherosclerosis, and survival in apolipoprotein E-deficient mice. *Circulation* . doi: 10.1161/01.CIR.0000141735.13202.B6.

Booth, A.M. et al. 2006. Exosomes and HIV Gag bud from endosome-like domains of the T cell plasma membrane. *Journal of Cell Biology* 172(6), pp. 923–935. doi: 10.1083/jcb.200508014.

Braga, M. et al. 2014. Follistatin promotes adipocyte differentiation, browning, and energy metabolism. *Journal of Lipid Research* 55(3), pp. 375–384. Available at: <http://www.jlr.org/lookup/doi/10.1194/jlr.M039719>.

Brett, S.I. et al. 2017. Immunoaffinity based methods are superior to kits for purification of prostate derived extracellular vesicles from plasma samples. *Prostate* 77(13), pp. 1335–1343. doi: 10.1002/pros.23393.

Bruno, S. et al. 2012. Microvesicles derived from mesenchymal stem cells enhance survival in a lethal model of acute kidney injury. *PLoS ONE* . doi: 10.1371/journal.pone.0033115.

Bruun, J.M. et al. 2003. Regulation of adiponectin by adipose tissue-derived cytokines: in vivo and in vitro investigations in humans. *Am J Physiol Endocrinol Metab* . doi: 10.1152/ajpendo.00110.2003.

Bunnell, B.A. et al. 2008. Adipose-derived stem cells: Isolation, expansion and differentiation. *Methods* 45(2), pp. 115–120. doi: 10.1016/j.ymeth.2008.03.006.

Buschow, S.I. et al. 2009. MHC II In dendritic cells is targeted to lysosomes or t cell-induced exosomes via distinct multivesicular body pathways. *Traffic* 10(10), pp. 1528–1542. doi: 10.1111/j.1600-0854.2009.00963.x.

Caby, M.-P. et al. 2005. Exosomal-like Vesicles are present in Human Blood Plasma. *International Immunology* 17(7), pp. 879–887. Available at: <https://academic.oup.com/intimm/article-lookup/doi/10.1093/intimm/dxh267>.

Cai, Z. et al. 2012. Immunosuppressive exosomes from TGF- β 1 gene-modified dendritic cells attenuate Th17-mediated inflammatory autoimmune disease by inducing regulatory T cells. *Cell Research* . doi: 10.1038/cr.2011.196.

Calles-Escandon, J. and Cipolla, M. 2001. Diabetes and endothelial dysfunction: A

clinical perspective. *Endocrine Reviews* . doi: 10.1210/edrv.22.1.0417.

Calzadilla, P. et al. 2013. N-Acetylcysteine affects obesity-related protein expression in 3T3-L1 adipocytes. *Redox report : communications in free radical research* 18(6), pp. 210–8. Available at: <http://www.ncbi.nlm.nih.gov/pubmed/24112955>.

Camp, H.S. et al. 2002. Adipogenesis and fat-cell function in obesity and diabetes. *Trends in Molecular Medicine* 8(9), pp. 442–447. doi: 10.1016/S1471-4914(02)02396-1.

de Candia, P. et al. 2013. Intracellular Modulation, Extracellular Disposal and Serum Increase of MiR-150 Mark Lymphocyte Activation. *PLoS ONE* . doi: 10.1371/journal.pone.0075348.

Caniuguir, A. et al. 2016. Markers of early endothelial dysfunction in intrauterine growth restriction-derived human umbilical vein endothelial cells revealed by 2D-DIGE and mass spectrometry analyses. *Placenta* . doi: 10.1016/j.placenta.2016.02.016.

Cannon, B. and Nedergaard, J. 2004. Brown Adipose Tissue: Function and Physiological Significance. *Physiol Rev* 84, pp. 277–359. doi: 10.1152/physrev.00015.2003.

Cao, Y. et al. 2017. The use of human umbilical vein endothelial cells (HUVECs) as an in vitro model to assess the toxicity of nanoparticles to endothelium: a review. *Journal of Applied Toxicology* . doi: 10.1002/jat.3470.

Caprio, M. et al. 2007. Pivotal role of the mineralocorticoid receptor in corticosteroid-induced adipogenesis. *FASEB journal : official publication of the Federation of American Societies for Experimental Biology* 21(9), pp. 2185–94. Available at: <http://www.ncbi.nlm.nih.gov/pubmed/17384139>.

Carayon, K. et al. 2011. Proteolipidic composition of exosomes changes during reticulocyte maturation. *Journal of Biological Chemistry* 286(39), pp. 34426–34439. doi: 10.1074/jbc.M111.257444.

Cardillo, C. et al. 2000. Interactions between nitric oxide and endothelin in the regulation of vascular tone of human resistance vessels in vivo. *Hypertension* . doi:

10.1161/01.HYP.35.6.1237.

Cavallari, C. et al. 2017. Serum-derived extracellular vesicles (EVs) impact on vascular remodeling and prevent muscle damage in acute hind limb ischemia. *Scientific Reports* . doi: 10.1038/s41598-017-08250-0.

Cawthorn, W.P. et al. 2012. Adipose tissue stem cells meet preadipocyte commitment: going back to the future. *Journal of Lipid Research* 53(2), pp. 227–246. Available at: <http://www.jlr.org/lookup/doi/10.1194/jlr.R021089>.

Chandler, W.L. et al. 2011. A new microparticle size calibration standard for use in measuring smaller microparticles using a new flow cytometer. *Journal of Thrombosis and Haemostasis* . doi: 10.1111/j.1538-7836.2011.04283.x.

Chang, C.-C. et al. 2015. Resveratrol exerts anti-obesity effects in high-fat diet obese mice and displays differential dosage effects on cytotoxicity, differentiation, and lipolysis in 3T3-L1 cells. *Endocrine journal* 63(2), pp. 169–178. doi: 10.1507/endocrj.EJ15-0545.

CHARGAFF, E. and WEST, R. 1946. The biological significance of the thromboplastic protein of blood. *The Journal of biological chemistry*

Charrière, G. et al. 2003. Preadipocyte conversion to macrophage: Evidence of plasticity. *Journal of Biological Chemistry* . doi: 10.1074/jbc.M210811200.

Chen, P.L. et al. 1996. Retinoblastoma protein positively regulates terminal adipocyte differentiation through direct interaction with C/EBPs. *Genes and Development* 10(21), pp. 2794–2804. doi: 10.1101/gad.10.21.2794.

Chen, Y.-W. et al. 2013. Absolute hypoxic exercise training enhances *in vitro* thrombin generation by increasing procoagulant platelet-derived microparticles under high shear stress in sedentary men. *Clinical Science* 124(10), pp. 639–649. Available at: <http://clinsci.org/lookup/doi/10.1042/CS20120540>.

Cheruvanky, A. et al. 2007. Rapid isolation of urinary exosomal biomarkers using a nanomembrane ultrafiltration concentrator. *AJP: Renal Physiology* 292(5), pp. F1657–F1661. Available at: <http://ajprenal.physiology.org/cgi/doi/10.1152/ajprenal.00434.2006>.

- Chironi, G. et al. 2006. Circulating leukocyte-derived microparticles predict subclinical atherosclerosis burden in asymptomatic subjects. *Arteriosclerosis, Thrombosis, and Vascular Biology* . doi: 10.1161/01.ATV.0000249639.36915.04.
- Chistiakov, D.A. et al. 2015. Endothelial barrier and its abnormalities in cardiovascular disease. *Frontiers in Physiology* . doi: 10.3389/fphys.2015.00365.
- Chiva-Blanch, G. et al. 2016. CD3+/CD45+ and SMA- α + circulating microparticles are increased in individuals at high cardiovascular risk who will develop a major cardiovascular event. *International Journal of Cardiology* . doi: 10.1016/j.ijcard.2016.01.211.
- Choi, H.Y. et al. 2011. Association of adiponectin, resistin, and vascular inflammation: Analysis with ¹⁸F-fluorodeoxyglucose positron emission tomography. *Arteriosclerosis, Thrombosis, and Vascular Biology* . doi: 10.1161/ATVBAHA.110.220673.
- Choi, K.M. et al. 2004. Serum adiponectin concentrations predict the developments of type 2 diabetes and the metabolic syndrome in elderly Koreans. *Clinical Endocrinology* . doi: 10.1111/j.1365-2265.2004.02063.x.
- Chow, A. et al. 2014. Macrophage immunomodulation by breast cancer-derived exosomes requires Toll-like receptor 2-mediated activation of NF- κ B. *Scientific Reports* . doi: 10.1038/srep05750.
- Church, C. et al. 2015. Conditional immortalization of primary adipocyte precursor cells. *Adipocyte* 4(3), pp. 203–211. Available at: <http://www.ncbi.nlm.nih.gov/pubmed/26257993>.
- Cocucci, E. et al. 2009. Shedding microvesicles: artefacts no more. *Trends in Cell Biology* 19(2), pp. 43–51. doi: 10.1016/j.tcb.2008.11.003.
- Collino, F. et al. 2009. Mesenchymal Stem Cell-Derived Microvesicles Protect Against Acute Tubular Injury. *Journal of the American Society of Nephrology* . doi: 10.1681/asn.2008070798.
- Colombo, M. et al. 2013. Analysis of ESCRT functions in exosome biogenesis, composition and secretion highlights the heterogeneity of extracellular vesicles.

Journal of Cell Science 126(24), pp. 5553–5565. Available at:
<http://jcs.biologists.org/lookup/doi/10.1242/jcs.128868>.

Colombo, M. et al. 2014. Biogenesis, Secretion, and Intercellular Interactions of Exosomes and Other Extracellular Vesicles. *Annual Review of Cell and Developmental Biology* 30(1), pp. 255–289. Available at:
<http://www.annualreviews.org/doi/10.1146/annurev-cellbio-101512-122326>.

Del Conde, I. et al. 2005. Tissue-factor-bearing microvesicles arise from lipid rafts and fuse with activated platelets to initiate coagulation. *Blood* 106(5), pp. 1604–1611. doi: 10.1182/blood-2004-03-1095.

Connolly, K.D. et al. 2015. Characterisation of adipocyte-derived extracellular vesicles released pre- and post-adipogenesis. *Journal of extracellular vesicles* 4, p. 29159. Available at: <http://www.ncbi.nlm.nih.gov/pubmed/26609807>.

Connolly, K.D. et al. 2018. Evidence for adipocyte-derived extracellular vesicles in the human circulation. *Endocrinology* . doi: 10.1210/en.2018-00266.

Corsini, A. et al. 1987. (5Z)-carbacyclin discriminates between prostacyclin-receptors coupled to adenylate cyclase in vascular smooth muscle and platelets. *British Journal of Pharmacology* . doi: 10.1111/j.1476-5381.1987.tb16847.x.

Coumans, F.A.W. et al. 2017. Bulk immunoassays for analysis of extracellular vesicles. *Platelets* 28(3), pp. 242–248. doi: 10.1080/09537104.2016.1265926.

Cousin, B. et al. 1996. Cellular changes during cold acclimation in adipose tissues. *Journal of Cellular Physiology* 167(2), pp. 285–289. doi: 10.1002/(SICI)1097-4652(199605)167:2<285::AID-JCP12>3.0.CO;2-7.

Crewe, C. et al. 2018. An Endothelial-to-Adipocyte Extracellular Vesicle Axis Governed by Metabolic State. *Cell* . doi: 10.1016/j.cell.2018.09.005.

Cristancho, A.G. and Lazar, M.A. 2011. Forming functional fat: a growing understanding of adipocyte differentiation. *Nature Reviews Molecular Cell Biology* 12(11), pp. 722–734. Available at:
<http://www.nature.com/doi/10.1038/nrm3198>.

Cybulsky, M.I. et al. 2001. A major role for VCAM-1, but not ICAM-1, in early

- atherosclerosis. *Journal of Clinical Investigation* . doi: 10.1172/JCI11871.
- Cybulsky, M.I. and Gimbrone, M.A. 1991. Endothelial expression of a mononuclear leukocyte adhesion molecule during atherogenesis. *Science* . doi: 10.1126/science.1990440.
- D'Uscio, L. V. et al. 2001. Hypercholesterolemia impairs endothelium-dependent relaxations in common carotid arteries of apolipoprotein E-deficient mice. *Stroke* . doi: 10.1161/hs1101.097393.
- Dalli, J. and Serhan, C.N. 2012. Specific lipid mediator signatures of human phagocytes: Microparticles stimulate macrophage efferocytosis and pro-resolving mediators. *Blood* 120(15). doi: 10.1182/blood-2012-04-423525.
- Dandona, P. et al. 2004. Inflammation: The link between insulin resistance, obesity and diabetes. *Trends in Immunology* 25(1), pp. 4–7. doi: 10.1016/j.it.2003.10.013.
- Darimont, C. and Macé, K. 2003. Immortalization of human preadipocytes. In: *Biochimie.*, pp. 1231–1233. doi: 10.1016/j.biochi.2003.10.015.
- Darlington, G.J. et al. 1998. The role of C/EBP genes in adipocyte differentiation. *Journal of Biological Chemistry* 273(46), pp. 30057–30060. doi: 10.1074/jbc.273.46.30057.
- Dear, J.W. et al. 2013. Urinary exosomes: A reservoir for biomarker discovery and potential mediators of intrarenal signalling. *Proteomics* 13(10–11), pp. 1572–1580. doi: 10.1002/pmic.201200285.
- Declercq, V. et al. 2015. Fatty acids increase adiponectin secretion through both classical and exosome pathways. *Biochimica et Biophysica Acta - Molecular and Cell Biology of Lipids* 1851(9), pp. 1123–1133. doi: 10.1016/j.bbalip.2015.04.005.
- Deng, Z. Bin et al. 2009. Adipose tissue exosome-like vesicles mediate activation of macrophage-induced insulin resistance. *Diabetes* 58(11), pp. 2498–2505. doi: 10.2337/db09-0216.
- Deregibus, M.C. et al. 2007. Endothelial progenitor cell - Derived microvesicles activate an angiogenic program in endothelial cells by a horizontal transfer of mRNA. *Blood* 110(7), pp. 2440–2448. doi: 10.1182/blood-2007-03-078709.

- Desarzens, S. et al. 2014. Hsp90 blockers inhibit adipocyte differentiation and fat mass accumulation. *PLoS ONE* 9(4). doi: 10.1371/journal.pone.0094127.
- Van Deun, J. et al. 2014. The impact of disparate isolation methods for extracellular vesicles on downstream RNA profiling. *Journal of Extracellular Vesicles* . doi: 10.3402/jev.v3.24858.
- Dirat, B. et al. 2010. Unraveling the obesity and breast cancer links: A role for cancer-associated adipocytes? *Endocrine Development* 19, pp. 45–52. doi: 10.1159/000316896.
- Divoux, A. et al. 2014. Identification of a novel lncRNA in gluteal adipose tissue and evidence for its positive effect on preadipocyte differentiation. *Obesity* 22(8), pp. 1781–1785. doi: 10.1002/oby.20793.
- Donnarumma, E. et al. 1959. Cancer-associated fibroblasts release exosomal microRNAs that dictate an aggressive phenotype in breast cancer. *Oncotarget*
- Dragovic, R.A. et al. 2011. Sizing and phenotyping of cellular vesicles using Nanoparticle Tracking Analysis. *Nanomedicine: Nanotechnology, Biology, and Medicine* 7(6), pp. 780–788. doi: 10.1016/j.nano.2011.04.003.
- Dragovic, R.A. et al. 2013. Multicolor Flow Cytometry and Nanoparticle Tracking Analysis of Extracellular Vesicles in the Plasma of Normal Pregnant and Pre-eclamptic Women1. *Biology of Reproduction* 89(6). Available at: <https://academic.oup.com/biolreprod/article-lookup/doi/10.1095/biolreprod.113.113266>.
- Duque, G.A. and Descoteaux, A. 2014. Macrophage cytokines: Involvement in immunity and infectious diseases. *Frontiers in Immunology* . doi: 10.3389/fimmu.2014.00491.
- Durcin, M. et al. 2017. Characterisation of adipocyte-derived extracellular vesicle subtypes identifies distinct protein and lipid signatures for large and small extracellular vesicles. *Journal of Extracellular Vesicles* 6(1). Available at: <http://dx.doi.org/10.1080/20013078.2017.1305677>.
- Egorina, E.M. et al. 2008. Regulation of tissue factor procoagulant activity by post-

translational modifications. *Thrombosis Research* 122(6), pp. 831–837. doi: 10.1016/j.thromres.2007.11.004.

Eguchi, A. et al. 2015. Microparticles release by adipocytes act as ‘find-me’ signals to promote macrophage migration. *PLoS ONE* 10(4). doi: 10.1371/journal.pone.0123110.

Eguchi, A. et al. 2016. Circulating adipocyte-derived extracellular vesicles are novel markers of metabolic stress. *Journal of Molecular Medicine* 94(11), pp. 1241–1253. Available at: <http://dx.doi.org/10.1007/s00109-016-1446-8>.

van Eijk, I.C. et al. 2010. Circulating microparticles remain associated with complement activation despite intensive anti-inflammatory therapy in early rheumatoid arthritis. *Annals of the rheumatic diseases* 69(7), pp. 1378–1382. doi: 10.1136/ard.2009.118372.

Elabd, C. et al. 2009. Human multipotent adipose-derived stem cells differentiate into functional brown adipocytes. *Stem Cells* 27(11), pp. 2753–2760. doi: 10.1002/stem.200.

Elberg, G. et al. 2000. Modulation of the Murine Peroxisome Proliferator-Activated Receptor gamma 2 Promoter Activity by CCAAT/Enhancer Binding Proteins. *Journal of Biological Chemistry* 275(36), pp. 27815–22. Available at: <http://www.ncbi.nlm.nih.gov/pubmed/10862621> <http://www.jbc.org/cgi/doi/10.1074/jbc.M003593200>.

Eldh, M. et al. 2010. Exosomes Communicate Protective Messages during Oxidative Stress; Possible Role of Exosomal Shuttle RNA. *PLoS ONE* . doi: 10.1371/journal.pone.0015353.

Engin, A. 2017. Endothelial dysfunction in obesity. In: *Advances in Experimental Medicine and Biology*. doi: 10.1007/978-3-319-48382-5_15.

Enomoto, K. et al. 2002. High-throughput miniaturized immunoassay for human interleukin-13 secreted from NK3.3 cells using homogenous time-resolved fluorescence. *Journal of Pharmaceutical and Biomedical Analysis* 28(1), pp. 73–79. doi: 10.1016/S0731-7085(01)00596-9.

- Erl, W. et al. 1998. Monocytic cell adhesion to endothelial cells stimulated by oxidized low density lipoprotein is mediated by distinct endothelial ligands. *Atherosclerosis* . doi: 10.1016/S0021-9150(97)00223-2.
- Escudier, B. et al. 2005. Vaccination of metastatic melanoma patients with autologous dendritic cell (DC) derived-exosomes: results of the first phase I clinical trial. *Journal of translational medicine* 3(1), p. 10. doi: 10.1186/1479-5876-3-10.
- Eseberri, I. et al. 2015. Doses of quercetin in the range of serum concentrations exert delipidating effects in 3T3-L1 preadipocytes by acting on different stages of adipogenesis, but not in mature adipocytes. *Oxidative Medicine and Cellular Longevity* 2015. doi: 10.1155/2015/480943.
- Esteve Ràfols, M. 2014. Adipose tissue: Cell heterogeneity and functional diversity. *Endocrinología y Nutrición (English Edition)* 61(2), pp. 100–112. Available at: <http://linkinghub.elsevier.com/retrieve/pii/S2173509314000336>.
- Farmer, S.R. 2006. Transcriptional control of adipocyte formation. *Cell Metabolism* 4(4), pp. 263–273. doi: 10.1016/j.cmet.2006.07.001.
- Félétou, M. and Vanhoutte, P.M. 2006. Endothelial dysfunction : a multifaceted disorder. *American Journal of Physiology - Heart and Circulatory Physiology* . doi: 10.1152/ajpheart.00292.2006.
- Fenech, M. et al. 2015. Effect of tissue inhibitor of metalloproteinases 3 on DLK1 shedding in cultured human pre-adipocytes and implications for adipose tissue remodelling. *Lancet (London, England)* 385 Suppl, p. S35. Available at: <http://ovidsp.ovid.com/ovidweb.cgi?T=JS%7B%7DPAGE=reference%7B%7DD=prem%7B%7DNEWS=N%7B%7DAN=26312857>.
- Feng, Y. et al. 2014. Ischemic preconditioning potentiates the protective effect of stem cells through secretion of exosomes by targeting Mecp2 via miR-22. *PLoS ONE* 9(2). doi: 10.1371/journal.pone.0088685.
- Ferrante, S.C. et al. 2015. Adipocyte-derived exosomal miRNAs: a novel mechanism for obesity-related disease. *Pediatric Research* 77(3), pp. 447–454. Available at: <http://www.nature.com/doi/10.1038/pr.2014.202>.

- Ferri, C. et al. 1997. Circulating endothelin-1 levels in obese patients with the metabolic syndrome. *Exp Clin Endocrinol Diabetes*
- Filipe, V. et al. 2010. Critical evaluation of nanoparticle tracking analysis (NTA) by NanoSight for the measurement of nanoparticles and protein aggregates. *Pharmaceutical Research* 27(5), pp. 796–810. doi: 10.1007/s11095-010-0073-2.
- Filková, M. et al. 2009. The role of resistin as a regulator of inflammation: Implications for various human pathologies. *Clinical Immunology* . doi: 10.1016/j.clim.2009.07.013.
- Fitzner, D. et al. 2011. Selective transfer of exosomes from oligodendrocytes to microglia by macropinocytosis. *Journal of Cell Science* . doi: 10.1242/jcs.074088.
- Flavahan, N.A. 2007. Balancing prostanoid activity in the human vascular system. *Trends in Pharmacological Sciences* . doi: 10.1016/j.tips.2007.01.003.
- Fleming, I. and Busse, R. 1999. Signal transduction of eNOS activation. *Cardiovascular Research* . doi: 10.1016/S0008-6363(99)00094-2.
- Foster, M.T. and Bartness, T.J. 2006. Sympathetic but not sensory denervation stimulates white adipocyte proliferation. *American journal of physiology. Regulatory, integrative and comparative physiology* 291(6), pp. R1630-7. Available at: <http://www.ncbi.nlm.nih.gov/pubmed/16887921>.
- Freiman, P.C. et al. 1986. Atherosclerosis impairs endothelium-dependent vascular relaxation to acetylcholine and thrombin in primates. *Circulation Research* . doi: 10.1161/01.RES.58.6.783.
- Freytag, S.O. et al. 1994. Ectopic expression of the CCAAT/enhancer-binding protein α promotes the adipogenic program in a variety of mouse fibroblastic cells. *Genes and Development* 8(14), pp. 1654–1663. doi: 10.1101/gad.8.14.1654.
- Fried, S.K. et al. 1998. Omental and subcutaneous adipose tissues of obese subjects release interleukin-6: Depot difference and regulation by glucocorticoid. *Journal of Clinical Endocrinology and Metabolism* . doi: 10.1210/jc.83.3.847.
- Furuhashi, M. et al. 2008. Adipocyte/macrophage fatty acid-binding proteins contribute to metabolic deterioration through actions in both macrophages and

- adipocytes in mice. *Journal of Clinical Investigation* . doi: 10.1172/JC134750.
- Furuhashi, M. et al. 2011. Serum fatty acid-binding protein 4 is a predictor of cardiovascular events in end-stage renal disease. *PLoS ONE* . doi: 10.1371/journal.pone.0027356.
- Furuhashi, M. et al. 2014. Fatty acid-binding protein 4 (FABP4): Pathophysiological insights and potent clinical biomarker of metabolic and cardiovascular diseases. *Clinical Medicine Insights: Cardiology* 2014, pp. 23–33. doi: 10.4137/CMC.S17067.
- Furuhashi, M. et al. 2016. Local production of fatty acid-binding protein 4 in epicardial/perivascular fat and macrophages is linked to coronary atherosclerosis. *Arteriosclerosis, Thrombosis, and Vascular Biology* . doi: 10.1161/ATVBAHA.116.307225.
- Furuhashi, M. and Hotamisligil, G.S. 2008. Fatty acid-binding proteins: Role in metabolic diseases and potential as drug targets. *Nature Reviews Drug Discovery* . doi: 10.1038/nrd2589.
- Fuseya, T. et al. 2017. Ectopic fatty acid-binding protein 4 expression in the vascular endothelium is involved in neointima formation after vascular injury. *Journal of the American Heart Association* . doi: 10.1161/JAHA.117.006377.
- Van Gaal, L.F. et al. 2006. Mechanisms linking obesity with cardiovascular disease. *Nature* . doi: 10.1038/nature05487.
- Gómez-Valero, A. et al. 2016. Size-Exclusion Chromatography-based isolation minimally alters Extracellular Vesicles' characteristics compared to precipitating agents. *Scientific Reports* 6. doi: 10.1038/srep33641.
- Gao, X. et al. 2007. Tumor necrosis factor- α induces endothelial dysfunction in Lepr^{db} mice. *Circulation* . doi: 10.1161/CIRCULATIONAHA.106.650671.
- Gao, X. et al. 2017. Extracellular vesicles from adipose tissue-A potential role in obesity and type 2 diabetes? *Frontiers in Endocrinology* 8(AUG). doi: 10.3389/fendo.2017.00202.
- Gardiner, C. et al. 2014. Measurement of refractive index by nanoparticle tracking analysis reveals heterogeneity in extracellular vesicles. *Journal of Extracellular*

Vesicles . doi: 10.3402/jev.v3.25361.

Gardiner, C. et al. 2016. Techniques used for the isolation and characterization of extracellular vesicles: Results of a worldwide survey. *Journal of Extracellular Vesicles* 5(1). doi: 10.3402/jev.v5.32945.

Garfield, A.S. 2010. Derivation of primary mouse embryonic fibroblast (PMEF) cultures. *Methods in molecular biology (Clifton, N.J.)* 633, pp. 19–27. doi: 10.1007/978-1-59745-019-5_2.

Garin-Shkolnik, T. et al. 2014. FABP4 attenuates PPAR γ and adipogenesis and is inversely correlated with PPAR γ in adipose tissues. *Diabetes* 63(3), pp. 900–911. doi: 10.2337/db13-0436.

Gawaz, M. et al. 2000. Platelets induce alterations of chemotactic and adhesive properties of endothelial cells mediated through an interleukin-1-dependent mechanism. Implications for atherogenesis. *Atherosclerosis* . doi: 10.1016/S0021-9150(99)00241-5.

Geddings, J.E. and Mackman, N. 2013. Tumor-derived tissue factor-positive microparticles and venous thrombosis in cancer patients. *Blood* 122(11), pp. 1873–1880. doi: 10.1182/blood-2013-04-460139.

Géminard, C. et al. 2004. Degradation of AP2 during reticulocyte maturation enhances binding of hsc70 and Alix to a common site on TfR for sorting in exosomes. *Traffic* 5(3), pp. 181–193. doi: 10.1111/j.1600-0854.2004.0167.x.

Gercel-Taylor, C. et al. 2012. Nanoparticle analysis of circulating cell-derived vesicles in ovarian cancer patients. *Analytical Biochemistry* 428(1), pp. 44–53. doi: 10.1016/j.ab.2012.06.004.

Ghossoub, R. et al. 2014. Syntenin-ALIX exosome biogenesis and budding into multivesicular bodies are controlled by ARF6 and PLD2. *Nature Communications* 5. Available at: <http://www.nature.com/doi/10.1038/ncomms4477>.

Gillilan, R.E. et al. 2007. Structural Basis for Activation of Fatty Acid-binding Protein 4. *Journal of Molecular Biology* . doi: 10.1016/j.jmb.2007.07.040.

Giordano, a et al. 1998. Sensory nerves affect the recruitment and differentiation of

rat periovarian brown adipocytes during cold acclimation. *Journal of cell science* 111 (Pt 1, pp. 2587–2594.

Giordano, A. et al. 2014. White, brown and pink adipocytes: The extraordinary plasticity of the adipose organ. *European Journal of Endocrinology* 170(5). doi: 10.1530/EJE-13-0945.

Giorgino, F. et al. 2005. Regional differences of insulin action in adipose tissue: insights from in vivo and in vitro studies. *Acta Physiologica Scandinavica* 183(1), pp. 13–30. Available at: <http://doi.wiley.com/10.1111/j.1365-201X.2004.01385.x>.

Giusti, I. et al. 2018. Ovarian cancer-derived extracellular vesicles affect normal human fibroblast behavior. *Cancer Biology and Therapy* . doi: 10.1080/15384047.2018.1451286.

Goettsch, C. et al. 2016. Sortilin mediates vascular calcification via its recruitment into extracellular vesicles. *Journal of Clinical Investigation* . doi: 10.1172/JCI80851.

Goetzl, E.J. et al. 2017. Altered cargo proteins of human plasma endothelial cell–derived exosomes in atherosclerotic cerebrovascular disease. *FASEB Journal* . doi: 10.1096/fj.201700149.

Goichot, B. et al. 2006. Circulating procoagulant microparticles in obesity. *Diabetes and Metabolism* . doi: 10.1016/S1262-3636(07)70251-3.

Goralski, K.B. et al. 2007. Chemerin, a novel adipokine that regulates adipogenesis and adipocyte metabolism. *Journal of Biological Chemistry* . doi: 10.1074/jbc.M700793200.

Gould, G.W. and Lippincott-Schwartz, J. 2009. New roles for endosomes: from vesicular carriers to multi-purpose platforms. *Nature Reviews Molecular Cell Biology* 10(4), pp. 287–292. Available at: <http://www.nature.com/doi/10.1038/nrm2652>.

Grassi, G. et al. 2010. Structural and functional alterations of subcutaneous small resistance arteries in severe human obesity. *Obesity* . doi: 10.1038/oby.2009.195.

Green, H. and Kehinde, O. 1976. Spontaneous heritable changes leading to increased adipose conversion in 3T3 cells. *Cell* 7(1), pp. 105–113. doi: 10.1016/0092-

8674(76)90260-9.

Green, H. and Meuth, M. 1974. An established pre-adipose cell line and its differentiation in culture. *Cell* 3(2), pp. 127–133. doi: 10.1016/0092-8674(74)90116-0.

Gregoire, F.M. et al. 1998. Understanding adipocyte differentiation. *Physiological reviews* 78(3), pp. 783–809. Available at: <http://www.ncbi.nlm.nih.gov/pubmed/9674695>.

Van Guilder, G.P. et al. 2011. Enhanced endothelin-1 system activity with overweight and obesity. *American Journal of Physiology-Heart and Circulatory Physiology* . doi: 10.1152/ajpheart.00206.2011.

Gupta, R.K. 2014. Adipocytes. *Current biology : CB* 24(20), pp. R988-93. Available at: <http://www.sciencedirect.com/science/article/pii/S096098221401118X>.

Gustafson, B. et al. 2015a. BMP4 and BMP antagonists regulate human white and beige adipogenesis. *Diabetes* 64(5), pp. 1670–1681. doi: 10.2337/db14-1127.

Gustafson, C.M. et al. 2015b. Age- and sex-specific differences in blood-borne microvesicles from apparently healthy humans. *Biology of Sex Differences* . doi: 10.1186/s13293-015-0028-8.

Hadi, H.A.R. et al. 2005. Endothelial dysfunction: cardiovascular risk factors, therapy, and outcome. *Vascular health and risk management*

Hagan, A.K. and Zuchner, T. 2011. Lanthanide-based time-resolved luminescence immunoassays. *Analytical and Bioanalytical Chemistry* 400(9), pp. 2847–2864. doi: 10.1007/s00216-011-5047-7.

Han, J. et al. 2013. ER stress signalling through eIF2 α and CHOP, but not IRE1 α , attenuates adipogenesis in mice. *Diabetologia* 56(4), pp. 911–924. doi: 10.1007/s00125-012-2809-5.

Hansen, H.O. et al. 1991. Induction of acyl-CoA-binding protein and its mRNA in 3T3-L1 cells by insulin during preadipocyte-to-adipocyte differentiation. *The Biochemical journal* 277 (Pt 2, pp. 341–4. Available at: <http://www.pubmedcentral.nih.gov/articlerender.fcgi?artid=1151239&tool=pmcentre>

z&rendertype=abstract.

Hansen, J.B. et al. 1999. Activation of peroxisome proliferator-activated receptor gamma bypasses the function of the retinoblastoma protein in adipocyte differentiation. *The Journal of biological chemistry* 274(4), pp. 2386–2393.

Available at:

<http://eutils.ncbi.nlm.nih.gov/entrez/eutils/elink.fcgi?dbfrom=pubmed&id=9891007&retmode=ref&cmd=prlinks%5Cnpapers3://publication/uuid/DFAAC7C9-CF3F-49A4-A31A-49D741F9B9AC>.

Hanson, P.I. and Cashikar, A. 2012. Multivesicular Body Morphogenesis. *Annual Review of Cell and Developmental Biology* 28(1), pp. 337–362. Available at:

<http://www.annualreviews.org/doi/10.1146/annurev-cellbio-092910-154152>.

Harms, M. and Seale, P. 2013. Brown and beige fat: development, function and therapeutic potential. *Nature Medicine* 19(10), pp. 1252–1263. Available at:

<http://www.nature.com/doi/10.1038/nm.3361>.

Harshman, S.W. et al. 2016. Proteomic characterization of circulating extracellular vesicles identifies novel serum myeloma associated markers. *Journal of Proteomics* 136, pp. 89–98. doi: 10.1016/j.jprot.2015.12.016.

Hart, R. and Greaves, D.R. 2010. Chemerin Contributes to Inflammation by Promoting Macrophage Adhesion to VCAM-1 and Fibronectin through Clustering of VLA-4 and VLA-5. *The Journal of Immunology* . doi: 10.4049/jimmunol.0902154.

Hattori, Y. et al. 1991. Effect of glucose and insulin on immunoreactive endothelin-1 release from cultured porcine aortic endothelial cells. *Metabolism* . doi:

10.1016/0026-0495(91)90168-V.

Hausman, G.J. et al. 2014. Preadipocyte and Adipose Tissue Differentiation in Meat Animals: Influence of Species and Anatomical Location. *Annual Review of Animal Biosciences* 2(1), pp. 323–351. Available at:

<http://www.annualreviews.org/doi/10.1146/annurev-animal-022513-114211>.

Heijnen, H.F. et al. 1999. Activated platelets release two types of membrane vesicles: microvesicles by surface shedding and exosomes derived from exocytosis of multivesicular bodies and alpha-granules. *Blood* 94(11), pp. 3791–3799.

Available at:

http://www.ncbi.nlm.nih.gov/entrez/query.fcgi?cmd=Retrieve&db=PubMed&dopt=Citation&list_uids=10572093.

Heiss, M. et al. 2015. Endothelial cell spheroids as a versatile tool to study angiogenesis in vitro. *FASEB Journal* . doi: 10.1096/fj.14-267633.

Heming, M. et al. 2018. Peroxisome proliferator-activated receptor- γ modulates the response of macrophages to lipopolysaccharide and glucocorticoids. *Frontiers in Immunology* . doi: 10.3389/fimmu.2018.00893.

Hemmilä, I. et al. 1984. Europium as a label in time-resolved immunofluorometric assays. *Analytical Biochemistry* 137(2), pp. 335–343. doi: 10.1016/0003-2697(84)90095-2.

Hernández-Mosqueira, C. et al. 2015. Tissue alkaline phosphatase is involved in lipid metabolism and gene expression and secretion of adipokines in adipocytes. *Biochimica et Biophysica Acta - General Subjects* 1850(12), pp. 2485–2496. doi: 10.1016/j.bbagen.2015.09.014.

Hertzel, A. V et al. 2017. Fatty acid binding protein 4/aP2-dependent BLT1R expression and signaling. *Journal of lipid research* . doi: 10.1194/jlr.M074542.

Hiebert, S.W. et al. 1992. The interaction of RB with E2F coincides with an inhibition of the transcriptional activity of E2F. *Genes and Development* 6(2), pp. 177–185. doi: 10.1101/gad.6.2.177.

Hiemstra, T.F. et al. 2014. Human Urinary Exosomes as Innate Immune Effectors. *Journal of the American Society of Nephrology* 25(9), pp. 2017–2027. Available at: <http://www.jasn.org/cgi/doi/10.1681/ASN.2013101066>.

Higuchi, M. et al. 2013. Differentiation of Human Adipose-Derived Stem Cells into Fat Involves Reactive Oxygen Species and Forkhead Box O1 Mediated Upregulation of Antioxidant Enzymes. *Stem Cells and Development* 22(6), pp. 878–888. Available at: <http://online.liebertpub.com/doi/abs/10.1089/scd.2012.0306>.

Himms-Hagen, J. et al. 2000. Multilocular fat cells in WAT of CL-316243-treated rats derive directly from white adipocytes. *American journal of physiology. Cell*

physiology 279(3), pp. C670–C681. doi: 10.1292/jvms.61.403.

Hoehn, E.N.M.N. t. et al. 2012. Quantitative and qualitative flow cytometric analysis of nanosized cell-derived membrane vesicles. *Nanomedicine: Nanotechnology, Biology, and Medicine* 8(5), pp. 712–720. doi: 10.1016/j.nano.2011.09.006.

Holm, S. et al. 2011. Fatty acid binding protein 4 is associated with carotid atherosclerosis and outcome in patients with acute ischemic stroke. *PLoS ONE* . doi: 10.1371/journal.pone.0028785.

Holme, P.A. et al. 1994. Demonstration of platelet-derived microvesicles in blood from patients with activated coagulation and fibrinolysis using a filtration technique and Western blotting. *Thrombosis and Haemostasis* 72(5), pp. 666–671.

Holven, K.B. et al. 2003. Patients with familial hypercholesterolaemia show enhanced spontaneous chemokine release from peripheral blood mononuclear cells ex vivo: Dependency of xanthomas/xanthelasms, smoking and gender. *European Heart Journal* . doi: 10.1016/S0195-668X(03)00467-6.

Hong, C.S. et al. 2014a. Isolation and characterization of CD34+ blast-derived exosomes in acute myeloid leukemia. *PLoS ONE* 9(8). doi: 10.1371/journal.pone.0103310.

Hong, C.S. et al. 2014b. Plasma exosomes as markers of therapeutic response in patients with acute myeloid leukemia. *Front Immunol* 5, p. 160. Available at: <http://www.ncbi.nlm.nih.gov/pubmed/24782865>.

Horowitz, J.F. et al. 1999. Effect of short-term fasting on lipid kinetics in lean and obese women. *The American journal of physiology*

Hosseinkhani, B. et al. 2018. Extracellular vesicles work as a functional inflammatory mediator between vascular endothelial cells and immune cells. *Frontiers in Immunology* . doi: 10.3389/fimmu.2018.01789.

Hotamisligil, G.S. et al. 1993. Adipose expression of tumor necrosis factor- α : Direct role in obesity-linked insulin resistance. *Science* . doi: 10.1126/science.7678183.

Hotamisligil, G.S. 1999. The role of TNF α and TNF receptors in obesity and insulin resistance. *Journal of internal medicine* 245(6), pp. 621–625. doi:

10.1046/j.1365-2796.1999.00490.x.

Hristov, M. et al. 2004. Apoptotic bodies from endothelial cells enhance the number and initiate the differentiation of human endothelial progenitor cells in vitro. *Blood* 104(9), pp. 2761–2766. doi: 10.1182/blood-2003-10-3614.

Huang, X. et al. 2012. The COP9 signalosome, cullin 3 and Keap1 supercomplex regulates CHOP stability and adipogenesis. *Biology Open* 1(8), pp. 705–710. Available at: <http://bio.biologists.org/cgi/doi/10.1242/bio.20121875>.

Huang, X. et al. 2013. Characterization of human plasma-derived exosomal RNAs by deep sequencing. *BMC Genomics* . doi: 10.1186/1471-2164-14-319.

Hubal, M.J. et al. 2017. Circulating adipocyte-derived exosomal MicroRNAs associated with decreased insulin resistance after gastric bypass. *Obesity* . doi: 10.1002/oby.21709.

Hunter, M.P. et al. 2008. Detection of microRNA expression in human peripheral blood microvesicles. *PLoS ONE* 3(11). doi: 10.1371/journal.pone.0003694.

Hwang, S.J. et al. 1997. Circulating adhesion molecules VCAM-1, ICAM-1, and E-selectin in carotid atherosclerosis and incident coronary heart disease cases: The Atherosclerosis Risk In Communities (ARIC) study. *Circulation* . doi: 10.1161/01.CIR.96.12.4219.

Iantorno, M. et al. 2014. Obesity, inflammation and endothelial dysfunction. *Journal of Biological Regulators and Homeostatic Agents*

Ibrahim, M.M. 2010. Subcutaneous and visceral adipose tissue: Structural and functional differences. *Obesity Reviews* 11(1), pp. 11–18. doi: 10.1111/j.1467-789X.2009.00623.x.

Inglis, H.C. et al. 2015. Techniques to improve detection and analysis of extracellular vesicles using flow cytometry. *Cytometry. Part A : the journal of the International Society for Analytical Cytology* (14), pp. 1–12. Available at: <http://www.ncbi.nlm.nih.gov/pubmed/25847910>.

Ismail, N. et al. 2013. Macrophage microvesicles induce macrophage differentiation and miR-223 transfer. *Blood* 121(6), pp. 984–995. doi: 10.1182/blood-2011-08-

374793.

Jaffe, E.A. et al. 1973. Culture of human endothelial cells derived from umbilical veins. Identification by morphologic and immunologic criteria. *Journal of Clinical Investigation* . doi: 10.1172/JCI107470.

Jaiswal, J.K. et al. 2002. Membrane proximal lysosomes are the major vesicles responsible for calcium-dependent exocytosis in nonsecretory cells. *Journal of Cell Biology* 159(4), pp. 625–635. doi: 10.1083/jcb.200208154.

Jayachandran, M. et al. 2015. Extracellular vesicles in urine of women with but not without kidney stones manifest patterns similar to men: a case control study. *Biology of sex differences* 6, p. 2. Available at: <http://www.pubmedcentral.nih.gov/articlerender.fcgi?artid=4345020&tool=pmcentrez&rendertype=abstract>.

Jenster, G. et al. 2019. Extracellular Vesicle Quantification and Characterization: Common Methods and Emerging Approaches. *Bioengineering* . doi: 10.3390/bioengineering6010007.

Jia, B. et al. 2012. Activation of protein kinase a and exchange protein directly activated by cAMP promotes adipocyte differentiation of human mesenchymal stem cells. *PLoS ONE* 7(3). doi: 10.1371/journal.pone.0034114.

Jia, L.-X. et al. 2017. ER stress dependent microparticles derived from smooth muscle cells promote endothelial dysfunction during thoracic aortic aneurysm and dissection. *Clinical Science* . doi: 10.1042/CS20170252.

Johansson, S.M. et al. 2008. Different types of in vitro generated human monocyte-derived dendritic cells release exosomes with distinct phenotypes. *Immunology* 123(4), pp. 491–499. doi: 10.1111/j.1365-2567.2007.02714.x.

Jones, B.H. et al. 1997. Angiotensin II increases lipogenesis in 3T3-L1 and human adipose cells. *Endocrinology* 138(4), pp. 1512–1519. doi: 10.1210/en.138.4.1512.

Jones, K.A. et al. 1999. cGMP modulation of Ca²⁺ sensitivity in airway smooth muscle. *The American journal of physiology*

Jørgensen, M. et al. 2013. Extracellular Vesicle (EV) array: Microarray capturing of

exosomes and other extracellular vesicles for multiplexed phenotyping. *Journal of Extracellular Vesicles* 2(1). doi: 10.3402/jev.v2i0.20920.

Jørgensen, M.M. et al. 2015. Potentials and capabilities of the extracellular vesicle (EV) array. *Journal of Extracellular Vesicles* 4(2015), pp. 1–8. doi: 10.3402/jev.v4.26048.

Juncker, D. et al. 2014. Cross-reactivity in antibody microarrays and multiplexed sandwich assays: Shedding light on the dark side of multiplexing. *Current Opinion in Chemical Biology* 18(1), pp. 29–37. doi: 10.1016/j.cbpa.2013.11.012.

Kang, I. et al. 2016a. Urolithin A, C, and D, but not iso-urolithin A and urolithin B, attenuate triglyceride accumulation in human cultures of adipocytes and hepatocytes. *Molecular Nutrition and Food Research* 60(5), pp. 1129–1138. doi: 10.1002/mnfr.201500796.

Kang, M.-C. et al. 2016b. Anti-obesity effects of seaweeds of Jeju Island on the differentiation of 3T3-L1 preadipocytes and obese mice fed a high-fat diet. *Food and Chemical Toxicology* 90, pp. 36–44. Available at: <http://linkinghub.elsevier.com/retrieve/pii/S0278691516300230>.

Kang, Y.E. et al. 2016c. The roles of adipokines, proinflammatory cytokines, and adipose tissue macrophages in obesity-associated insulin resistance in modest obesity and early metabolic dysfunction. *PLoS ONE* 11(4). doi: 10.1371/journal.pone.0154003.

Karaca, Ü. et al. 2014. Microvascular dysfunction as a link between obesity, insulin resistance and hypertension. *Diabetes Research and Clinical Practice* . doi: 10.1016/j.diabres.2013.12.012.

Kato, H. et al. 2015. Melatonin promotes adipogenesis and mitochondrial biogenesis in 3T3-L1 preadipocytes. *Journal of Pineal Research* 59(2), pp. 267–275. doi: 10.1111/jpi.12259.

Kaur, J. et al. 2010. Identification of chemerin receptor (ChemR23) in human endothelial cells: Chemerin-induced endothelial angiogenesis. *Biochemical and Biophysical Research Communications* . doi: 10.1016/j.bbrc.2009.12.150.

Kawanami, D. et al. 2004. Direct reciprocal effects of resistin and adiponectin on vascular endothelial cells: A new insight into adipocytokine-endothelial cell interactions. *Biochemical and Biophysical Research Communications* . doi: 10.1016/j.bbrc.2003.12.104.

Kawano, J. and Arora, R. 2009. The role of adiponectin in obesity, diabetes, and cardiovascular disease. *Journal of the CardioMetabolic Syndrome* . doi: 10.1111/j.1559-4572.2008.00030.x.

Kershaw, E.E. and Flier, J.S. 2004. Adipose tissue as an endocrine organ. *The Journal of clinical endocrinology and metabolism* 89(6), pp. 2548–56. Available at: <http://www.ncbi.nlm.nih.gov/pubmed/15181022>.

Khan, S.Y. et al. 2017. Premature senescence of endothelial cells upon chronic exposure to TNF α can be prevented by N-acetyl cysteine and plumericin. *Scientific Reports* . doi: 10.1038/srep39501.

Kieffer, T.J. and Habener, J.F. 2000. The adipoinsular axis: effects of leptin on pancreatic β -cells. *American Journal of Physiology - Endocrinology And Metabolism* 278(1), p. E1 LP-E14. Available at: <http://ajpendo.physiology.org/content/278/1/E1.abstract>.

Kim, H.R. et al. 2014a. Inhibitory effects of *Pericarpium zanthoxyli* extract on adipocyte differentiation. *International Journal of Molecular Medicine* 33(5), pp. 1140–1146. doi: 10.3892/ijmm.2014.1667.

Kim, J.-H. et al. 2014b. Suppression of PPAR γ through MKRN1-mediated ubiquitination and degradation prevents adipocyte differentiation. *Cell death and differentiation* 21(4), pp. 594–603. Available at: <http://www.ncbi.nlm.nih.gov/pubmed/24336050>.

Kim, J.B. and Spiegelman, B.M. 1996. ADD1/SREBP1 promotes adipocyte differentiation and gene expression linked to fatty acid metabolism. *Genes & Development* 10(9), pp. 1096–1107. Available at: <http://genesdev.cshlp.org/content/10/9/1096.abstract>.

Kim, N.H. et al. 2011. Circulating Chemerin Level is Independently Correlated with Arterial Stiffness. *Journal of Atherosclerosis and Thrombosis* . doi:

10.5551/jat.9647.

King, H.W. et al. 2012. Hypoxic enhancement of exosome release by breast cancer cells. *BMC Cancer* . doi: 10.1186/1471-2407-12-421.

Kjelsberg, M.O. 1982. Multiple Risk Factor Intervention Trial: Risk Factor Changes and Mortality Results. *JAMA: The Journal of the American Medical Association* . doi: 10.1001/jama.1982.03330120023025.

Klang, V. et al. 2013. Electron microscopy of pharmaceutical systems. *Micron* 44(1), pp. 45–74. doi: 10.1016/j.micron.2012.07.008.

Klumperman, J. and Raposo, G. 2014. The complex ultrastructure of the endolysosomal system. *Cold Spring Harbor Perspectives in Biology* 6(10). doi: 10.1101/cshperspect.a016857.

Knepper, M.A. and Pisitkun, T. 2007. Exosomes in urine: Who would have thought...? *Kidney International* 72(9), pp. 1043–1045. Available at: <http://linkinghub.elsevier.com/retrieve/pii/S0085253815528056>.

Kodidela, S. et al. 2018. Cytokine profiling of exosomes derived from the plasma of HIV-infected alcohol drinkers and cigarette smokers. *PLoS ONE* . doi: 10.1371/journal.pone.0201144.

Koeck, E.S. et al. 2014. Adipocyte exosomes induce transforming growth factor beta pathway dysregulation in hepatocytes: A novel paradigm for obesity-related liver disease. *Journal of Surgical Research* 192(2), pp. 268–275. doi: 10.1016/j.jss.2014.06.050.

Komai, A.M. et al. 2014. PKA-independent cAMP stimulation of white adipocyte exocytosis and adipokine secretion: modulations by Ca²⁺ and ATP. *The Journal of Physiology* 592(23), pp. 5169–5186. Available at: <http://doi.wiley.com/10.1113/jphysiol.2014.280388>.

Konoshenko, M.Y. et al. 2018. Isolation of Extracellular Vesicles: General Methodologies and Latest Trends. *BioMed Research International* . doi: 10.1155/2018/8545347.

Kranendonk, M.E. et al. 2014a. Effect of extracellular vesicles of human adipose

tissue on insulin signaling in liver and muscle cells. *Obesity (Silver Spring)* 22(10), pp. 2216–2223. Available at: <http://www.ncbi.nlm.nih.gov/pubmed/25045057>.

Kranendonk, M.E.G. et al. 2014b. Effect of extracellular vesicles of human adipose tissue on insulin signaling in liver and muscle cells. *Obesity* . doi: 10.1002/oby.20847.

Kranendonk, M.E.G. et al. 2014c. Extracellular vesicle markers in relation to obesity and metabolic complications in patients with manifest cardiovascular disease. *Cardiovascular Diabetology* . doi: 10.1186/1475-2840-13-37.

Kranendonk, M.E.G. et al. 2014d. Human adipocyte extracellular vesicles in reciprocal signaling between adipocytes and macrophages. *Obesity* 22(5), pp. 1296–1308. doi: 10.1002/oby.20679.

Kreimer, S. and Ivanov, A.R. 2017. Rapid Isolation of Extracellular Vesicles from Blood Plasma with Size-Exclusion Chromatography Followed by Mass Spectrometry-Based Proteomic Profiling. *Methods in molecular biology (Clifton, N.J.)* . doi: 10.1007/978-1-4939-7253-1_24.

Krzyzanowska, K. et al. 2004. Weight loss reduces circulating asymmetrical dimethylarginine concentrations in morbidly obese women. *Journal of Clinical Endocrinology and Metabolism* . doi: 10.1210/jc.2004-0672.

Kubes, P. et al. 2006. Nitric oxide: an endogenous modulator of leukocyte adhesion. *Proceedings of the National Academy of Sciences* . doi: 10.1073/pnas.88.11.4651.

Kubota, N. et al. 1999. PPAR γ mediates high-fat diet-induced adipocyte hypertrophy and insulin resistance. *Molecular Cell* 4(4), pp. 597–609. doi: 10.1016/S1097-2765(00)80210-5.

Kubota, N. et al. 2002. Disruption of adiponectin causes insulin resistance and neointimal formation. *Journal of Biological Chemistry* 277(29), pp. 25863–25866. doi: 10.1074/jbc.C200251200.

Lai, C.S. et al. 2016. Bisdemethoxycurcumin Inhibits Adipogenesis in 3T3-L1 Preadipocytes and Suppresses Obesity in High-Fat Diet-Fed C57BL/6 Mice. *Journal of Agricultural and Food Chemistry* 64(4), pp. 821–830. doi:

10.1021/acs.jafc.5b05577.

Lai, R.C. et al. 2010. Exosome secreted by MSC reduces myocardial ischemia/reperfusion injury. *Stem Cell Research* 4(3), pp. 214–222. doi: 10.1016/j.scr.2009.12.003.

Lane, J.M. et al. 2014. Development of an OP9 derived cell line as a robust model to rapidly study adipocyte differentiation. *PLoS ONE* 9(11). doi: 10.1371/journal.pone.0112123.

Langer, H.F. and Chavakis, T. 2009. Leukocyte - Endothelial interactions in inflammation. *Journal of Cellular and Molecular Medicine* . doi: 10.1111/j.1582-4934.2009.00811.x.

Larsen, M.R. et al. 2012. Characterization of Membrane-shed Microvesicles from Cytokine-stimulated β -Cells Using Proteomics Strategies. *Molecular & Cellular Proteomics* . doi: 10.1074/mcp.m111.012732.

Lässer, C. 2013. Identification and analysis of circulating exosomal microRNA in human body fluids. *Methods in molecular biology (Clifton, N.J.)* 1024, pp. 109–128. doi: 10.1007/978-1-62703-453-1_9.

Laulagnier, K. et al. 2004. Mast cell- and dendritic cell-derived exosomes display a specific lipid composition and an unusual membrane organization. *The Biochemical journal* 380(Pt 1), pp. 161–71. Available at: <http://www.pubmedcentral.nih.gov/articlerender.fcgi?artid=1224152&tool=pmcentrez&rendertype=abstract>.

Lawrie, A.S. et al. 2009. Microparticle sizing by dynamic light scattering in fresh-frozen plasma. *Vox Sanguinis* 96(3), pp. 206–212. doi: 10.1111/j.1423-0410.2008.01151.x.

Lawson, C. et al. 2016. Microvesicles and exosomes: New players in metabolic and cardiovascular disease. *Journal of Endocrinology* 228(2), pp. R57–R71. doi: 10.1530/JOE-15-0201.

Lazar, I. et al. 2016. Adipocyte Exosomes Promote Melanoma Aggressiveness through Fatty Acid Oxidation: A Novel Mechanism Linking Obesity and Cancer.

Cancer Research 76(14), pp. 4051–4057. doi: 10.1158/0008-5472.CAN-16-0651.

Lee, D. et al. 2014a. Expression of fatty acid binding protein 4 is involved in the cell growth of oral squamous cell carcinoma. *Oncology Reports* . doi: 10.3892/or.2014.2975.

Lee, J. et al. 2017. Interaction of IL-6 and TNF- α contributes to endothelial dysfunction in type 2 diabetic mouse hearts. *PLoS ONE* . doi: 10.1371/journal.pone.0187189.

Lee, M.J. et al. 2014b. Prolonged efficiency of siRNA-mediated gene silencing in primary cultures of human preadipocytes and adipocytes. *Obesity* 22(4), pp. 1064–1069. doi: 10.1002/oby.20641.

Lee, M.J. and Fried, S.K. 2014. Optimal protocol for the differentiation and metabolic analysis of human adipose stromal cells. *Methods in Enzymology* 538, pp. 49–65. doi: 10.1016/B978-0-12-800280-3.00004-9.

Lee, T.S. et al. 2009. Resistin increases lipid accumulation by affecting class A scavenger receptor, CD36 and ATP-binding cassette transporter-A1 in macrophages. *Life Sciences* . doi: 10.1016/j.lfs.2008.11.004.

Lessard, J. et al. 2014. Low abdominal subcutaneous preadipocyte adipogenesis is associated with visceral obesity, visceral adipocyte hypertrophy, and a dysmetabolic state. *Adipocyte* 3(3), pp. 197–205. Available at: <http://www.pubmedcentral.nih.gov/articlerender.fcgi?artid=4110096&tool=pmcentrez&rendertype=abstract>.

Li, P. et al. 2017a. Progress in exosome isolation techniques. *Theranostics* 7(3), pp. 789–804. doi: 10.7150/thno.18133.

Li, P. et al. 2017b. Progress in Exosome Isolation Techniques. *Theranostics* 7(3), pp. 789–804. Available at: <http://www.thno.org/v07p0789.htm>.

Libby, P. 2012. Inflammation in atherosclerosis. *Arteriosclerosis, Thrombosis, and Vascular Biology* . doi: 10.1161/ATVBAHA.108.179705.

Libby, P. and Aikawa, M. 1998. New insights into plaque stabilisation by lipid lowering. In: *Drugs*. doi: 10.2165/00003495-199856001-00002.

- Lim, Y.M. et al. 2014. Systemic autophagy insufficiency compromises adaptation to metabolic stress and facilitates progression from obesity to diabetes. *Nature Communications* . doi: 10.1038/ncomms5934.
- Lin, F.T. and Lane, M.D. 1992. Antisense CCAAT/enhancer-binding protein RNA suppresses coordinate gene expression and triglyceride accumulation during differentiation of 3T3-L1 preadipocytes. *Genes and Development* 6(4), pp. 533–544. doi: 10.1101/gad.6.4.533.
- Lin, Z. et al. 2013. Adiponectin mediates the metabolic effects of FGF21 on glucose homeostasis and insulin sensitivity in mice. *Cell Metabolism* 17(5), pp. 779–789. doi: 10.1016/j.cmet.2013.04.005.
- Linares, R. et al. 2015. High-speed centrifugation induces aggregation of extracellular vesicles. *Journal of Extracellular Vesicles* . doi: 10.3402/jev.v4.29509.
- Livshits, M.A. et al. 2015. Isolation of exosomes by differential centrifugation: Theoretical analysis of a commonly used protocol. *Scientific Reports* 5(1), p. 17319. Available at: <http://www.nature.com/articles/srep17319>.
- Llorente, A. et al. 2013. Molecular lipidomics of exosomes released by PC-3 prostate cancer cells. *Biochimica et Biophysica Acta - Molecular and Cell Biology of Lipids* 1831(7), pp. 1302–1309. doi: 10.1016/j.bbalip.2013.04.011.
- Lo, J.C. et al. 2014. Adipsin is an adipokine that improves β cell function in diabetes. *Cell* 158(1), pp. 41–53. doi: 10.1016/j.cell.2014.06.005.
- Looze, C. et al. 2009. Proteomic profiling of human plasma exosomes identifies PPAR γ as an exosome-associated protein. *Biochemical and Biophysical Research Communications* 378(3), pp. 433–438. Available at: <http://dx.doi.org/10.1016/j.bbrc.2008.11.050>.
- Lopez-Candales, A. et al. 2017. Linking Chronic Inflammation with Cardiovascular Disease: From Normal Aging to the Metabolic Syndrome. *Journal of nature and science*
- Lötvall, J. et al. 2014. Minimal experimental requirements for definition of extracellular vesicles and their functions: a position statement from the International

Society for Extracellular Vesicles. *Journal of extracellular vesicles* 3, p. 26913.

Louet, J.-F. et al. 2006. Oncogenic steroid receptor coactivator-3 is a key regulator of the white adipogenic program. *Proceedings of the National Academy of Sciences of the United States of America* 103, pp. 17868–17873. doi: 10.1073/pnas.0608711103.

Lozano-Ramos, I. et al. 2015. Size-exclusion chromatography-based enrichment of extracellular vesicles from urine samples. *Journal of Extracellular Vesicles* . doi: 10.3402/jev.v4.27369.

Ludmer, P.L. et al. 1986. Paradoxical vasoconstriction induced by acetylcholine in atherosclerotic coronary arteries. *The New England Journal of Medicine* . doi: 10.1056/NEJM198610233151702.

Lumeng, C.N. et al. 2008. Phenotypic switching of adipose tissue macrophages with obesity is generated by spatiotemporal differences in macrophage subtypes. *Diabetes* . doi: 10.2337/db08-0872.

Mackay, F. 1993. Tumor necrosis factor alpha (TNF-alpha)-induced cell adhesion to human endothelial cells is under dominant control of one TNF receptor type, TNF-R55. *Journal of Experimental Medicine* . doi: 10.1084/jem.177.5.1277.

Maeda, N. et al. 2002. Diet-induced insulin resistance in mice lacking adiponectin/ACRP30. *Nature Medicine* 8(7), pp. 731–737. Available at: <http://www.nature.com/doi/10.1038/nm724>.

Makó, V. et al. 2010. Proinflammatory activation pattern of human umbilical vein endothelial cells induced by IL-1 β , TNF- α , and LPS. *Cytometry Part A* . doi: 10.1002/cyto.a.20952.

Makowski, L. et al. 2001. Lack of macrophage fatty-acid-binding protein aP2 protects mice deficient in apolipoprotein E against atherosclerosis. *Nature Medicine* . doi: 10.1038/89076.

Martinet, W. and De Meyer, G.R.Y. 2009. Autophagy in atherosclerosis: A cell survival and death phenomenon with therapeutic potential. *Circulation Research* . doi: 10.1161/CIRCRESAHA.108.188318.

Martins-Marques, T. et al. 2016. Presence of Cx43 in extracellular vesicles reduces

the cardiotoxicity of the anti-tumour therapeutic approach with doxorubicin. *Journal of Extracellular Vesicles* 5(1). doi: 10.3402/jev.v5.32538.

Mateescu, B. et al. 2017. Obstacles and opportunities in the functional analysis of extracellular vesicle RNA - An ISEV position paper. *Journal of Extracellular Vesicles* 6(1). doi: 10.1080/20013078.2017.1286095.

Mathivanan, S. et al. 2010. Proteomics Analysis of A33 Immunoaffinity-purified Exosomes Released from the Human Colon Tumor Cell Line LIM1215 Reveals a Tissue-specific Protein Signature. *Molecular & Cellular Proteomics* 9(2), pp. 197–208. Available at: <http://www.mcponline.org/lookup/doi/10.1074/mcp.M900152-MCP200>.

Matsumoto, N. et al. 2004. Increased level of oxidized LDL-dependent monocyte-derived microparticles in acute coronary syndrome. *Thrombosis and Haemostasis* 91(1), pp. 146–154. doi: 10.1160/TH03-04-0247.

McDonald, M.K. et al. 2014. Functional significance of macrophage-derived exosomes in inflammation and pain. *Pain* . doi: 10.1016/j.pain.2014.04.029.

Melo, S.A. et al. 2014. Cancer Exosomes Perform Cell-Independent MicroRNA Biogenesis and Promote Tumorigenesis. *Cancer Cell* . doi: 10.1016/j.ccell.2014.09.005.

Melton, L. 2004. Protein arrays: proteomics in multiplex. *Nature* 429(6987), pp. 101–107. doi: 10.1038/429101a.

Menck, K. et al. 2017. Isolation and Characterization of Microvesicles from Peripheral Blood. *Journal of Visualized Experiments* . doi: 10.3791/55057.

de Menezes-Neto, A. et al. 2015. Size-exclusion chromatography as a stand-alone methodology identifies novel markers in mass spectrometry analyses of plasma-derived vesicles from healthy individuals. *Journal of Extracellular Vesicles* 4(1). doi: 10.3402/jev.v4.27378.

Merkstein, M. et al. 2015. FTO influences adipogenesis by regulating mitotic clonal expansion. *Nature Communications* 6, p. 6792. Available at: <http://www.nature.com/doi/10.1038/ncomms7792>.

- Mesri, M. and Altieri, D.C. 1998. Endothelial Cell Activation by Leukocyte Microparticles. *The Journal of Immunology* 161(8), pp. 4382–4387. Available at: <http://www.jimmunol.org/content/161/8/4382>.
- Mesri, M. and Altieri, D.C. 1999. Leukocyte microparticles stimulate endothelial cell cytokine release and tissue factor induction in a JNK1 signaling pathway. *Journal of Biological Chemistry* 274(33), pp. 23111–23118. doi: 10.1074/jbc.274.33.23111.
- Michaud, A. et al. 2014. Expression of genes related to prostaglandin synthesis or signaling in human subcutaneous and omental adipose tissue: Depot differences and modulation by adipogenesis. *Mediators of Inflammation* 2014. doi: 10.1155/2014/451620.
- Miettinen, S. et al. 2008. Adipose Tissue and Adipocyte Differentiation: Molecular and Cellular Aspects and Tissue Engineering Applications. *Topics in Tissue Engineering* 4, pp. 1–26.
- Minciacchi, V.R. et al. 2017. MYC mediates large oncosome-induced fibroblast reprogramming in prostate cancer. *Cancer Research* . doi: 10.1158/0008-5472.CAN-16-2942.
- Miranda, K.C. et al. 2014. Massively parallel sequencing of human urinary exosome/microvesicle RNA reveals a predominance of non-coding RNA. *PLoS ONE* 9(5). doi: 10.1371/journal.pone.0096094.
- Mitchell, M.D. 2017. Exosome enrichment by ultracentrifugation and size exclusion chromatography. *Frontiers in Bioscience* . doi: 10.2741/4621.
- Mittelbrunn, M. et al. 2011. Unidirectional transfer of microRNA-loaded exosomes from T cells to antigen-presenting cells. *Nature Communications* 2, p. 282. Available at: <http://www.nature.com/doi/10.1038/ncomms1285>.
- Miyazaki, T. et al. 2018. Extracellular vesicle-mediated EBAG9 transfer from cancer cells to tumor microenvironment promotes immune escape and tumor progression. *Oncogenesis* . doi: 10.1038/s41389-017-0022-6.
- Mol, E.A. et al. 2017. Higher functionality of extracellular vesicles isolated using size-exclusion chromatography compared to ultracentrifugation. *Nanomedicine*:

Nanotechnology, Biology, and Medicine 13(6), pp. 2061–2065. doi:
10.1016/j.nano.2017.03.011.

Molchadsky, A. et al. 2013. p53 is required for brown adipogenic differentiation and has a protective role against diet-induced obesity. *Cell Death and Differentiation* 20(5), pp. 774–783. Available at:
<http://www.nature.com/doifinder/10.1038/cdd.2013.9>.

Molestina, R.E. et al. 2000. Requirement for NF- κ B in transcriptional activation of monocyte chemotactic protein 1 by *Chlamydia pneumoniae* in human endothelial cells. *Infection and Immunity* . doi: 10.1128/IAI.68.7.4282-4288.2000.

Momen-Heravi, F. et al. 2013. Current methods for the isolation of extracellular vesicles. *Biological Chemistry* 394(10), pp. 1253–1262. doi: 10.1515/hsz-2013-0141.

Moncada, S. and Higgs, E.A. 2006. The discovery of nitric oxide and its role in vascular biology. *British Journal of Pharmacology* . doi: 10.1038/sj.bjp.0706458.

Montecalvo, A. et al. 2008. Exosomes As a Short-Range Mechanism to Spread Alloantigen between Dendritic Cells during T Cell Allorecognition. *The Journal of Immunology* . doi: 10.4049/jimmunol.180.5.3081.

Moreno-Navarrete, J.M. et al. 2011. Circulating omentin as a novel biomarker of endothelial dysfunction. *Obesity* . doi: 10.1038/oby.2010.351.

Morita, E. et al. 2007. Human ESCRT and ALIX proteins interact with proteins of the midbody and function in cytokinesis. *EMBO Journal* . doi:
10.1038/sj.emboj.7601850.

Morrison, R.F. and Farmer, S.R. 1999. Role of PPAR γ in regulating a cascade expression of cyclin-dependent kinase inhibitors, p18(INK4c) and p21(Waf1/Cip1), during adipogenesis. *Journal of Biological Chemistry* 274(24), pp. 17088–17097. doi: 10.1074/jbc.274.24.17088.

Morton, G.J. and Schwartz, M.W. 2011. Leptin and the Central Nervous System Control of Glucose Metabolism. *Physiological Reviews* . doi:
10.1152/physrev.00007.2010.

Moseti, D. et al. 2016. Molecular regulation of adipogenesis and potential anti-adipogenic bioactive molecules. *International Journal of Molecular Sciences* 17(1). doi: 10.3390/ijms17010124.

Mueller, E. et al. 2002. Genetic analysis of adipogenesis through peroxisome proliferator-activated receptor γ isoforms. *Journal of Biological Chemistry* . doi: 10.1074/jbc.M206950200.

Muir, L.A. et al. 2016. Adipose tissue fibrosis, hypertrophy, and hyperplasia: Correlations with diabetes in human obesity. *Obesity* . doi: 10.1002/oby.21377.

Müller, G. 2011. Let's shift lipid burden-From large to small adipocytes. *European Journal of Pharmacology* 656(1–3), pp. 1–4. doi: 10.1016/j.ejphar.2011.01.035.

Müller, G. et al. 2011a. Microvesicles released from rat adipocytes and harboring glycosylphosphatidylinositol-anchored proteins transfer RNA stimulating lipid synthesis. *Cellular Signalling* . doi: 10.1016/j.cellsig.2011.03.013.

Müller, G. et al. 2011b. Upregulation of Lipid Synthesis in Small Rat Adipocytes by Microvesicle-Associated CD73 From Large Adipocytes. *Obesity* 19(8), pp. 1531–1544. Available at: <http://doi.wiley.com/10.1038/oby.2011.29>.

Muller, L. et al. 2014a. Isolation of biologically-active exosomes from human plasma. *Journal of Immunological Methods* 411, pp. 55–65. doi: 10.1016/j.jim.2014.06.007.

Muller, L. et al. 2014b. Isolation of biologically-active exosomes from human plasma. *Journal of Immunological Methods* 411(Lm), pp. 55–65. doi: 10.1016/j.jim.2014.06.007.

Muller, W.A. 2003. Leukocyte-endothelial-cell interactions in leukocyte transmigration and the inflammatory response. *Trends in Immunology* . doi: 10.1016/S1471-4906(03)00117-0.

Muralidharan-Chari, V. et al. 2009. ARF6-Regulated Shedding of Tumor Cell-Derived Plasma Membrane Microvesicles. *Current Biology* 19(22), pp. 1875–1885. doi: 10.1016/j.cub.2009.09.059.

Musante, L. et al. 2013. Recovery of urinary nanovesicles from ultracentrifugation

- supernatants. *Nephrology Dialysis Transplantation* . doi: 10.1093/ndt/gfs564.
- Nakashima, Y. et al. 1998. Upregulation of VCAM-1 and ICAM-1 at atherosclerosis-prone sites on the endothelium in the apoE-deficient mouse. *Arteriosclerosis, Thrombosis, and Vascular Biology* . doi: 10.1161/01.ATV.18.5.842.
- Nam, D. et al. 2015. Novel Function of Rev-erb α in Promoting Brown Adipogenesis. *Scientific Reports* 5(1), p. 11239. Available at: <http://www.nature.com/articles/srep11239>.
- Naour, N. et al. 2010. Cathepsins in human obesity: Changes in energy balance predominantly affect cathepsin S in adipose tissue and in circulation. *Journal of Clinical Endocrinology and Metabolism* . doi: 10.1210/jc.2009-1894.
- Nardi, F. da S. et al. 2016. High levels of circulating extracellular vesicles with altered expression and function during pregnancy. *Immunobiology* . doi: 10.1016/j.imbio.2016.03.001.
- Narvaez, C.J. et al. 2013. Induction of STEAP4 correlates with 1,25-dihydroxyvitamin D3 stimulation of adipogenesis in mesenchymal progenitor cells derived from human adipose tissue. *Journal of Cellular Physiology* 228(10), pp. 2024–2036. doi: 10.1002/jcp.24371.
- Nedergaard, J. et al. 2011. New powers of brown fat: Fighting the metabolic syndrome. *Cell Metabolism* 13(3), pp. 238–240. doi: 10.1016/j.cmet.2011.02.009.
- Nedvídková, J. et al. 2005. Adiponectin, an adipocyte-derived protein. *Physiological Research* 54(2), pp. 133–140.
- New, S.E.P. et al. 2013. Macrophage-derived matrix vesicles : An alternative novel mechanism for microcalcification in atherosclerotic plaques. *Circulation Research* . doi: 10.1161/CIRCRESAHA.113.301036.
- Nguyen, D. and Coull, B.M. 2017. Thrombosis. In: *Primer on Cerebrovascular Diseases: Second Edition*. doi: 10.1016/B978-0-12-803058-5.00021-7.
- van Niel, G. et al. 2011. The Tetraspanin CD63 Regulates ESCRT-Independent and -Dependent Endosomal Sorting during Melanogenesis. *Developmental Cell* . doi:

10.1016/j.devcel.2011.08.019.

Nielsen, M.H. et al. 2014. A flow cytometric method for characterization of circulating cell-derived microparticles in plasma. *Journal of Extracellular Vesicles* 3(1), pp. 1–12. doi: 10.3402/jev.v3.20795.

Nomura, S. et al. 2001. High-shear-stress-induced activation of platelets and microparticles enhances expression of cell adhesion molecules in THP-1 and endothelial cells. *Atherosclerosis* . doi: 10.1016/S0021-9150(01)00433-6.

O'Brien, K.D. et al. 1993. Vascular cell adhesion molecule-1 is expressed in human coronary atherosclerotic plaques: Implications for the mode of progression of advanced coronary atherosclerosis. *Journal of Clinical Investigation* . doi: 10.1172/JCI116670.

O'Neill, H.C. and Quah, B.J.C. 2008. Exosomes Secreted by Bacterially Infected Macrophages Are Proinflammatory. *Science Signaling* 1(6), pp. pe8–pe8. Available at: <http://stke.sciencemag.org/cgi/doi/10.1126/stke.16pe8>.

Ogawa, R. et al. 2010. Adipocyte-derived microvesicles contain RNA that is transported into macrophages and might be secreted into blood circulation. *Biochemical and Biophysical Research Communications* . doi: 10.1016/j.bbrc.2010.07.008.

Öhman, M.K. et al. 2008. Visceral adipose tissue inflammation accelerates atherosclerosis in apolipoprotein E-deficient mice. *Circulation* . doi: 10.1161/CIRCULATIONAHA.107.717595.

Olefsky, J.M. and Glass, C.K. 2010. Macrophages, Inflammation, and Insulin Resistance. *Annual Review of Physiology* 72(1), pp. 219–246. Available at: <http://www.annualreviews.org/doi/10.1146/annurev-physiol-021909-135846>.

Oliveira-Rodríguez, M. et al. 2016. Development of a rapid lateral flow immunoassay test for detection of exosomes previously enriched from cell culture medium and body fluids. *Journal of Extracellular Vesicles* 5(1), p. 31803. Available at: <https://www.tandfonline.com/doi/full/10.3402/jev.v5.31803>.

Onat, D. et al. 2011. Human vascular endothelial cells: A model system for studying

vascular inflammation in diabetes and atherosclerosis. *Current Diabetes Reports* . doi: 10.1007/s11892-011-0182-2.

Orozco, A.F. and Lewis, D.E. 2010. Flow cytometric analysis of circulating microparticles in plasma. *Cytometry Part A* 77(6), pp. 502–514. doi: 10.1002/cyto.a.20886.

Ostrowski, M. et al. 2010. Rab27a and Rab27b control different steps of the exosome secretion pathway. *Nature Cell Biology* 12(1), pp. 19–30. Available at: <http://www.nature.com/doi/10.1038/ncb2000>.

Otu, H. et al. 2005. Preconditioning of primary human endothelial cells with inflammatory mediators alters the “set point” of the cell. *The FASEB Journal* . doi: 10.1096/fj.05-4037fje.

Ouchi, N. et al. 2000. Adiponectin, an adipocyte-derived plasma protein, inhibits endothelial NF- κ B signaling through a cAMP-dependent pathway. *Circulation* . doi: 10.1161/01.CIR.102.11.1296.

Ouchi, N. et al. 2006. Cardioprotection by Adiponectin. *Trends in Cardiovascular Medicine* . doi: 10.1016/j.tcm.2006.03.001.

Owens, A.P. and MacKman, N. 2011. Microparticles in hemostasis and thrombosis. *Circulation Research* 108(10), pp. 1284–1297. doi: 10.1161/CIRCRESAHA.110.233056.

Paggetti, J. et al. 2015. Exosomes released by chronic lymphocytic leukemia cells induce the transition of stromal cells into cancer-associated fibroblasts. *Blood* . doi: 10.1182/blood-2014-12-618025.

Palmieri, V. et al. 2014. Dynamic light scattering for the characterization and counting of extracellular vesicles: a powerful noninvasive tool. *Journal of Nanoparticle Research* 16(9). doi: 10.1007/s11051-014-2583-z.

Pan, B.T. and Johnstone, R.M. 1983. Fate of the transferrin receptor during maturation of sheep reticulocytes in vitro: Selective externalization of the receptor. *Cell* 33(3), pp. 967–978. doi: 10.1016/0092-8674(83)90040-5.

Peeters, W. et al. 2011. Adipocyte fatty acid binding protein in atherosclerotic

- plaques is associated with local vulnerability and is predictive for the occurrence of adverse cardiovascular events. *European Heart Journal* . doi: 10.1093/eurheartj/ehq387.
- Pellegrinelli, V. et al. 2016. Adipose tissue plasticity: how fat depots respond differently to pathophysiological cues. *Diabetologia* 59(6), pp. 1075–1088. doi: 10.1007/s00125-016-3933-4.
- Perreault, M. and Marette, A. 2001. Targeted disruption of inducible nitric oxide synthase protects against obesity-linked insulin resistance in muscle. *Nature Medicine* . doi: 10.1038/nm1001-1138.
- Perticone, F. et al. 2001. Obesity and body fat distribution induce endothelial dysfunction by oxidative stress: Protective effect of vitamin C. *Diabetes* . doi: 10.2337/diabetes.50.1.159.
- Pettit, E.J. and Hallett, M.B. 1998. Release of ‘caged’ cytosolic Ca²⁺ triggers rapid spreading of human neutrophils adherent via integrin engagement. *Journal of Cell Science*
- Phoonsawat, W. et al. 2014. Adiponectin is partially associated with exosomes in mouse serum. *Biochemical and Biophysical Research Communications* . doi: 10.1016/j.bbrc.2014.04.114.
- Picchi, A. et al. 2006. Tumor necrosis factor- α induces endothelial dysfunction in the prediabetic metabolic syndrome. *Circulation Research* . doi: 10.1161/01.RES.0000229685.37402.80.
- Pilch, P.F. et al. 2011. Caveolae and lipid trafficking in adipocytes. *Clinical lipidology* 6(1), pp. 49–58. Available at: <http://www.pubmedcentral.nih.gov/articlerender.fcgi?artid=3103140&tool=pmcentrez&rendertype=abstract>.
- Pisani, D.F. et al. 2011. Differentiation of human adipose-derived stem cells into ‘brite’ (brown-in-white) adipocytes. *Frontiers in Endocrinology* 2(NOV). doi: 10.3389/fendo.2011.00087.
- Pisitkun, T. et al. 2004. Identification and proteomic profiling of exosomes in human

urine. *Proc. Natl. Acad. Sci. USA* 101(36), pp. 13368–13373. Available at: <http://www.pubmedcentral.nih.gov/articlerender.fcgi?artid=516573&tool=pmcentrez&rendertype=abstract>.

Pitt, J.M. et al. 2016. Extracellular vesicles: Masters of intercellular communication and potential clinical interventions. *Journal of Clinical Investigation* . doi: 10.1172/JCI87316.

van der Pol, E. et al. 2014. Particle size distribution of exosomes and microvesicles determined by transmission electron microscopy, flow cytometry, nanoparticle tracking analysis, and resistive pulse sensing. *Journal of Thrombosis and Haemostasis* 12(7), pp. 1182–1192. doi: 10.1111/jth.12602.

van der Pol, E. et al. 2016. Recent developments in the nomenclature, presence, isolation, detection and clinical impact of extracellular vesicles. *Journal of Thrombosis and Haemostasis* 14(1), pp. 48–56. doi: 10.1111/jth.13190.

Van Der Pol, E. et al. 2010. Optical and non-optical methods for detection and characterization of microparticles and exosomes. *Journal of Thrombosis and Haemostasis* 8(12), pp. 2596–2607. doi: 10.1111/j.1538-7836.2010.04074.x.

Pomatto, M.A.C. et al. 2018. Noncoding RNAs carried by extracellular vesicles in endocrine diseases. *International Journal of Endocrinology* . doi: 10.1155/2018/4302096.

Poulos, S.P. et al. 2010. Cell line models for differentiation: preadipocytes and adipocytes. *Experimental Biology and Medicine* 235(10), pp. 1185–1193. Available at: <http://journals.sagepub.com/doi/10.1258/ebm.2010.010063>.

Prunotto, M. et al. 2013. Proteomic analysis of podocyte exosome-enriched fraction from normal human urine. *Journal of Proteomics* 82, pp. 193–229. doi: 10.1016/j.jprot.2013.01.012.

Public Health England 2017. Health matters: obesity and the food environment. doi: 10.1142/S179352451350040X.

Pugholm, L.H. et al. 2015. Antibody-based assays for phenotyping of extracellular vesicles. *BioMed Research International* 2015. doi: 10.1155/2015/524817.

Rafieian-Kopaei, M. et al. 2014. Atherosclerosis: Process, indicators, risk factors and new hopes. *International Journal of Preventive Medicine*

Rahimi, N. 2017. Defenders and challengers of endothelial barrier function. *Frontiers in Immunology* . doi: 10.3389/fimmu.2017.01847.

Rahman, F. et al. 2014. Ascorbic acid is a dose-dependent inhibitor of adipocyte differentiation, probably by reducing cAMP pool. *Frontiers in Cell and Developmental Biology* 2, p. 29. Available at:
<http://journal.frontiersin.org/article/10.3389/fcell.2014.00029/abstract>.

Rajendran, L. et al. 2006. Alzheimer's disease beta-amyloid peptides are released in association with exosomes. *Proceedings of the National Academy of Sciences* 103(30), pp. 11172–11177. Available at:
<http://www.pnas.org/cgi/doi/10.1073/pnas.0603838103>.

Ramirez, M.I. et al. 2018. Technical challenges of working with extracellular vesicles. *Nanoscale* . doi: 10.1039/c7nr08360b.

Raposo, G. et al. 1996. B lymphocytes secrete antigen-presenting vesicles. *The Journal of experimental medicine* 183(3), pp. 1161–72. Available at:
<http://www.pubmedcentral.nih.gov/articlerender.fcgi?artid=2192324&tool=pmcentrez&rendertype=abstract>.

Raposo, G. and Stoorvogel, W. 2013a. Extracellular vesicles: Exosomes, microvesicles, and friends. *Journal of Cell Biology* 200(4), pp. 373–383. doi: 10.1083/jcb.201211138.

Raposo, G. and Stoorvogel, W. 2013b. Extracellular vesicles: Exosomes, microvesicles, and friends. *Journal of Cell Biology* 200(4), pp. 373–383. doi: 10.1083/jcb.201211138.

Rautou, P.E. et al. 2011. Microparticles from human atherosclerotic plaques promote endothelial ICAM-1-dependent monocyte adhesion and transendothelial migration. *Circulation Research* . doi: 10.1161/CIRCRESAHA.110.237420.

Razani, B. et al. 2012. Autophagy links inflammasomes to atherosclerotic progression. *Cell Metabolism* . doi: 10.1016/j.cmet.2012.02.011.

Rechavi, O. et al. 2009. Cell contact-dependent acquisition of cellular and viral nonautonomously encoded small RNAs. *Genes and Development* 23(16), pp. 1971–1979. doi: 10.1101/gad.1789609.

Reichert, M. and Eick, D. 1999. Analysis of cell cycle arrest in adipocyte differentiation. *Oncogene* 18(2), pp. 459–466. doi: 10.1038/sj.onc.1202308.

Ren, D. et al. 2002. PPAR γ knockdown by engineered transcription factors: Exogenous PPAR γ 2 but not PPAR γ 1 reactivates adipogenesis. *Genes and Development* 16(1), pp. 27–32. doi: 10.1101/gad.953802.

Rhee, E.J. et al. 2009. The association of serum adipocyte fatty acid-binding protein with coronary artery disease in Korean adults. *European Journal of Endocrinology* . doi: 10.1530/EJE-08-0665.

Rhee, J.-S. et al. 2004. The functional role of blood platelet components in angiogenesis. *Thrombosis and Haemostasis* . Available at: http://www.schattauer.de/index.php?id=1214&doi=10.1160/TH03-04-0213&no_cache=1.

Richards, K.E. et al. 2017. Cancer-associated fibroblast exosomes regulate survival and proliferation of pancreatic cancer cells. *Oncogene* . doi: 10.1038/onc.2016.353.

Ritchie, S.A. and Connell, J.M.C. 2007. The link between abdominal obesity, metabolic syndrome and cardiovascular disease. *Nutrition, Metabolism and Cardiovascular Diseases* . doi: 10.1016/j.numecd.2006.07.005.

Robbins, P.D. et al. 2016. Regulation of chronic inflammatory and immune processes by extracellular vesicles. *Journal of Clinical Investigation* . doi: 10.1172/JCI81131.

Robinson, K. et al. 2011. Clinical review: adiponectin biology and its role in inflammation and critical illness. *Critical care (London, England)* 15(2), p. 221. Available at: <http://www.pubmedcentral.nih.gov/articlerender.fcgi?artid=3219307&tool=pmcentrez&rendertype=abstract>.

Rodríguez-Calvo, R. et al. 2017. Role of the fatty acid-binding protein 4 in heart

failure and cardiovascular disease. *Journal of Endocrinology* . doi: 10.1530/JOE-17-0031.

Rodriguez, A. et al. 2007. Visceral and subcutaneous adiposity: Are both potential therapeutic targets for tackling the metabolic syndrome? *Current pharmaceutical design*

Rohde, E. et al. 2007. Immune cells mimic the morphology of endothelial progenitor colonies in vitro. *Stem cells* 25(7), pp. 1746–1752. doi: 10.1634/stemcells.2006-0833.

Romano, M. et al. 2000. Inhibition of monocyte chemotactic protein-1 synthesis by statins. *Laboratory Investigation* . doi: 10.1038/labinvest.3780115.

Rosen, E.D. et al. 2002. C/EBPalpha induces adipogenesis through PPARgamma: a unified pathway. *Genes & Development* (16), pp. 22–26. doi: 10.1101/gad.948702.nuclear.

Rosen, E.D. and MacDougald, O.A. 2006. Adipocyte differentiation from the inside out. *Nature Reviews Molecular Cell Biology* 7(12), pp. 885–896. Available at: <http://www.nature.com/doi/10.1038/nrm2066>.

Rosen, E.D. and Spiegelman, B.M. 2000. Molecular Regulation of Adipogenesis. *Annual Review of Cell and Developmental Biology* 16(1), pp. 145–171. Available at: <http://www.annualreviews.org/doi/10.1146/annurev.cellbio.16.1.145>.

Rosen, E.D. and Spiegelman, B.M. 2006. Adipocytes as regulators of energy balance and glucose homeostasis. *Nature* 444(7121), pp. 847–853. Available at: <http://www.nature.com/doi/10.1038/nature05483>.

Rosenwald, M. et al. 2013. Bi-directional interconversion of brite and white adipocytes. *Nature Cell Biology* 15(6), pp. 659–667. Available at: <http://www.nature.com/doi/10.1038/ncb2740>.

Ruiz-Ojeda, F.J. et al. 2016a. Cell models and their application for studying adipogenic differentiation in relation to obesity: A review. *International Journal of Molecular Sciences* 17(7). doi: 10.3390/ijms17071040.

Ruiz-Ojeda, F.J. et al. 2016b. Impact of 3-amino-1,2,4-triazole (3-AT)-derived

increase in hydrogen peroxide levels on inflammation and metabolism in human differentiated adipocytes. *PLoS ONE* 11(3). doi: 10.1371/journal.pone.0152550.

Rupert, D. et al. 2016. Methods for the physical characterization and quantification of extracellular vesicles in biological samples. *Biochimica et Biophysica Acta (BBA) - General Subjects* 1861(1), pp. 3164–3179. Available at: <http://dx.doi.org/10.1016/j.bbagen.2016.07.028>.

Saavedra, P. et al. 2015. New insights into circulating FABP4: Interaction with cytokeratin 1 on endothelial cell membranes. *Biochimica et Biophysica Acta - Molecular Cell Research* . doi: 10.1016/j.bbamcr.2015.09.002.

Sadaf Farooqi, I. et al. 2002. Beneficial effects of leptin on obesity, T cell hyporesponsiveness, and neuroendocrine/metabolic dysfunction of human congenital leptin deficiency. *Journal of Clinical Investigation* 110(8), pp. 1093–1103. doi: 10.1172/JCI200215693.

Sahu, R. et al. 2011. Microautophagy of Cytosolic Proteins by Late Endosomes. *Developmental Cell* 20(1), pp. 131–139. doi: 10.1016/j.devcel.2010.12.003.

Sáinz, N. et al. 2015. Leptin resistance and diet-induced obesity: Central and peripheral actions of leptin. *Metabolism: Clinical and Experimental* 64(1), pp. 35–46. doi: 10.1016/j.metabol.2014.10.015.

Saitoh, Y. et al. 2012. Polyhydroxylated fullerene C₆₀(OH)₄₄ suppresses intracellular lipid accumulation together with repression of intracellular superoxide anion radicals and subsequent PPAR α expression during spontaneous differentiation of OP9 preadipocytes into adipocyte. *Molecular and Cellular Biochemistry* 366(1–2), pp. 191–200. doi: 10.1007/s11010-012-1297-8.

Salvolini, E. et al. 1999. A study on human umbilical cord endothelial cells: Functional modifications induced by plasma from insulin-dependent diabetes mellitus patients. *Metabolism: Clinical and Experimental* . doi: 10.1016/S0026-0495(99)90049-5.

Salzer, U. et al. 2008. Vesicles generated during storage of red cells are rich in the lipid raft marker stomatin. *Transfusion* . doi: 10.1111/j.1537-2995.2007.01549.x.

- Samad, F. et al. 2018. Elevated Expression of Transforming Growth Factor- β in Adipose Tissue from Obese Mice. *Molecular Medicine* . doi: 10.1007/bf03401666.
- Sandoo, A. et al. 2015. The Endothelium and Its Role in Regulating Vascular Tone. *The Open Cardiovascular Medicine Journal* . doi: 10.2174/1874192401004010302.
- Sano, S. et al. 2014. Lipid synthesis is promoted by hypoxic adipocyte-derived exosomes in 3T3-L1 cells. *Biochemical and Biophysical Research Communications* 445(2), pp. 327–333. doi: 10.1016/j.bbrc.2014.01.183.
- Sansbury, B.E. et al. 2012. Overexpression of endothelial nitric oxide synthase prevents diet-induced obesity and regulates adipocyte phenotype. *Circulation Research* . doi: 10.1161/CIRCRESAHA.112.266395.
- Sarkar, A. et al. 2009. Monocyte derived microvesicles deliver a cell death message via encapsulated caspase-1. *PLoS ONE* 4(9). doi: 10.1371/journal.pone.0007140.
- Sartipy, P. and Loskutoff, D.J. 2003. Monocyte chemoattractant protein 1 in obesity and insulin resistance. *Proceedings of the National Academy of Sciences* . doi: 10.1073/pnas.1133870100.
- Schulz, T.J. and Tseng, Y.-H. 2013. Brown adipose tissue: development, metabolism and beyond. *The Biochemical journal* 453(2), pp. 167–78. Available at: <http://www.pubmedcentral.nih.gov/articlerender.fcgi?artid=3887508&tool=pmcentrez&rendertype=abstract>.
- Scroyen, I. et al. 2015. The anti-adipogenic potential of COUP-TFII is mediated by downregulation of the Notch target gene Hey1. *PLoS ONE* 10(12). doi: 10.1371/journal.pone.0145608.
- Sell, H. et al. 2009. Chemerin is a novel adipocyte-derived factor inducing insulin resistance in primary human skeletal muscle cells. *Diabetes* . doi: 10.2337/db09-0277.
- Sell, H. et al. 2010. Chemerin correlates with markers for fatty liver in morbidly obese patients and strongly decreases after weight loss induced by bariatric surgery. *Journal of Clinical Endocrinology and Metabolism* . doi: 10.1210/jc.2009-2374.
- Seo, Y.S. et al. 2015. Quercetin prevents adipogenesis by regulation of

transcriptional factors and lipases in OP9 cells. *International Journal of Molecular Medicine* 35(6), pp. 1779–1785. doi: 10.3892/ijmm.2015.2185.

Sepa-Kishi, D.M. and Ceddia, R.B. 2018. White and beige adipocytes: are they metabolically distinct? *Hormone Molecular Biology and Clinical Investigation* . doi: 10.1515/hmbci-2018-0003.

Shan, T. et al. 2013. Fatty acid binding protein 4 expression marks a population of adipocyte progenitors in white and brown adipose tissues. *FASEB Journal* . doi: 10.1096/fj.12-211516.

Shang, J. and Gao, X. 2014. Nanoparticle counting: towards accurate determination of the molar concentration. *Chem. Soc. Rev.* 43(21), pp. 7267–7278. Available at: <http://xlink.rsc.org/?DOI=C4CS00128A>.

Sharma, S. et al. 2010. Structural-mechanical characterization of nanoparticle exosomes in human saliva, using correlative AFM, FESEM, and force spectroscopy. *ACS Nano* 4(4), pp. 1921–1926. doi: 10.1021/nn901824n.

Shulman, G.I. 2000. Cellular mechanisms of insulin resistance. *Journal of Clinical Investigation* . doi: 10.1172/JCI10583.

Sidossis, L. and Kajimura, S. 2015. Brown and beige fat in humans: Thermogenic adipocytes that control energy and glucose homeostasis. *Journal of Clinical Investigation* 125(2), pp. 478–486. doi: 10.1172/JCI78362.

Siersbæk, R. et al. 2010. PPAR γ in adipocyte differentiation and metabolism - Novel insights from genome-wide studies. *FEBS Letters* . doi: 10.1016/j.febslet.2010.06.010.

Simonsen, J.B. 2017. What are we looking at? Extracellular vesicles, lipoproteins, or both? *Circulation Research* . doi: 10.1161/CIRCRESAHA.117.311767.

Singh, R. et al. 2003. Androgens Stimulate Myogenic Differentiation and Inhibit Adipogenesis in C3H 10T1/2 Pluripotent Cells through an Androgen Receptor-Mediated Pathway. *Endocrinology* 144(11), pp. 5081–5088. doi: 10.1210/en.2003-0741.

Singh, R.B. et al. 2002. Pathogenesis of atherosclerosis: A multifactorial process.

- Experimental and Clinical Cardiology* . doi: 10.1007/978-94-007-7920-4_9.
- Sinha, A. et al. 2014. In-depth proteomic analyses of ovarian cancer cell line exosomes reveals differential enrichment of functional categories compared to the NCI 60 proteome. *Biochemical and Biophysical Research Communications* . doi: 10.1016/j.bbrc.2013.12.070.
- Skogberg, G. et al. 2013. Characterization of Human Thymic Exosomes. *PLoS ONE* . doi: 10.1371/journal.pone.0067554.
- Skurk, T. et al. 2009. Expression and secretion of RANTES (CCL5) in human adipocytes in response to immunological stimuli and hypoxia. *Hormone and metabolic research = Hormon- und Stoffwechselforschung = Hormones et métabolisme* . doi: 10.1055/s-0028-1093345.
- Smorlesi, A. et al. 2012. The adipose organ: White-brown adipocyte plasticity and metabolic inflammation. *Obesity Reviews* 13(SUPPL.2), pp. 83–96. doi: 10.1111/j.1467-789X.2012.01039.x.
- Sódar, B.W. et al. 2016. Low-density lipoprotein mimics blood plasma-derived exosomes and microvesicles during isolation and detection. *Scientific Reports* . doi: 10.1038/srep24316.
- Sokolova, V. et al. 2011. Characterisation of exosomes derived from human cells by nanoparticle tracking analysis and scanning electron microscopy. *Colloids and Surfaces B: Biointerfaces* 87(1), pp. 146–150. Available at: <http://linkinghub.elsevier.com/retrieve/pii/S0927776511002724>.
- Song, Y.H. et al. 2017. Breast cancer-derived extracellular vesicles stimulate myofibroblast differentiation and pro-angiogenic behavior of adipose stem cells. *Matrix Biology* . doi: 10.1016/j.matbio.2016.11.008.
- Soukka, T. et al. 2003. Highly sensitive immunoassay of free prostate-specific antigen in serum using europium(III) nanoparticle label technology. *Clinica Chimica Acta* 328(1–2), pp. 45–58. doi: 10.1016/S0009-8981(02)00376-5.
- Steen, K.A. et al. 2016. FABP4/aP2 Regulates Macrophage Redox Signaling and Inflammasome Activation via Control of UCP2. *Molecular and Cellular Biology* .

doi: 10.1128/mcb.00282-16.

Steinberg, H.O. et al. 1994. Insulin-mediated skeletal muscle vasodilation is nitric oxide dependent: A novel action of insulin to increase nitric oxide release. *Journal of Clinical Investigation* . doi: 10.1172/JCI117433.

Steinberg, H.O. et al. 1996. Obesity/insulin resistance is associated with endothelial dysfunction: Implications for the syndrome of insulin resistance. *Journal of Clinical Investigation* . doi: 10.1172/JCI118709.

Steinberg, H.O. et al. 1997. Endothelial dysfunction is associated with cholesterol levels in the high normal range in humans. *Circulation* . doi: 10.1161/01.CIR.96.10.3287.

Steinbrecher, U. et al. 1984. Modification of low density lipoprotein by endothelial cells involves lipid peroxidation and degradation of low density lipoprotein phospholipids. *Proceedings of the National Academy of Sciences of the United States of America*

Stephens, J.M. 2012. The Fat Controller: Adipocyte Development. *PLoS Biology* 10(11), pp. 11–13. doi: 10.1371/journal.pbio.1001436.

Stephens, J.M. and Vidal Puig, A.J. 2006. An update on visfatin/pre-B cell colony-enhancing factor, an ubiquitously expressed, illusive cytokine that is regulated in obesity. *Current opinion in lipidology* 17(2), pp. 128–131. doi: 10.1097/01.mol.0000217893.77746.4b.

Steppan, C.M. et al. 2001. The hormone resistin links obesity to diabetes. *Nature* . doi: 10.1038/35053000.

Stoorvogel, W. et al. 1991. Late endosomes derive from early endosomes by maturation. *Cell* 65(3), pp. 417–427. doi: 10.1016/0092-8674(91)90459-C.

Stranska, R. et al. 2018. Comparison of membrane affinity-based method with size-exclusion chromatography for isolation of exosome-like vesicles from human plasma. *Journal of Translational Medicine* . doi: 10.1186/s12967-017-1374-6.

Stuffers, S. et al. 2009. Multivesicular endosome biogenesis in the absence of ESCRTs. *Traffic* 10(7), pp. 925–937. doi: 10.1111/j.1600-0854.2009.00920.x.

- Suades, R. et al. 2012. Circulating and platelet-derived microparticles in human blood enhance thrombosis on atherosclerotic plaques. *Thrombosis and Haemostasis* 108(6), pp. 1208–1219. doi: 10.1160/TH12-07-0486.
- Suárez, H. et al. 2017. A bead-assisted flow cytometry method for the semi-quantitative analysis of Extracellular Vesicles. *Scientific Reports* . doi: 10.1038/s41598-017-11249-2.
- Suzuki, H. et al. 1997. A role for macrophage scavenger receptors in atherosclerosis and susceptibility to infection. *Nature* . doi: 10.1038/386292a0.
- Szatanek, R. et al. 2015. Isolation of extracellular vesicles: Determining the correct approach (review). *International Journal of Molecular Medicine* 36(1), pp. 11–17. doi: 10.3892/ijmm.2015.2194.
- Szatanek, R. et al. 2017. The methods of choice for extracellular vesicles (EVs) characterization. *International Journal of Molecular Sciences* . doi: 10.3390/ijms18061153.
- Takov, K. et al. 2019. Comparison of small extracellular vesicles isolated from plasma by ultracentrifugation or size-exclusion chromatography: yield, purity and functional potential. *Journal of Extracellular Vesicles* . doi: 10.1080/20013078.2018.1560809.
- Taleb, S. et al. 2005. Cathepsin S, a novel biomarker of adiposity: relevance to atherogenesis. *FASEB J.* . doi: 10.1096/fj.05-3673fje.
- Tamai, K. et al. 2010. Exosome secretion of dendritic cells is regulated by Hrs, an ESCRT-0 protein. *Biochemical and Biophysical Research Communications* 399(3), pp. 384–390. doi: 10.1016/j.bbrc.2010.07.083.
- Tan, B.K. et al. 2010. Metformin treatment may increase omentin-1 levels in women with polycystic ovary syndrome. *Diabetes* . doi: 10.2337/db10-0124.
- Tanaka, T. et al. 1997. Defective adipocyte differentiation in mice lacking the C/EBPbeta and/or C/EBPdelta gene. *The EMBO journal* 16(24), pp. 7432–43. Available at:
<http://www.pubmedcentral.nih.gov/articlerender.fcgi?artid=1170343&tool=pmcentre>

z&rendertype=abstract.

Tansey, J.T. et al. 2004. The central role of perilipin A in lipid metabolism and adipocyte lipolysis. *IUBMB Life* 56(7), pp. 379–385. doi: 10.1080/15216540400009968.

Tataruch-Weinert, D. et al. 2016. Urinary extracellular vesicles for RNA extraction: optimization of a protocol devoid of prokaryote contamination. *Journal of Extracellular Vesicles* . doi: 10.3402/jev.v5.30281.

Tauro, B.J. et al. 2012. Comparison of ultracentrifugation, density gradient separation, and immunoaffinity capture methods for isolating human colon cancer cell line LIM1863-derived exosomes. *Methods* 56(2), pp. 293–304. doi: 10.1016/j.ymeth.2012.01.002.

Tavafi, M. 2013. Complexity of diabetic nephropathy pathogenesis and design of investigations. *J Renal Inj Prev* . doi: 10.12861/jrip.2013.20.

Taylor, D.D. et al. 2011. Exosome isolation for proteomic analyses and RNA profiling. *Methods in Molecular Biology* 728, pp. 235–246. doi: 10.1007/978-1-61779-068-3_15.

Taylor, D.D. and Gercel-Taylor, C. 2008. MicroRNA signatures of tumor-derived exosomes as diagnostic biomarkers of ovarian cancer. *Gynecologic Oncology* 110(1), pp. 13–21. doi: 10.1016/j.ygyno.2008.04.033.

Taylor, D.D. and Shah, S. 2015. Methods of isolating extracellular vesicles impact down-stream analyses of their cargoes. *Methods* . doi: 10.1016/j.ymeth.2015.02.019.

Theos, A.C. et al. 2006. A luminal domain-dependent pathway for sorting to intraluminal vesicles of multivesicular endosomes involved in organelle morphogenesis. *Developmental Cell* 10(3), pp. 343–354. doi: 10.1016/j.devcel.2006.01.012.

Théry, C. et al. 2018. Minimal information for studies of extracellular vesicles 2018 (MISEV2018): a position statement of the International Society for Extracellular Vesicles and update of the MISEV2014 guidelines. *Journal of Extracellular Vesicles* . doi: 10.1080/20013078.2018.1535750.

Thomas, D. and Apovian, C. 2017. Macrophage functions in lean and obese adipose tissue. *Metabolism: Clinical and Experimental* . doi: 10.1016/j.metabol.2017.04.005.

Thomas, D.W. et al. 1998. Coagulation defects and altered hemodynamic responses in mice lacking receptors for thromboxane A₂. *Journal of Clinical Investigation* . doi: 10.1172/JCI5116.

Thomou, T. et al. 2017. Adipose-derived circulating miRNAs regulate gene expression in other tissues. *Nature* . doi: 10.1038/nature21365.

Thompson, B.R. et al. 2010. Fatty acid flux in adipocytes: The in's and out's of fat cell lipid trafficking. *Molecular and Cellular Endocrinology* 318(1–2), pp. 24–33. doi: 10.1016/j.mce.2009.08.015.

Tomlinson, P.R. et al. 2015. Identification of distinct circulating exosomes in Parkinson's disease. *Annals of Clinical and Translational Neurology* 2(4), pp. 353–361. Available at: <http://doi.wiley.com/10.1002/acn3.175>.

Tontonoz, P. et al. 1994a. mPPAR γ 2: Tissue-specific regulator of an adipocyte enhancer. *Genes and Development* . doi: 10.1101/gad.8.10.1224.

Tontonoz, P. et al. 1994b. Stimulation of adipogenesis in fibroblasts by PPAR gamma 2, a lipid-activated transcription factor. *Cell* 79(7), pp. 1147–1156. doi: 10.1016/0092-8674(94)90006-X.

Tontonoz, P. et al. 1995. PPAR α 2 Regulates Adipose Expression of the Phosphoenolpyruvate Carboxykinase Gene. *MOLECULAR AND CELLULAR BIOLOGY* . doi: 10.1021/ac9610117.

Toti, F. et al. 1996. Scott syndrome, characterized by impaired transmembrane migration of procoagulant phosphatidylserine and hemorrhagic complications, is an inherited disorder. *Blood* 87(4), pp. 1409–15. Available at: <http://www.ncbi.nlm.nih.gov/pubmed/8608230>.

Trajkovic, K. et al. 2008. Ceramide Triggers Budding of Exosome Vesicles into Multivesicular Endosomes. *Science* 319(5867), pp. 1244–1247. Available at: <http://www.sciencemag.org/cgi/doi/10.1126/science.1153124>.

Tran, Q.K. et al. 2000. Calcium signalling in endothelial cells. *Cardiovascular*

Research . doi: 10.1016/S0008-6363(00)00172-3.

Traupe, T. et al. 2002. Obesity increases prostanoid-mediated vasoconstriction and vascular thromboxane receptor gene expression. *Journal of Hypertension* . doi: 10.1097/00004872-200211000-00024.

Turner, D.A. et al. 2010. Physiological levels of TNF stimulation induce stochastic dynamics of NF- κ B responses in single living cells. *Journal of Cell Science* . doi: 10.1242/jcs.069641.

Turner, P.A. et al. 2015. Three-dimensional spheroid cell model of in vitro adipocyte inflammation. *Tissue engineering. Part A* 21(11–12), pp. 1837–47. Available at: <http://www.ncbi.nlm.nih.gov/pubmed/25781458>.

Ueda, K. et al. 2014. Antibody-coupled monolithic silica microtips for highthroughput molecular profiling of circulating exosomes. *Scientific Reports* 4. doi: 10.1038/srep06232.

Umezu, T. et al. 2014. Exosomal miR-135b shed from hypoxic multiple myeloma cells enhances angiogenesis by targeting factor-inhibiting HIF-1. *Blood* 124(25), pp. 3748–3757. doi: 10.1182/blood-2014-05-576116.

Utsugi-Kobukai, S. et al. 2003. MHC class I-mediated exogenous antigen presentation by exosomes secreted from immature and mature bone marrow derived dendritic cells. *Immunology Letters* . doi: 10.1016/S0165-2478(03)00128-7.

Varga, Z. et al. 2014. Towards traceable size determination of extracellular vesicles. *Journal of Extracellular Vesicles* 3(1), pp. 1–10. doi: 10.3402/jev.v3.23298.

Verderio, C. et al. 2012. Myeloid microvesicles are a marker and therapeutic target for neuroinflammation. *Annals of Neurology* 72(4), pp. 610–624. doi: 10.1002/ana.23627.

Vestad, B. et al. 2017. Size and concentration analyses of extracellular vesicles by nanoparticle tracking analysis: a variation study. *Journal of Extracellular Vesicles* 6(1), p. 1344087. Available at: <https://www.tandfonline.com/doi/full/10.1080/20013078.2017.1344087>.

Villarroya-Beltri, C. et al. 2013. Sumoylated hnRNPA2B1 controls the sorting of

miRNAs into exosomes through binding to specific motifs. *Nature Communications* . doi: 10.1038/ncomms3980.

Villarroya-Beltri, C. et al. 2014. Sorting it out: Regulation of exosome loading. *Seminars in Cancer Biology* . doi: 10.1016/j.semcancer.2014.04.009.

Virtue, S. and Vidal-Puig, A. 2008. It's not how fat you are, it's what you do with it that counts. *PLoS Biology* 6(9), pp. 1819–1823. doi: 10.1371/journal.pbio.0060237.

Vishwanath, D. et al. 2013. Novel method to differentiate 3T3 L1 cells in vitro to produce highly sensitive adipocytes for a GLUT4 mediated glucose uptake using fluorescent glucose analog. *Journal of Cell Communication and Signaling* 7(2), pp. 129–140. doi: 10.1007/s12079-012-0188-9.

Vitali, A. et al. 2012. The adipose organ of obesity-prone C57BL/6J mice is composed of mixed white and brown adipocytes. *Journal of Lipid Research* 53(4), pp. 619–629. Available at: <http://www.jlr.org/lookup/doi/10.1194/jlr.M018846>.

van der Vlist, E.J. et al. 2012. Fluorescent labeling of nano-sized vesicles released by cells and subsequent quantitative and qualitative analysis by high-resolution flow cytometry. *Nature Protocols* 7(7), pp. 1311–1326. Available at: <http://www.nature.com/doi/10.1038/nprot.2012.065>.

Volgers, C. et al. 2017. Bead-based flow-cytometry for semi-quantitative analysis of complex membrane vesicle populations released by bacteria and host cells. *Microbiological Research* . doi: 10.1016/j.micres.2017.04.003.

Wabitsch, M. et al. 2000. LiSa-2, a novel human liposarcoma cell line with a high capacity for terminal adipose differentiation. *International Journal of Cancer* 88(6), pp. 889–894. doi: 10.1002/1097-0215(20001215)88:6<889::AID-IJC8>3.0.CO;2-N.

Wabitsch, M. et al. 2001. Characterization of a human preadipocyte cell strain with high capacity for adipose differentiation. *International Journal of Obesity* 25(1), pp. 8–15. Available at: <http://www.ncbi.nlm.nih.gov/pubmed/11244452>.

Wadey, R.M. et al. 2019. Inflammatory adipocyte-derived extracellular vesicles promote leukocyte attachment to vascular endothelial cells. *Atherosclerosis* . doi: 10.1016/j.atherosclerosis.2019.01.013.

- Wahlgren, J. et al. 2012. Activated Human T Cells Secrete Exosomes That Participate in IL-2 Mediated Immune Response Signaling. *PLoS ONE* . doi: 10.1371/journal.pone.0049723.
- Wang, J. et al. 2016. The Novel Methods for Analysis of Exosomes Released from Endothelial Cells and Endothelial Progenitor Cells. *Stem Cells International* 2016. doi: 10.1155/2016/2639728.
- Wang, Q.A. et al. 2013. Tracking adipogenesis during white adipose tissue development, expansion and regeneration. *Nature Medicine* 19(10), pp. 1338–1344. Available at: <http://www.nature.com/doi/10.1038/nm.3324>.
- Wang, Y. et al. 2003. Perilipin expression in human adipose tissues: Effects of severe obesity, gender, and depot. *Obesity Research* . doi: 10.1038/oby.2003.128.
- Wang, Y. et al. 2006. Pref-1, a Preadipocyte Secreted Factor That Inhibits Adipogenesis. *The Journal of Nutrition* 136, pp. 2953–2956. doi: 136/12/2953 [pii].
- Webber, J. et al. 2014a. Proteomics Analysis of Cancer Exosomes Using a Novel Modified Aptamer-based Array (SOMAscan™) Platform. *Molecular & Cellular Proteomics* 13(4), pp. 1050–1064. Available at: <http://www.mcponline.org/lookup/doi/10.1074/mcp.M113.032136>.
- Webber, J. et al. 2014b. Proteomics Analysis of Cancer Exosomes Using a Novel Modified Aptamer-based Array (SOMAscan™) Platform. *Molecular & Cellular Proteomics* . doi: 10.1074/mcp.M113.032136.
- Webber, J. and Clayton, A. 2013. How pure are your vesicles? *Journal of Extracellular Vesicles* 2(1). doi: 10.3402/jev.v2i0.19861.
- Webber, J.P. et al. 2015. Differentiation of tumour-promoting stromal myofibroblasts by cancer exosomes. *Oncogene* . doi: 10.1038/onc.2013.560.
- Weisberg, S.P. et al. 2003. Obesity is associated with macrophage accumulation in adipose tissue. *Journal of Clinical Investigation* . doi: 10.1172/JCI200319246.
- Weiss, H.J. et al. 1979. Isolated deficiency of platelet procoagulant activity. *The American Journal of Medicine* 67(2), pp. 206–213. doi: 10.1016/0002-9343(79)90392-9.

Welsh, J.A. et al. 2017a. Extracellular Vesicle Flow Cytometry Analysis and Standardization. *Frontiers in Cell and Developmental Biology* 5. Available at: <http://journal.frontiersin.org/article/10.3389/fcell.2017.00078/full>.

Welsh, P. et al. 2017b. Targeting inflammation to reduce cardiovascular disease risk: a realistic clinical prospect? *British Journal of Pharmacology* . doi: 10.1111/bph.13818.

Welton, J.L. et al. 2015. Ready-made chromatography columns for extracellular vesicle isolation from plasma. *Journal of Extracellular Vesicles* 4(2015), pp. 1–9. doi: 10.3402/jev.v4.27269.

Welton, J.L. et al. 2016. Proteomics analysis of vesicles isolated from plasma and urine of prostate cancer patients using a multiplex, aptamer-based protein array. *Journal of Extracellular Vesicles* 5(1). doi: 10.3402/jev.v5.31209.

Welton, J.L. et al. 2017. Cerebrospinal fluid extracellular vesicle enrichment for protein biomarker discovery in neurological disease; multiple sclerosis. *Journal of Extracellular Vesicles* 6(1), p. 1369805. Available at: <https://www.tandfonline.com/doi/full/10.1080/20013078.2017.1369805>.

Wen, C. et al. 2017. Biological roles and potential applications of immune cell-derived extracellular vesicles. *Journal of Extracellular Vesicles* . doi: 10.1080/20013078.2017.1400370.

White, I.J. et al. 2006. EGF stimulates annexin 1-dependent inward vesiculation in a multivesicular endosome subpopulation. *The EMBO Journal* 25(1), pp. 1–12. Available at: <http://emboj.embopress.org/cgi/doi/10.1038/sj.emboj.7600759>.

Willerson, J.T. 2004. Inflammation as a Cardiovascular Risk Factor. *Circulation* . doi: 10.1161/01.cir.0000129535.04194.38.

Willis, G.R. et al. 2014. Young women with polycystic ovary syndrome have raised levels of circulating annexin V-positive platelet microparticles. *Human Reproduction* 29(12), pp. 2756–2763. doi: 10.1093/humrep/deu281.

Willms, E. et al. 2018. Extracellular vesicle heterogeneity: Subpopulations, isolation techniques, and diverse functions in cancer progression. *Frontiers in Immunology* .

doi: 10.3389/fimmu.2018.00738.

Witczak, J. et al. 2017. Alterations in concentration and characteristics of circulating extracellular vesicles in morbid obesity. *Endocrine Abstracts* . doi: 10.1530/endoabs.50.p331.

Wolf, P. 1967. The nature and significance of platelet products in human plasma. *British journal of haematology* 13(3), pp. 269–288. doi: 10.1111/j.1365-2141.1967.tb08741.x.

Wolins, N.E. et al. 2006. OP9 mouse stromal cells rapidly differentiate into adipocytes: characterization of a useful new model of adipogenesis. *Journal of lipid research* 47(2), pp. 450–60. Available at: <http://www.ncbi.nlm.nih.gov/pubmed/16319419>.

Woo, H.K. et al. 2019. Urine-based liquid biopsy: Non-invasive and sensitive AR-V7 detection in urinary EVs from patients with prostate cancer. *Lab on a Chip* . doi: 10.1039/c8lc01185k.

World Health Organization 2015. Cardiovascular diseases (CVDs). doi: 19 Jan 2014.

Wu, G. et al. 2014. Mechanism and clinical evidence of lipocalin-2 and adipocyte fatty acid-binding protein linking obesity and atherosclerosis. *Diabetes/Metabolism Research and Reviews* . doi: 10.1002/dmrr.2493.

Wu, Z. et al. 1999. Cross-regulation of C/EBP α and PPAR γ controls the transcriptional pathway of adipogenesis and insulin sensitivity. *Molecular Cell* 3(2), pp. 151–158. doi: 10.1016/S1097-2765(00)80306-8.

Xiao, L. et al. 2011. Highly hydroxylated fullerene localizes at the cytoskeleton and inhibits oxidative stress in adipocytes and a subcutaneous adipose-tissue equivalent. *Free Radical Biology and Medicine* 51(7), pp. 1376–1389. doi: 10.1016/j.freeradbiomed.2011.05.026.

Xie, Z. et al. 2018. Adipose-derived exosomes exert proatherogenic effects by regulating macrophage foam cell formation and polarization. *Journal of the American Heart Association* . doi: 10.1161/JAHA.117.007442.

- Xu, A. et al. 2003a. The fat-derived hormone adiponectin alleviates alcoholic and nonalcoholic fatty liver diseases in mice. *Journal of Clinical Investigation* 112(1), pp. 91–100. doi: 10.1172/JCI200317797.
- Xu, A. et al. 2006. Adipocyte fatty acid-binding protein is a plasma biomarker closely associated with obesity and metabolic syndrome. *Clinical Chemistry* . doi: 10.1373/clinchem.2005.062463.
- Xu, A. et al. 2007. Circulating adipocyte-fatty acid binding protein levels predict the development of the metabolic syndrome: A 5-year prospective study. *Circulation* . doi: 10.1161/CIRCULATIONAHA.106.647503.
- Xu, H. et al. 2003b. Chronic inflammation in fat plays a crucial role in the development of obesity-related insulin resistance. *The Journal of clinical investigation* 112(12), pp. 1821–30. Available at: <http://www.ncbi.nlm.nih.gov/pubmed/14679177> <http://www.pubmedcentral.nih.gov/articlerender.fcgi?artid=PMC296998>.
- Yamawaki, H. et al. 2011. Omentin, a novel adipocytokine inhibits TNF-induced vascular inflammation in human endothelial cells. *Biochemical and Biophysical Research Communications* . doi: 10.1016/j.bbrc.2011.04.039.
- Yáñez-Mó, M. et al. 2015. Biological properties of extracellular vesicles and their physiological functions. *Journal of Extracellular Vesicles* 4(2015), pp. 1–60. doi: 10.3402/jev.v4.27066.
- Yang, R.-Z. et al. 2006. Identification of omentin as a novel depot-specific adipokine in human adipose tissue: possible role in modulating insulin action. *American Journal of Physiology-Endocrinology and Metabolism* . doi: 10.1152/ajpendo.00572.2004.
- Yang, X. et al. 2003. Reduced expression of {FOXC}2 and brown adipogenic genes in human subjects with insulin resistance. *Obesity Research* 11(10), pp. 1182–1191. Available at: <http://www.ncbi.nlm.nih.gov/pubmed/14569043>.
- Yeh, W.C. et al. 1995. Cascade regulation of terminal adipocyte differentiation by three members of the C/EBP family of leucine zipper proteins. *Genes and Development* 9(2), pp. 168–181. doi: 10.1101/GAD.9.2.168.

- Yin, W. et al. 2008. Expression of complement components and inhibitors on platelet microparticles. *Platelets* 19(3), pp. 225–233. doi: 10.1080/09537100701777311.
- Yiran, W. et al. 2015. Global scientific trends on exosome research during 2007-2016: A bibliometric analysis. *Oncotarget* . doi: 10.18632/oncotarget.17223.
- Yuana, Y. et al. 2013. Cryo-electron microscopy of extracellular vesicles in fresh plasma. *Journal of Extracellular Vesicles* 2(1), p. 21494. Available at: <https://www.tandfonline.com/doi/full/10.3402/jev.v2i0.21494>.
- Yuana, Y. et al. 2014. Co-isolation of extracellular vesicles and high-density lipoproteins using density gradient ultracentrifugation. *Journal of Extracellular Vesicles* . doi: 10.3402/jev.v3.23262.
- Zaborowski, M.P. et al. 2015. Extracellular Vesicles: Composition, Biological Relevance, and Methods of Study. *BioScience* . doi: 10.1093/biosci/biv084.
- Zarovni, N. et al. 2015. Integrated isolation and quantitative analysis of exosome shuttled proteins and nucleic acids using immunocapture approaches. *Methods* 87, pp. 46–58. doi: 10.1016/j.ymeth.2015.05.028.
- Zebisch, K. et al. 2012. Protocol for effective differentiation of 3T3-L1 cells to adipocytes. *Analytical Biochemistry* 425(1), pp. 88–90. doi: 10.1016/j.ab.2012.03.005.
- Zeringer, E. et al. 2015. Strategies for isolation of exosomes. *Cold Spring Harbor Protocols* 2015(4), pp. 319–323. doi: 10.1101/pdb.top074476.
- Zhang, H. et al. 2009. Role of TNF-alpha in vascular dysfunction. *Clinical Science* . doi: 10.1042/CS20080196.
- Zhang, H. et al. 2011. CD4 T cell-released exosomes inhibit CD8 cytotoxic T-lymphocyte responses and antitumor immunity. *Cellular and Molecular Immunology* . doi: 10.1038/cmi.2010.59.
- Zhang, J. et al. 2008. The Role of Lipocalin 2 in the Regulation of Inflammation in Adipocytes and Macrophages. *Molecular Endocrinology* . doi: 10.1210/me.2007-0420.

Zhang, J. et al. 2014. Inflammation induced-endothelial cells release angiogenesis associated-microRNAs into circulation by microparticles. *Chinese Medical Journal* . doi: 10.3760/cma.j.issn.0366-6999.20133228.

Zhang, Y. et al. 2010. Secreted Monocytic miR-150 Enhances Targeted Endothelial Cell Migration. *Molecular Cell* . doi: 10.1016/j.molcel.2010.06.010.

Zhang, Y. et al. 2017. Inflammasome-Derived Exosomes Activate NF- κ B Signaling in Macrophages. *Journal of Proteome Research* . doi: 10.1021/acs.jproteome.6b00599.

Zhao, W. et al. 2015a. Exosome and its roles in cardiovascular diseases. *Heart Failure Reviews* 20(3), pp. 337–348. doi: 10.1007/s10741-014-9469-0.

Zhao, X.Y. et al. 2015b. Effects of high glucose on human umbilical vein endothelial cell permeability and myosin light chain phosphorylation. *Diabetology and Metabolic Syndrome* . doi: 10.1186/s13098-015-0098-0.

Zhou, Q. et al. 2011. Immune-related microRNAs are abundant in breast milk exosomes. *International Journal of Biological Sciences* . doi: 10.7150/ijbs.8.118.

Zhu, H. et al. 2013. Mutation of SIMPLE in Charcot-Marie-Tooth 1C Alters Production of Exosomes. *Molecular biology of the cell* . doi: 10.1091/mbc.E12-07-0544.

Zuchner, T. et al. 2009. Highly sensitive protein detection based on lanthanide chelates with antenna ligands providing a linear range of five orders of magnitude. *Analytical Chemistry* 81(22), pp. 9449–9453. doi: 10.1021/ac902175g.

Appendix 1

Dialysis

In an attempt to purify the EV prep, dialysis device called Slide-A-Lyzer™ MINI (ThermoScientific) was employed with the use of appropriately sized membrane pores and 1ml sample volume. This system was initially validated by assessing a starting sample of albumin (mol weight 67kDa) and lysozyme (mol weight 14kDa) using a 17kDa cut off pore. This molecular weight was chosen to be directly comparable with that of FABP4 (one of the key adipocyte markers that also exist as a free protein). Having verified the method, this was then applied to 3T3-L1 cell line and results are presented in Table I.

There was no significant change in EV protein concentration over time in the sample holder (as assessed by NanoDrop), and a small but measurable increase in buffer protein concentration was detected, which implies the amount of free FABP4 protein was negligible in the sample. It can be concluded that the FABP4 is less likely to exist as free protein instead bound to the EV. However, in the case of plasma EVs, owing to the high protein content in blood, one step dialysis is precarious for plasma EVs. Hence, other alternate approaches of EV purification was explored.

(A) Albumin

Time (hrs)	Buffer conc (mg/ml)	Sample conc (mg/ml)
0	0	0.65
2	0.01	0.65
4	0	0.66
overnight	0.01	0.65

(B) Lysozyme

Time (hrs)	Buffer conc (mg/ml)	Sample conc (mg/ml)
0	0	4.02
2	0.01	3.74
4	1.77	2.68
overnight	1.77	2.66

(C) 3T3-L1 cell culture media

Time (hrs)	Buffer conc(mg/ml),	3T3 EV sample conc (mg/ml),
0	0	0.8
2	0.01	0.79
4	0.01	0.77
6	0.01	0.77
overnight	0.01	0.77

Table I: Dialysis of control proteins and 3T3 EVs using a 17kDa cut off pore.

0.1ml of protein sample of albumin, lysozyme and 3T3-L1 culture media supernatant were loaded into the sample cup and placed into the dialysis buffer. Protein concentration of the samples were measured by Nanodrop at regular interval at hour 1, 2 and 4 during an overnight dialysis. The mean concentration was recorded for (A) Albumin (B) Lysozyme and (C) cell culture supernatant, $n=3$.